



Role of Flavonoids in the resistance of Carrot to *Alternaria dauci*

Marie Louisa Ramaroson

► To cite this version:

Marie Louisa Ramaroson. Role of Flavonoids in the resistance of Carrot to *Alternaria dauci*. Agricultural sciences. Université d'Angers, 2023. English. NNT : 2023ANGE0030 . tel-04448147

HAL Id: tel-04448147

<https://theses.hal.science/tel-04448147>

Submitted on 9 Feb 2024

HAL is a multi-disciplinary open access archive for the deposit and dissemination of scientific research documents, whether they are published or not. The documents may come from teaching and research institutions in France or abroad, or from public or private research centers.

L'archive ouverte pluridisciplinaire **HAL**, est destinée au dépôt et à la diffusion de documents scientifiques de niveau recherche, publiés ou non, émanant des établissements d'enseignement et de recherche français ou étrangers, des laboratoires publics ou privés.

THESE DE DOCTORAT

DE
L'UNIVERSITÉ D'ANGERS

SOUS LE SCEAU DE
LA COMUE ANGERS – LE MANS

ECOLE DOCTORALE N° 642
Ecole doctorale Végétal, Animal, Aliment, Mer, Environnement
Spécialité : *Sciences Agronomiques*

Par **Marie Louisa RAMAROSON**

Role of Flavonoids in the resistance of Carrot to *Alternaria dauci*

Le rôle des flavonoïdes dans la résistance de la carotte à *Alternaria dauci*

Thèse présentée et soutenue à Angers le 10 octobre 2023
Unité de recherche : UMR 1345 IRHS

Rapporteurs avant soutenance :

Fabienne Baillieu
Antoine Gravot

Professeure, Université de Reims Champagne-Ardenne
Professeur, Université de Rennes

Composition du Jury :

Présidente :

Julie Chong

Examineurs : Julie Chong
Romain Larbat

Professeure, Université de Haute Alsace
Chargé de Recherche, INRAE

Dir. de thèse : Mathilde Briard
Co-encadrant : Jean-Jacques Helesbeux

Professeure, Institut Agro Rennes Angers
Maître de Conférences, Université d'Angers

Invité(s)

Co-encadrante : Latifa Hamama

Ingénieure de Recherche, IRHS, Université d'Angers

L'auteur du présent document vous autorise à le partager, reproduire, distribuer et communiquer selon les conditions suivantes :



- Vous devez le citer en l'attribuant de la manière indiquée par l'auteur (mais pas d'une manière qui suggérerait qu'il approuve votre utilisation de l'œuvre).
- Vous n'avez pas le droit d'utiliser ce document à des fins commerciales.
- Vous n'avez pas le droit de le modifier, de le transformer ou de l'adapter.

Consulter la licence creative commons complète en français :
<http://creativecommons.org/licences/by-nc-nd/2.0/fr/>

Ces conditions d'utilisation (attribution, pas d'utilisation commerciale, pas de modification) sont symbolisées par les icônes positionnées en pied de page.



*“Ka dera no atolotro ho Anao ry Tompo ô,
Fa tsara Ianao, tsara Ianao, sady Mpanao ny tsara koa.
Izay rehetra ataonao sy avelanao hitranga koa,
Dia mahasoia satria Tsara Ianao, sady Mpanao ny tsara koa.”*

Experiencing this doctoral journey was a blessing, as I believe that I would not have been able to learn so much about life, about myself, otherwise. Through all the good people I have met, the joyful moments, the hardships and uncomfortable circumstances I have faced, I have discovered a new facet of my identity, my strengths, my weaknesses and have learned how to walk straight to a better version of myself.

Scientifically, I am humbled by the passion that G. Barroso and A. Calonnec have for the fungi kingdom and plant pathology respectively. Today, I dedicate the fruits of this three-year study to both of you, for being my source of inspiration and for significantly contributing to my development.

My gratitude goes to my supervisors for giving me the opportunity to work on a topic that means a lot to me. Thank you for welcoming me in your lab and for all the priceless time you spared to encourage me and lead me to this day. M. Briard, thank you for being always there and for your boundless support during the darkest moments of my journey. It was an honour indeed, to be your PhD student. L. Hamama, I am grateful to you for the skills you keenly have passed on to me in plant biotechnology. Thank you for your motherly emotional support and for showing me the way during my hardships. J-J Helesbeux, I acknowledge your willingness to push me forward with my skill development in phytochemistry. Thank you for not giving up on me when I felt helpless in the lab or in other aspects of my doctoral life. Thank you for your constructive criticism which has enabled me to strive for excellence.

Many thanks to the members of the SONAS lab, for their warm welcome and for providing a work space for me. J-J Helesbeux, for showing me the way at my début in compound purification and for patiently accompanying me all the way long. D. Bréard, for willing to pass on as much knowledge as possible, which enabled me to work confidently and independently with diverse equipment in the phytochemistry lab. K. Al Sabil, for helping in solving casual lab issues and for his advices during method optimisation. A. Schinkovitz, S.Boisard and D. Guilet for their expert opinion and advices on analytical analyses. A. Ghidini, for being my ears and being there to discuss my results with. Thank you for guiding me with many tasks in the lab and for relentlessly sharing your knowledge in chemistry with me. T. Charpentier, for his advices on chemical analysis. S. Pecnard for all the discussions we had on career development. To all students and colleagues I had the chance to spend great times with.

Likewise, I would also like to thank every member of the QuaRVeg team and colleagues from other research teams of the IRHS lab, for their significant involvement in this thesis. L. Voisine and P. Berthelot, for taking the time to train me in tissue culture techniques and for putting a lot of effort into keeping the vitroplants and calluses in good condition. L. Hamama for the enormous work done to keep the biological materials alive during the COVID lockdown. C. Dubois-Laurent and M. Briard, for all the hours of work in a dark room to help me with image acquisition. S. Huet, for all the energy spent following up field trials and greenhouse experiments, often during heat waves. Again, L. Hamama and M. Briard for their significant involvement in callus extract biological assays and many other tasks. A. Suel, for training me in pathological assays and in molecular analysis of carrot tissues, but also for lending a hand with sample preparations in the lab. D. Peltier for helping a lot with administrative stuff at the University of Angers and for letting me use his office when I needed a quiet place to work. Thank you for the advices during our occasional lunches in the University cafeteria. V. Le Clerc and E. Geoffriau for their expert point of view during team meetings and their suggestions in various publication manuscript writings. S. Moussa and C. Koutouan for preparing the launch of the Ph.D. programme. E. Brémand, for helping with tissue culture, field work and method optimisation for *in vitro* biological assays during his internship.

ACKNOWLEDGEMENT

To S. Ouchetto for contributing to the tissue culture work. W. Chevalier, for his advices on gene expression analyses and statistics. To O. Posylayeva, for giving me a quick lecture on plant breeding techniques and for letting me benefit from her expertise in psychology. L. Ogé from GDO team, for his colossal involvement in the production of carrot transformants and in molecular analyses. C. Vilfroy, for his assistance with culture medium sterilisation. My gratitude also goes to D. Rousseau and members of the ImHorPhen team, for collaborating with us on the automation of the *A. dauci* image analysis. To A-G. Gouerec and S. Dussot for building the pillars of the model and to H. Metuarea for fine-tuning as well as for helping me get to grips with the tool. To A. El Ghaziri for the huge amount of time she spent in helping me with the statistical analysis of my data. P. Santagostini for his advices on statistics. To L. Ismaila and A. Moufidi for sparing time to solve some of the issues I had with R and for sharing tips on mathematics, artificial intelligence or career plan. To all colleagues and students of the IRHS lab who took part of this journey by their presence.

Many thanks to colleagues from the INEM and Phenotic platform for field and greenhouse trial follow up, especially M. Robert, C. Boursier, P. Ponce and D. Sochard. Also to A. Rolland and F. Simoneau from the IMAC platform for training me and for their assistance in microscopy. I also express my gratitude to I. Freuze from the ASTRAL platform for offering her help during the first stage of the purification of Chry7R, by providing the LC-MS profile of my leaf extracts. To colleagues from the SVQV team in Colmar for metabolite quantification and for generously answering our questions.

I extend my thanks to the members of the thesis committee for their hindsight and guidance over the years.

Many thanks to the members of the Jury who agreed to lend their expertise to the evaluation of my work.

Thanks to the RFI Objectif Végétal programme of the Région Pays-de-la-Loire and to the Ministère de l'Enseignement Supérieur, de la Recherche et de l'Innovation (MESRI) for financially supporting the FLARESCAD project.

Last but not least, I would like to thank all the people at the University of Angers, who went to great lengths to help international students find accommodation, manage administrative paperwork and for providing emotional support during the COVID lockdown. I treasure all the good times I had with my Latin and ballroom dancing friends, who gave a positive weight to my mental health. I am deeply grateful to my friends and colleagues who made a home for me when I was weak, helpless and hopeless. I could write a thick manuscript telling the world how you all lifted me up. But I would rather give you a piece of my heart. Most importantly, I dedicate this work to my family for their invaluable contribution to every aspect of my life to this day. May this path God has set me on be a blessing to the younger generations !

Contents

GENERAL INTRODUCTION	1
CHAPTER I: CARROT, CARROT-A. DAUCI PATHOSYSTEM AND INVOLVEMENT OF FLAVONOIDS IN PLANT IMMUNITY	5
1.1. <i>From Queen Anne's Lace to modern carrots</i>	<i>5</i>
1.2. <i>Challenges for carrot production</i>	<i>8</i>
1.3. <i>Daucus carota - A. dauci interaction</i>	<i>9</i>
1.4. <i>Flavonoids</i>	<i>13</i>
CHAPTER II: ACCUMULATION PATTERN OF THE THREE CANDIDATE FLAVONOIDS IN CARROT LEAVES AT DIFFERENT PHENOLOGICAL STAGES AND THEIR CONSISTENCY ACROSS DIVERSE GENETIC BACKGROUNDS	21
2.1 <i>Quantitative differentials between H1 and I2 along the vegetative growth</i>	<i>22</i>
2.2 <i>Correspondence between disease expression level and metabolite enrichment in eight accessions</i>	<i>25</i>
2.3 <i>Contrast between accessions: ALB symptoms</i>	<i>29</i>
2.4 <i>Contrast between accessions: candidate metabolite content</i>	<i>30</i>
2.5 <i>Analysis of the correlation between candidate metabolites</i>	<i>36</i>
DISCUSSION AND PERSPECTIVES.....	36
APPENDICES	40
CHAPTER III: SHEDDING LIGHT ON THE PLACE HELD BY THE THREE FLAVONE GLYCOSIDES IN THE D.CAROTA - A.DAUCI INTERACTION - BIOLOGICAL ACTIVITY AND MECHANISMS OF ACTION.....	46
3.1 <i>Scouting for natural sources enriched with the candidate flavones.....</i>	<i>48</i>
3.2 <i>Method development and flavonoid purification</i>	<i>49</i>
3.3 <i>Biological activity of the flavonoids of interest.....</i>	<i>63</i>
DISCUSSION AND PERSPECTIVES.....	79
APPENDICES	83
CHAPTER IV: FUNCTIONAL ANALYSIS OF CANDIDATE GENES PUTATIVELY DICTATING THE ACCUMULATION OF THE CANDIDATE FLAVONOIDS IN CARROT LEAVES	92
4.1 <i>Investigation of candidate gene function on calli</i>	<i>94</i>
4.2 <i>Follow up of H1 and I2 T₀ regenerants.....</i>	<i>102</i>
DISCUSSION AND PERSPECTIVES.....	104
APPENDICES	108
CHAPTER V: MATERIALS AND METHODOLOGIES	110
5.1 <i>CHAPTER II.....</i>	<i>110</i>
5.2 <i>CHAPTER III</i>	<i>116</i>
5.3 <i>CHAPTER IV</i>	<i>124</i>
GENERAL DISCUSSION	130
BIBLIOGRAPHY	138

GENERAL INTRODUCTION

The Food and Agriculture Organization of the United Nations (FAO) has encouraged fruit and vegetable uptake for a more balanced and healthier diet, during the International Year of Fruits and Vegetables in 2021. At the same time, the world's population is constantly growing and is expected to exceed 9 billion by 2050, according to UN estimates. Meeting with this demographic challenge will require an effective reshaping of the agricultural system, in a way to ensure an optimal and sustainable food supply. Another challenge is the growing demand for food that is safe for animals and humans, while minimising its impact on the environment. Recently, the European Union's Green Deal initiatives recommended a 50% reduction in the use of more toxic chemical pesticides by the horizon 2030; thus, encouraging the deployment of Integrated Pest Management (IPM) strategies, as well as the development of organic farming by 25%. In addition to these directives, the French authorities have launched the Ecophyto plan to reduce the local pesticide use by 50% by 2025 (<https://agriculture.gouv.fr/telecharger/98894>). Beside the expansion of natural alternatives to pesticides, organic farming is also constantly developing, representing 10% of the total production area in 2021 (French Ministry of Agriculture, <https://agriculture.gouv.fr/quels-sont-les-chiffres-du-bio-en-2021>).

The production of carrots as part of the health-promoting vegetables recommended for consumption by the FAO (FAO, 2020), is more than ever concerned by this transition. In France alone, its large field production is highly dependent on phytopharmaceutical products, mainly fungicides with an IFT (Indicator of Frequency of Treatment) of 2.9 over a total of 8 for this crop in 2018 (Agreste 2022). Growers continue to rely on these products to ensure their production is optimal and marketable during a period of high disease pressure in the field. One of the most common and threatening pre-harvest diseases in carrot production is a leaf blight caused by *Alternaria dauci*, which threatens root filling if established early in plant development (Davis, 2004) and can lead to 100% losses in severe attacks, as harvesting relies on foliage grasping (Farrar et al., 2004; Ben-Noon et al., 2001; Boedo et al., 2012). As this pathogen is transmissible through seeds if occurring during seed set (Maude et al., 1992), carrot seed treatment is also of practice to a lesser extent, with an IFT of 0.6 (Agreste 2022). An increasing number of conventional pesticides are withdrawn from use, while certified natural alternatives are not yet available. The use of the carrot genetic resources seems to be one evident approach, as genotypes with good resistance to this disease exist (Boedo et al., 2008). Nevertheless, more needs to be done to obtain a highly resistant cultivar that will assort the rapid expansion of organic production system for this crop. In fact, according to France Agrimer, it has reached 14 % of the total area cultivated with carrot in 2020 (<https://www.franceagrimer.fr/fam/content/download/69332/document/SYN-FL-2022-VEILLE-CAROTTE-2020.pdf?version=1>). To reach the FAO and Ecophyto targets will therefore imply a good knowledge of the genetic factors responsible for the resistance trait, although no major resistance genes have yet been discovered. A recent *de novo* assembly of the carrot genome predicted more than 600 genes, putatively determining disease and pest resistance (Iorizzo et al., 2016). This breakthrough has given real hope for the incorporation of multiple resistance genes into future cultivars.

The Institute of Research on Horticulture and Seeds (IRHS) in Angers is a multidisciplinary research unit, comprising 14 research teams working on the quality and resistance to biotic / abiotic stresses of horticultural and seed crops (<https://www6.angers-nantes.inrae.fr/irhs/L-Institut>). Vegetable crops, in particular carrots, have been the focus of the QuaRVeg team (Quality and Resistance to bio-aggressors of Vegetable crops) for years. While a part of the team's work is dedicated to understanding the overall nutrient and carotenoid accumulation in carrot roots, the search for more resistant cultivars to *A. dauci* also holds a major part. Indeed, screening for new sources of resistance has been fruitful, leading to the identification of new resistance-related quantitative trait loci (rQTL) mapped on the carrot's genome (Le Clerc et al., 2009; Le Clerc et al., 2015). By characterising these sources of resistance, the team demonstrated the ability of cells of some resistant cultivars to withstand the toxins secreted by this fungus (Lecomte et al., 2014; Courtial et al., 2018). With the growing evidence of metabolite-mediated resistance to plant pathogens, the role of polyacetylenes in the resistance to *A. dauci* was also confirmed by the team in cultivars grown in France (Lecomte et al., 2012). Echoing this first approach, the exploration of the metabolome and transcriptome of carrot leaves led to the discovery of flavonoids associated with resistance to *A. dauci* and of genes putatively responsible for their accumulation. This was done on a correlative basis, in part published in (Koutouan et al., 2018). On the basis of co-localisation between metaboliteQTL (mQTL) and rQTL, three specific flavonoids were selected, together with two genes that were up-regulated by the resistant genotype compared to a susceptible one and co-localised with major rQTL mapped on the chromosome 6 (under publication). These candidate compounds were identified as apigenin-7-O-rutinoside, luteolin-7-O-rutinoside and chrysoeriol-7-O-rutinoside, from the flavone subfamily. The candidate genetic determinants of their accumulation in the leaves were annotated as a *basic helix loop helix 118-like* gene, and an *anthocyanidin-3-O-UDP-glucosyltransferase 2* gene, based on the publication of (Iorizzo et al., 2016).

The discovery of this resistance-related trait was promising in improving carrot's resistance to leaf blight. However, these results were mainly exploratory and carried out on a very limited number of accessions (1 susceptible and 3 partially resistant). Additional evidence of the metabolite-resistance relationship in a larger number of carrot accessions seems important. Understanding the accumulation pattern of these flavones in the leaves is also worth investigating to know if they could be accumulated early during development. Also, substantial evidence highlighting their mechanism of action would fully support their role in the disease resistance. Future exploitation in a breeding programme will involve the introgression of the flavonoid accumulation trait into cultivars, if these three compounds are indeed markers of resistance. Subsequently, a sound knowledge of their corresponding biosynthetic genes and their regulators will allow the development of molecular tools that can be widely used for a high-throughput screening of genotypes, during varietal selection processes.

Before reaching that phase, four main research questions were to be studied and investigated thoroughly:

1. Is the correlation between the candidate metabolite contents and the level of resistance still observable in different accessions throughout the developmental stage of the carrot?
2. Could they have an inhibitory effect on the development of *A. dauci*?
3. Are the candidate genes responsible for the accumulation of the candidate flavonoids?
4. Is their expression responsible for resistance by controlling flavonoid accumulation?

The Flaescad doctoral project (For **fl**avonoids and **re**sistance of the **car**rot to *Alternaria dauci*) was conceived by the QuaRVeg team of the IRHS, in collaboration with the SONAS laboratory (Natural Substances and Structural Analogues) in Angers, to provide answers to these questions. The present document reports on the investigations undertaken throughout this 3-year research programme, discusses the main findings and proposes prospects for future applications. To allow a full understanding of this research topic, a review of the state of the art on the carrot-*A. dauci* pathosystem, as well as on the involvement of flavonoids in plant immunity is proposed in Chapter I.

CHAPTER I: CARROT, CARROT-A. DAUCI PATHOSYSTEM AND INVOLVEMENT OF FLAVONOIDS IN PLANT IMMUNITY

1.1. From Queen Anne's Lace to modern carrots

Carrot (*Daucus carota* L. subsp. *sativus*) is a diploid plant ($2n = 18$) belonging to the *Apiaceae* family (formerly the *Umbelliferae* family), that is ubiquitously cultivated for its edible taproot. Historical records indicated that the carrot was first domesticated in Arab countries and in Central Asia from the wild carrot species referred to as Queen Anne's Lace (*D. carota* L. subsp. *carota*) (Stolarczyk and Janick, 2011; Simon et al., 2017). Phylogenetic analyses, however, have shown that domesticated carrots are more closely related to wild carrot relatives from Asia (Iorizzo et al., 2013; Rong et al., 2014). Modern cultivated carrots are the result of sequential genetic improvements, from the reduction of root branching to the formation of fleshy roots of various colours (white, purple, yellow, orange and red) (**Figure 1**) and shapes (conical, cylindrical, round, long, short) (**Figure 2**). Orange carrots in Western countries have been shown to be derived from cultivated carrot varieties with yellow roots, rather than through domestication of European wild relatives (Banga, 1957; Iorizzo et al., 2013). According to the "Carottes de France" Organisation, there are more than 500 cultivars classified into market types according to their colour and shape. For example, the most appreciated and produced carrot in France is of Nantes type (**Figure 2**), which is cylindrical and orange.

Extensive selection for traits of agricultural interest resulted in high genetic differentiation between wild relatives and cultivated varieties, and the reduction in genetic diversity among cultivated carrots (Rong et al., 2014). First of all, cultivated carrots complete their life cycle in two years. During the vegetative phase, seedlings emerge and develop the aerial parts concomitantly to root filling (**Figure 3**). At the end of the vegetative phase, they go through a period of vernalisation before entering the generative or reproductive phase in spring. The shoots begin to elongate and the apical meristem differentiates to form umbrella-shaped inflorescences called umbels. After inflorescence pollination, carrot plants begin to senesce and die when seeds are fully developed and mature (Linke et al., 2017). However, for carrot production, the roots are harvested much earlier than the end of the vegetative phase, as the roots would then become more fibrous and no longer palatable. Known to be an excellent source of provitamin A, carotenoids and antioxidant compounds depending on the root colour (predominantly carotenes in orange roots, anthocyanins in purple roots, lycopene in red roots and lutein in yellow carrots), carrot consumption is increasingly recommended by health authorities to prevent deterioration of vision and prevent inflammatory diseases in human health (Surles et al., 2004; Arscott and Tanumihardjo, 2010; Leja et al., 2013; Ahmad et al., 2019). Since the advent of palatable roots from the first domestication, improvement of the sensory and organoleptic quality of cultivars has therefore been a constant focus, while at the same time considering new traits to adapt to modern farming practices (e.g. mechanical harvesting) and changing climatic conditions (Stein and Nothnagel, 1995; Foury, 2003; Surles et al., 2004; Garcia-Mas and Rodriguez-Concepcion, 2016; Acosta-Motos et al., 2021; Bhandari et al., 2022). The recent publication of

the carrot genome sequence is expected to provide insights into finding genes of interest to meet with agricultural needs, improve nutritional value, and increase disease and pest resistance (Iorizzo et al., 2016). The discovery of the mechanism of somatic embryogenesis from carrot cells (Steward, 1958) pioneered the validation of candidate gene function and the use of genetic engineering to evolve towards these objectives (Tokuji and Hiroo, 1999; Punja, 2005; Klimek-Chodacka et al., 2018).

Today, China is the world's leading carrot producer with more than 17 million tons in average, followed by Ouzbekistan, Russia, the United States and Europeans countries (FAOSTAT, carrot and parsnip production from 2010 to 2021). In Europe, France is the fifth carrot producer with 547000 tons in 2020, after the Netherlands, the United Kingdom, Italy and Spain, (FranceAgrimer, 2022). It is also the second world carrot seed producer and the first in Europe (Le Clerc et al., 2021). The French fresh market is supplied throughout the year, by three main production areas located in the south-west (Les Landes and Gironde) and north-west (Manche) of the country. Spring carrots or early carrots, called “carotte de primeur”, are planted in December-February and harvested between May and July. Seasonal carrots are harvested in the summer. Late season carrots, called “carotte de conservation”, are those planted during summer and harvested in winter or stored in the field for a late harvest. Carrot is the second most consumed vegetable in France (Carottes de France Organisation).

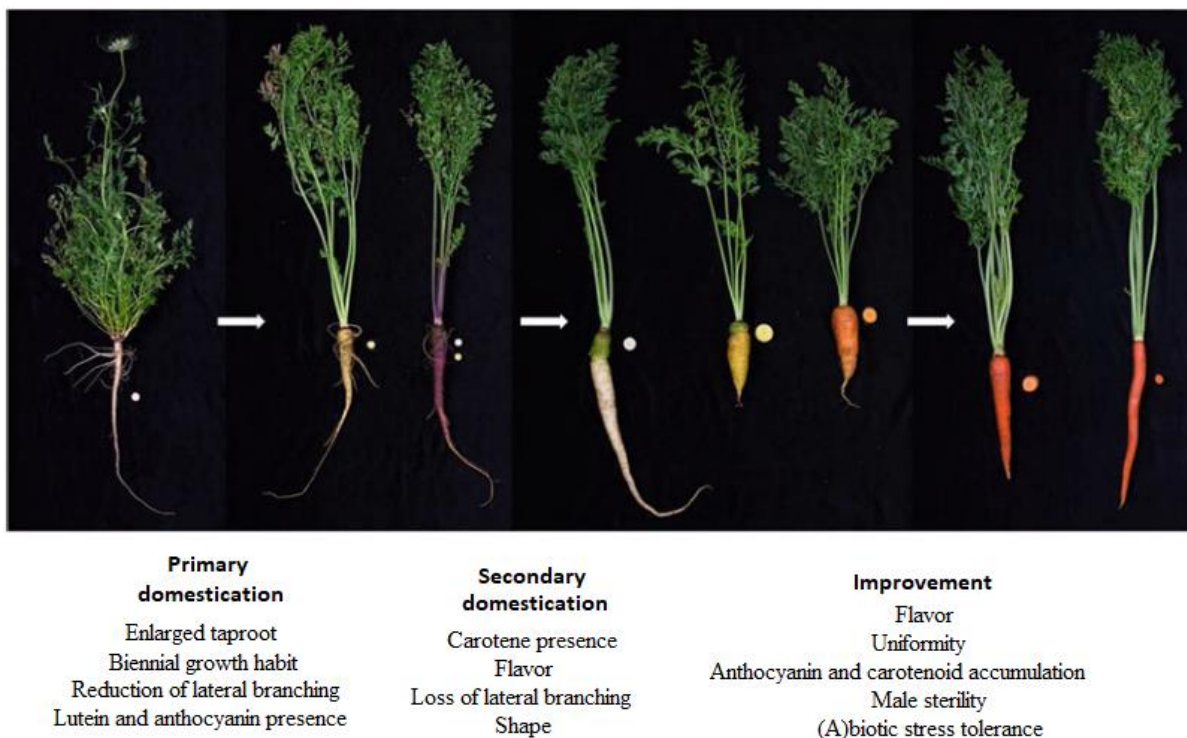


Figure 1: Trajectory of the carrot domestication from wild species to modern cultivars. Adapted from (Ellison, 2017).

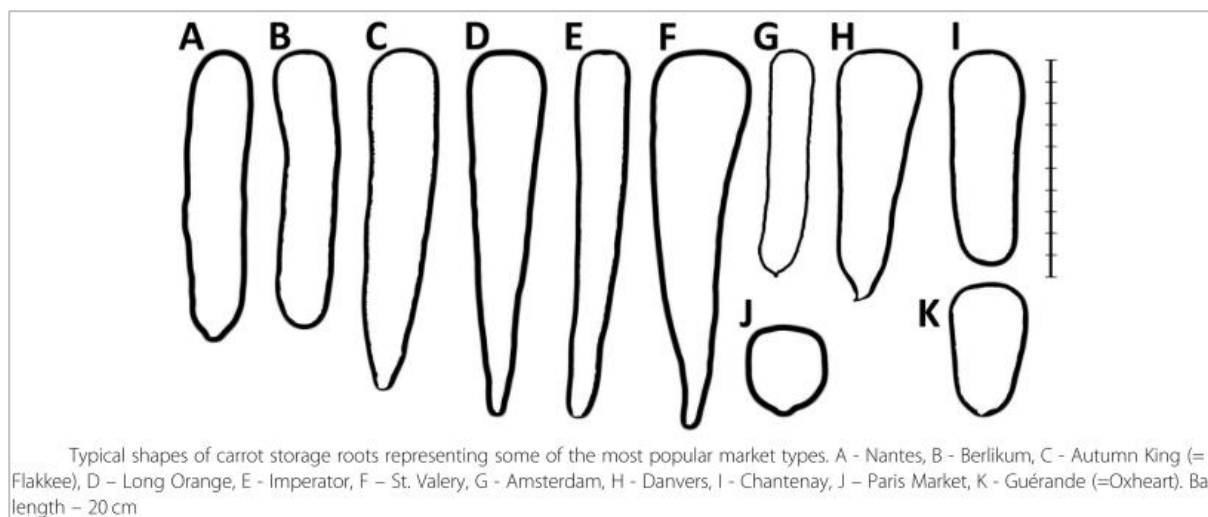


Figure 2: Typical shapes of cultivated carrot roots produced around the world (Stelmach et al., 2021)

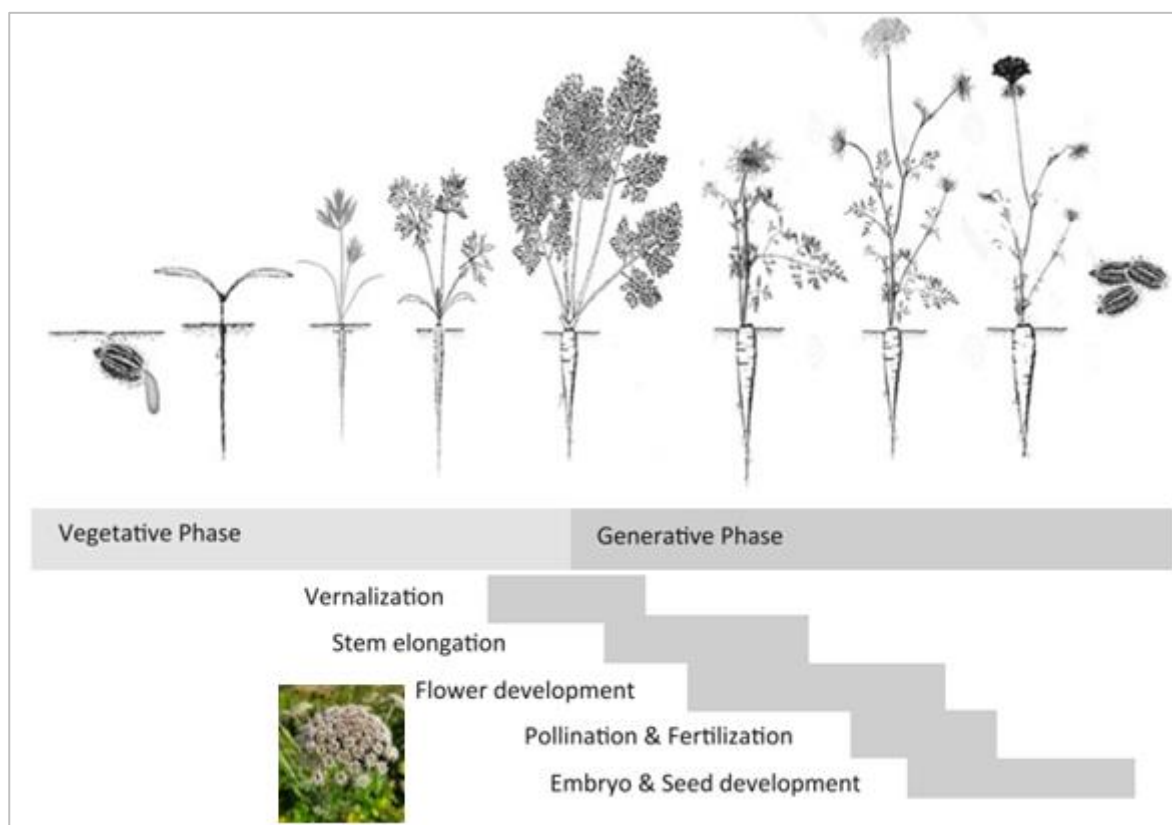


Figure 3: Full life cycle of the carrot. Adapted from (Linke et al., 2017).

1.2. Challenges for carrot production

Root shape is highly dependent on plant density and soil type. It is, therefore, essential to grow carrots in the most favourable pedoclimatic conditions in order to meet the commercial production specifications. Growth is more optimal in well irrigated sandy soils and at cool temperatures, than on clay (Ahmad and Siddiqui, 2017). Besides, carrot is subject to several weed invasions in the field, including species of the genera *Amaranthus* and *Chenopodium*, or by *Senecio vulgaris* (Grace and Müller-Schärer, 2003; Swanton et al., 2010). Effective weed management is required at the earliest stages of development, to avoid competition for space with developing seedlings.

Root filling and harvestability could be dramatically impacted by the occurrence of foliar diseases such as *Alternaria* leaf blight (ALB, caused by the fungus *Alternaria dauci*), *Cercospora* leaf blight (CLB, caused by the fungus *Cercospora carotae*) and bacterial leaf blight (caused by the bacterium *Xanthomonas campestris* pv. *carotae*), leading to a reduction in photosynthetic leaf area (Davis, 2004; Ahmad and Siddiqui, 2017) and foliage robustness for mechanical harvesting. Other foliar diseases, such as the powdery mildew *Erysiphe heraclei*, may have an indirect impact through a weakening of leaf tissue, which promote the development of blights.

The marketing or consumption of the roots may also be threatened by the fungus *Alternaria radicina*, the causal agent of black rot, *Pythium* species causing cavity spot (Chen and Punja, 2002), (Hiltunen and White, 2002) and species of *Meloidogyne* or *Heterodera* parasitic nematodes, pathogens causing root rot (*Erwinia carotovora* subsp. *carotovora*), *Rhizoctonia solani* or *violacea* causing root splitting or damaged roots. Insect infestation (especially the carrot fly *Psila rosae*) can also dramatically affect root quality (CAB International, 2021). Viral diseases of carrot also cause reduce the commercial value of roots. The most common post-harvest diseases of carrot include cottony rot (*Sclerotinia sclerotiorum* (Lib.) de Bary, *Mycocentrospora acerina* Hartig, *Botrytis cinerea* and *Rhizoctonia carotae* Rader).

Seed production is generally challenged by the presence of wild carrot relatives growing everywhere in nature, which makes it difficult to obtain pure varieties. Bidirectional gene flow between cultivated and wild relatives can occur, depending on the density of both populations and on the ability of the pollinators to disperse pollen over relatively long distances (Hauser and Shim, 2007; Rong et al., 2010; Mandel et al., 2016). Carrot inflorescences can also be attacked by pathogens such as *Alternaria dauci* (Maude et al., 1992), *Xanthomonas campestris* pv. *carotae* (Du Toit et al., 2005), *Cercospora carotae* and *Alternaria radicina* pathogen (Davis, 2004); thus amplifying the risk of disease transmission to the next production or abortion of seed development or dampening of seedling development (Maude et al., 1992). Although there are no comprehensive data on the economic losses due to all these diseases, *Alternaria dauci* is considered to be the most damaging carrot pathogen (Davis, 2004).

1.3. *Daucus carota* - *A. dauci* interaction

1.3.1. The fungus *Alternaria dauci*

Alternaria dauci (J.G. Kühn) J.W. Groves & Skolko described by J.W. Groves & Skolko in 1944 is a seed-borne fungus belonging to the phylum Ascomycota, the *Pleosporaceae* family and the genus *Alternaria* (<https://www.mycobank.org/>). At its early developmental stage, it has a melanised multicellular conidial body (80 - 100 µm long) which is prolonged by the presence of a very long beak (200 - 250 µm) typical of the species (**Figure 4**). *A. dauci* is thought to be homokaryotic only as there is, till date, no evidence of a sexual reproduction event or a trace of nuclear heterokaryosis (Netzer and Kenneth, 1970). Different strains of *A. dauci* have different levels of aggressiveness towards broad host range of hosts, including plants in the *Apiaceae* family (e.g. carrot, chervil, dill, fennel, or coriander), but also Corn salad, Cress, Radish and Tomato (Boedo et al., 2012). As a necrotrophic fungus, it operates by producing toxins -phytotoxic metabolites (Courtial et al., 2018; Leyte-Lugo et al., 2020).

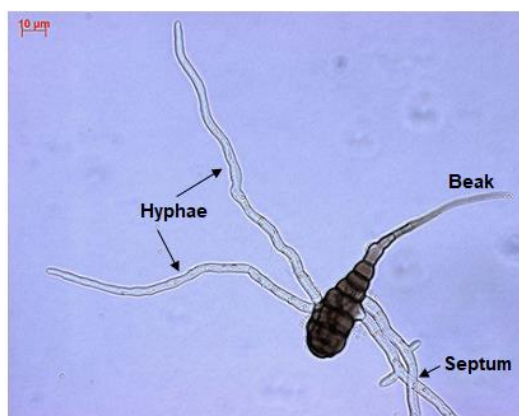


Figure 4: Germinating conidium of *Alternaria dauci*.

1.3.2. Disease cycle

During the reproductive phase of carrots, in the case of early attacks, *A. dauci* can drastically prevent the fecundity if the sexual organs are infected, as shown in wild relatives (Schouten et al., 2002), or be transmitted to seeds, which will become one of the putative sources of inoculum for a new crop. Plant debris are the second inoculum source, which can harbour live conidia over the winter (Pryor et al., 2002). Wild relatives can also be reservoirs of inoculum. Conidia are able to germinate over a very wide temperature range (8 - 28°C) with an optimum around 22-24°C when relative humidity exceeds 96% or when open water remains on the leaf surface (Rottem, 1994). As described in **Figure 5**, this stage could be reached in less than 5 hours under optimal weather conditions. The germ tubes adhere to the plant leaf thanks to a mucilage made of polysaccharides or glycoproteins (Hatzipapas et al., 2002; Boedo et al., 2008). Tissue invasion apparatuses, such as appressoria have not been observed. *A. dauci* penetrates epidermal cells directly (L., J., Dugdale et al., 2000) by means of appressoria-like structures, probably containing lytic enzymes, or through stomata before colonising inter- and intracellular spaces (Boedo et al., 2008). A subsequent dense

subcuticular net of hyphae leads to cell wall breakage and cytoplasmic disorder within 8 to 18 days, resulting in symptoms. New conidia are emitted from infected tissues and dispersed into the environment by wind, splashing water or human practices.

If infected seeds are sown, seedling damping-off may occur (Maude, 1966). In adult plants, the first symptoms appear on older leaves. Small green lesions of 1 mm in diameter gradually develop into brown infected zones, eventually surrounded by a yellow halo. After a few weeks, the necrotic spots could merge into large lesions, which may end in a completely blighted foliage. If the season is still favourable, a new foliage can be produced from root reserves, otherwise, the disease can lead to 100% losses in case of severe attacks, as the harvesting relies on foliage grasping (Ben-Noon et al., 2001; Farrar et al., 2004; Boedo et al., 2012). Although the effects of ALB on root quality are not known in great detail, it has been shown that inoculation with *A. dauci* reduces both leaf and root carotenoid content and chlorophyll content, which can also affect root filling (Ahmad and Siddiqui, 2017; Perrin et al., 2017).

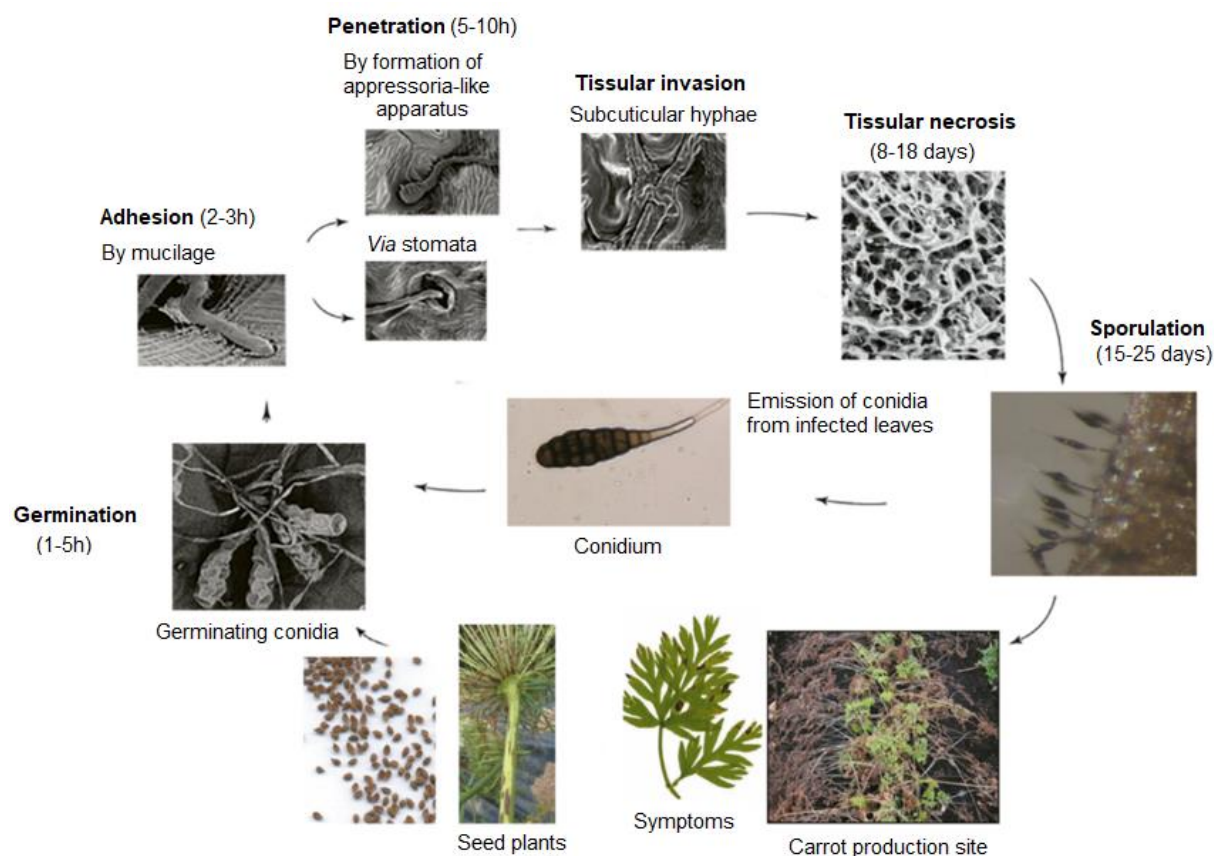


Figure 5: Life cycle of the fungus *Alternaria dauci*, the causal agent of leaf blight on ware and seed carrots. (Adapted from the conception by Charrier L, Photos: QuaRVeg and Fungisem / IRHS)

1.3.3. Disease management strategies

As reviewed by (Le Clerc and Briard, 2020) both preventive and curative levers are used by growers to protect carrots from ALB. Chemical control remains the first and the use of predictive models allows to reduce fungicide applications, TOM-CAST being the most widespread predictive model (Bounds et al., 2007; Marcuzzo and Tomasoni, 2020). For about 20 years, protection methods based on Biological Control Agents (BCA) have been largely investigated by researchers. These include a wide varieties of virulent or avirulent pathogens, cell wall fragments, synthetic chemicals or plant extracts that can i) induce plant defence responses , ii) jeopardize fungal integrity or iii) interfere with pathogenesis. To date, although many promising weapons have been described in the literature, none has been registered and effectively used by growers. The biggest challenge in developing such control strategies is to transfer from lab to field conditions and to define the right timing and dosage of treatments. Agro-technical measures such as crop rotation, planting density, nitrogen applications, foliage trimming, drip irrigation are also of great importance in ALB prevention (Vintal et al., 1999; Ben-Noon et al., 2003; Rogers and Stevenson, 2010a; McIsaac et al., 2013; Saude et al., 2014). Seed treatment is crucial to avoid the first inoculum as mentioned above (Maude, 1992; Koch et al., 2010). Finally, varietal resistance is one of the most important levers and will be described with more details below.

For sure, integrative management strategies relying on a combination of all levers are probably the only way to reach a sustainable cropping system. The Optima European H2020 project has focused on this question in detail and new insights should be published within a few months (<http://optima-h2020.eu>).

1.3.4. Resistance against ALB

(Du Toit et al., 2019) reported the long history of carrot screening for resistance to *A. dauci*, from 1972 to 2015. The main take-home messages are, firstly, the existence of different sources of resistance in Kuroda-type carrots, in Brazilian open-field populations and in several French old varieties or landraces (Strandberg et al., 1972; Silva et al., 2009; Pereira et al., 2012; Amirov et al., 2014; Le Clerc et al., 2015; Carvalho et al., 2015). However, complete resistance has never been found. Only partial quantitative resistance has been described. Secondly, while (Rogers and Stevenson, 2010b) detected variety-by-isolate interactions with three commercial carrot cultivars, (Le Clerc et al., 2015) tested *A. dauci* isolates from different parts of the world on eight varieties or inbred lines and a segregating population for *A. dauci* resistance. They found no significant interaction between isolates and varieties. Differences may be due to isolate-specific resistance factors conferring varying degrees of resistance in different environments as suggested by Clerc et al., 2015). Thirdly, a large number of different types of phenotyping assays have been developed ranging from whole plants in the field, greenhouses, tunnels, or growth chambers to detached leaflets, petioles or hypocotyls in laboratory conditions (Simon and Strandberg, 1998; Pawelec et al., 2006; Baranski et al., 2007; Rogers and Stevenson, 2010b; Le Clerc et al., 2015). From the point of view of the QuaRVeg team, in the context of breeding programmes, of all these phenotyping methods, field phenotyping remains one of the most robust methods for screening a large set of genotypes at once, while, greenhouse trials may be an efficient alternative with

fewer climatic or biotic hazards when the number of accessions to be screened is limited. Other types of screening tests have also been successfully developed in the context of resistance mechanism investigation, but have been too costly or heavy to manage to be applied to high-throughput phenotyping. Among these, (Dugdale et al., 2000) measured the susceptibility of regenerant somaclonal plants by the chlorophyll loss of infected detached leaves. (Boedo et al., 2010) developed a single non-detached leaf drop inoculation method that allowed for mini-scaled greenhouse assessment, *in vivo* conidial germination evaluation and *in planta* quantification of fungal biomass by quantitative PCR (qPCR). (Lecomte et al., 2014) and (Courtial et al., 2018) challenged embryogenic cell cultures with fungal extracts.

(Du Toit et al., 2019) also reported on the genetics and mechanisms of resistance of carrot to *A. dauci*. The heritability of resistance was calculated for different cultivars and environments: 40% narrow-sense heritability (h^2) for the open-pollinated cultivar Brasília (Boiteux et al., 1993) and broad-sense heritability ranging from 45 to 82% (Vieira et al., 1991) for the cultivars Kuroda and Nantes. The polygenic nature of resistance to *A. dauci* has been identified by several authors (Simon and Strandberg, 1998; Le Clerc et al., 2009). To date, no major gene is known and only resistance quantitative trait loci (rQTL) have been described (Le Clerc et al., 2009; Le Clerc et al., 2015). Using electron microscopy and qPCR analyses, (Boedo et al., 2008; Boedo et al., 2010) showed that fungal invasion of carrot leaf tissue was much faster and denser in a susceptible genotype than in resistant ones. Interestingly, they also showed that the germination of *A. dauci* conidia and the number of germ tubes emitted per conidium on carrot leaves *in vivo* were significantly higher on two partially resistant cultivars than on the susceptible one. They suggested that it might reflect multiple attempts by the fungus to penetrate the host epidermis. (Lecomte et al., 2012; Lecomte et al., 2014) concluded a possible but limited effect of 6-methoxy-mellein and a higher effect of faltarindiol, both accumulated more in the resistant genotype Boléro than in the susceptible Presto. These two defence molecules could respectively slow down fungal development and permeabilise the plasma membrane of *A. dauci*. The same authors also showed, by challenging embryogenic cells with fungal exudates, that resistance could involve detoxification of fungal toxins (Lecomte et al., 2014), including the one identified later as aldaulactone (Courtial et al., 2018). Finally, based on the co-localisation of metabolite QTL (mQTL) with rQTL, the flavones apigenin-7-O-rutinoside, luteolin-7-O-rutinoside and chrysoeriol-7-O-rutinoside were identified as candidates to sustain the resistance mechanism through flavonoid accumulation, along with the identification of camphene, α -pinene, α -bisabolene, β -cubebene, caryophyllene, germacrene D and α -humulene as candidates for terpene-mediated resistance (Koutouan et al., 2018). (Lecomte et al., 2014) suggested the involvement of the jasmonate pathway, in the resistant carrot genotype K3, through the overexpression of the *PR4* gene compared to the susceptible H1, but not in another resistant genotype I2. These differences between K3 and I2 supported the hypothesis that the genotypes could achieve partial resistance by quite distinct mechanisms. Using micro-array analysis and rQTL-mQTL co-localization approach, (Koutouan et al., 2018; Koutouan et al., 2023) highlighted two genes for I2 and five terpene synthases and twenty transcription factors for K3 that were up-regulated in the resistant genotype compared to H1. For I2, whose resistance seems to rely on the flavonoid pathway, the two candidate genetic determinants were annotated as a *basic*

helix loop helix 118-like gene, and an *anthocyanidin-3-O-UDP-glucosyltransferase 2* gene, based on the publication of the carrot genome (Iorizzo et al., 2016).

Transgenic carrot plants expressing genes encoding a human lysozyme (possibly able to cleave chitin in the fungal cell wall) or a microbial factor 3 (possibly involved in the signalling pathway affecting induced systemic resistance) or over-expressing a thaumatin-like protein (possibly associated with host defence) have been described as slightly less susceptible to *A. dauci* than non-transformed plants (Takaichi and Oeda, 2000; Punja, 2005; Baranski et al., 2007). No further application has been reported. (Klimek-Chodacka et al., 2018) reported the first use of the CRISPR/Cas9 system for efficient site-targeted mutagenesis of the carrot genome.

1.4. Flavonoids

A review about the “Role of Phenylpropanoids and Flavonoids in Plant Resistance to Pests and Diseases” has been published in *Molecules* in 2022 (Ramaroson et al., 2022)

1.4.1. Molecular structure and diversity

Flavonoids form a large family of low molecular weight compounds, produced by plants from the specialised metabolism. They are found at different locations in the plant, such as in epidermal and mesophyll cells (Agati et al., 2009), also in glandular trichomes (Tattini et al., 2000). In the mesophyll cells, they are mostly stored in the vacuoles (Anhalt and Weissenböck, 1992). Together with phenylpropanoids, they form the big family of polyphenolic compounds, with the generic carbon backbone structure C6-C3-C6. The flavonoid pathway derives from the phenylpropanoid pathway, and starts by the isomerisation of naringenin chalcone to give the flavanone naringenin (**Figure 6**). Naringenin is in turn the common precursor of diverse subfamilies of flavonoids: flavones, flavanols, anthocyanidins and isoflavonoids and so on. The structural diversity can be extended through the conjugation of flavonoid nuclei, the genins, by C- or O-methylation, sulfation, or glycosylation (Hannoufa et al., 1991; Jean Bruneton, 1999; Zagrean-Tuza et al., 2020). As an illustration, the flavone apigenin can be hydroxylated at the carbon in 3' of the ring B to produce luteolin (**Figure 7**). This new compound can even undergo a further transfer of a methyl group at the newly added 3'-OH to produce a methoxylated form of apigenin at this position, which is chrysoeriol. As shown in **Figure 7**, several glycoconjugates can be obtained by the action of more or less substrate specific glycosyltransferases (Griesser et al., 2008; Wu et al., 2022). Less regioselective enzymes can add sugar moieties at different positions of the genin backbone (Liu et al., 2018), giving the possibility of producing a plethora of structurally similar, yet, different compounds.

Reflecting their structural diversity, they are involved in a myriad of biological processes in plants. In plant development, for example, flavonols are essential to pollen germination (Vogt and Taylor, 1995; Taylor and Grotewold, 2005). Pollen viability and seed set are guaranteed by the protective action of flavonols through

quenching of reactive oxygen species (ROS) (Muhlemann et al., 2018). Flavonoids are also key players in ensuring a successful reproductive phase to plants, by attracting pollinators through the pigmentation of floral organs (Mierziak et al., 2014). In addition, the accumulation of flavonoids in the roots of *A. thaliana* has been shown to negatively influence polar auxin transport (Buer et al., 2013). However, there is another line of evidence highlighting that they can exert opposite effects on this developmental process, depending on the structure of the genins (Zhang et al., 2021).

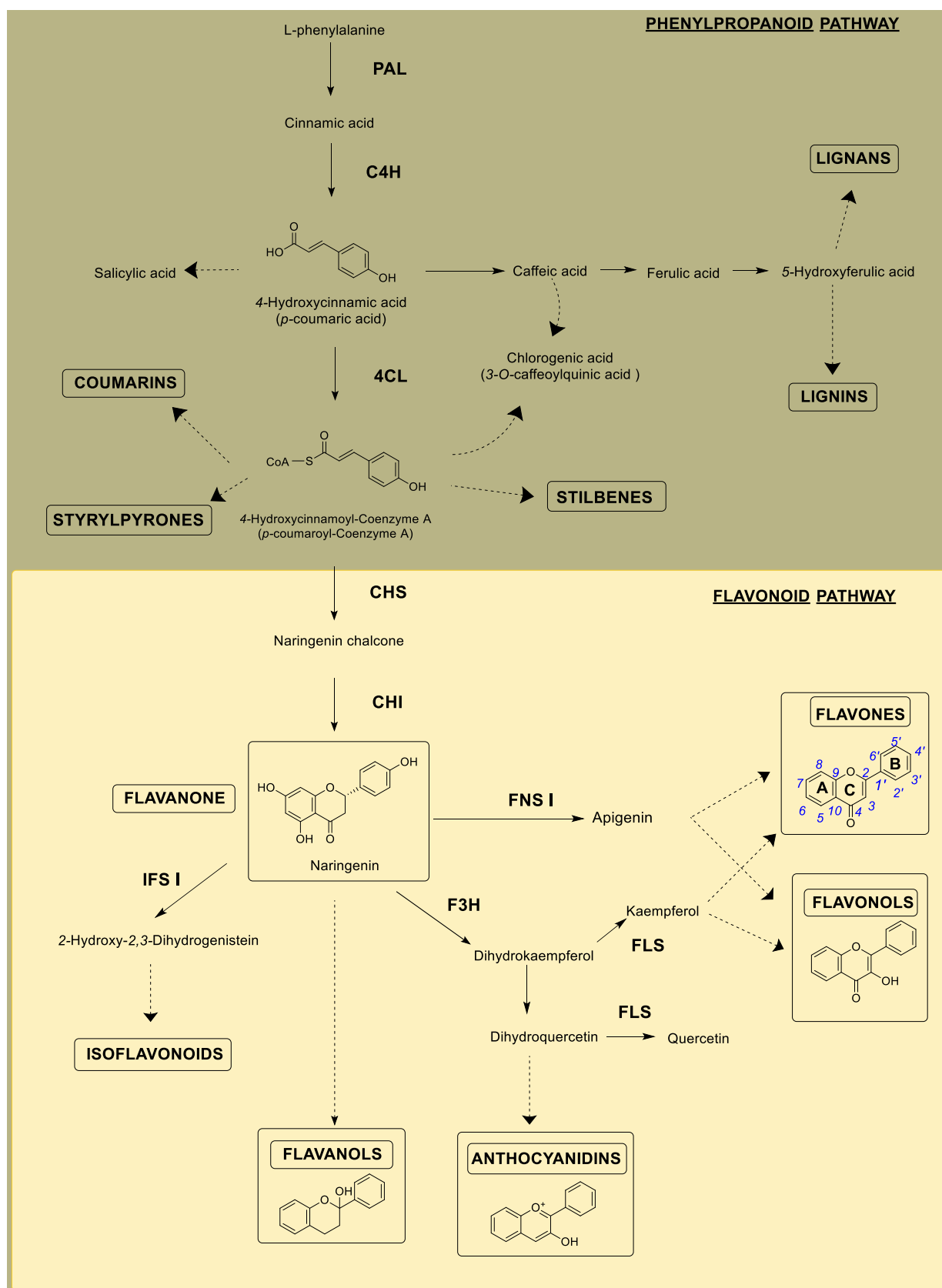


Figure 6: Major steps of the phenylpropanoid and flavonoid pathways leading to compound subfamilies, based on the pathway described in KEGG database (Kyoto Encyclopedia of Genes and Genomes).

Solid arrow: one enzymatic reaction. Dashed arrow: several enzymatic reactions.

PAL: phenylalanine ammonia-lyase; C4H: cinnamate 4-hydroxylase; 4CL: 4-coumarate CoA ligase, CHS: chalcone synthase; CHI: chalcone isomerase; FNS I: flavone synthase I, F3H: flavanone 3-hydroxylase; IFS I: isoflavonoid synthase I; FLS: flavonol synthase.

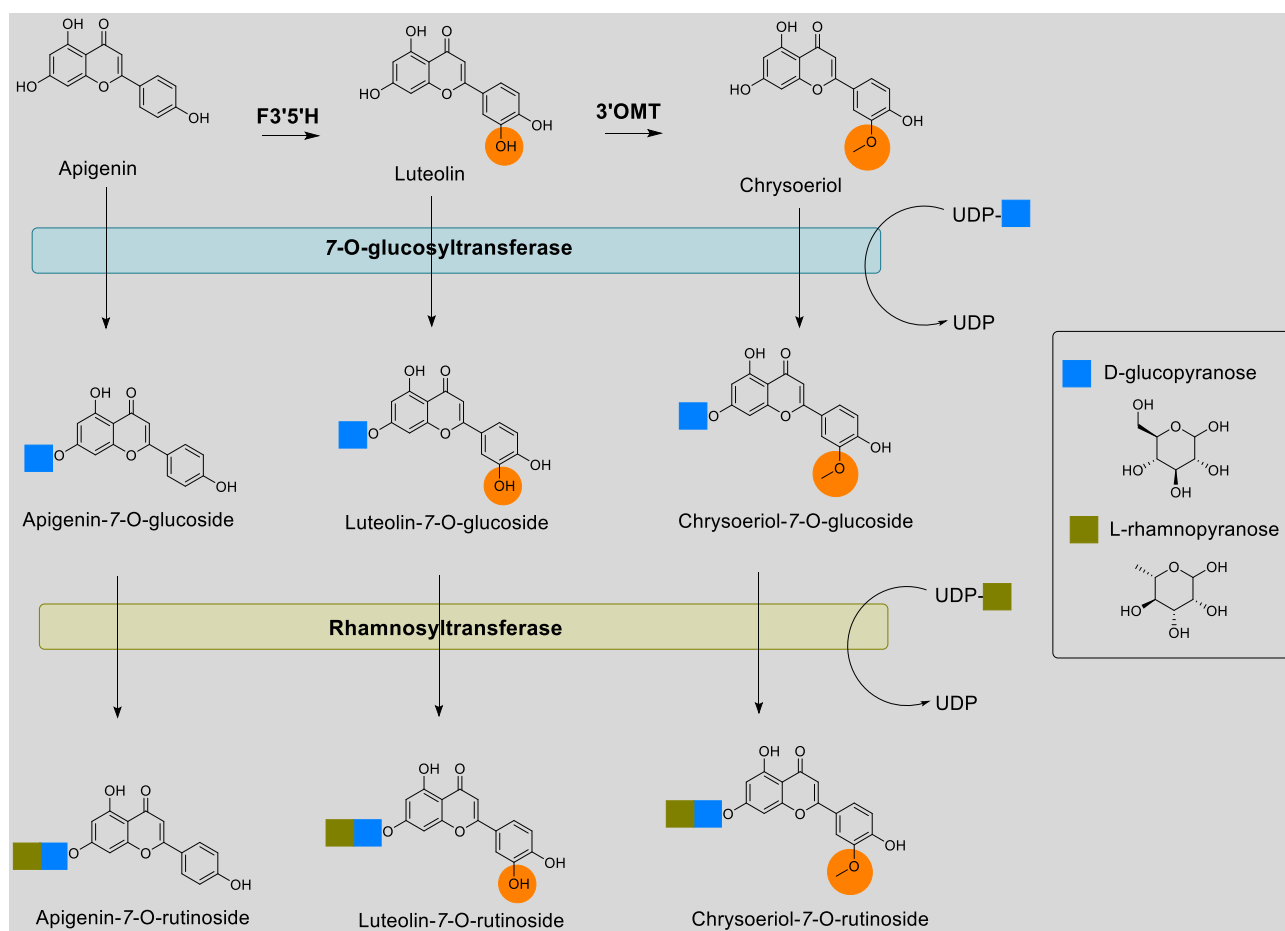


Figure 7: Biosynthesis of the three candidate flavones starting from apigenin, based on the pathway from the KEGG database. *F3'5'H*: flavone 3',5'-hydroxylase; *3'OMT*: 3'-O-methyltransferase.

1.4.2. Control and regulation of the biosynthesis

Exploration of the transcriptome in various plant species allowed to understand that the flavonoid biosynthesis is regulated by the ternary transcription factor (TF) complex, formed by R2R3-MYB, bHLH and WD repeats (Li et al., 2017; Kodama et al., 2018). Functional validation of genes of interest pointed out that TFs in the bHLH and the MYB families can be up-regulators or down-regulators of the flavonoid biosynthesis (Wang et al., 2017), while WDR was described as the ubiquitous component of the complex (Nemesio-Goriz et al., 2017). Furthermore, Zhu and colleagues have demonstrated in *Camellia sinensis*, that the regulatory action of bHLH and MYB TFs on flavonoid biosynthesis can go either way, depending on the environmental factor, notably temperature changes (Zhu et al., 2020). Accordingly, flavonoids of the leaf-surface may quantitatively vary with seasonal phenological shift of the plant (Brooks and Feeny, 2004). These TFs can induce or repress the expression of genes of the central phenylpropanoid pathway such as *PAL* and from the flavonoid pathway such as *CHS* (Figure 6) (Nemesio-Goriz et al., 2017). This may signify that they mostly target early steps of the biosynthetic pathway. However, the up-regulation of glycosyltransferase genes have also been observed, meaning that they can control specific genes at the periphery of the pathway (Zhu et al., 2020).

1.4.3. Protection of the plant during abiotic stresses

The protective role of flavonoids in this context is often linked to the fact that plants have to maintain their redox homeostasis, following their exposure to abiotic stresses, which enhances ROS production. Peroxidation of membrane lipids would be prevented by the action of flavonoids with high antioxidant activity (Rackova et al., 2005; Haraguchi et al., 2010). This pattern can be observed either during water stress (Hodaei et al., 2018), salt or UV stresses (Markham et al., 1998; Tattini et al., 2000; Ryan et al., 2002; Agati et al., 2007). Mutation of a *MYB* TF and chalcone synthase/isomerase genes in *A. thaliana* revealed the essential role of this family of compounds in conferring a freezing tolerance (Schulz et al., 2016).

1.4.4. Role in plant-pathogenic fungi interactions

Plant defence can be mediated by the action of flavonoids acting indirectly as signalling molecules, or directly through the toxic effect of phytoanticipins (constitutively accumulated active compounds in plant tissues) and phytoalexins (newly synthesised active compounds following pathogen detection) (Naoumkina et al., 2010; Jeandet et al., 2014; Oros and Kállai, 2019). This has been described in the literature from two points of view. On the one hand, research focusing on basal defence addressed the different types of constitutive defence mechanisms, from physical to chemical barriers. Cell wall reinforcement involving flavonoid derivatives is one of them (Tan et al., 2016). On the other hand, research focusing on induced resistance investigated the potential toxicity of these metabolites that may suppress diseases or interfere with the pathogenicity of invaders. Although the study of this direct effect played by bioactive compounds against pathogens has been promoted by a rising interest in deciphering the molecular dialogue between the host and the pathogen, these mechanisms are still to be extensively addressed in plant science. The mechanistic studies published so far followed an overall trend emphasising a quantitative aspect and/or a spatio-temporal dimension of phenolic derivative accumulation in plant tissues associated with resistance to fungi.

The quantitative aspects can be illustrated by a case study on carrot (*Daucus carota* L.) leaves. Genotypes more resistant to *A. dauci* contained significantly higher levels of 4'-O- and 7-O-glycosides of apigenin, luteolin and chrysoeriol, compared to susceptible genotypes (Koutouan et al., 2018). Other studies have shown that the same compound can exert opposite actions between two different pathogens (Kröner et al., 2012). As an example, accumulation of rutin and nicotiflorin in potato tubers was positively correlated with resistance to *Pectobacterium atrosepticum*, whereas it was associated with their susceptibility to *Phytophthora infestans* (Kröner et al., 2012).

Flavonoids, as defence-related compounds against fungal pathogens, can accumulate at the infection site with the aim of containing the pathogen. The formation of tyloses has been observed in vascular diseases of plants, where a toxic environment is created around the site of infection to prevent a systemic spread of the pathogen (Mace et al., 1978; Del Rio et al., 2001).

The temporality of flavonoid-mediated resistance to fungi can be delineated with an early or constitutive availability of the compound of interest in the tissues, leading to an efficient defence response (Melake-Berhan et al., 1996; Bollina et al., 2010; Ardila et al., 2013; Wang et al., 2016). Moreover, plant resistance to fungal diseases is more complex than a simple quantitative differential between resistant and susceptible genotypes at the time of infection. The sustainability of this resistance also depends on the stability of metabolite contents in the tissues over time (Melake-Berhan et al., 1996). Thus, according to the development cycles of the disease and those of the plant, an efficient metabolic ratio must be maintained.

Regarding the biological activity of flavonoids, most papers report direct antifungal properties, by inhibiting fungal growth (Wang et al., 2010; Song et al., 2011; S., Xu et al., 2014). Others demonstrated their role in inhibiting mycotoxin biosynthesis in the pathogen (Bilska et al., 2018; Castano-Duque et al., 2021; Tian et al., 2023). However, the mechanistic is seldom detailed in plant-pathogen interactions. Observations in the field of medical microbiology have brought additional descriptions, that are potentially worth considering in studying plant fungal pathogens. Apigenin, for example, has been shown to cause leakage of the intracellular calcium and potassium to *C. albicans*, resulting in osmotic imbalance (Lee et al., 2018). The capacity of some compounds to cross cell boundaries suggests that they might reach and interfere with nuclear components. Despite the lack of clear evidence of a nucleic acid - flavonoid interaction, apoptosis-associated DNA fragmentation and chromatin condensation was observed in *Candida glabrata* following a treatment with glabridin (Moazeni et al., 2017).

OBJECTIVES AND STRATEGIES OF THE THESIS

We have seen that the leaf blight can be a very serious disease in carrot crops around the world. It leads growers to use synthetic pesticides to secure their harvest. One of the most promising alternatives for protecting crops from *Alternaria dauci*, the causal agent of the disease, is the use of resistant varieties. Genotypes with good resistance to this disease exist, although no major genes have been discovered. To date, marketed varieties do not have sufficient resistance to avoid fungicide treatments, therefore introgression of resistance factors discovered in non-commercial genetic resources into modern cultivars would be particularly relevant. However, more in-depth knowledge of the mechanisms involved in these resistances is essential. Resistance markers enabling breeders to guide their crosses or check the level of resistance of their different breeding lines could be of great interest. Resistance-related quantitative trait loci (rQTL) have already been mapped on the carrot genome and evidence for metabolite-mediated resistance has been confirmed. Through the exploration of the carrot leaf metabolome and transcriptome, and based on the co-localisation between metabolite QTL (mQTL) and rQTL, three specific flavonoids were selected along with two genes that were up-regulated in the resistant genotype compared to a susceptible one and co-localised with the major rQTL. These candidates were identified as apigenin-7-O-rutinoside, luteolin-7-O-rutinoside and chrysoeriol-7-O-rutinoside, belonging to the flavone sub-family. The candidate genetic determinants of their accumulation in the leaves were annotated as a *basic helix loop helix 118-like* gene, and an *anthocyanidin-3-O-UDP-glucosyltransferase 2* gene. As summarised in a review published in 2022, flavonoids are specialised metabolites frequently reported to be involved in plant defence against biotic or abiotic stresses. Their biosynthetic accumulation can be constitutive and/or induced in response to external stimuli. They may participate in plant signalling that drives plant defence responses, act as a physical or chemical barrier to prevent invasion, or as a direct toxic weapon against microbial or insect targets. We also pointed out that for their action to be effective, it is essential to maintain a high level of these metabolites throughout the infective process.

The present study therefore proposes to test whether flavonoids can be involved in the resistance of carrot to *Alternaria dauci*. It also aims to evaluate their persistence during critical periods of disease incidence. Their mode of action is unravelled, and the genetic control of their accumulation is explored. To this end, the flavonoid content of a large number of accessions will be analysed over a long period of their vegetative development. After purification of the candidate molecules, their biological activity on the pathogen will be evaluated, and finally, the characterisation of the function of the candidate genes has been initiated by the obtention of transformants overexpressing the genes putatively involved in their biosynthesis.

From here, the results of the investigation are proposed as follows: Chapter II addresses the evidence supporting the relationship between flavonoid accumulation and resistance to *A. dauci*, as regards the first research question as edited in general introduction; Chapter III provides details on the biological activity of the candidate compounds and the methods developed for this purpose, in response to the second research question; Chapter IV highlights the

functional validation of two candidate genes putatively involved in the biosynthesis of the three flavonoids, as regards the third and fourth research questions. It is important to note that the details of the methods used in each chapter are presented in Chapter V.

CHAPTER II: ACCUMULATION PATTERN OF THE THREE CANDIDATE FLAVONOIDS IN CARROT LEAVES AT DIFFERENT PHENOLOGICAL STAGES AND THEIR CONSISTENCY ACROSS DIVERSE GENETIC BACKGROUNDS

The differential accumulation of these candidate metabolites in the leaves of susceptible (H1) and partially resistant (I2) accessions was previously observed at approximately (6-8)-leaf stage (Koutouan et al., 2018). However, it is known that the flavonoid content of leaves can change both quantitatively (Ancuceanu et al., 2017; Ryu et al., 2017; Petropoulos et al., 2018) as well as qualitatively (Omezzine et al., 2014) during the growth stages of the plant. This was also the case in carrot leaves with respect to glycosidic derivatives of luteolin, which fluctuated on the carrot leaf surface, especially during a phenological shift (Brooks and Feeny, 2004). In addition, the growing environment also influences the flavone content in the leaves, in interaction with the growth stage, as reported for *Mentha x piperita* (Ancuceanu et al., 2017). Koutouan and colleagues have already observed an environmental effect on the flavonoid content of carrot leaves over years of field experiments, but with a negligible ‘genotype x environment’ interaction. This variation in the leaf phytochemical composition is likely to affect the rate of fungal inhibition, as highlighted when target fungal pathogens were confronted with leaf extracts from different developmental stages of *Trigonella foenum-graecum*, *in vitro* (Omezzine et al., 2014). Such variations in flavonoid accumulation may also affect insect behaviour towards plants, as demonstrated by the differential accumulation of a luteolin derivative in or on the leaf surface, which may have conditioned the oviposition preference of the black swallowtail butterfly (*Papilio polyxenes*) on wild carrot leaves (Brooks and Feeny, 2004). Among other things, these case studies encouraged the consideration of the developmental stage as a primary factor in studying the stability of flavonoid accumulation as a resistance marker, and more importantly, to identify the optimal growth stage for any type of biological investigation. This approach will also provide an insight into the accumulation pattern that may differentiate susceptible from more resistant genotypes, as it has been shown in other pathosystems. *In extenso*, in addition to the abundance of defence-related compounds, the resistance status may lie in the maintained availability of a high metabolic content throughout a disease-prone season (Melake-Berhan et al., 1996).

To address these issues, the present chapter, therefore, seeks to provide a more dynamic view of the metabolic contrast between carrot accessions, by including a wide range of sampling times scattered along the vegetative growth of carrot. Furthermore, the evaluation of this trait in other accessions has been of interest in this study, in order to demonstrate the stability of the flavonoid-disease resistance relationship in carrots with potentially different genetic backgrounds. In other words, this chapter attempts to answer the following questions: i) What is the earliest stage of carrot development where a metabolic contrast between susceptible and partially resistant accessions is observed? ii) Could an early high metabolic accumulation be maintained along the vegetative growth? iii) Does the relationship

between the metabolite content and the disease resistance level depend on the genetic background of the carrot accessions?

To this end, data on leaf metabolite composition were acquired from two separate field trials including the same accessions as in previous studies: H1 and I2 (Koutouan et al., 2018), supplemented with eight carrot accessions from the seed industry and from carrot germplasm collection of the QuaRVeg team. A pathological assessment has also been undertaken on these accessions, to assess whether the correspondence between disease resistance level and flavonoid content is still true in other flavonoid - accumulating accessions.

2.1 Quantitative differentials between H1 and I2 along the vegetative growth

A two-way analysis of variance with a two-factor interaction model was applied after checking all the prerequisites: independence between observations, residual normal distribution and variance homogeneity. Residual normality and homogeneity of the variance were not respected, when working on the corrected raw data; therefore, a Box-Cox transformation was applied to recover these proprieties and allow the use of the intended ANOVA model. The result showed that there was no significant interaction between the two factors *i.e.*, developmental stages and accessions, regarding the accumulation of Api7R and Lut7R, but not Chry7R (**Figure 8**). Put simply, regardless of the quantitative aspects, the accumulation pattern of Api7R and Lut7R in the leaves evolved in a similar way in both susceptible and partially resistant accessions (H1 and I2, respectively) along the developmental stage of the plant. On the contrary, the accumulation kinetics of Chry7R along the developmental stage were highly accession-dependent. The quantitative difference between H1 and I2 was observable and statistically significant from the earliest developmental stage (2-leaf stage) and was maintained until the latest (12-leaf stage) for all three candidate metabolites (**Figure 9**). The level of Api7R in I2 was much higher than in H1 at all time-points and showed a gradual increase from the 4-leaf stage onwards. Meanwhile, it increased slightly in H1 at 4-leaf stage, but rapidly stabilised once 5-leaf stage was reached. The Lut7R content did not vary along the developmental stage in both accessions, although there was a marked difference between them. Finally, the level of Chry7R in I2 was relatively high and remained unchanged at all developmental stages, whereas it gradually increased in H1 following a relatively linear progression.

Anova Table (Type III tests)

Response: Api7R_bc

	Sum Sq	Df	F value	Pr(>F)
(Intercept)	2232.24	1	9.5059e+05	< 2.2e-16 ***
Accessions	0.70	1	2.9862e+02	< 2.2e-16 ***
Developmental_Stage	0.19	6	1.3367e+01	2.078e-08 ***
Accessions:Developmental_Stage	0.02	6	1.1831e+00	0.3338
Residuals	0.10	42		

signif. codes: 0 '***' 0.001 '**' 0.01 '*' 0.05 '.' 0.1 ' ' 1

Anova Table (Type III tests)

Response: Lut7R_bc

	Sum Sq	Df	F value	Pr(>F)
(Intercept)	1362.57	1	7.1203e+06	< 2e-16 ***
Accessions	0.12	1	6.5283e+02	< 2e-16 ***
Developmental_Stage	0.00	6	1.9418e+00	0.09625 .
Accessions:Developmental_Stage	0.00	6	1.0190e+00	0.42630
Residuals	0.01	42		

signif. codes: 0 '***' 0.001 '**' 0.01 '*' 0.05 '.' 0.1 ' ' 1

Anova Table (Type III tests)

Response: Chry7R_bc

	Sum Sq	Df	F value	Pr(>F)
(Intercept)	676.84	1	7.5608e+07	< 2.2e-16 ***
Accessions	0.02	1	1.8716e+03	< 2.2e-16 ***
Developmental_Stage	0.00	6	9.7084e+00	1.06e-06 ***
Accessions:Developmental_Stage	0.00	6	3.6902e+00	0.00492 **
Residuals	0.00	42		

signif. codes: 0 '***' 0.001 '**' 0.01 '*' 0.05 '.' 0.1 ' ' 1

Figure 8: Outputs of two-way ANOVA with interaction for each candidate metabolite content Api7R, Lut7R and Chry7R along 7 developmental stages of two carrot genotypes. A Box-Cox correction was applied to raw data (_bc).

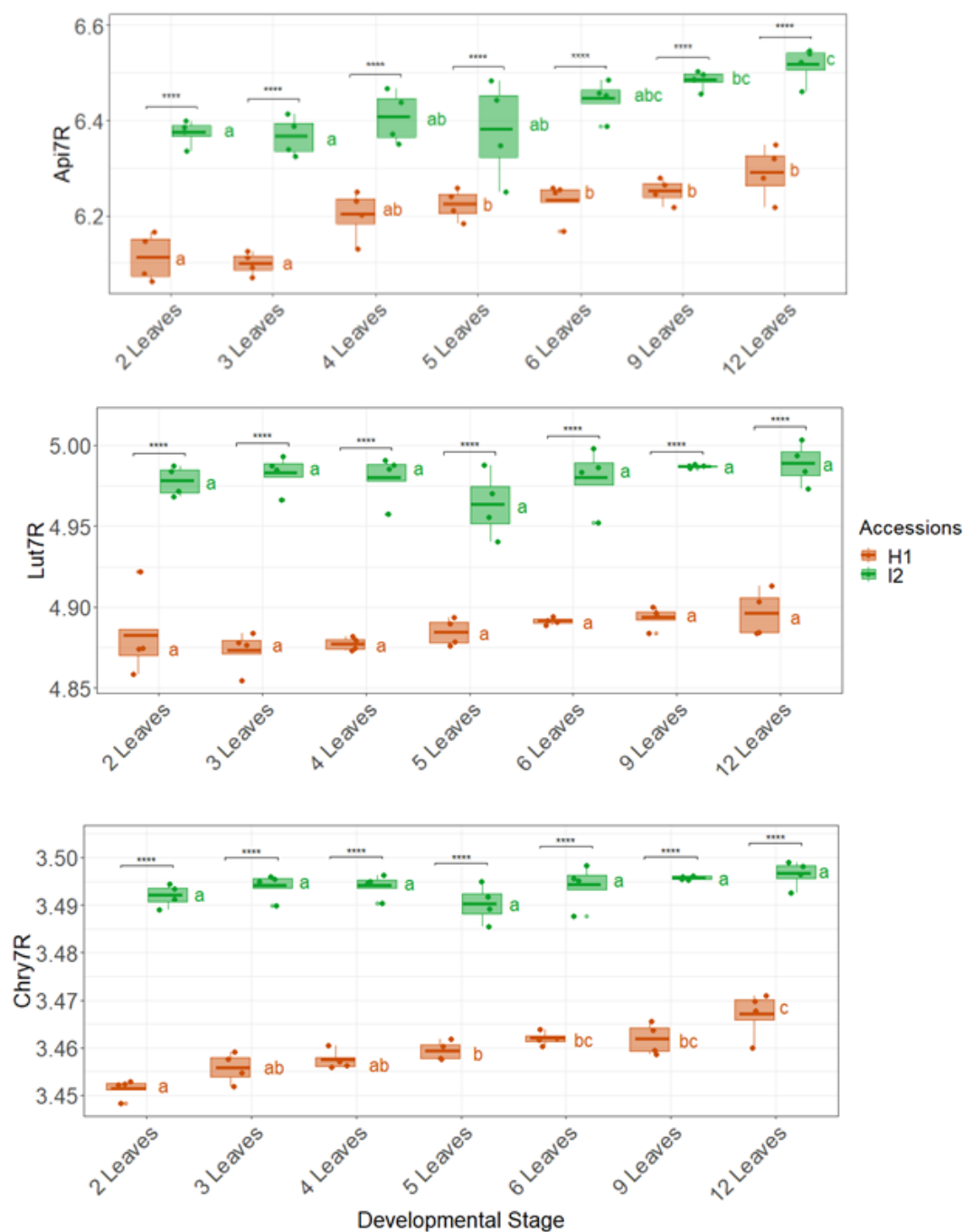


Figure 9: Accumulation kinetics of the three flavones in the leaves of H1 in red (Susceptible carrot genotype) and I2 in green (partially resistant one) along the vegetative growth.

Y axes are values of metabolite peak area from LC-DAD (280 nm), after a Box-Cox transformation. Letters near the boxes refer to group differentiation from Tukey's test, comparing the metabolite content of different developmental stages of the same accession. Significance symbols indicate statistical significance levels of metabolite content contrasting the two accessions at each developmental stage: $p < 0.0001$ '****', $p < 0.001$ '***', $p < 0.01$ '**', $p < 0.05$ '*', $p < 0.1$ '·'.

To provide a practical understanding of these differences in flavonoid quantity, the average flavonoid content in each accession, relative to the weight of dry carrot leaves, was estimated (**Table 1**). Irrespective of the developmental stage and the compound, it could be assumed overall that the average content was approximately 30-200 µg/g dry weight and 300-2000 µg/g dry weight in H1 and I2 respectively. In simple terms, 10 times more of the three candidates would be present in the leaves of I2 than in those of H1. This assumption was valid for most of the developmental stages, except for the 2- and 5-leaf stages with regard to the content of Lut7R, where the ratio would be lower (**Table 1**).

Table 1: Candidate flavonoid content at each developmental stage in carrot genotypes H1 and I2.

Quantification was based on the LC-DAD response of 1mg/mL of Apigenin-7-O-Glucoside. DW: dry weight. Values delineate the mean of four biological replications ± standard deviation.

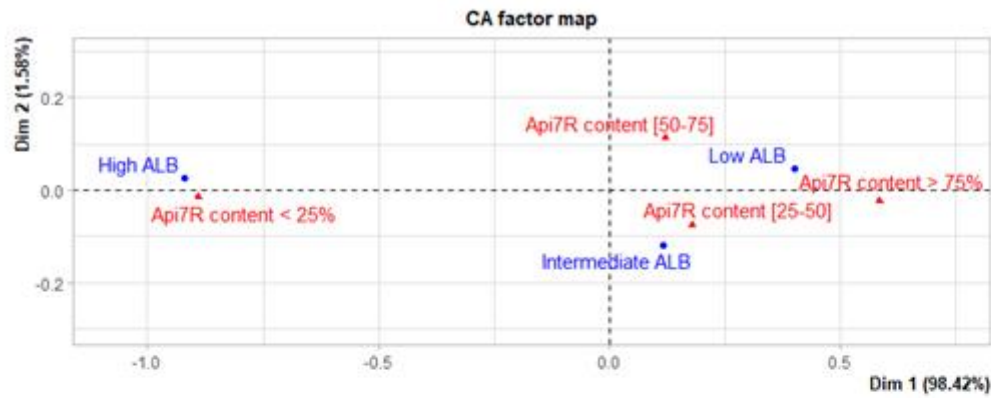
Leaf stages	Accessions	Api7R (µg/g DW)	Lut7R (µg/g DW)	Chry7R (µg/g DW)
2 Leaves	H1	43.88 ± 15.31	110.99 ± 63.68	31.91 ± 3.27
	I2	296.58 ± 95.07	588.93 ± 137.37	446.59 ± 102.01
3 Leaves	H1	33.09 ± 3.53	73.77 ± 9.99	34.47 ± 4.48
	I2	281.82 ± 118.25	688.53 ± 194.47	579.43 ± 187.28
4 Leaves	H1	74.48 ± 25.67	78.32 ± 7.35	37.26 ± 3.39
	I2	456.42 ± 229.1	687.22 ± 231.63	601.44 ± 170.75
5 Leaves	H1	84.32 ± 22.16	88.32 ± 11.16	40.89 ± 2.76
	I2	411.2 ± 311.89	431.18 ± 181.46	377.43 ± 126.93
6 Leaves	H1	87.33 ± 26.4	94.43 ± 8.96	44.88 ± 5.32
	I2	627.9 ± 278.22	672.65 ± 302.47	625.7 ± 284.26
9 Leaves	H1	108.61 ± 20.38	107.66 ± 10.93	49.02 ± 5.23
	I2	981.29 ± 198.15	786.13 ± 37.67	718.43 ± 37.87
12 Leaves	H1	155.86 ± 59.39	111.72 ± 22.47	66.21 ± 12.46
	I2	1433.77 ± 622.37	818.5 ± 335.43	791.91 ± 277.46

2.2 Correspondence between disease expression level and metabolite enrichment in eight accessions

A second experimental design focused on eight accessions with arbitrarily three levels of resistance to ALB and four levels of metabolite enrichment (based on quartile distribution) recorded at the 10-leaf stage. A correspondence analysis (CA) was performed after validating the dependence between these data by a Pearson's Chi-squared test of independence. Regarding the first dimension on the CA factor map (**Figure 10**), the enrichment in Api7R had a

reverse distribution to that of the disease score levels, such that a very low Api7R content ($< 25\%$, *i.e.*, first quartile) was positively associated with a relatively high disease expression, whereas a the highest Api7R content ($> 75\%$, *i.e.*, fourth quartile) was associated with low ALB expression. Regarding the intermediate cases, the description of the second dimension allowed to note that an Api7R content ranging within the third quartile ([50-75]) was associated with an intermediate ALB score (**Figure 10**). A similar trend was observed for Lut7R and its relationship with disease severity (**Figure 11**). That is, a relatively high ALB score was positively associated with a relatively low Lut7R level ($< 25\%$), whereas a Lut7R level within the last two quartiles ($> 50\%$), was positively associated with a low ALB score. Intermediate disease severity was associated with a Lut7R content between the second and third quartiles ([25-50]), as regards the second dimension of the factor map and the corresponding output data. However, the results seemed to indicate that a Lut7R content within the second quartile corresponded most closely to this level of disease score. For Chry7R, a content bellow the median (*i.e.*, $< 50\%$) was shown to cluster with a high ALB score, although to a greater extent for a content ranging within the first quartile ($< 25\%$) (**Figure 12**). In line with previous comments on Api7R and Lut7R, a Chry7R content above the median ($> 50\%$) was also associated with a low ALB symptom, with a stronger emphasis on the highest content ($> 75\%$). However, a content between [50-75] mostly corresponded to an intermediate level of ALB score according to the label distribution along the second dimension of the factor map.

Overall, this descriptive approach highlighted the pattern that accessions with the lowest metabolite content tended to develop the most ALB disease, as opposed to those that were relatively more enriched in each of the candidate compounds. A more analytical approach was then required to provide a detailed confirmation for each accession in the set.



The chi square of independence between the two variables is equal to 28.83333 (p-value = 6.541775e-05).

Eigenvalues

	Dim.1	Dim.2
Variance	0.296	0.005
% of var.	98.425	1.575
Cumulative % of var.	98.425	100.000

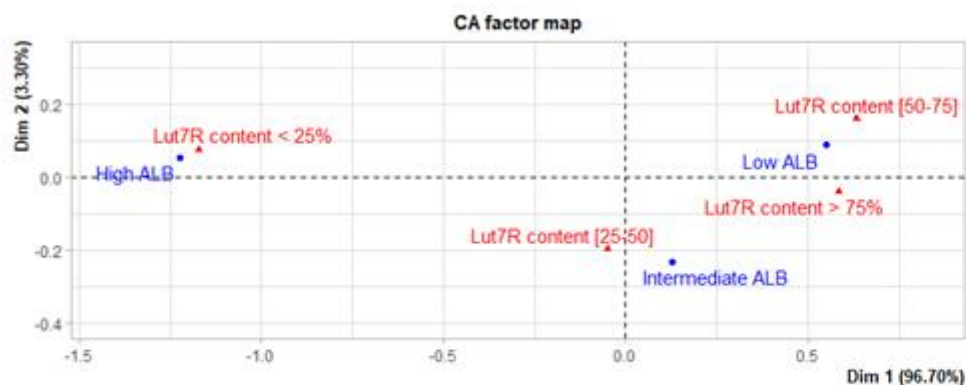
Rows

	Iner*1000	Dim.1	ctr	cos2	Dim.2	ctr	cos2
Low ALB	81.597	0.401	27.238	0.987	0.046	22.762	0.013
Intermediate ALB	6.944	0.117	1.168	0.497	-0.118	73.832	0.503
High ALB	211.806	-0.920	71.594	0.999	0.025	3.406	0.001

Columns

	Iner*1000	Dim.1	ctr	cos2	Dim.2	ctr	cos2
Api7R content < 25%	197.917	-0.890	66.932	1.000	-0.015	1.172	0.000
Api7R content [25-50]	9.549	0.181	2.764	0.856	-0.074	29.133	0.144
Api7R content [50-75]	6.944	0.123	1.280	0.545	0.112	66.824	0.455
Api7R content > 75%	85.938	0.586	29.025	0.998	-0.023	2.872	0.002

Figure 10: Factor map and output table of the correspondence analysis (CA) relating four classes of the Api7R content in red (four quartiles) and 3 levels of disease score in blue (low, intermediate and high ALB).



The chi square of independence between the two variables is equal to 52.5 (p-value = 1.479304e-09).

Eigenvalues

	Dim.1	Dim.2
Variance	0.529	0.018
% of var.	96.698	3.302
Cumulative % of var.	96.698	100.000

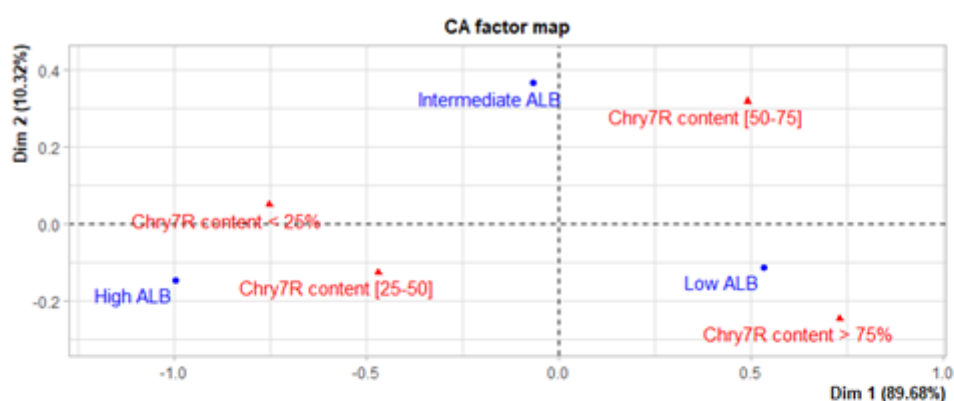
Rows

	Iner*1000	Dim.1	ctr	cos2	Dim.2	ctr	cos2
Low ALB	154.514	0.549	28.484	0.975	0.088	21.516	0.025
Intermediate ALB	17.361	0.126	0.748	0.228	-0.232	74.252	0.772
High ALB	375.000	-1.223	70.768	0.998	0.055	4.232	0.002

Columns

	Iner*1000	Dim.1	ctr	cos2	Dim.2	ctr	cos2
Lut7R content < 25%	343.750	-1.170	64.730	0.996	0.076	7.997	0.004
Lut7R content [25-50]	10.417	-0.048	0.111	0.056	-0.198	54.434	0.944
Lut7R content [50-75]	106.771	0.634	18.976	0.940	0.160	35.570	0.060
Lut7R content > 75%	85.938	0.585	16.183	0.996	-0.038	1.999	0.004

Figure 11: Factor map and output table of the correspondence analysis (CA) relating four classes of the Lut7R content in red (four quartiles) and 3 levels of disease score in blue (low, intermediate and high ALB).



The chi square of independence between the two variables is equal to 41.83333 (p-value = 1.983487e-07).

Eigenvalues

	Dim.1	Dim.2
Variance	0.391	0.045
% of var.	89.677	10.323
Cumulative % of var.	89.677	100.000

Rows

	Iner*1000	Dim.1	ctr	cos2	Dim.2	ctr	cos2
Low ALB	147.569	0.532	36.171	0.958	-0.112	13.829	0.042
Intermediate ALB	34.722	-0.067	0.285	0.032	0.367	74.715	0.968
High ALB	253.472	-0.997	63.544	0.980	-0.144	11.456	0.020

Columns

	Iner*1000	Dim.1	ctr	cos2	Dim.2	ctr	cos2
Chry7R content < 25%	142.361	-0.753	36.271	0.996	0.050	1.384	0.004
Chry7R content [25-50]	59.028	-0.469	14.099	0.933	-0.125	8.741	0.067
Chry7R content [50-75]	85.938	0.492	15.457	0.703	0.320	56.765	0.297
Chry7R content > 75%	148.438	0.731	34.173	0.900	-0.244	33.110	0.100

Figure 12: Factor map and output table of the correspondence analysis (CA) relating four classes of the Chry7R content in red (four quartiles) and 3 levels of disease score in blue (low, intermediate and high ALB).

2.3 Contrast between accessions: ALB symptoms

On the one hand, H1 and Presto could be considered as the most susceptible accessions of the set. Presto seemed to have a higher score than H1, although there was no significant difference between them (**Figure 13**). In addition, H1 shared a group letter with less blighted accessions, which were thought to belong to the intermediate group consisting of Valor and B18. This intermediate group, in turn, was not significantly different from the least affected accessions: A92, I2, Boléro and Brillyance. From these observations, the difference between less blighted accessions could not be statistically well resolved, although a visual classification could have been powerful enough to make a discrimination in the field. Thus, from the statistical point of view, the main information obtained therefrom is that two rough groups could be drawn: highly susceptible and partially resistant accessions.

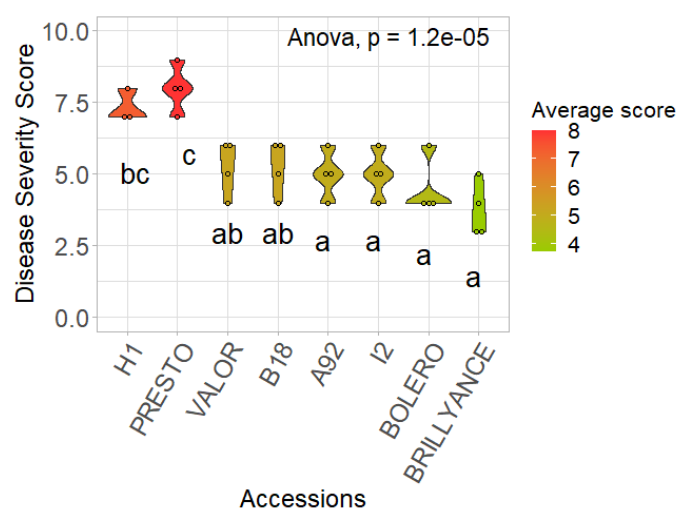


Figure 13: Disease symptom assessment on eight carrot accessions.

Dots indicate biological replications distributed in field blocks. Colour scale of the violins corresponds to the average disease score of 3-4 replications. Letters indicate group differences from Tukey's test (error threshold 0.05).

2.4 Contrast between accessions: candidate metabolite content

The difference in metabolite enrichment between accessions was analysed by ANOVA, using a two-factor interaction model described in CHAPTER V-5.1.4. All the necessary conditions for performing an ANOVA were validated after applying a Box-Cox transformation to the data. The results showed that the accumulation of all three candidate compounds followed the same pattern in all accessions along the three developmental stages, regardless of their respective levels of metabolic enrichment. In other words, there was no significant interaction between the effects of the two factors: developmental stage and accessions on metabolite accumulation (**Figure 14**). Furthermore, the results indicated that no significant difference could be made in the metabolite content at the three developmental stages in relation to each accession independently ($p > 0.05$) (**Appendix - Figure 1**, **Appendix - Figure 2**, **Appendix - Figure 3**). However, the accessions could be discriminated at each developmental stage based on the content of each candidate metabolite ($p < 0.05$) (**Figure 14**).

```

Anova Table (Type III tests)

Response: Api7R_bc

```

	Sum Sq	Df	F value	Pr(>F)
(Intercept)	11907.8	1	65455.9163	< 2.2e-16 ***
Accessions	13.3	7	10.4716	5.357e-09 ***
Developmental_Stage	0.9	2	2.5452	0.0855 .
Accessions:Developmental_Stage	0.4	14	0.1730	0.9996
Residuals	13.1	72		

```

---
Signif. codes:  0 '***' 0.001 '**' 0.01 '*' 0.05 '.' 0.1 ' ' 1

```



```

Anova Table (Type III tests)

Response: Lut7R_bc

```

	Sum Sq	Df	F value	Pr(>F)
(Intercept)	1465.02	1	2.7476e+07	<2e-16 ***
Accessions	0.03	7	7.3547e+01	<2e-16 ***
Developmental_Stage	0.00	2	1.5664e+00	0.2158
Accessions:Developmental_Stage	0.00	14	5.1730e-01	0.9154
Residuals	0.00	72		

```

---
Signif. codes:  0 '***' 0.001 '**' 0.01 '*' 0.05 '.' 0.1 ' ' 1

```



```

Anova Table (Type III tests)

Response: Chry7R_bc

```

	Sum Sq	Df	F value	Pr(>F)
(Intercept)	14222.6	1	82132.5272	< 2e-16 ***
Accessions	63.8	7	52.6597	< 2e-16 ***
Developmental_Stage	1.0	2	2.8100	0.06682 .
Accessions:Developmental_Stage	0.7	14	0.3086	0.99126
Residuals	12.5	72		

```

---
Signif. codes:  0 '***' 0.001 '**' 0.01 '*' 0.05 '.' 0.1 ' ' 1

```

Figure 14: Two-factor interaction ANOVA outputs for candidate metabolite content of eight carrot accessions, significance threshold at 0.05.

2.4.1. Group difference at the 10-leaf stage

This developmental stage was the latest at which the candidate metabolites were quantified prior to the disease occurrence in the field. It was therefore considered to be the most relevant time-point to address the correspondence between the resistance level of the accessions and their respective metabolite levels. A Tukey's *post hoc* (**Appendix - Figure 4**) test pointed out that H1 and Presto were not significantly different in their overall content of Api7R, Lut7R and Chry7R, being the least enriched of the set (**Figure 15, Figure 16, Figure 17**). I2 was also significantly different

from these accessions for the three compounds, following the trend contrasting less diseased and more diseased accessions in the correspondence analysis (**Figure 10, Figure 11, Figure 12**). For the other accessions, the content of Api7R did not allow a clear distinction to be made between the least and most enriched groups (**Appendix - Figure 4**). A look at the Lut7R content allowed to observe clearer separation of the groups: Valor belonged to the group least enriched in Lut7R, together with H1 and Presto; A92, B18 and I2 were among the most enriched; in between, there was Brillyance, which did not show any significant difference from the low enriched accessions; finally, Boléro also did not differ from Brillyance, but tended to join the higher content group (**Appendix - Figure 4**). A similar observation could be made for the Chry7R content, except that B18 shared the same trend as Boléro (**Appendix - Figure 4**).

In all, the metabolite contents and disease scores of the accessions varied indeed in opposite directions. The correspondence between low disease scores and high metabolite contents was confidently confirmed for I2 for all three compounds, but only for Lut7R and Chry7R contents for Boléro, B18 and A92. The opposite way was also true for H1 and Presto. However, the case of Valor and Brillyance however could be discussed hereafter.

2.4.2. Group difference at the 6-leaf stage

Group comparisons at this stage aimed at this stage to see if a better resolution could be observed than at the 10-leaf stage. The Api7R content still did not allow a good discrimination of the accessions in terms of their respective ALB scores (**Figure 15**). Similar to the distribution at 10-leaf stage, only I2 was significantly different from H1 and Presto (**Appendix - Figure 5**). With regard to the Lut7R content, no significant differences were found between Presto, H1 and Valor (**Figure 16**). The latter two were also not found to differ from Brillyance either. However, they were all statistically separated from Boléro, I2, A92 and B18 (**Appendix - Figure 5**). Finally, two groups could be drawn on the basis of the Chry7R content: the least enriched (Presto, Valor, H1 and Brillyance) and the most enriched (Boléro, B18, A92 and I2) (**Figure 17, Appendix - Figure 5**).

As for the analysis above, only Lut7R and Chry7R highlighted more the separation of partially resistant from susceptible accessions, yet not valid for Valor and Brillyance.

2.4.3. Group difference at the 2-leaf stage

A significant difference between H1 and I2 was observed for the three candidate compounds. Additional differences from I2 could be outlined with Presto and Valor for their Api7R content. Otherwise, all the other accessions were not significantly different from I2 or H1 (**Figure 15, Appendix - Figure 6**). In agreement with the observations at the 10-leaf and 6-leaf stages, the content of Lut7R and Chry7R was more discriminating for all accessions, except for Valor and Brillyance (**Figure 16, Figure 17 and Appendix - Figure 6**).

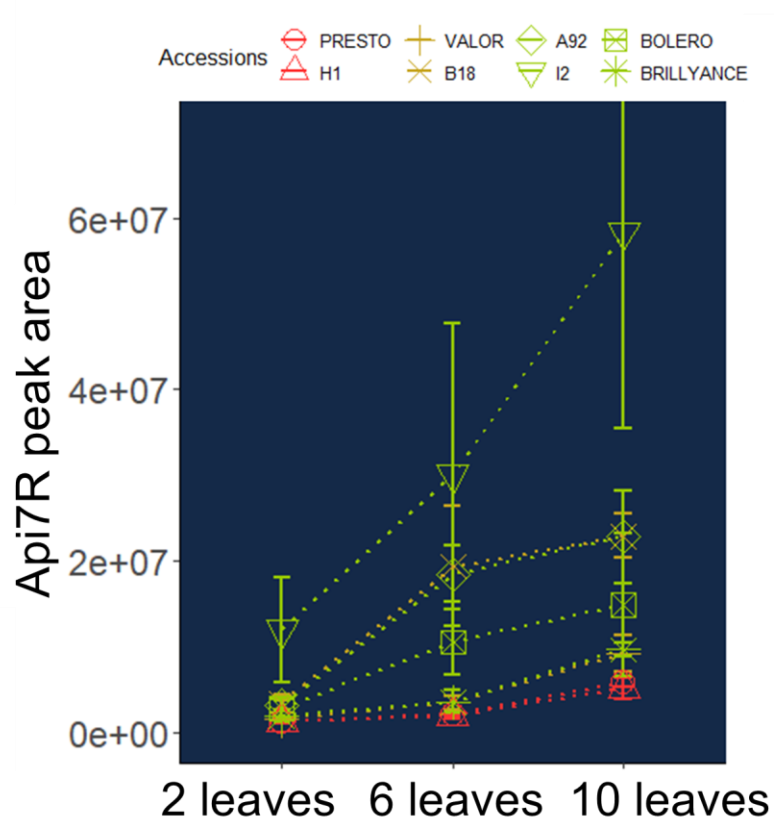


Figure 15: Accumulation of Api7R in the leaves of eight carrot accessions at three developmental stages.

Y axes are values of metabolite peak area from LC-DAD (280 nm). Statistics from group comparisons at each developmental stage are detailed in Appendix -Figure 4, 5 and 6. Colours of the lines refer to the ALB resistance : susceptible (red), intermediate (yellow) and partially resistant (green).

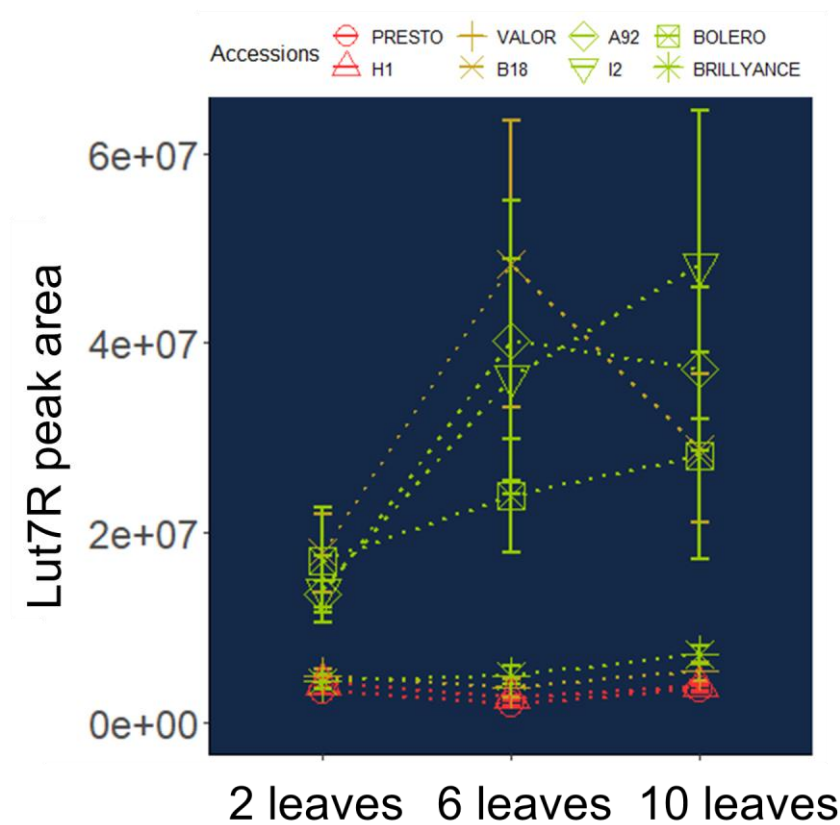


Figure 16: Accumulation of *Lut7R* in the leaves of eight carrot accessions at three developmental stages.

Y axes are values of metabolite peak area from LC-DAD (280 nm). Statistics from group comparisons at each developmental stage are detailed in Appendix -Figure 4, 5 and 6. Colours of the lines refer to the ALB resistance : susceptible (red), intermediate (yellow) and partially resistant (green).

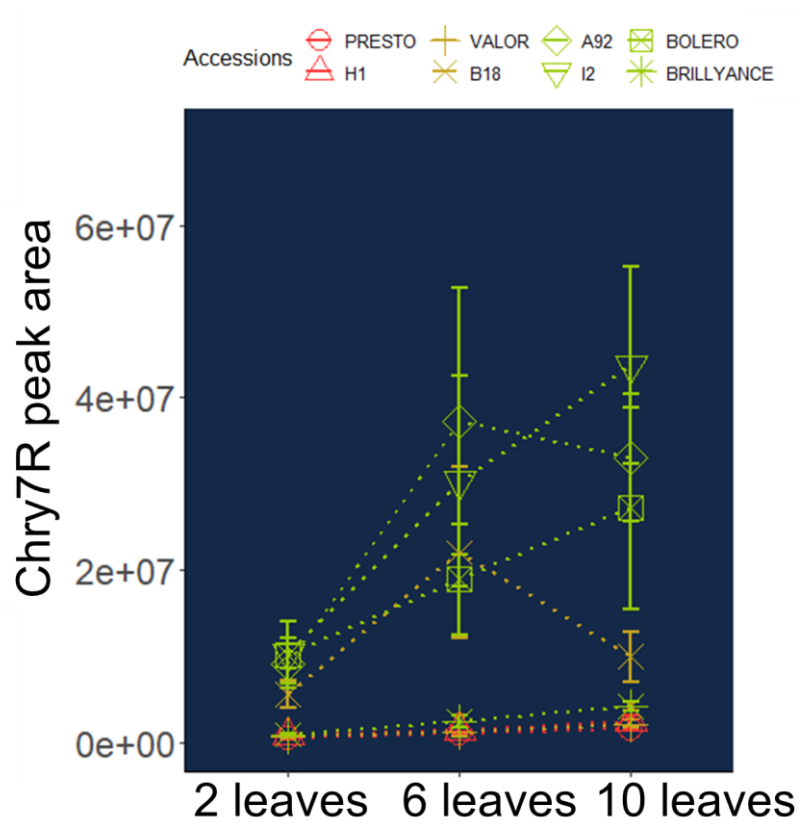


Figure 17: Accumulation of Chry7R in the leaves of eight carrot accessions at three developmental stages.

Y axes are values of metabolite peak area from LC-DAD (280 nm). Statistics from group comparisons at each developmental stage are detailed in Appendix -Figure 4, 5 and 6. Colours of the lines refer to the ALB resistance : susceptible (red), intermediate (yellow) and partially resistant (green).

2.5 Analysis of the correlation between candidate metabolites

A Pearson's correlation analysis showed that the three compounds had a relatively strong linear correlation with each other: $r = 0.76$ (Api7R-Lut7R), $r = 0.84$ (Api7R-Chry7R) and $r = 0.92$ (Lut7R -Chry7R) (**Figure 18**), suggesting a co-accumulation of the candidate compounds in the leaves.

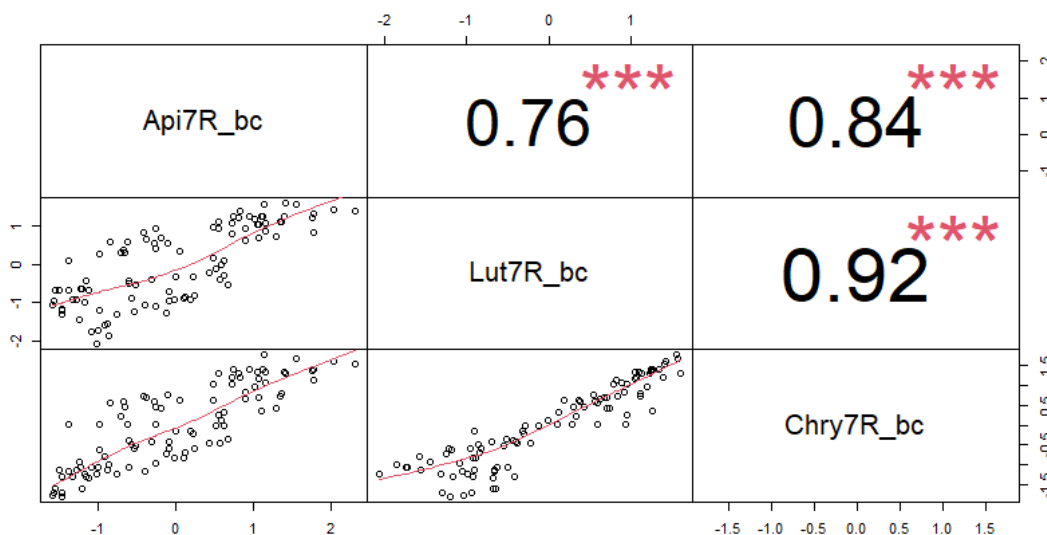


Figure 18: Spearman's correlation analysis relating the content of each candidate compound in the leaves.

Significance symbols: $p < 0.0001$ '****', $p < 0.001$ '***', $p < 0.01$ '**', $p < 0.05$ '*', $p < 0.1$ '·'.

DISCUSSION AND PERSPECTIVES

In previous studies, the quantitative differential in metabolites between two contrasting accessions, in terms of ALB resistance, was stated at approximately the 6-8 leaf stage (Koutouan et al., 2018). Here, the accumulation of the three candidate flavone-rutinosides in the carrot leaves was monitored at different time-points of the carrot vegetative growth. The aim of this evaluation was to observe the extent of their differential accumulation opposing the accessions H1 (susceptible) and I2 (partially resistant). The data collected were essential to determine whether this difference could be observed earlier and/or beyond the previous assessment date. In fact, I2 accumulated the three flavone-rutinosides about 10 times more than H1 at an early stage of development (2-leaf). Their relatively high levels in I2 were stabilised until 12-leaf stage, mainly for Lut7R and Chry7R, as the level of Api7R showed a gradual increase. The amplitude of this quantitative metabolic difference between these accessions is fully consistent with Koutouan's observation at 6-8-leaf stage (Koutouan et al., 2018). Although, the field trials may have exposed the carrot plants to potential biotic inducers of metabolite biosynthesis, in particular *A. dauci*, the findings of the QuaRVeg research team have already confirmed that this pathogen does not induce any change in the content of these

three candidate metabolites in the leaves of H1 and I2 (Ph.D. Koutouan 2019, data under publication process). Other environmental conditions such as sunlight exposure could also be pointed out, as a known enhancer of flavonoid accumulation in plant photosynthetic tissues (Tattini et al., 2000; Agati et al., 2011; Del Valle et al., 2018). Nevertheless, the absence of these data in the present evaluation does not invalidate the observations made, since the results are consistent with others obtained at the same developmental stage in different experimental years and under different conditions. Therefore, a constitutive biosynthesis of a relatively high amount of these three flavonoids in the leaves of I2 could be considered. Moreover, it is not new that constitutive accumulation of flavonoids from different subfamilies is found in target plant tissues, which helped more resistant plant genotypes to defend against pathogens (Ardila et al., 2013). A case study on kaempferol glycosidic derivatives from barley (*Hordeum vulgare*) spikelets contrasting barley genotypes resistant and susceptible to *Fusarium* head blight (FHB) showed comparable fold changes to those observed in the present study (Bollina et al., 2010).

With regard to the link between flavonoids and ALB resistance in carrot, an early and sustained availability in the leaves of I2 over time could be a factor determining the good performance of this accession against the pathogen, converging with the conclusion of an analogous phenomenon observed in sorghum (*Sorghum bicolor* (L) Moench), which similarly accumulates flavonoids in the group of flavanols, to resist against *Alternaria* spp. and *Fusarium* spp. (Melake-Berhan et al., 1996). The constitutive and early accumulation of the three candidate flavonoids in the partially resistant accession could be a key element allowing an early discrimination of carrot genotypes in future breeding programmes. Indeed, a major concern in carrot breeding is the search for a “shortcut” method to reduce the duration of field/greenhouse experiments to sort out genotypes with different levels of resistance. In practice, flavonoid enrichment could be a selectable trait that could be used to evaluate genotypes without going through the tedious and time-consuming disease scoring experiments. This type of approach has already been proposed, for example, for the carnation (*Dianthus caryophyllus* L.)-*Fusarium oxysporum* f. sp. *dianthi* L. pathosystem (Ardila et al., 2013), supported by the results of Galeotti and colleagues, who reported a successful cultivar discrimination by quantification of flavonoid-glycosides (Galeotti et al., 2008). However, to be routinely applicable, these putative markers need to be robust especially in diverse genetic backgrounds. Therefore, the co-occurrence of a higher metabolite accumulation and a better performance against *A. dauci* was investigated in other carrot accessions of different genetic background than that of I2. Disease evaluation of these accessions made it possible to identify which were the susceptible (H1 and Presto) or partially resistant (Valor, B18, A92, I2, Boléro, and Brilliance). These results are consistent with previous statements for H1 and I2, but also for commercial hybrids such as Presto and Boléro (Boedo et al., 2010; Le Clerc et al., 2014; Koutouan et al., 2018). Despite the lack of statistical significance, Valor and B18 could be visually qualified as intermediate resistant, performing not as well as A92 and I2 at one level, and Brilliance and Boléro at another. This would be in line with the previous performances known to experts for these two accessions (CHAPTER V-Table 8). This low discriminatory power is not surprising, since ALB resistance is a quantitative trait and the resistance levels of the accessions could be considered to be too close to each other, to be

efficiently discriminated by the statistical model used. Furthermore, heterogeneity of data within groups is another factor that could limit statistical power, due to the distribution of the biological replicates next to a set of carrot wild relatives in the field. Direct neighbours of each accession in a block are a potential source of heterogeneity in terms of inoculum load or due to the susceptibility / protective effect of the neighbouring plants (Pélissier et al., 2021). Additionally, the level of resistance to *A. dauci* in carrot wild relatives has been shown to be quite variable (Schouten et al., 2002; Nothnagel et al., 2017). The inclusion of a control susceptible accession along the field could have helped to assess the influence of neighbouring plants as well as the homogeneity of infection along the field plot, as already practised in similar field evaluations of disease resistance (Gugino et al., 2007; Le Clerc et al., 2015). A different experimental design with artificial inoculation may also have helped to overcome this issue. It should be noted that the initial objective of this trial was not to assess the level of resistance of the accessions but only to produce samples to assess their candidate metabolite content. Otherwise, for ALB evaluation, a more appropriate test could have been proposed.

Nonetheless, the coherence of the results with existing data allowed to make a bridge with the metabolic phenotype of each accession studied. Indeed, a low metabolite content was associated with a high disease score, while a higher metabolite content was associated with a lower disease score, except for Valor and Brilliance. Apart from these exceptions, zooming on the metabolite content showed that only Lut7R and Chry7R provided a statistical resolution to discriminate the accessions at the three developmental stages, in accordance with their presumed disease resistance level. The implication of this observation is that, on the one hand, other partially resistant accessions than I2 could also be significantly differentiated from H1 at an early, intermediate and late stage of the vegetative growth and, on the other hand, Lut7R and Chry7R would be the most reliable markers during a wide window of phenological stages. From this point of view, it could mean that Api7R is not as important as the other two compounds in mediating ALB resistance. This hypothesis could not be further evaluated by this type of experiment given the positive correlation between the accumulation of the three flavonoids. In other words, accessions that accumulate one of the candidate compounds are likely to accumulate the others as well, adding complexity to the investigation of their separate roles. Obtaining purified candidate compounds could be a way to rigorously assess their respective involvement in *A. dauci* resistance in any form. Furthermore, the present study did not seek to answer the question of the phenotypic gain that could be attributed to the accumulation of one or the other compound, given the diversity of the accessions under consideration. The case of Valor and Brilliance rightly emphasises the need for a different experimental design, based on the introgression of the metabolite accumulation trait in susceptible accessions such as H1 and Presto. The fact that the ALB scores of Valor were not considered to be different from those of the other partially resistant accessions suggests that it may harbour resistance factors other than the accumulation of the candidate flavonoids. This was even more evident in Brilliance, which was visually the most resistant of them all. Without mentioning all known resistance mechanisms, but only in the circle of the specialised metabolites only, terpenes and polyacetylenes are also mediators of ALB resistance in carrots (Lecomte et al., 2012; Koutouan et al., 2018; Koutouan et al., 2023).

Therefore, it could not be excluded that the two partially resistant accessions Valor and Brilliance might have better resisted to *A. dauci* by one of these other mechanisms. First of all, it would be interesting to evaluate their terpene content.

Overall, the co-occurrence of the disease resistance and metabolite accumulation traits in several genetic backgrounds supports the hypothesis of the robustness of the flavonoid-ALB resistance relationship, regardless of the genetic background. This relationship could even be extensively evaluated on a larger set of carrot accessions, to firmly support this statement.

To close this chapter, the accumulation of the candidate flavonoids in the leaves and a better performance against *A. dauci* coincided in several accessions presumably genetically diverse, making these candidate compounds robust resistance markers. The kinetics of their accumulation showed that carrot accessions with contrasted levels of ALB resistance could be efficiently discriminated at the 2-leaf stage based on Lut7R and Chry7R content, making them a potential tool for breeders at a very early stage of plant development. However, additional evidence as mentioned above, will undoubtedly add more elements to the present results, especially in unravelling the involvement of the candidate compounds in the resistance mechanism.

APPENDICES

```
## Accessions = A92:
## Developmental_Stage emmean SE df lower.CL upper.CL .group
## 2 Leaves 11.3 0.213 72 10.9 11.8 a
## 6 Leaves 11.4 0.213 72 11.0 11.9 a
## 10 Leaves 11.5 0.213 72 11.1 11.9 a
##
## Accessions = B18:
## Developmental_Stage emmean SE df lower.CL upper.CL .group
## 2 Leaves 11.2 0.213 72 10.8 11.6 a
## 10 Leaves 11.5 0.213 72 11.1 12.0 a
## 6 Leaves 11.6 0.213 72 11.1 12.0 a
##
## Accessions = BOLERO:
## Developmental_Stage emmean SE df lower.CL upper.CL .group
## 10 Leaves 11.1 0.213 72 10.7 11.5 a
## 2 Leaves 11.1 0.213 72 10.7 11.5 a
## 6 Leaves 11.4 0.213 72 11.0 11.8 a
##
## Accessions = BRILLIANCE:
## Developmental_Stage emmean SE df lower.CL upper.CL .group
## 2 Leaves 10.8 0.213 72 10.4 11.2 a
## 6 Leaves 11.0 0.213 72 10.6 11.4 a
## 10 Leaves 11.1 0.213 72 10.6 11.5 a
##
## Accessions = H1:
## Developmental_Stage emmean SE df lower.CL upper.CL .group
## 2 Leaves 10.6 0.213 72 10.1 11.0 a
## 6 Leaves 10.7 0.213 72 10.2 11.1 a
## 10 Leaves 10.8 0.213 72 10.4 11.2 a
##
## Accessions = I2:
## Developmental_Stage emmean SE df lower.CL upper.CL .group
## 2 Leaves 11.7 0.213 72 11.3 12.1 a
## 6 Leaves 11.8 0.213 72 11.3 12.2 a
## 10 Leaves 12.0 0.213 72 11.5 12.4 a
##
## Accessions = PRESTO:
## Developmental_Stage emmean SE df lower.CL upper.CL .group
## 2 Leaves 10.6 0.213 72 10.2 11.0 a
## 6 Leaves 10.7 0.213 72 10.3 11.1 a
## 10 Leaves 10.8 0.213 72 10.4 11.3 a
##
## Accessions = VALOR:
## Developmental_Stage emmean SE df lower.CL upper.CL .group
## 2 Leaves 10.7 0.213 72 10.3 11.1 a
## 6 Leaves 10.9 0.213 72 10.5 11.3 a
## 10 Leaves 11.1 0.213 72 10.7 11.5 a
##
## Confidence level used: 0.95
## P value adjustment: tukey method for comparing a family of 3 estimates
## significance level used: alpha = 0.05
## NOTE: If two or more means share the same grouping symbol,
## then we cannot show them to be different.
## But we also did not show them to be the same.
```

Appendix - Figure 1: Difference in the level of Api7R at three developmental stages in eight carrot accessions. Tukey's multiple comparison test. Error threshold = 0.05.

```

## Accessions = A92:
## Developmental_Stage emmean      SE df lower.CL upper.CL .group
## 2 Leaves            3.921 0.003651 72   3.914   3.928   a
## 10 Leaves           3.923 0.003651 72   3.915   3.930   a
## 6 Leaves            3.926 0.003651 72   3.919   3.934   a
##
## Accessions = B18:
## Developmental_Stage emmean      SE df lower.CL upper.CL .group
## 2 Leaves            3.921 0.003651 72   3.914   3.929   a
## 10 Leaves           3.923 0.003651 72   3.916   3.930   a
## 6 Leaves            3.929 0.003651 72   3.922   3.936   a
##
## Accessions = BOLERO:
## Developmental_Stage emmean      SE df lower.CL upper.CL .group
## 10 Leaves           3.916 0.003651 72   3.909   3.923   a
## 2 Leaves            3.922 0.003651 72   3.914   3.929   a
## 6 Leaves            3.923 0.003651 72   3.916   3.930   a
##
## Accessions = BRILLIANCE:
## Developmental_Stage emmean      SE df lower.CL upper.CL .group
## 2 Leaves            3.895 0.003651 72   3.887   3.902   a
## 6 Leaves            3.897 0.003651 72   3.890   3.905   a
## 10 Leaves           3.900 0.003651 72   3.893   3.908   a
##
## Accessions = H1:
## Developmental_Stage emmean      SE df lower.CL upper.CL .group
## 2 Leaves            3.883 0.003651 72   3.876   3.891   a
## 6 Leaves            3.888 0.003651 72   3.880   3.895   a
## 10 Leaves           3.888 0.003651 72   3.881   3.896   a
##
## Accessions = I2:
## Developmental_Stage emmean      SE df lower.CL upper.CL .group
## 2 Leaves            3.921 0.003651 72   3.914   3.929   a
## 10 Leaves           3.923 0.003651 72   3.915   3.930   a
## 6 Leaves            3.926 0.003651 72   3.919   3.933   a
##
## Accessions = PRESTO:
## Developmental_Stage emmean      SE df lower.CL upper.CL .group
## 6 Leaves            3.880 0.003651 72   3.873   3.887   a
## 2 Leaves            3.884 0.003651 72   3.877   3.891   a
## 10 Leaves           3.884 0.003651 72   3.877   3.892   a
##
## Accessions = VALOR:
## Developmental_Stage emmean      SE df lower.CL upper.CL .group
## 2 Leaves            3.891 0.003651 72   3.884   3.899   a
## 6 Leaves            3.895 0.003651 72   3.888   3.902   a
## 10 Leaves           3.895 0.003651 72   3.888   3.902   a
##
## Confidence level used: 0.95
## P value adjustment: tukey method for comparing a family of 3 estimates
## significance level used: alpha = 0.05
## NOTE: If two or more means share the same grouping symbol,
##       then we cannot show them to be different.
##       But we also did not show them to be the same.

```

Appendix - Figure 2: Difference in the level of Lut7R at three developmental stages in eight carrot accessions. Tukey's multiple comparison test. Error threshold = 0.05.

```

## Accessions = A92:
## Developmental_Stage emmean    SE df lower.CL upper.CL .group
## 2 Leaves             13.0 0.208 72    12.6    13.4    a
## 10 Leaves            13.1 0.208 72    12.7    13.5    a
## 6 Leaves             13.2 0.208 72    12.8    13.6    a
##
## Accessions = B18:
## Developmental_Stage emmean    SE df lower.CL upper.CL .group
## 2 Leaves             12.4 0.208 72    12.0    12.8    a
## 10 Leaves            12.7 0.208 72    12.3    13.1    a
## 6 Leaves             12.9 0.208 72    12.5    13.3    a
##
## Accessions = BOLERO:
## Developmental_Stage emmean    SE df lower.CL upper.CL .group
## 10 Leaves            12.8 0.208 72    12.4    13.2    a
## 2 Leaves             13.0 0.208 72    12.6    13.4    a
## 6 Leaves             13.0 0.208 72    12.6    13.4    a
##
## Accessions = BRILLYANCE:
## Developmental_Stage emmean    SE df lower.CL upper.CL .group
## 2 Leaves             11.5 0.208 72    11.1    11.9    a
## 6 Leaves             11.7 0.208 72    11.3    12.1    a
## 10 Leaves            11.9 0.208 72    11.5    12.3    a
##
## Accessions = H1:
## Developmental_Stage emmean    SE df lower.CL upper.CL .group
## 2 Leaves             11.2 0.208 72    10.8    11.6    a
## 6 Leaves             11.5 0.208 72    11.1    11.9    a
## 10 Leaves            11.5 0.208 72    11.1    12.0    a
##
## Accessions = I2:
## Developmental_Stage emmean    SE df lower.CL upper.CL .group
## 10 Leaves            13.1 0.208 72    12.7    13.5    a
## 2 Leaves             13.1 0.208 72    12.7    13.5    a
## 6 Leaves             13.2 0.208 72    12.8    13.7    a
##
## Accessions = PRESTO:
## Developmental_Stage emmean    SE df lower.CL upper.CL .group
## 2 Leaves             11.0 0.208 72    10.6    11.4    a
## 6 Leaves             11.1 0.208 72    10.7    11.5    a
## 10 Leaves            11.2 0.208 72    10.8    11.6    a
##
## Accessions = VALOR:
## Developmental_Stage emmean    SE df lower.CL upper.CL .group
## 2 Leaves             11.1 0.208 72    10.7    11.5    a
## 6 Leaves             11.4 0.208 72    11.0    11.8    a
## 10 Leaves            11.4 0.208 72    11.0    11.8    a
##
## Confidence level used: 0.95
## P value adjustment: tukey method for comparing a family of 3 estimates
## significance level used: alpha = 0.05
## NOTE: If two or more means share the same grouping symbol,
##       then we cannot show them to be different.
##       But we also did not show them to be the same.

```

Appendix - Figure 3: Difference in the level of Chry7R at three developmental stages in eight carrot accessions. Tukey's multiple comparison test. Error threshold = 0.05.

Developmental_Stage = 10 Leaves:						(Api7R)
Accessions	emmean	SE	df	lower.CL	upper.CL	.group
H1	10.8	0.213	72	10.4	11.2	a
PRESTO	10.8	0.213	72	10.4	11.3	a
BRILLYANCE	11.1	0.213	72	10.6	11.5	ab
VALOR	11.1	0.213	72	10.7	11.5	ab
BOLERO	11.1	0.213	72	10.7	11.5	ab
A92	11.5	0.213	72	11.1	11.9	ab
B18	11.5	0.213	72	11.1	12.0	ab
I2	12.0	0.213	72	11.5	12.4	b

Developmental_Stage = 10 Leaves:						(Lut7R)
Accessions	emmean	SE	df	lower.CL	upper.CL	.group
PRESTO	3.884	0.003651	72	3.877	3.892	a
H1	3.888	0.003651	72	3.881	3.896	a
VALOR	3.895	0.003651	72	3.888	3.902	a
BRILLYANCE	3.900	0.003651	72	3.893	3.908	ab
BOLERO	3.916	0.003651	72	3.909	3.923	bc
A92	3.923	0.003651	72	3.915	3.930	c
I2	3.923	0.003651	72	3.915	3.930	c
B18	3.923	0.003651	72	3.916	3.930	c

Developmental_Stage = 10 Leaves:						(Chry7R)
Accessions	emmean	SE	df	lower.CL	upper.CL	.group
PRESTO	11.2	0.208	72	10.8	11.6	a
VALOR	11.4	0.208	72	11.0	11.8	a
H1	11.5	0.208	72	11.1	12.0	a
BRILLYANCE	11.9	0.208	72	11.5	12.3	ab
B18	12.7	0.208	72	12.3	13.1	bc
BOLERO	12.8	0.208	72	12.4	13.2	bc
I2	13.1	0.208	72	12.7	13.5	c
A92	13.1	0.208	72	12.7	13.5	c

Appendix - Figure 4 : Tukey's multiple pairwise comparison test based on the content of each metabolite observed at the 10-leaf stage in eight carrot accessions. Accessions sharing the same letters are not significantly different at the error rate of 0.05.

Developmental_Stage = 6 Leaves: (Api7R)						
Accessions	emmean	SE	df	lower.CL	upper.CL	.group
H1	10.7	0.213	72	10.2	11.1	a
PRESTO	10.7	0.213	72	10.3	11.1	a
VALOR	10.9	0.213	72	10.5	11.3	ab
BRILLYANCE	11.0	0.213	72	10.6	11.4	ab
BOLERO	11.4	0.213	72	11.0	11.8	ab
A92	11.4	0.213	72	11.0	11.9	ab
B18	11.6	0.213	72	11.1	12.0	ab
I2	11.8	0.213	72	11.3	12.2	b

Developmental_Stage = 6 Leaves: (Lut7R)						
Accessions	emmean	SE	df	lower.CL	upper.CL	.group
PRESTO	3.880	0.003651	72	3.873	3.887	a
H1	3.888	0.003651	72	3.880	3.895	ab
VALOR	3.895	0.003651	72	3.888	3.902	ab
BRILLYANCE	3.897	0.003651	72	3.890	3.905	b
BOLERO	3.923	0.003651	72	3.916	3.930	c
I2	3.926	0.003651	72	3.919	3.933	c
A92	3.926	0.003651	72	3.919	3.934	c
B18	3.929	0.003651	72	3.922	3.936	c

Developmental_Stage = 6 Leaves: (Chry7R)						
Accessions	emmean	SE	df	lower.CL	upper.CL	.group
PRESTO	11.1	0.208	72	10.7	11.5	a
VALOR	11.4	0.208	72	11.0	11.8	a
H1	11.5	0.208	72	11.1	11.9	a
BRILLYANCE	11.7	0.208	72	11.3	12.1	a
B18	12.9	0.208	72	12.5	13.3	b
BOLERO	13.0	0.208	72	12.6	13.4	b
A92	13.2	0.208	72	12.8	13.6	b
I2	13.2	0.208	72	12.8	13.7	b

Appendix - Figure 5 : Tukey's multiple pairwise comparison test based on the content of each metabolite observed at 6-leaf stage.

Accessions sharing the same letters are not significantly different at the error rate of 0.05.

Developmental_Stage = 2 Leaves: (Api7R)

Accessions	emmean	SE	df	lower.CL	upper.CL	.group
H1	10.6	0.213	72	10.1	11.0	a
PRESTO	10.6	0.213	72	10.2	11.0	a
VALOR	10.7	0.213	72	10.3	11.1	a
BRILLYANCE	10.8	0.213	72	10.4	11.2	ab
BOLERO	11.1	0.213	72	10.7	11.5	ab
B18	11.2	0.213	72	10.8	11.6	ab
A92	11.3	0.213	72	10.9	11.8	ab
I2	11.7	0.213	72	11.3	12.1	b

Developmental_Stage = 2 Leaves: (Lut7R)

Accessions	emmean	SE	df	lower.CL	upper.CL	.group
H1	3.883	0.003651	72	3.876	3.891	a
PRESTO	3.884	0.003651	72	3.877	3.891	a
VALOR	3.891	0.003651	72	3.884	3.899	a
BRILLYANCE	3.895	0.003651	72	3.887	3.902	a
A92	3.921	0.003651	72	3.914	3.928	b
I2	3.921	0.003651	72	3.914	3.929	b
B18	3.921	0.003651	72	3.914	3.929	b
BOLERO	3.922	0.003651	72	3.914	3.929	b

Developmental_Stage = 2 Leaves: (Chry7R)

Accessions	emmean	SE	df	lower.CL	upper.CL	.group
PRESTO	11.0	0.208	72	10.6	11.4	a
VALOR	11.1	0.208	72	10.7	11.5	a
H1	11.2	0.208	72	10.8	11.6	a
BRILLYANCE	11.5	0.208	72	11.1	11.9	ab
B18	12.4	0.208	72	12.0	12.8	bc
BOLERO	13.0	0.208	72	12.6	13.4	c
A92	13.0	0.208	72	12.6	13.4	c
I2	13.1	0.208	72	12.7	13.5	c

Appendix - Figure 6 : Tukey's multiple pairwise comparison test based on the content of each metabolite observed at the 2-leaf stage in eight carrot accessions. Accessions sharing the same letters are not significantly different at the error rate of 0.05.

CHAPTER III: SHEDDING LIGHT ON THE PLACE HELD BY THE THREE FLAVONE GLYCOSIDES IN THE *D.CAROTA* - *A.DAUCI* INTERACTION - BIOLOGICAL ACTIVITY AND MECHANISMS OF ACTION

Leaf enrichment in the three candidate flavonoids was seen to be indeed associated with a higher resistance to *A. dauci*, both in I2 and in three highly divergent accessions. However, it is not certain how close they are genetically. Furthermore, despite the diversity of their metabolic phenotype, the candidate metabolite-accumulating accessions showed similar behaviour in the presence of *A. dauci*, with respect to the candidate flavonoids. Two hypothetical scenarii could be considered: either the metabolite content covaries with an undefined resistance factor that is common to these accessions or the three compounds are resistance factors but are interchangeable as long as each of them is present at relatively high levels. Drawing conclusions from a correlative observation alone could be very misleading and should be carefully considered before implementation in a breeding programme, as illustrated by a case study in apple (Bernonville et al., 2011). Driven by a joint analysis of the carrot leaf transcriptome, resistance and metabolite QTL mapping by the QuaRVeg team, this chapter aims to decipher the mechanism of action of the candidate flavonoids through their direct effect on *A. dauci* growth.

The most frequently investigated mechanism of action of flavonoid-mediated resistance is their putative inhibitory activity on fungal phytopathogens; either through antifungal or fungistatic activities (Sung and Lee, 2010; El-Nagar et al., 2020; Koutouan et al., 2023) or through inhibition of mycotoxin production (Tian et al., 2023). Two main questions were therefore addressed: i) do the three candidate flavonoids directly interfere with *A. dauci* development? ii) If so, what is the extent of their role in the pathogen-host interaction in the context of disease resistance? To achieve these objectives, exposure of *A. dauci* to each of the candidate compounds required a sufficient amount of pure compounds, which was initially set at around 500 mg each. The easiest and most convenient way to obtain these was to purchase them from the market. However, this approach was ruled out by the unattractive cost / quantity ratio identified at the start of this study. Indeed, 10 mg of Api7R cost 168 € at Extrasynthèse France (178 € in 2023); 1 mg of Lut7R cost 326 € in 2020 (439 € in 2023) at Sigma-Aldrich USA, while Chry7R was not and is still not commercially available. To overcome this limitation, there are several alternatives: 1) total organic synthesis or semi-synthesis, 2) *in vitro* enzymatic synthesis or through biotransformation by a genetically engineered microbial organism and 3) purification from sources naturally enriched in the compounds of interest.

The Chemical synthesis of aglycones has been proposed, to overcome the lack of suitable natural sources for purification. Apigenin could be obtained this way with a five-step strategy described in (Zhang et al., 2013), starting from 1,3,5-trimethoxybenzene; later optimised by (Wang et al., 2015). This strategy was more efficient than the one starting from phloroglucinol (Wang et al, 2012), which was limited to 40% yield in 5 steps. To shorten the process, purified genins could also be purchased directly if available and affordable. Apigenin is relatively cheap (123 € for 25

mg at Sigma Aldrich, in 2023) compared to luteolin (96 € for 5 mg at Sigma Aldrich, in 2023) and chrysoeriol (424 € for 5 mg at Sigma Aldrich, in 2023). The obtained aglycones could become the acceptor substrates for subsequent enzymatic reactions (**Figure 19**) aimed at adding sugar moieties and producing glycosylated conjugates (Jang et al., 2018; Liu et al., 2021). Yet, as their native production machineries, this step often requires activated sugars, *i.e.* attached to a nucleotide-diphosphate (NDP), which are not always commercially available or very costly. UDP-glucose could be affordable, although a very strategic way to limit reaction costs is to regenerate the sugar donor at each reaction cycle, by means of a coupled enzymatic transglucosylation system (Liu et al., 2021). As an illustration, the C-glucosylation of luteolin to give rise to orientin (luteolin-8-C-glucoside) implied the activity of a sucrose synthase (SuSy) taking up sucrose and UDP as substrates to produce a fructose and a UDP-glucose unit. Glucose transfer by the C-glycosyltransferase to the aglycone in turn releases the UDP, which is revalorised in the next round by the sucrose synthase, and so on (Liu et al., 2021). To obtain the flavones of interest (Api7R, Lut7R and Chry7R), an additional reaction should be considered to attach a rhamnose to the glucosyl group of 7-O-glucosylated genins. As UDP-rhamnose is difficult to obtain and expensive, bioconversion in *Escherichia coli* is an attractive solution to overcome this obstacle. Providing the host (*E.coli*) with the biosynthetic genes that lead to UDP-rhamnose, including preferred glycosyltransferase genes, has been fruitful for the 3-O-rhamnosylation of kaempferol (Chung et al., 2015), and quercetin (Gu et al., 2020). However, the most challenging aspect of this approach is the low regioselectivity of some O-glycosyltransferases (Ko et al., 2008; Griesser et al., 2008), resulting in the glycosylation of hydroxyl groups at undesired positions on the genin; hence, leading to the obtention of a relatively complex mixture of structurally very similar compounds (**Figure 19**). Purification of the candidate compound can thereafter be very tedious. Obviously, several parameters need to be established for a synthetic biology approach, starting with the selection and characterisation of enzymes with a relatively good substrate specificity and a strict regioselectivity. Therefore, this route did not seem suitable for a very short period of time during a 3-year Ph.D. project.

The third and most documented alternative is the extraction of flavonoids from natural sources such as vegetables, fruits, or medicinal plants. In fact, flavonoids present in food and beverages have been extensively characterised for human health purposes, leading to an advanced knowledge of different isolation methods (Fecka et al., 2004; Lin et al., 2015; Pardede et al., 2017; Tagousop et al., 2018). Purification methods adapted to a wide range of plant matrices are available. Slight adaptations could be made according to the physicochemical properties of the compounds of interest and the accessibility of laboratory facilities (Barba et al., 2016; Vinatoru et al., 2017; Zhang et al., 2018; Rodríguez De Luna et al., 2020). A rapid survey of the literature encouraged the adoption of this methodology.

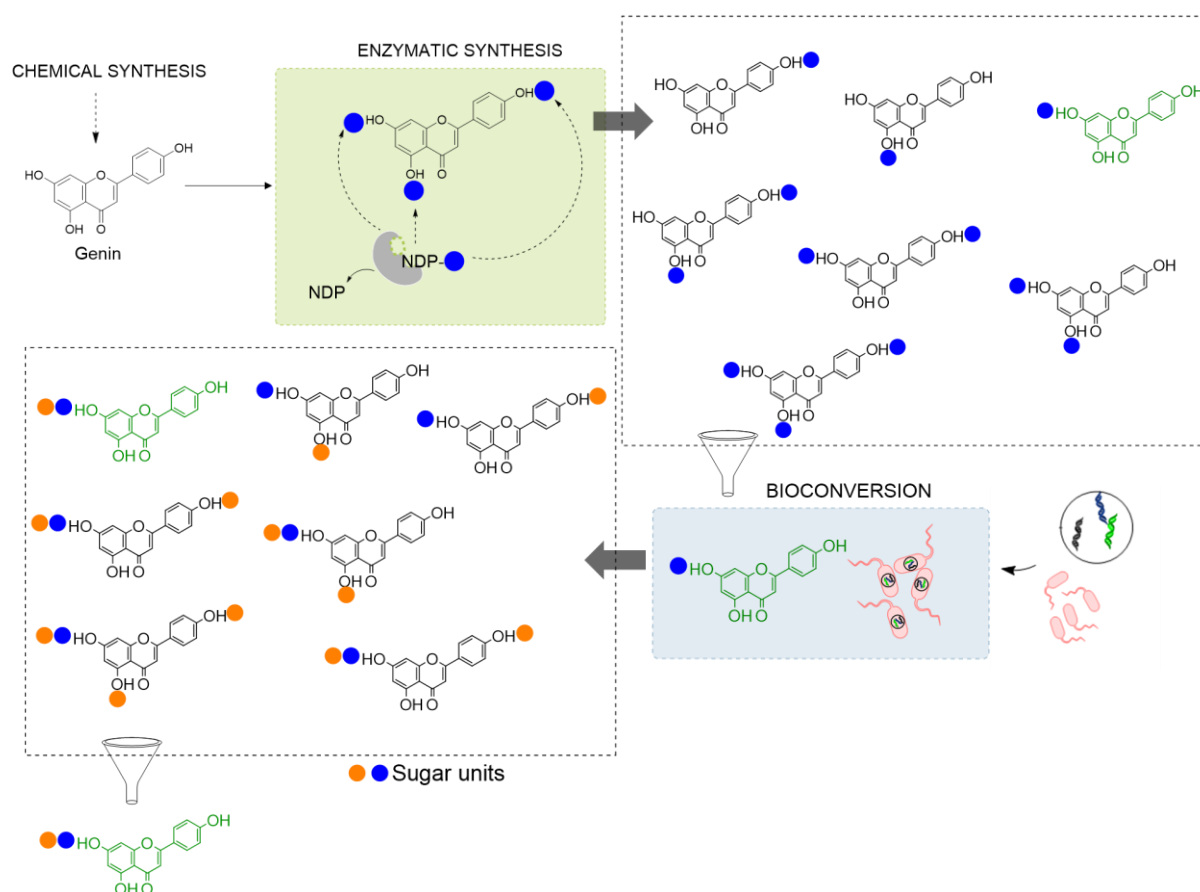


Figure 19: Strategy for the addition of two consecutive sugar moieties at the 7-OH of a genin (ex: apigenin).

NDP: nucleotide-diphosphate

3.1 Scouting for natural sources enriched with the candidate flavones

Literature review enabled to spot plants known to contain a decent content of Api7R and Lut7R, but not Chy7R. A plethora of studies reported the potential of globe artichoke (*Cynara cardunculus* L. subsp. *scolymus* (L.)) in promoting health through its high content in phenolic compounds, to name only a few (Wang et al., 2003; Zhu et al., 2004; Lattanzio et al., 2009; Abu-Reidah et al., 2013; Hassabou and Farag, 2020; Shallan et al., 2020). Artichoke heads (capitula) and leaves showed interesting concentration in Api7R and Lut7R for the purpose of the present investigation. Depending on the cultivar, the Api7R content in the heads varied from 174-554 mg/kg dry weight (Schütz et al., 2004; Pandino et al., 2011). Lut7R could be found in both heads and leaves but mainly in the heads, that can reach 34000 mg/kg fresh weight (Schütz et al., 2006; Negro et al., 2012). Thereupon, the *Green Globe* cultivar stood out from the cultivar set identified, to isolate Api7R as it had the highest content. It was also a good source of Lut7R. Local supplier (Evear, Coutures) in Maine-et-Loire provided artichoke extracts that we analysed by HPLC-UV, but did not result in the detection of Api7R. Therefore, there was a need to obtain the *Green Globe* cultivar. While waiting for the artichokes to grow, peppermint leaves (*Mentha x piperita* L.) was identified as an interesting source of Lut7R, which could quickly be retrieved from a relatively limited dry plant material (650 mg/kg fresh weight) (Guédon and Pasquier, 1994; Inoue et al., 2002).

The few publications mentioning the presence of Chry7R in plant tissues did not always report a precise enrichment, if not a signal below the detection limit in liquid chromatography analyses (El-Negoumy et al., 1986; Plazonić et al., 2009; Fialova et al., 2015). The immediate solution was thereafter, to start with in-house carrot accessions already known to have a higher amount of this compound in their leaves, compared to others from the carrot biological resource collection of the QuaRVeg team.

3.2 Method development and flavonoid purification

Available information from the literature were intended to be optimised to suit the facilities at the SONAS laboratory. Given the immediate disposability of the materials to purify Lut7R and Chry7R and their limited accessibility in the market, the process was launched in priority regarding these compounds. A common generic pipeline comprising four main steps was applied (**Figure 20**): extraction, fractionation of the crude extract, purification of the compound of interest from enriched fractions and in the end, compound identity validation through chromatographic comparison with available standard derivatives. More in depth, the first challenge to overcome lied in the optimisation of the extraction method to find the most suitable solvent ratio, followed by the development of an analytical method to optimally resolve the leaf matrix components. Afterwards, applying an efficient fractionation method was sought to minimise the iteration of this step until the obtaining of a sufficient amount of quality fractions.

Lut7R was more in the first scenario, for which the process was relatively more fluid than it was for Chry7R. Starting with the isolation of Lut7R, method optimisations were made at every scale of the workflow. Afterwards, these methods were intended to be applied for the obtaining of Chry7R, although it demanded more time and adjustments than expected. With no available standard for this last compound, the main challenge resided in the difficulty to identify the peak on HPLC-UV chromatograms without a routinely accessible mass spectrometer. For this reason, a consequent amount of time was allocated in the development of suitable analytical method. This left insufficient time to purify the Api7R as initially planned, and prompted us to purchase small amount of this candidate for various biological assays.

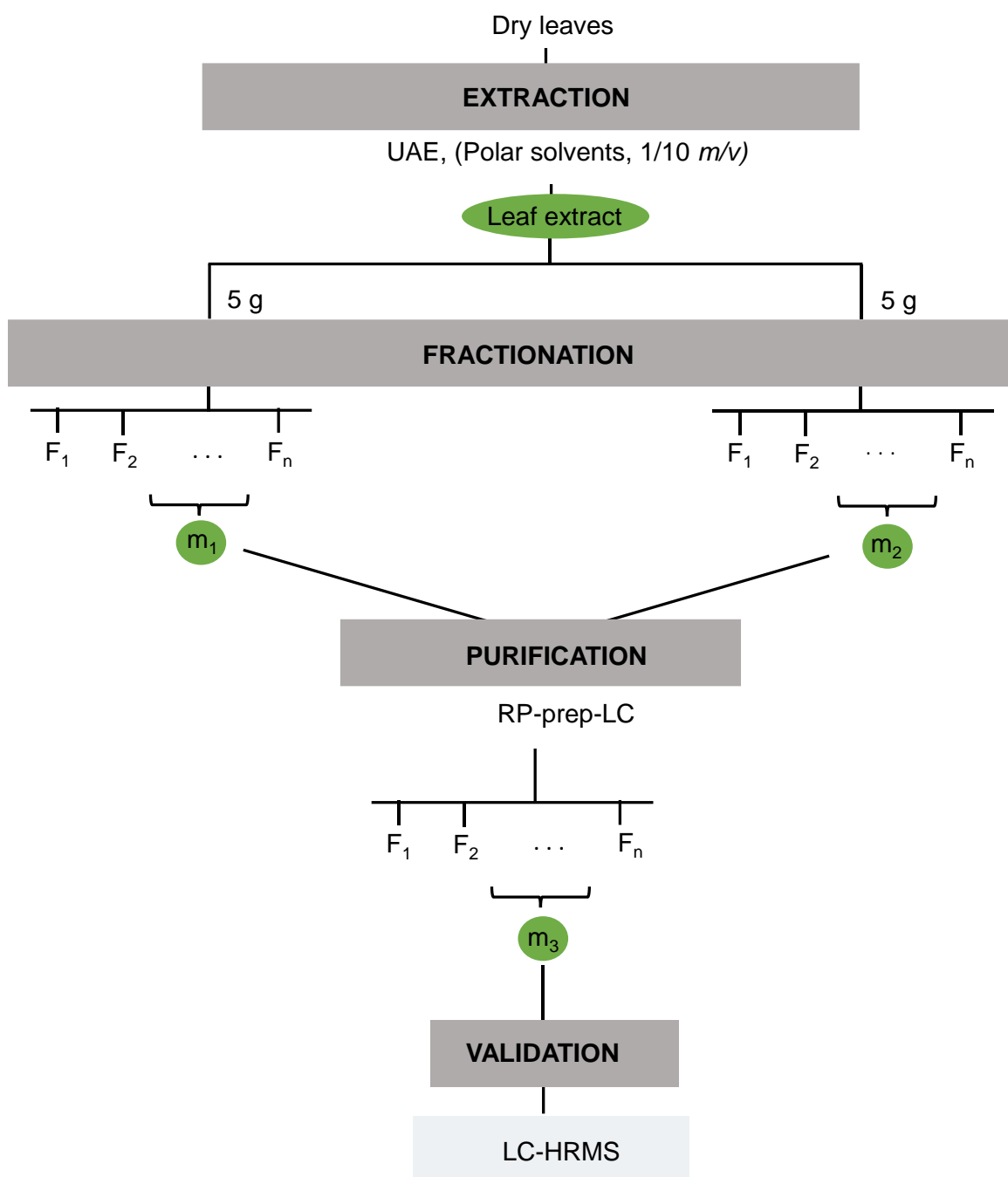


Figure 20: General pipeline for the target compound isolation from dry leaf materials. UAE: ultrasound-assisted extraction. RP-prep-LC: reverse phase liquid preparative liquid chromatography. LC-HRMS: liquid chromatography-high resolution mass spectrometry.

3.2.1. Isolation of Lut7R from *Mentha x piperita* (peppermint) leaves

3.2.1.1 Optimisation of the HPLC-UV method

A methanolic extraction from *Mentha x piperita* leaves has yielded in 14.2% of dry crude extract, i.e. 40.60 g out of 285 g starting material. The leaf extract was analysed using a reversed phase high-pressure liquid chromatography and eluted peaks were monitored at 254nm and 320nm. A methanol gradient method allowed to elute most of the

constituents of this extract between 10 and 18 minutes (**Figure 21**). The injection of a standard solution allowed to uncover that Lut7R was not the major peak detected at 254nm, and it was eluted at ($RT_{254nm} = 15.301$ min). The vicinity of this peak with others of the same polarity made the region between 14-18min a region of interest (ROI) subjected to close attention during method development, for a better peak resolution. Considering all methods tested (Chapter V-5.2), increasing the methanol percentage earlier in the gradient allowed to efficiently separate these peaks (**Figure 22**).

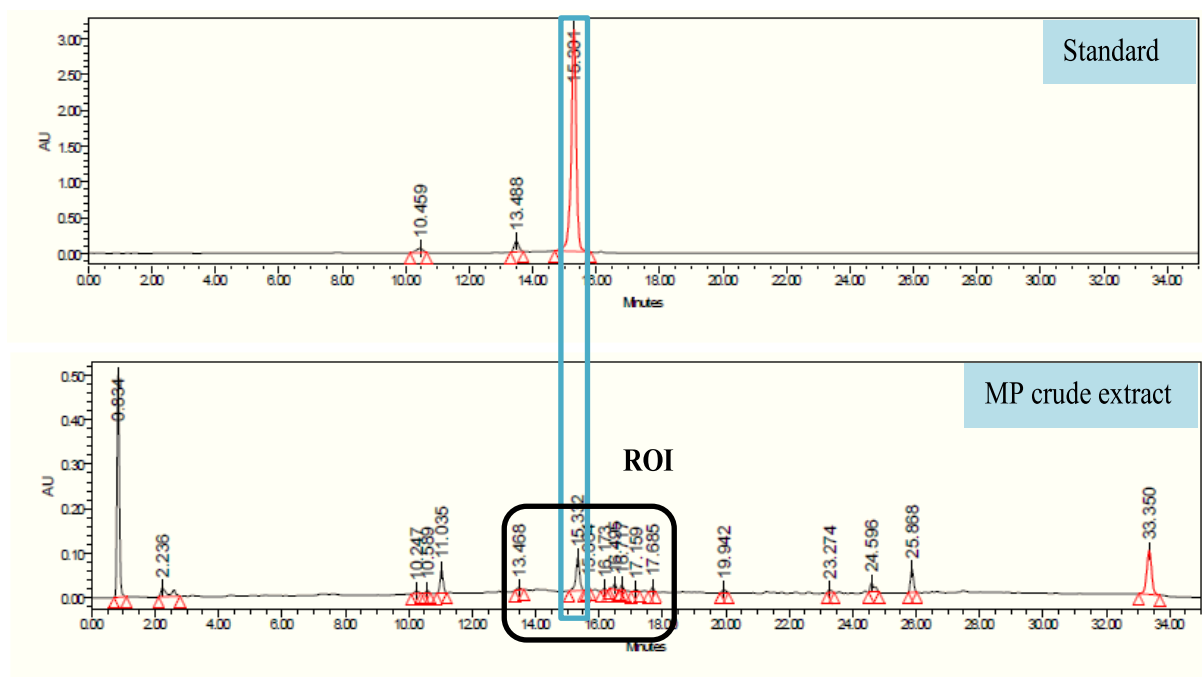


Figure 21: Identification of the Lut7R peak and retention time by HPLC-UV analysis at 254nm, using a non-optimised method. ROI: region of interest. MP: *Mentha x piperita*. Blue frame: peaks corresponding to Lut7R. C18 (150 x 4.6 mm, 3 μ m). A: H_2O and B: MeOH/ H_2O 50/50. Flow 0.7 mL/min.

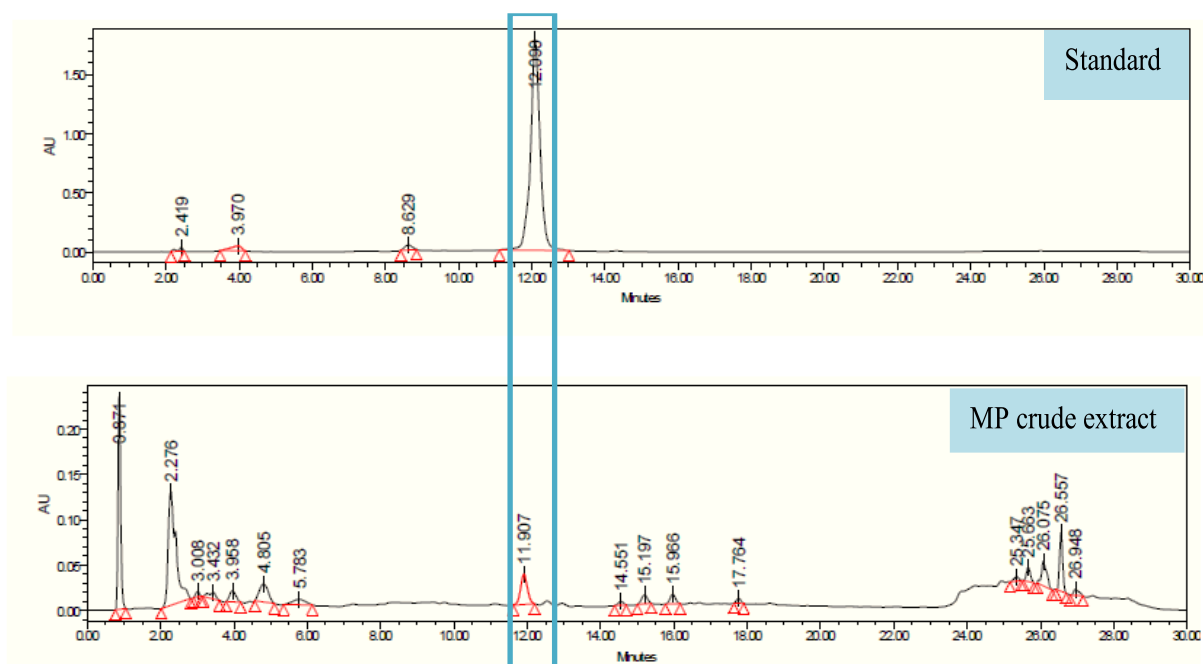


Figure 22: HPLC-UV (254nm) chromatograms of the standard and the *Mentha x piperita* leaf crude extract, using the optimised method. MP: *Mentha x piperita*. Blue frame: peaks corresponding to Lut7R. C18 (150 x 4.6 mm, 3 μ m). A: H₂O and B: MeOH/H₂O 50/50. Flow 0.7 mL/min.

3.2.1.2 Optimisation of the fractionation and purification protocol

Qualitatively non-complex fractions and more enriched in the peak of interest (POI) eluted at ~12min were sought at this step. Assuming the transposability of the analytical method to a preparative scale, the ROI would be accessible through polarity-based separation methods. However, as a first step to discard unwanted compounds of the matrix, reverse phase adsorbents may not be the most cost-effective when it deals with multi-gram scale fractionation. Therefore, a comparative evaluation of two systems was set, lying on the polarity (normal phase) of the compounds or their size (size exclusion).

Purification of fractions deriving from normal phase fractionation (silica) had a lower yield and a less qualitative profile compared to when they came from exclusion-based separation (Sephadex LH-20) (**Table 2**), with 7.8 mg and between 32-35 mg of fractions of interest obtained, respectively, from 5 g of starting material. The results also suggested that size exclusion-based approach was more compatible with the *Mentha x piperita* leaf extract, hence, allowing to discard undesired compounds without losing much of the target compound (**Figure 23**). Moreover, fractionation with this type of adsorbent was reproducible (**Table 2**, entry 2 and 3). The slight improvement of the yield obtained for F_D (**Table 2**) was assumed to be linked to the continuous optimisation of the elution method in C18 purification step. Among all obtained qualitative fractions, the attention was put on F_D (76 mg), in which 93% of the

total peak area accounted for the peak of interest at 254 nm (**Table 2, Figure 23**). This purity rate at 254nm required further confirmation by means of a RP-HPLC-DAD-ELSD analysis.

Table 2: Comparative overview of the purification yield along modulation of the stationary phase during the fractionation.

Starting material	Fractionation	Purification	Lut7R area at 254nm	Dry weight (mg)	Fraction name
5g	Silica	C18	80%	7.8	F _A
5g	Sephadex LH-20	C18	84%	35.4	F _B
5g	Sephadex LH-20	C18	83%	32.7	F _C
5g * 2	Sephadex LH-20 * 2	C18	93%	75.8	F _D

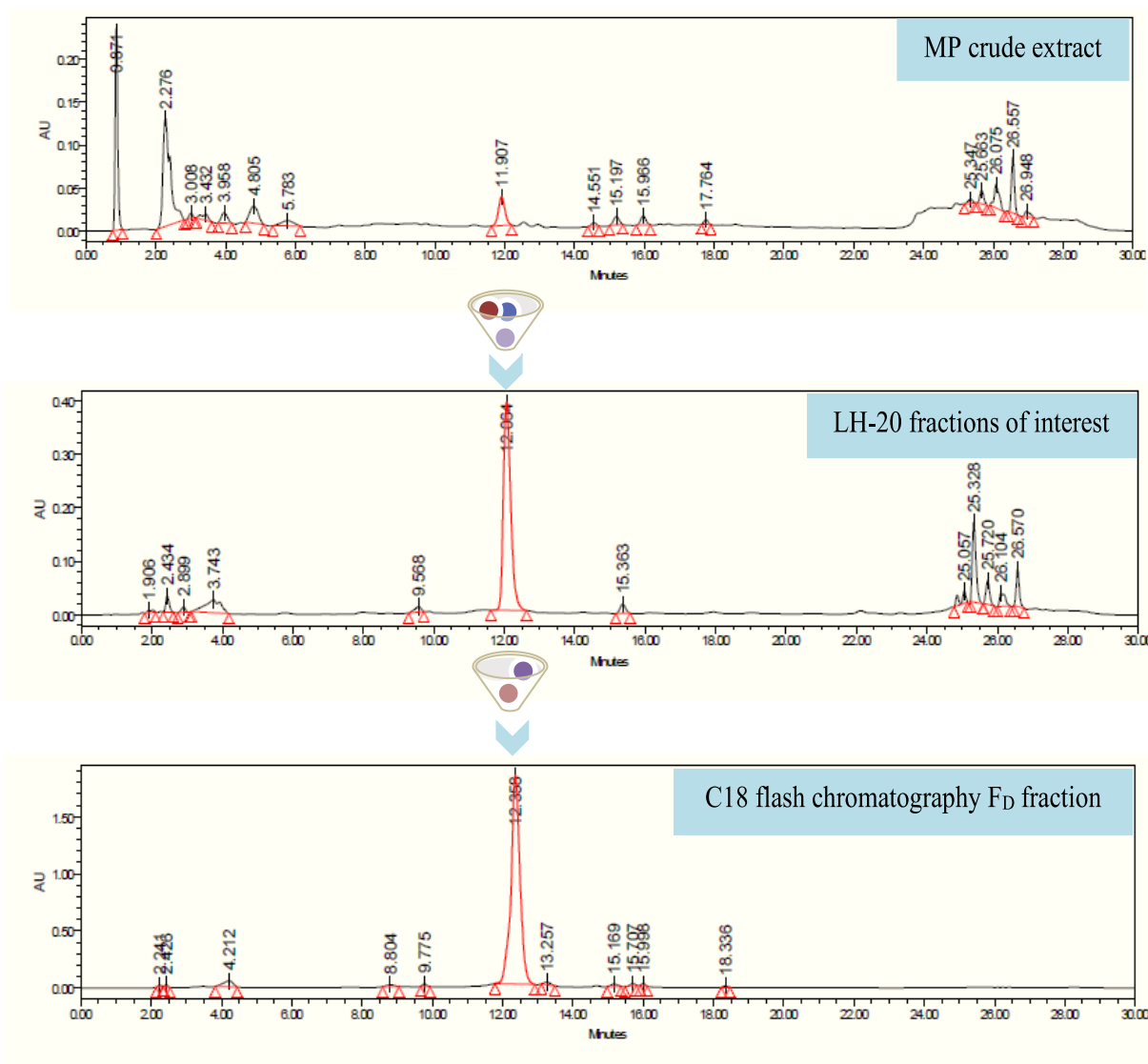


Figure 23: HPLC-UV chromatograms at 254nm depicting the qualitative profiles of the crude extract (top), the fraction of interest after a fractionation through a LH-20 column (middle) and a purification through a C18 column thereof (bottom). The height of the Y-axes is not representative of the compound proportion retrieved from the crude extract. C18 (150 x 4.6 mm, 3 μ m). A: H₂O and B: MeOH/ H₂O 50/50. Flow 0.7 mL/min.

3.2.1.3 Purity rate of the POI in the F_D fraction

Signal from ELSD showed that the FD fraction was a highly purified with 95.781- 97.258 % of the total fraction accounting for the peak eluted at RT = 12.577 min (**Figure 24A**). UV signal overlapping between 190-400 nm suggested a pure peak at this retention time, that was exempt from co-eluting with compound (s) which would be revealed by the presence of shifting peaks (**Figure 24B**). The results were congruent with known absorption wavelengths of Lut7R from 229 to 279 nm (**Figure 24C**). At this stage, the purity rate of the isolated compound was considered sufficient, for this fraction to be used in a biological assay.

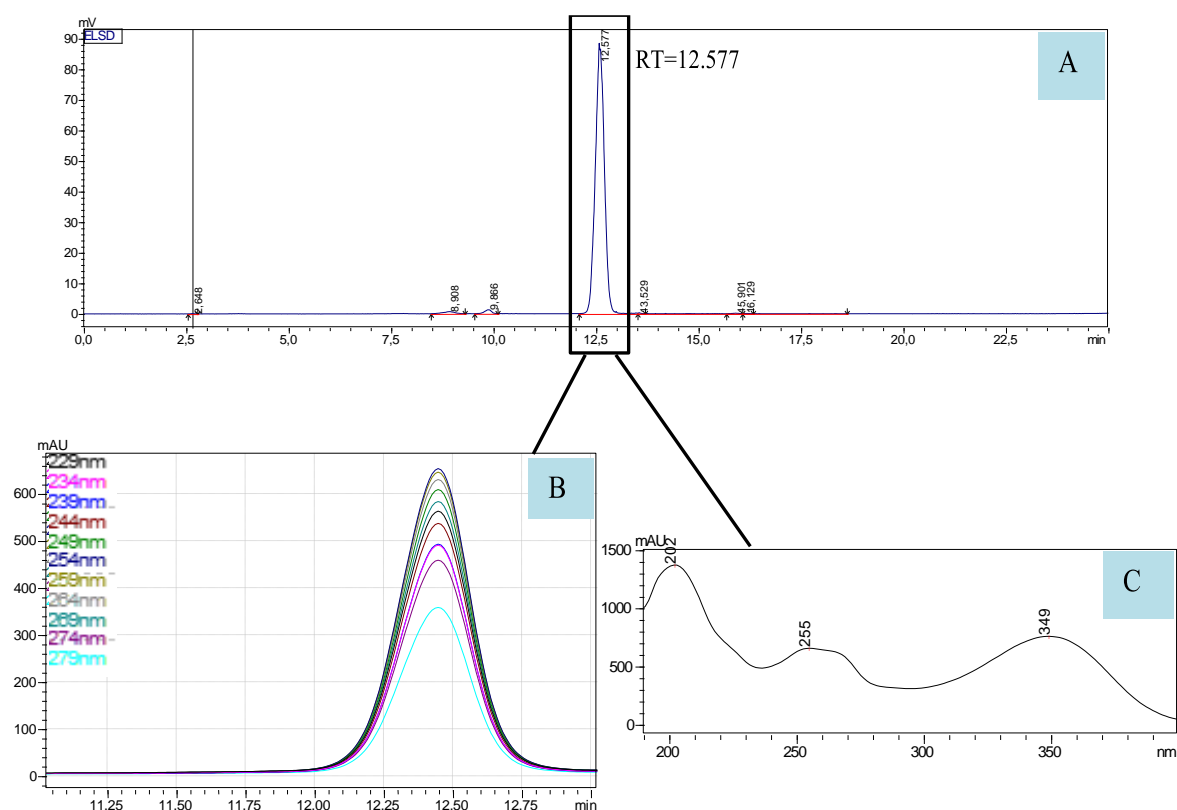


Figure 24: HPLC-DAD-ELSD confirmation of the purity rate of the F_D fraction. A: ELSD signal along the LC program. B: overlapping of signals detected at different wavelengths from 229 to 279 nm at RT =12.577min. C: Absorption spectrum of the compound at RT=12.577min. C18 (150 x 4.6 mm, 3 μ m). Eluent A: H₂O and B: MeOH/ H₂O 50/50. Flow 0.7 mL/min.

3.2.1.4 Peak identity validation by LC-HRMS and LC-DAD-MS

The LC method from the HPLC-UV system was adjusted to fit into LC-HRMS conditions. The characteristic molecular ion for Lut7R was detected in negative mode with a mass over charge ratio (m/z) of 593.1067 (**Figure 25**). Fragmentation of this molecular ion indicated the loss of the sugar moiety and the detection of the luteolin aglycone ion with $m/z = 285.0436$ (**Figure 26**). This fragmentation pattern was consistent with reported data in the literature (Plazonić et al., 2009) and provided to emphasize peak identification based on the LC retention time of the commercial standard. Results from LC-DAD-MS analysis in positive mode at the SVQV team of INRAe Colmar was in line with these observations (**Figure 27**).

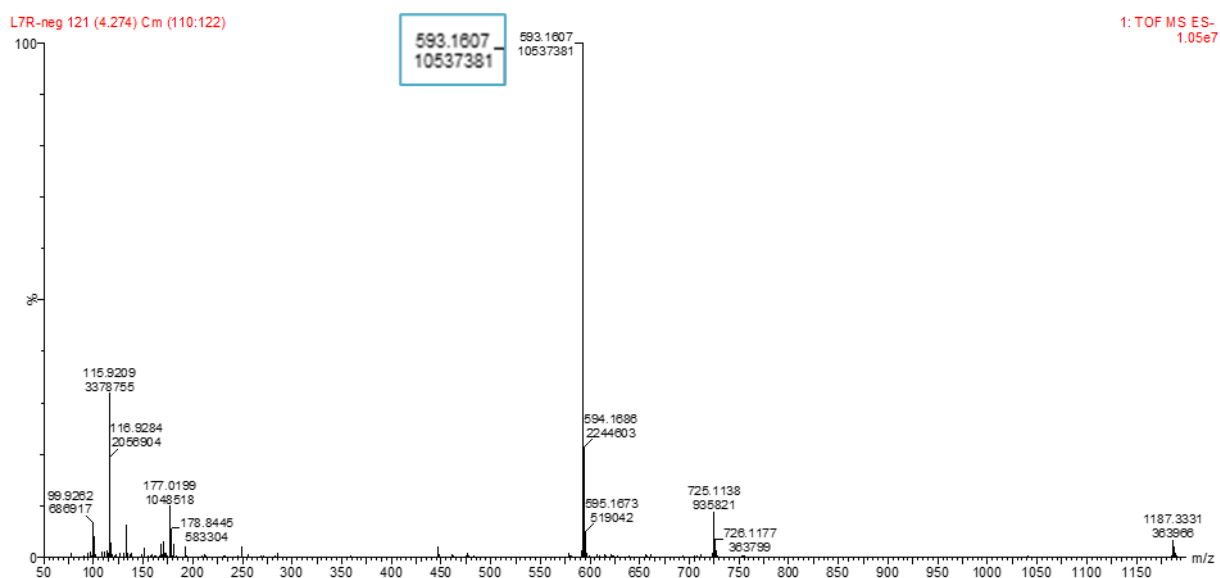


Figure 25: Mass detection of the target molecular ion $[M-H]^-$ with $m/z = 593.1607$ in negative mode.

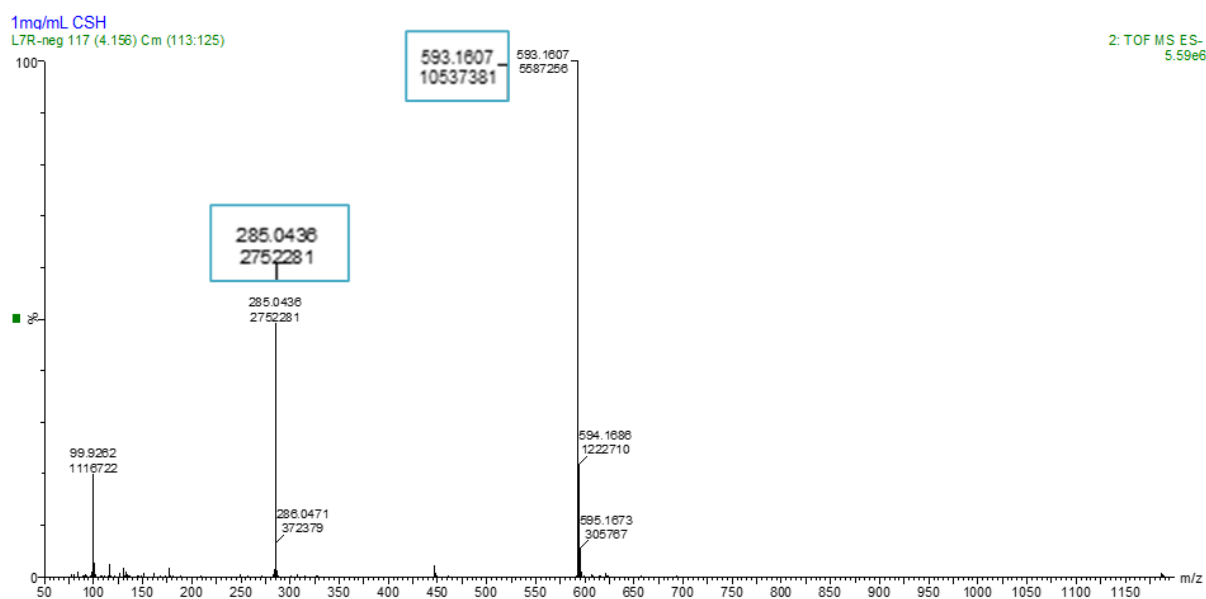


Figure 26: Fragmentation pattern of $m/z = 593.1607$.

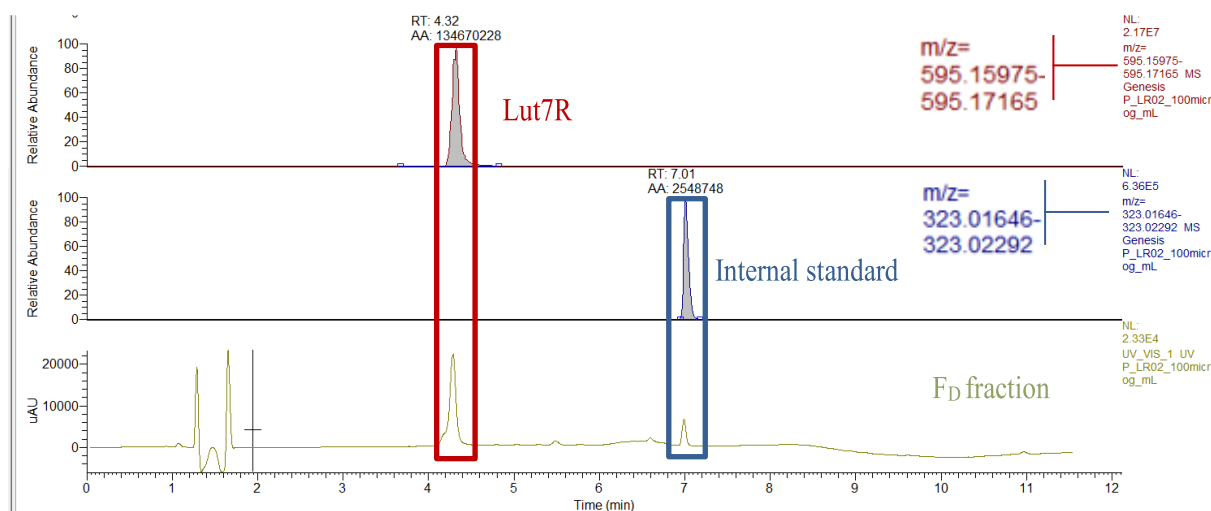


Figure 27: UPLC-DAD (280nm) chromatogram of the compound purified of the F_D fraction (bottom), referring to recorded retention time and mass data (top) of isolated peaks. Mass detection focused on positively charged ions ($m/z = 595.1575$ for Lut7R). C18 (150×2 mm, $1.8 \mu\text{m}$), eluent A: ACN + 0.1 % FA and B: H_2O + 0.1% FA. Flow rate: 0.25 mL/min.

3.2.2. Obtention of Chry7R from *Daucus carota* leaves

The purification of Chry7R was challenged, primarily, by the fact that the quantities of Chry7R produced by certain carrot accessions are only relative and not absolute. Delving into this process was risky, as the purification of a minor compound would require time consuming and several purifications from a colossal amount of leaf extracts, to result in limited amount of purified product. In addition, the absence of a pure standard implied that the characterisation of the leaf extracts immensely relied on the availability of tools combining LC-UV and a mass spectrometer at least at the beginning of the process, to identify the retention time of Chry7R. Collaboration with the ASTRAL technical platform at the University of Angers and the SVQV team in Colmar was very helpful in unlocking this first step.

3.2.2.1 Characterisation of the carrot leaf crude extract by HPLC-UV

A preliminary small-scale screening of different solvent systems was carried out to select the one that would provide the best yield through an ultrasound-assisted extraction procedure (UAE). During this experiment, two carrot accessions (A92 and C12) were studied. Between 100% MeOH, 50/50 MeOH/ H_2O and 75/25 MeOH/ H_2O , the latter system was validated (not shown) for further application to a larger scale. Qualitative analysis of the extracts (5 mg/mL) was performed using the previously optimized MeOH gradient. In sum, all extracts shared a similar chromatographic profile as portrayed in (Figure 28). Apart from the highly polar peaks and thus rapidly eluted peaks, one major peak, eluted at $\text{RT}=11.891$ min (Figure 28) was detected with all the extracts. Five other minor peaks, in terms of relative intensity, were also observed, mostly eluted or co-eluted ($\text{RT}=14.624$ min) from 13 to 16 minutes. This co-elution would be eventually challenging at an analytical scale first, especially if the target compound is in this zone. Moreover, without any Chry7R standard available on the market it limited the possibility of ascertaining the

identity of the concerned peaks through UV detection only. Hence, through a collaboration with the ASTRAL technical platform at the University of Angers, mass detection (not shown) allowed to affirm that the first part of the peak was likely to be Api7R followed by Chry7R. From this information, only the A92 carrot accession was chosen for a large scale extraction as the peak intensity corresponding to Chry7R was more intense than in the C12 accession (not shown). A large scale UAE made from 200 g of dry leaves resulted thereafter, in 36.3 g of dry crude extract, equivalent to 18.2 % extraction yield.

The first challenge faced was to analytically improve the resolution of the peaks of Api7R and Chry7R, to ensure that the right conclusions are made during the fractionation step, and that the right fractions of interest are selected for further purification. However, fractionation of the extract was also primordial to obtain a fraction that would be more concentrated in Chry7R compared to others, intended for peak identification by LC-MS.

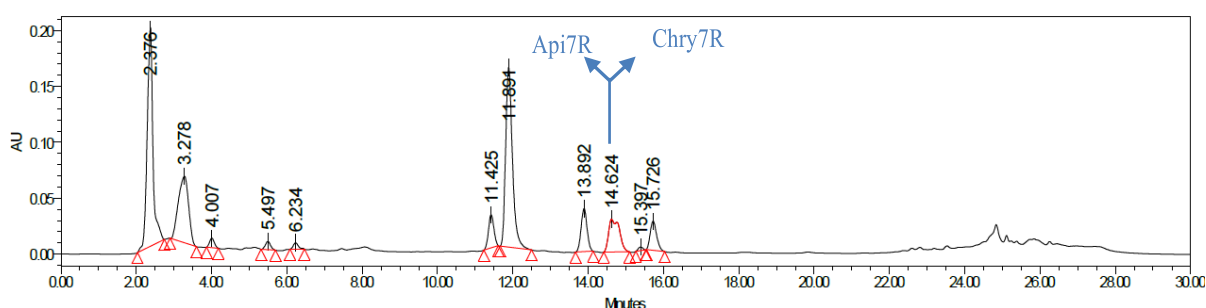


Figure 28: HPLC-UV chromatogram of the carrot hydroalcoholic (MeOH/H₂O 75/25) leaf extract at 254 nm. Arrows: co-eluted peaks at RT = 14.624 min corresponding to Api7R and Chry7R based on MS detection (not shown). C18 (150 x 4.6 mm, 3 μ m). Eluent A: H₂O and B: MeOH/H₂O 50/50. Flow 0.7 mL/min.

3.2.2.2 Preliminary fractionation of the leaf extract and LC method optimisation

Fractionation through a Sephadex LH-20 column was performed on 1.2 g of dry crude extract obtained from all preliminary extractions made during the optimisation process. Compounds were eluted with MeOH/H₂O 50/50. Five groups of fractions were obtained and analysed by LC-MS at INRAE Colmar to identify fractions containing Chry7R. From this analysis, one fraction of interest named F₁ (120 mg) was found to contain some Chry7R. However, this peak co-eluted with Luteolin-glucuronide under the analytical conditions applied in Colmar (**Figure 29**). Under the conditions applied in Angers, however, it was difficult to affirm on the identity of the peak eluted at RT = 30.817 min (**Figure 30**, bottom). Despite this observation and because Chry7R was scarcely detected in other fractions, the F₁ fraction was used thereafter as a contaminated reference for peak identification during LC method development.

The LC method published by Plazonić and colleagues (2009) studying the composition of *Caucalis platycarpos* L. or Burr parsley from the *Apiaceae* family was found to be potentially transferable to the analysis of carrot leaf extract. Chry7R was detected for the first time in this plant and structurally characterised by ¹H NMR. In the aftermath, this method seemed lengthy and not resolutive enough (**Figure 30**). Therefore, the method was altered by taking into

account the acetonitrile gradient used by the SVQV team in Colmar, in order to maintain peak elution order while expecting a better resolution. This approach allowed to shorten the initial method from 120 min to 60 min (**Figure 30**). The parallel with the F₁ fraction chromatogram showed that with this final method, the retention time of the putative Chry7R peak could be at RT = 30.817 min. An evident retention time shift between the two chromatograms for F₁ and the crude extract was observed. This shift might be imputable to chromatographic bias such as temperature fluctuations in the laboratory during the day and between days of the analysis, thus impacting the column pressure while injections were made on the same HPLC module. Regulation of the column temperature was set at 25°C and helped to stabilize the retention time of this peak around RT = 31 min, with unfortunately still some fluctuations. Furthermore, this comparative view clearly showed that the fractionation method could be considered satisfactory to decomplexify the initial mixture, thus leading to fractions whose purification through flash chromatography should be easier to develop.

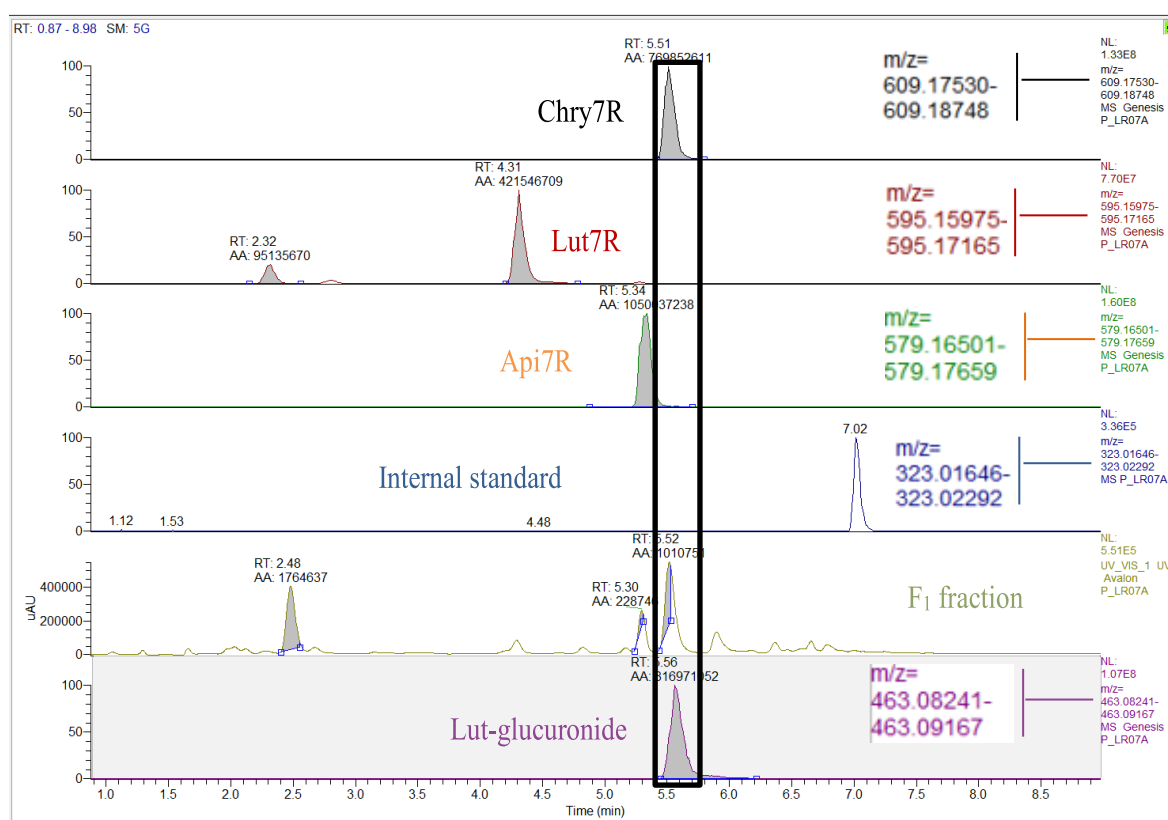


Figure 29: UPLC-DAD (280nm) chromatogram of the F₁ fraction referring to known retention times and mass data of isolated peaks. Mass detection focused on positively charged ions ($m/z = 609.1753$ for Chry7R). C18 (150 × 2 mm, 1.8 μm), eluent A: ACN + 0.1 % FA and B: H₂O + 0.1% FA. Flow rate: 0.25 mL/min.

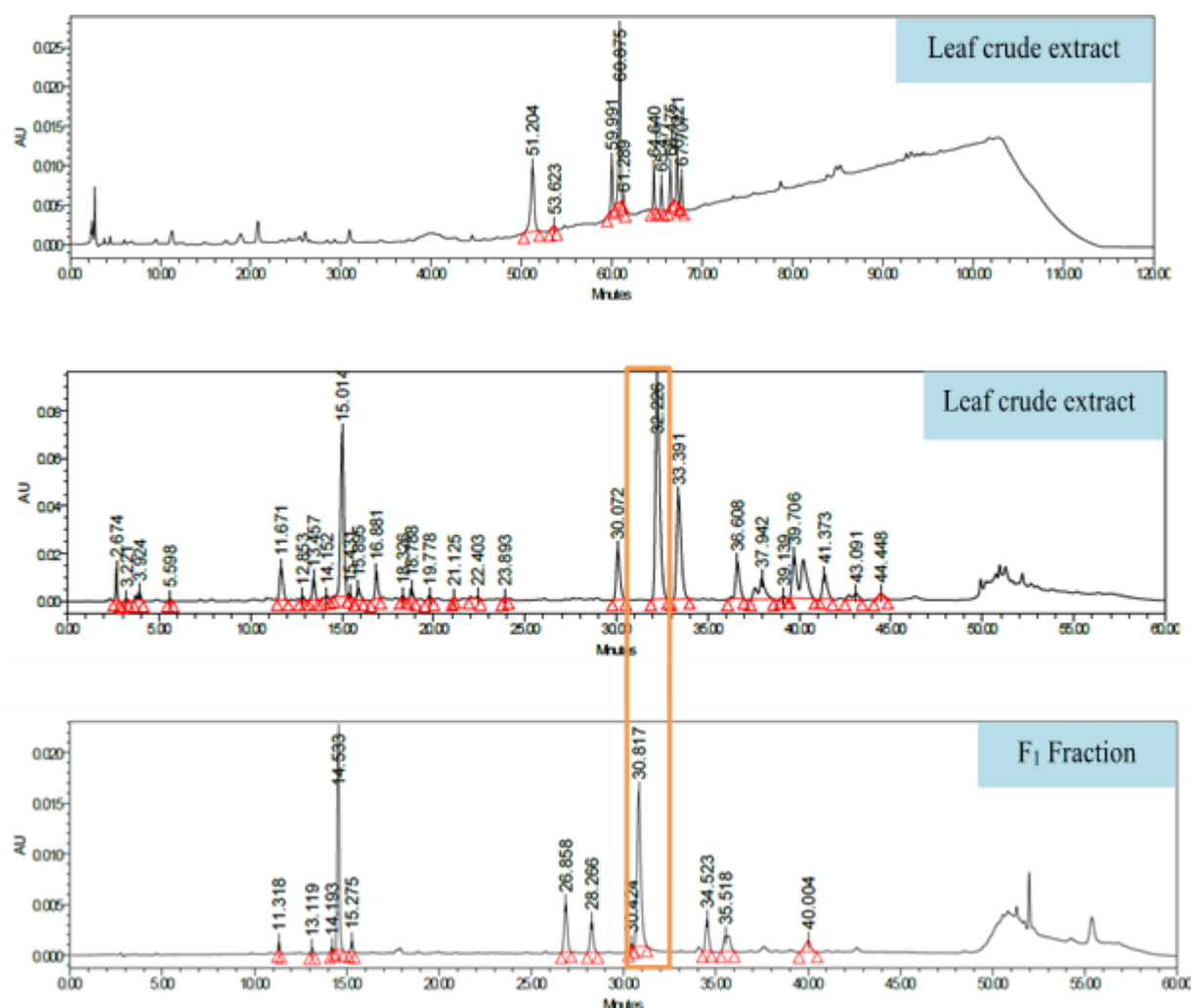


Figure 30: HPLC-UV chromatogram at 254nm of the carrot leaf crude extract (5 gm/mL) according to the method from the literature (top), at 280 nm for the same extract analysed with the optimised method (middle) and at 280nm for the F₁ fraction as a Chry7R reference sample (bottom). Conditions in the final method: C18 (150 x 4.6 mm, 3µm); A: ACN / H₂O 5/95 + FA 0.1% and B: ACN / H₂O 50/50 + FA 0.1%; Flow: 0.7 mL/min.

3.2.2.3 Large scale fractionation and reversed phase flash chromatography

From 5 g of crude extract, two groups of fractions from a Sephadex LH-20 separation were found to be qualitatively and quantitatively worth being admitted to the next step. F_I and F_{II} of 57.6 mg and 48 mg respectively had the potential peak of interest eluted at RT = 31.043-31.63 min (**Figure 31**) as the major peak detected at 345 nm.

The similitude of these profiles enabled to combine these fractions as one starting mixture (105.6 mg) for flash chromatography. Two majors peaks were eluted as shown in **Figure 32**, but only F_β (9 mg) was confirmed by LC-MS to contain Chry7R. The molecular ion corresponding to Chry7R with an exact mass of 608.17412 amu was detected in positive mode (**Figure 33**) with the associated fragmentation pattern that is reported in the literature (**Figure 34**) (Plazonić et al., 2009). However, an HPLC-ELSD analysis of this fraction showed that there are other constituents in

this fraction (**Figure 35**), with one contaminant eluted at RT = 35.836 min, identified as Api7R by LC-MS (not shown). The chromatogram highlighted the fact that Chry7R was rather eluted at RT = 37.058 min instead and was a rather a minor constituent of the F_I fraction (**Figure 29**, **Figure 30**). The AUC of the Chry7R peak in this fraction represented 73.2 % of the fraction and the one for Api7R peak 8.7 % (**Appendix - Table 1**).

This far, Chry7R was the major peak, although not with the expected purity as the one reached for the previously purified compound Lut7R. However, the available amount was quite small to be further purified through preparative HPLC. Moreover, at an advanced time course of this Ph.D. programme, the process was ended and this fraction was used in biological assay, bearing in mind that the biggest contaminant of this batch of Chry7R was one of the candidate flavonoid. The shortage in time also prevented the purification of Api7R from the *Green Globe* artichoke heads obtained locally and justified its acquisition from the market.

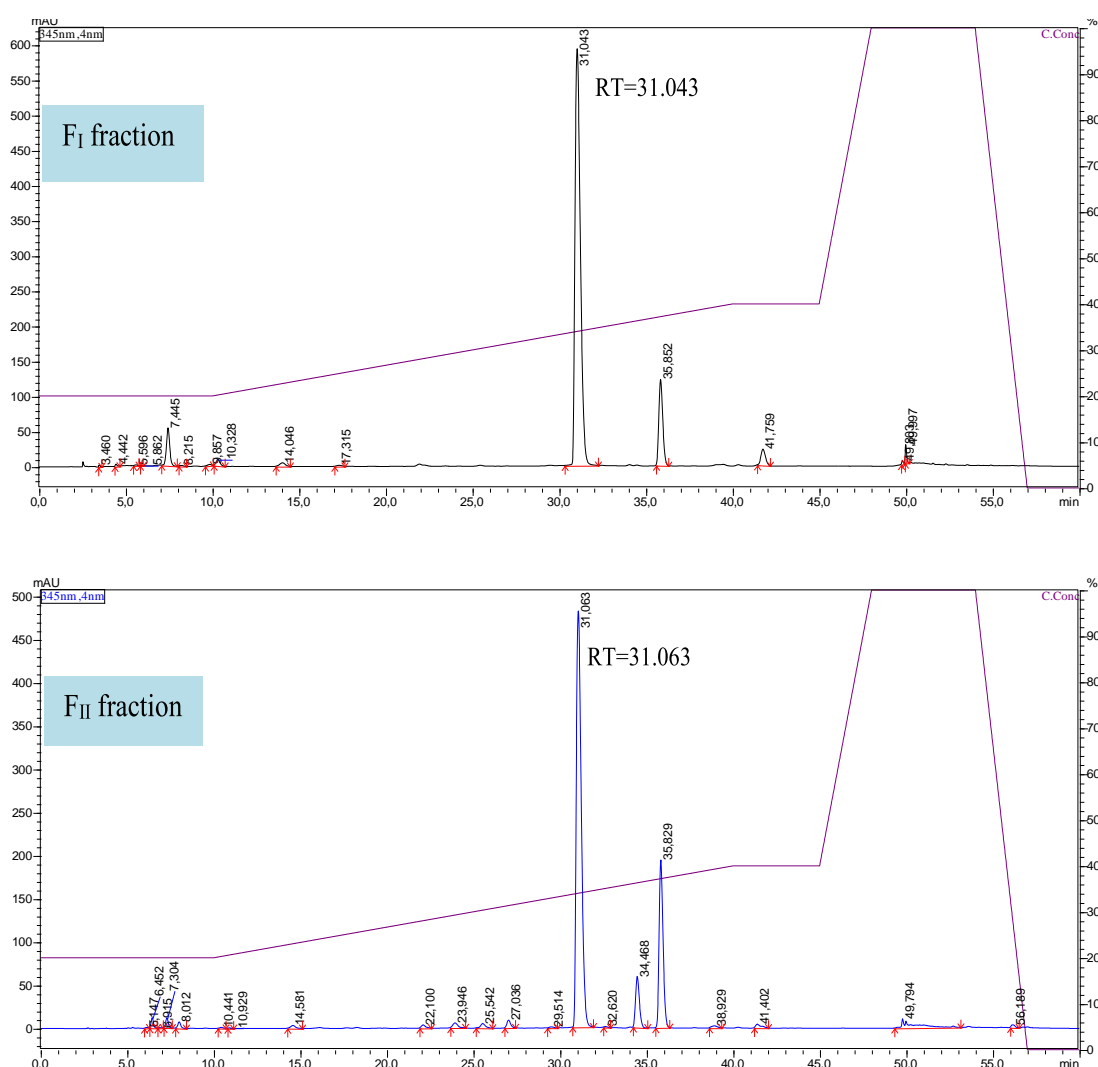


Figure 31: HPLC-UV chromatograms at 345 nm of the two fractions of interest, obtained from a fractionation of the carrot leaf extract. Peaks of interest has RT = 31.043-31.063 min. C18 (150 x 4.6 mm, 3 μ m). A: ACN / H₂O 5/95 + FA 0.1% and B: ACN / H₂O 50/50 + FA 0.1%. Flow 0.7 mL/min.

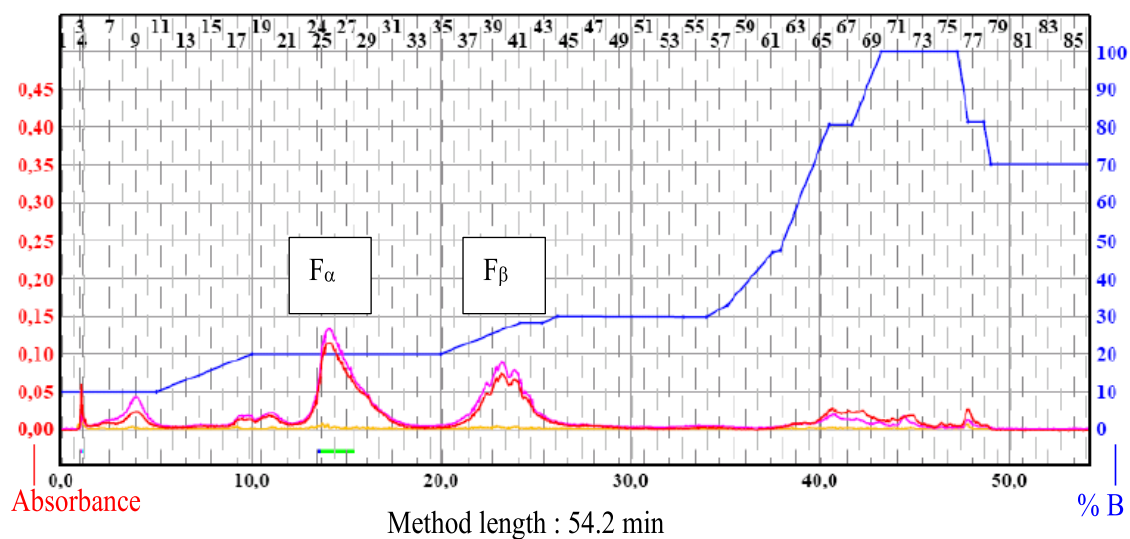


Figure 32: Flash chromatography separation on a 4 g C18 column. Eluent A: ACN / H₂O 5/95 + FA 0.1% and B: ACN / H₂O 50/50 + FA 0.1%. Flow 12 mL/min.

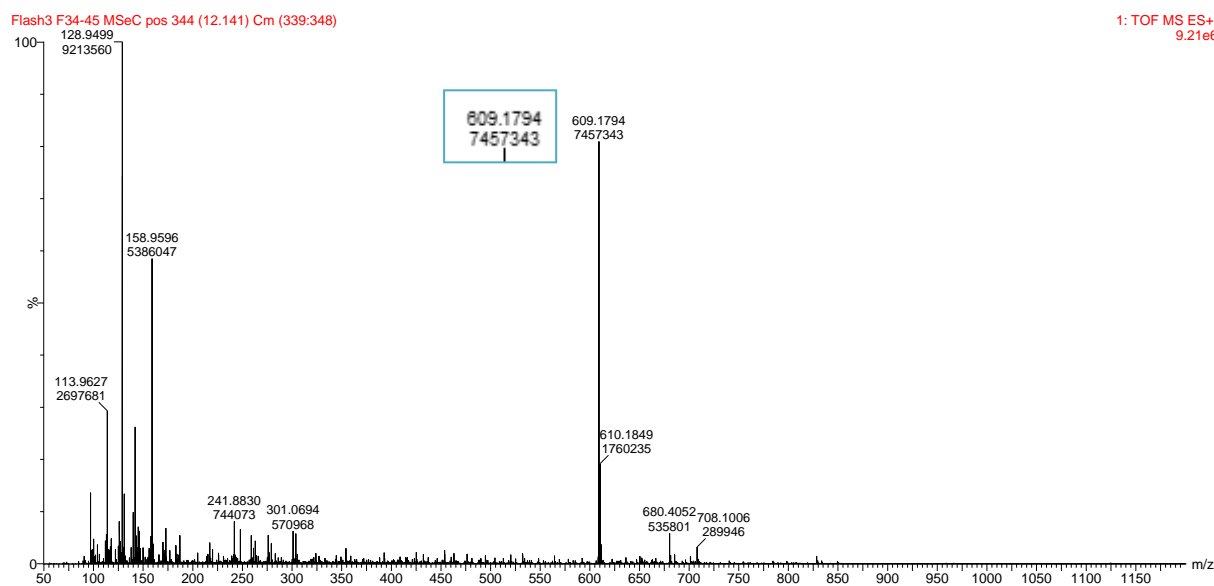
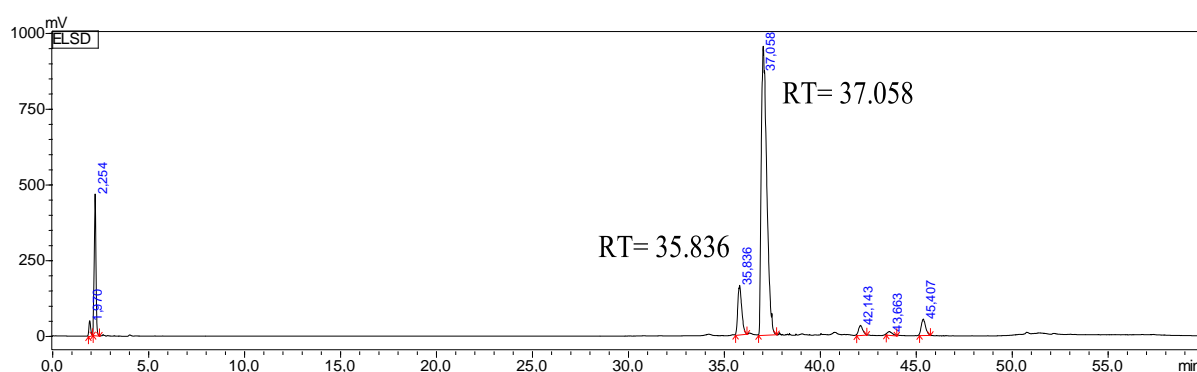
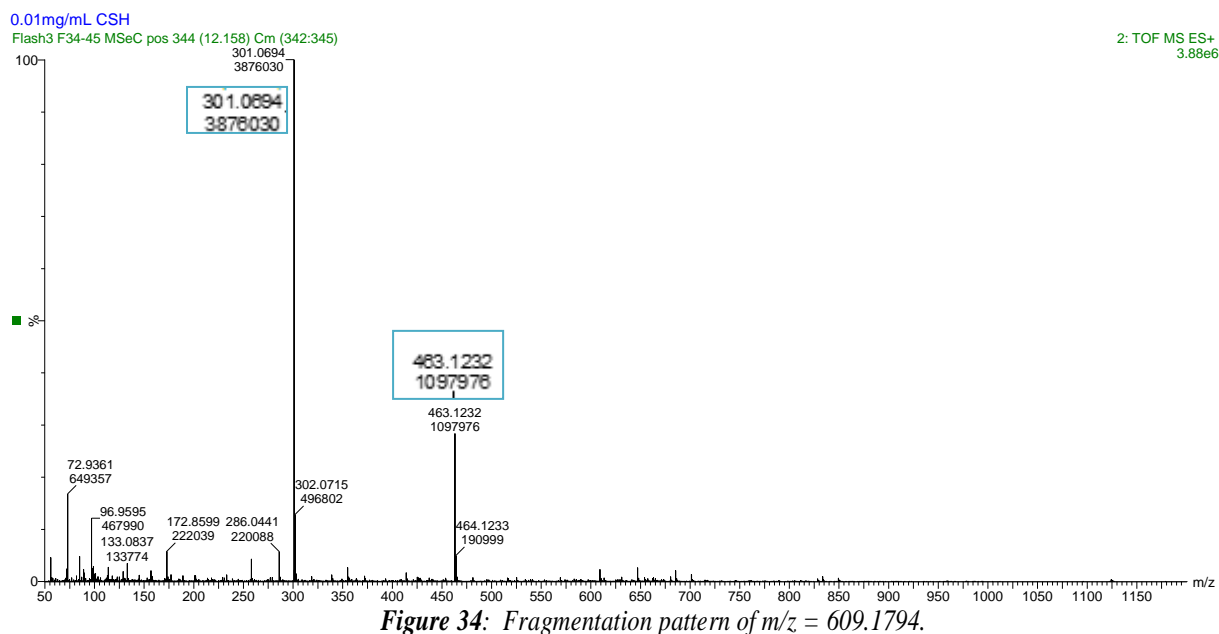


Figure 33: Detection of positive ion with $m/z = 609.1794$.



3.3 Biological activity of the flavonoids of interest

To cope with the limited amount of compounds, a protocol for a slide assay was optimised from an existing protocol in the QuaRVeg team. Its application to the candidate flavonoids required a preliminary adjustment of the culture conditions, taking into account the solubility of the compounds in the culture medium used. The effect of four concentrations (0.2 mM, 0.5 mM, 1 mM and 2 mM) of the candidate flavonoids on *A. dauci* conidia was assessed in terms of conidial germination rate, hypha number per conidium and average hypha surface per conidium. The hyphal surface was used as a proxy for the length of each developed hypha and was measured using an image analysis tool developed for this purpose. The duration of the culture incubation was also set at 4 hours to allow a relatively advanced conidial growth and an automated analysis of individual conidia on the same microscope slide. A further

experiment was carried out on carrot leaves under greenhouse conditions to assess the pathogenicity of *A. dauci* conidia exposed to Api7R and Lut7R at 0.2 and 2 mM.

3.3.1. Development of an image analysis tool

An image segmentation model was developed in collaboration with the ImHorphen team of the IRHS lab, which specialises in digital phenotyping. Different parts of *A. dauci* conidia had to be accurately classified and separated from the background or potential noise, using a random forest model through a training with a set of 32 images acquired from preliminary biological assays. The model was then tested and validated on a larger dataset, consisting of 1959 images. Visual inspection of the segmented images showed that the model accurately predicted the different classes in general, *i.e.* conidial cells, hyphae and the background (**Figure 36**). However, data inspection revealed that the number of hyphae formed per conidium was not correctly predicted by the model, despite a faithful definition of the object class by the model, as portrayed in **Figure 36A** (6 detected hyphae instead of 8) and **Figure 36B** (3 instead of 5). This occurred when hyphae were distributed in too different planes or when the bases of several hyphae were very closed to each other. For this reason, the number of hyphae per conidium was manually counted instead, in the following experiments. Furthermore, noisy images were not successfully segmented as imposing aggregates in the field of view prevented the model from detecting the correct target (**Figure 36C**), or led to an overestimation of a particular class such as hyphal or conidial surface (**Figure 36D**). Based on these observations, additional steps had to be implemented in the preparation of the microscope slides, in order to discard mycelial fragments or aggregates from the culture. During the light microscopic visualisation of the slides, only images of individual conidia were captured for a more accurate estimation of the total hyphal surface area per conidium and the extent of the conidial cells. The quality of the subsequent images was set as in **Figure 36A** and **Figure 36B**.

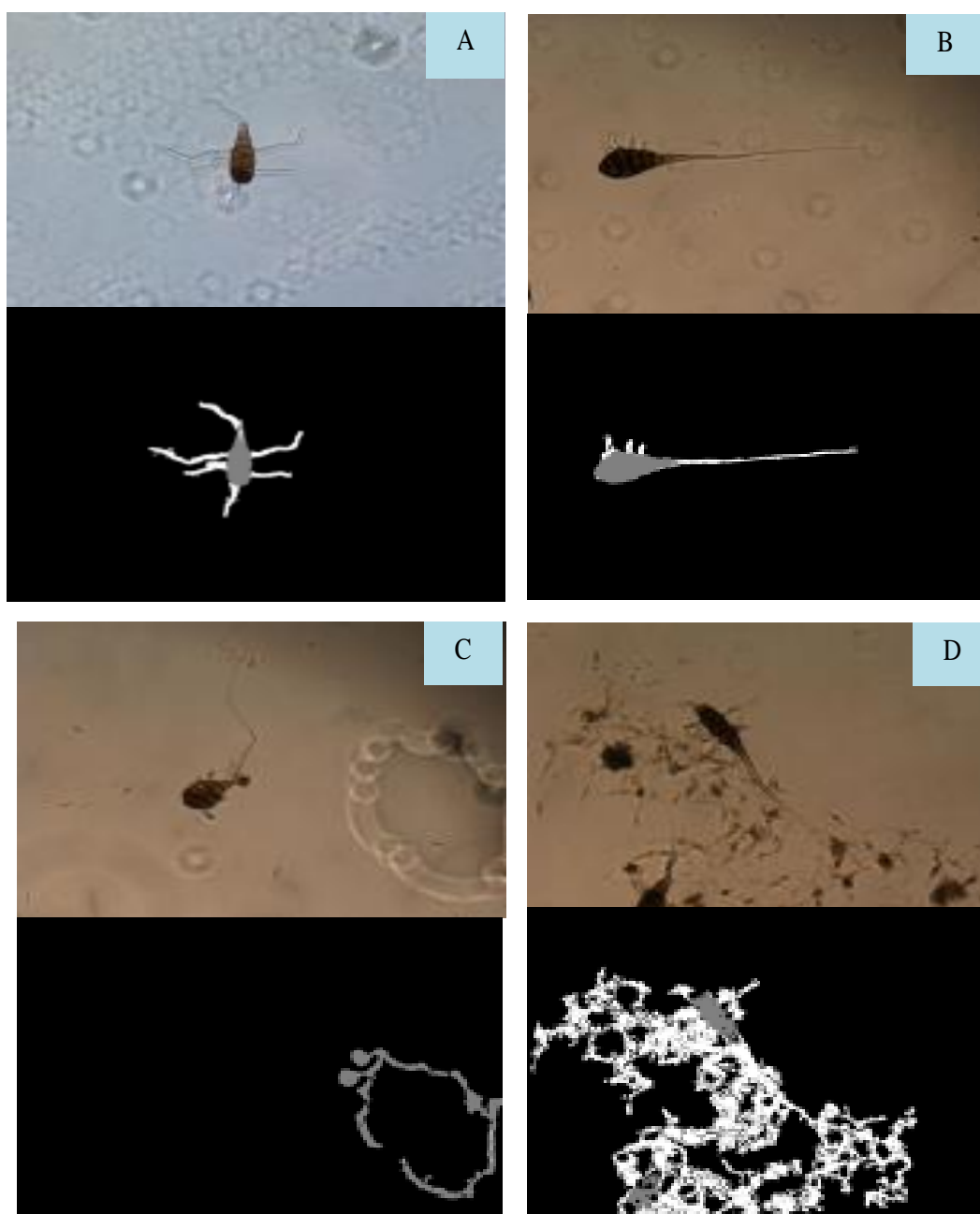


Figure 36: Performance of the model in different backgrounds and image quality during the testing phase of a new image analysis tool. Detected hyphae are coloured in white and conidial cells in grey.

3.3.2. Effect of the tested compounds on conidial germination

The germination rate of *A. dauci* conidia in the different treatments was related to the control condition (DMSO), which showed a relatively wide range of variation. During the evaluation of Api7R and Lut7R, this baseline DMSO was rather low, between 25-50% (**Figure 37**, **Figure 38**), whereas it was between 70-90% during the evaluation of the F_β fraction containing 73% of Chry7R (**Figure 39**). This suggested that the activation of the germination process was not homogenous between conidia, with some germinating more rapidly than others, and in the first case (evaluation of Api7R and Lut7R) because of ambient conditions the experiment would probably required a bit longer incubation time. Nonetheless, this discrepancy did not interfere with the evaluation of the different solutions, as the germination

process still occurred in both cases. In this context, it was observed that Api7R significantly accelerated the germination process of *A. dauci* conidia ($p < 0.05$) from 0.2 mM to 1 mM but not at 2 mM, compared to the DMSO treatment (**Figure 37**). From a practical point of view, a similar effect would also be worth considering at 2mM, but the statistical method used may not have detected the difference due to the lower number of replicates in this modality (3 instead of 4). With respect to the concentrations used, the above-mentioned effect was observed at the lowest concentration (0.2 mM), where almost a complete germination of all conidia observed was achieved. This trend was maintained in the modalities with a slight decrease as the solution became more concentrated in Api7R, although the difference between groups was not evaluated at this stage. In the same series of tests, Lut7R was shown to have the same effect on the germination of *A. dauci* conidia (**Figure 38**). The germination rate was also relatively high, with a slight decrease from 1 mM to 2 mM.

In the other set of tests (F_β fraction), where conidia germinated more rapidly in the control condition, a gradual decrease in germination rate was observed as the concentration of Chry7R in the F_β fraction increased, although this difference was not statistically significant ($p > 0.05$) from 0.2 mM to 1 mM (**Figure 39**). However, the statistical significance observed at 2 mM may have come from data scatter, resulting in a false positive, which is further highlighted by comparing the fold change in germination rate between treatments (**Figure 40**).

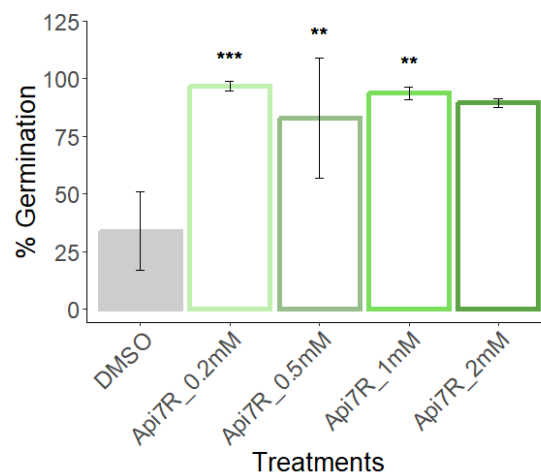


Figure 37: Effect of *ApiR* on the conidial germination.

Kruskal-wallis test, $p = 0.015$. 4. Four replications of 100 conidia per modality except at 2mM (three replications). Symbols signify Conover's comparing groups to DMSO as the reference group: **** $p < 0.0001$, *** $p < 0.001$, ** $p < 0.01$, * $p < 0.05$, . $p < 0.1$. Error bars display standard deviations.

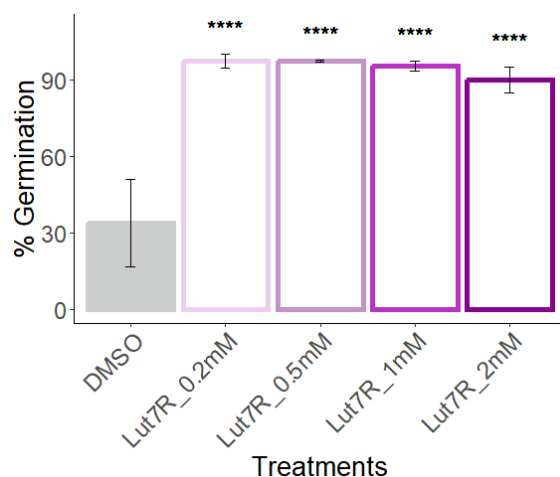


Figure 38: Effect of *Lut7R* on the conidial germination.

ANOVA on power transformed data (Boc-Cox), $p = 4.51 \times 10^{-10}$. Four replications of 1000 conidia per modality. Symbols signify Dunnett's comparison test to DMSO as a reference group: **** $p < 0.0001$, *** $p < 0.001$, ** $p < 0.01$, * $p < 0.05$, . $p < 0.1$. Error bars display standard deviations.

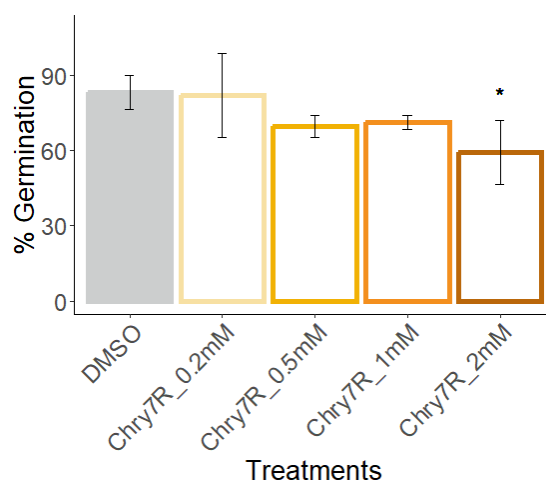


Figure 39: Effect of the F_{β} fraction (containing 73% *Chry7R* and 8.7% *Api7R*) on the conidial germination.

ANOVA with Welch's correction, $p = 0.041$. Four replications of 100 conidia per modality. Symbols signify Dunnett's test significance referring to DMSO as the reference group: **** $p < 0.0001$, *** $p < 0.001$, ** $p < 0.01$, * $p < 0.05$, . $p < 0.1$. Error bars display standard deviations.

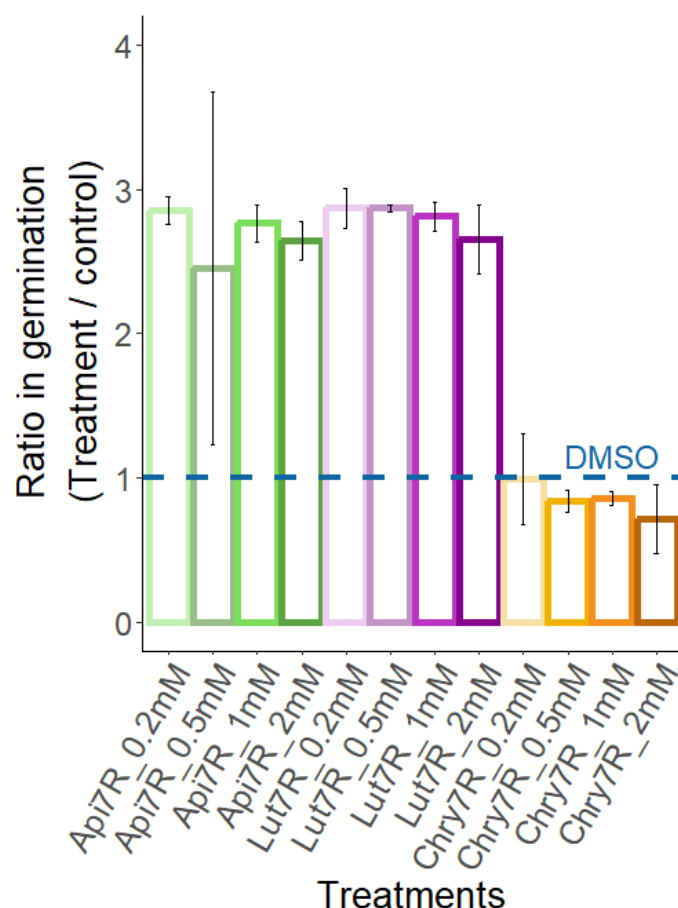


Figure 40: Effect of different concentrations of Api7R, Lut7R and of Chry7R (contained in the F_{β} fraction) on the conidial germination.

Y axis represent the fold change of the germination percentage. Dashed horizontal line refers to the control condition (1% DMSO). Error bars display standard deviations.

3.3.3. Effect on hyphal number and growth

In view of the clear stimulatory effect on conidial germination exhibited by Api7R and Lut7R, the investigation continued with a close examination of the hyphae formed. Visual examination of approximately 80 germinating conidia per modality showed no evidence of hyphal disruption in the presence of the tested flavonoids and fractions, as in the control condition at the time of analysis (Table 3, Table 4, Table 5). Even so, a difference was observed in the number of hyphae formed and their surface area. Irrespective of the treatment, relatively larger conidia with a higher number of cells tended to form more hyphae, but these appeared to be shorter compared to the smaller conidia, where they were scarce but relatively long. This observation was supported by the linear regression of conidial area data (proxy for conidial size) on both the number of hyphae and their measured area (proxy for hyphal length) shown in Figure 41, Figure 43 and Figure 45.

For all conidium shapes combined, the stimulation of germination by Api7R was characterised by a germ tube emission from a greater number of conidial cells, compared to DMSO alone. In other words, more conidial cells were activated, resulting in the production of more hyphae per conidium (Table 3, Figure 42). The effect was statistically

significant ($p < 0.05$) at all concentrations, but was even higher at 1 mM and 2 mM (**Figure 42**). The flip side of this was that the measured hyphal area in these groups was indeed smaller than in the groups treated with 0.2 mM and 0.5 mM of Api7R (**Figure 42**). It is important to note, however, that the groups treated with 0.2 mM and 2 mM of the compound were not significantly different in terms of hyphal area, probably due to a few outliers in the 2 mM modality pulling up the mean.











When treated with Lut7R, the conidia also produced more hyphae, compared to DMSO (**Table 4, Figure 44**). The difference was statistically significant ($p < 0.05$), but the group comparison *post hoc* test indicated that the conidial response was comparable at all concentrations, except at 1 mM where it increased slightly (**Figure 44**). The statement about the hypha number-hyphal area relationship was also applicable here, as a reminder, that the relationship between number of hyphae and hyphal area was again applicable, as a reminder that the hyphae were numerous but of smaller area and vice versa. In fact, the hyphae were significantly smaller in area at all concentrations Lut7R compared to DMSO. No significant dose effect was observed, except between 1 mM and 2 mM modalities (**Figure 44**).

Finally, conidia exposed to the F_β fraction had fewer hyphae than in the DMSO group as the concentration in Chry7R increased (**Table 5, Figure 46**), although there was no significant effect on the germination rate. The decrease in the number of hyphae was statistically significant ($p < 0.05$) when the concentration of Chry7R in this fraction was at 1 mM or 2 mM. The area of a hypha in these conditions was on average slightly higher than in the other groups and was only statistically confirmed at 2 mM of Chry7R (**Figure 46**).

To summarise on the results obtained from these *in vitro* tests, an overview is proposed in **Table 6**.

Table 3: Illustration of hyphal growth in two sized *A. dauci* conidial (large and small) exposed to four concentrations of Api7R, in comparison to DMSO.

Object magnification: 250x

	DMSO	
	Api7R 0.2 mM	
	Api7R 0.5 mM	
	Api7R 1 mM	
	Api7R 2 mM	

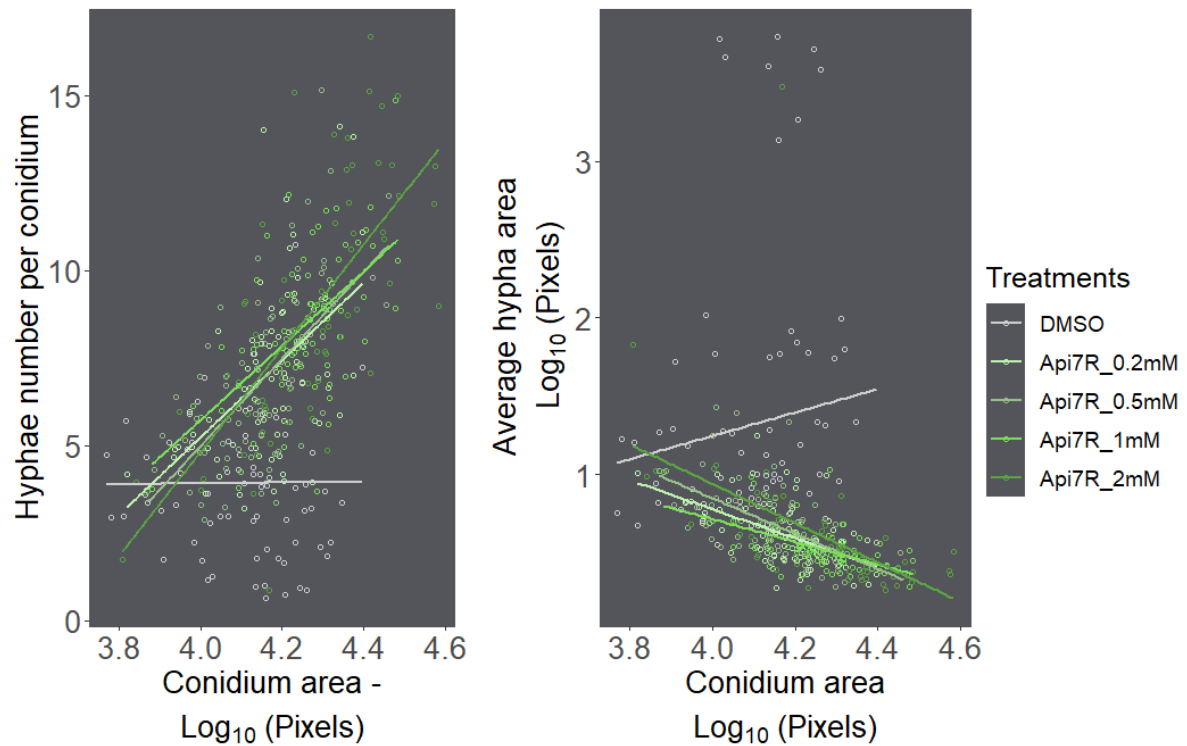


Figure 41: Variation in hypha number (left) and the average area of a hypha (right) on conidia of various size, exposed to four concentrations of Api7R, compared to DMSO.

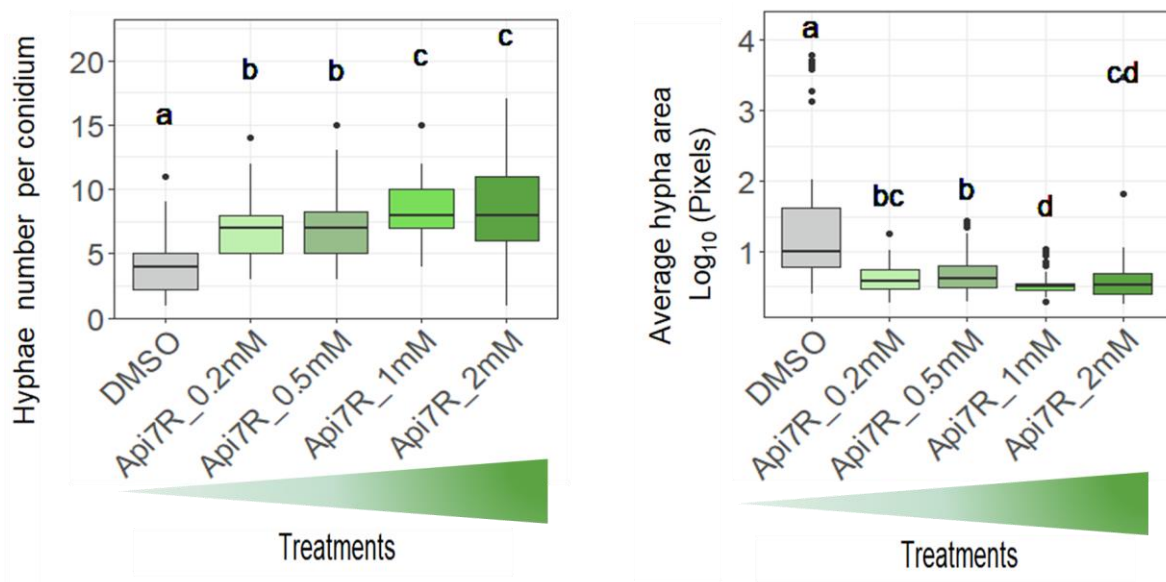












Figure 42: Difference in emitted hyphae number (left) and in the average area of a hypha (right), between modalities treated with four concentrations of Api7R and DMSO.

80 conidia per modality. Hyphae number: Kruskal-Wallis test, $p < 2.2 \times 10^{-16}$. Hypha area: Kruskal-Wallis test, $p < 2.2 \times 10^{-16}$.

Letters display group significant differences from Conover's multiple comparisons test.

Table 4: Illustration of hyphal growth in two sized *A. dauci* conidial (large and small) exposed to four concentrations of Lut7R, in comparison to DMSO.
Object magnification: 250x

	DMSO	
	Lut7R 0.2 mM	
	Lut7R 0.5 mM	
	Lut7R 1 mM	
	Lut7R 2 mM	

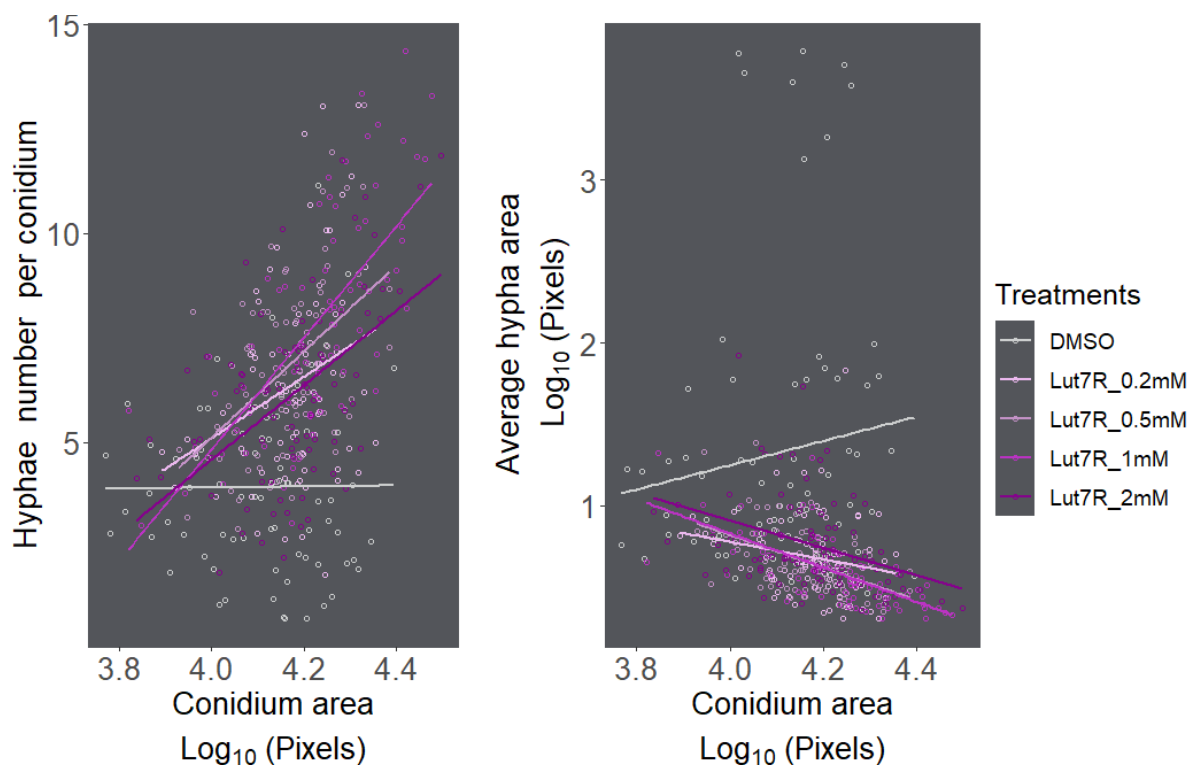


Figure 43: Variation in hypha number (left) and the average area of a hypha (right) on conidia of various size, exposed to four concentrations of Lut7R, compared to DMSO.

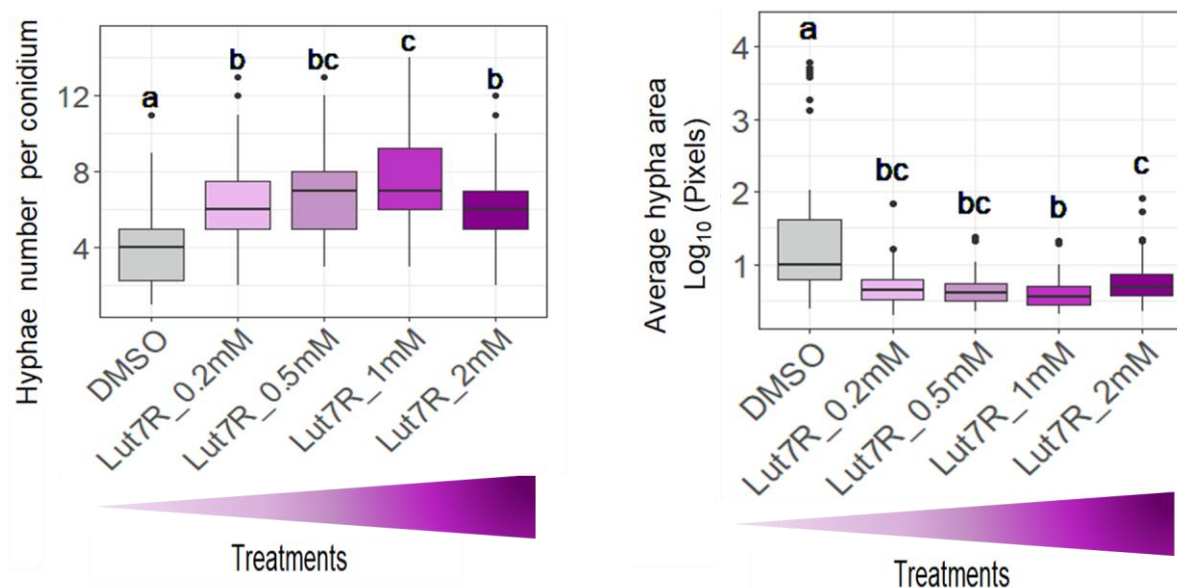












Figure 44: Difference in emitted hyphae number (left) and in the average area of a hypha (right), between modalities treated with four concentrations of Lut7R and DMSO.

80 conidia per modality. Hyphae number: Kruskal-Wallis test, $p < 2.2 \times 10^{-16}$. Hypha area: Kruskal-Wallis test, $p < 2.2 \times 10^{-16}$. Letters display group significant differences from Conover's multiple comparisons test.

Table 5: Illustration of hyphal growth in two sized *A. dauci* conidial (large and small) exposed to four concentrations of Chry7R, in comparison to DMSO.

* A specific amount of the F_{β} fraction was weighted to reach the indicated concentration of Chry7R in the final solution. Object magnification: 200x.

	DMSO	
	Chry7R 0.2 mM *	
	Chry7R 0.5 mM *	
	Chry7R 1 mM *	
	Chry7R 2 mM *	

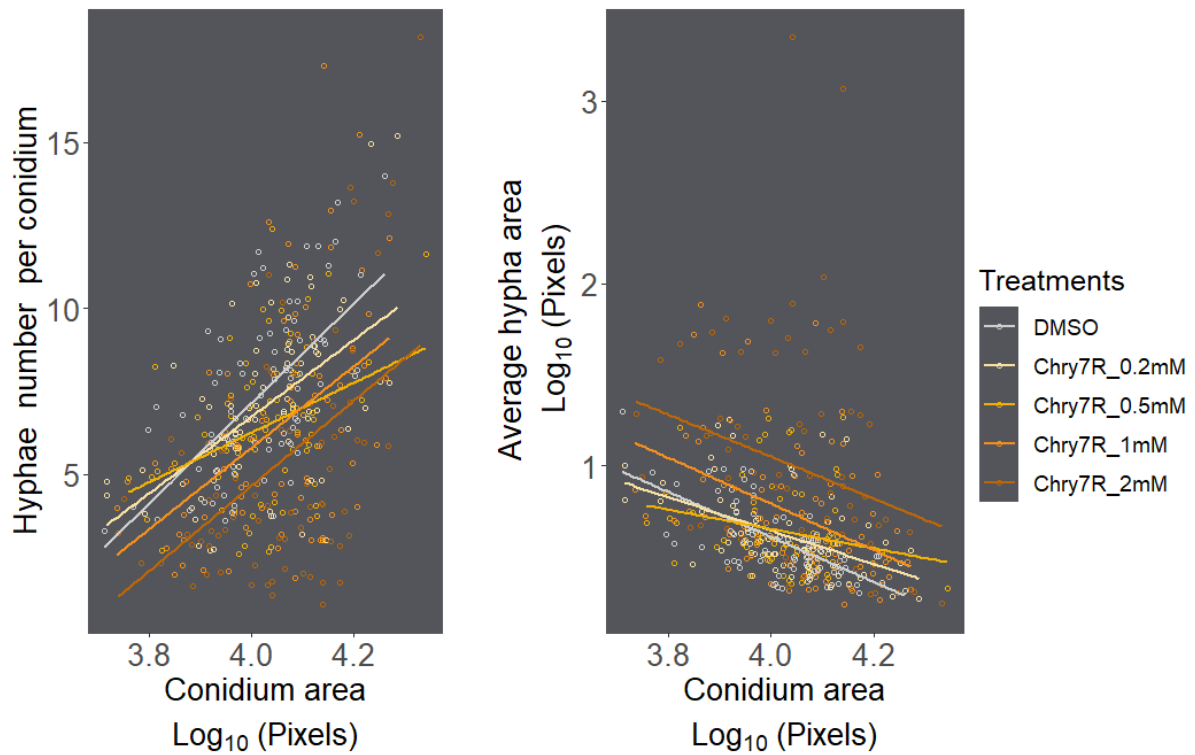


Figure 45: Variation in hypha number (left) and the average area of a hypha (right) on conidia of various size, exposed to four concentrations of Chry7R contained in the F_{β} fraction, compared to DMSO.

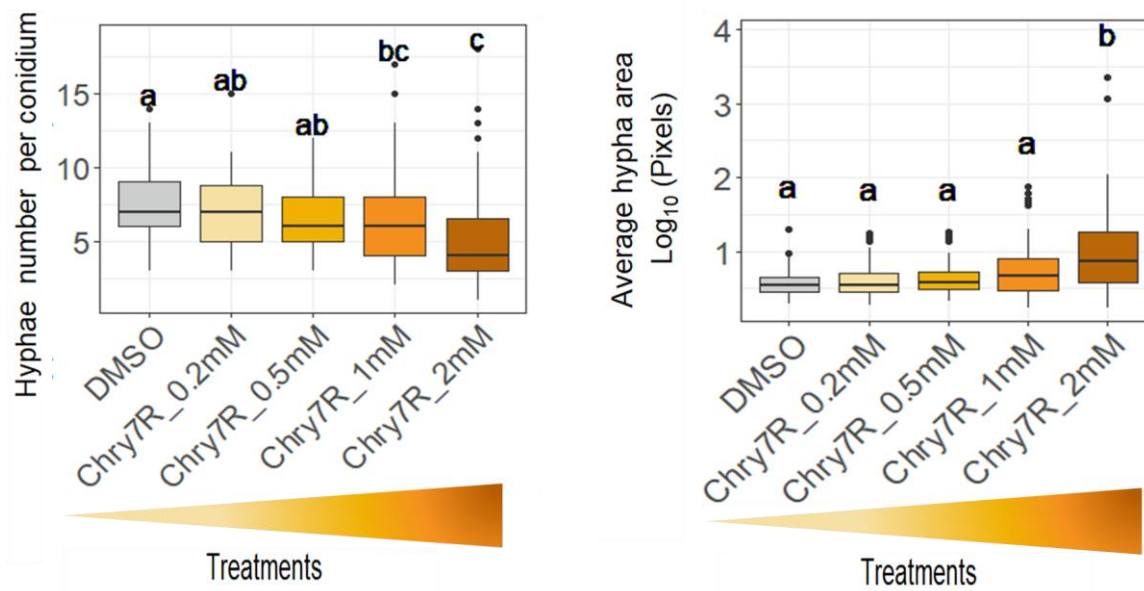


Figure 46: Difference in emitted hyphae number (left) and in the average area of a hypha (right), between modalities treated with four concentrations of Chry7R in the F_{β} fraction and DMSO.

80 conidia per modality. Hypha number: Kruskal-Wallis test, $p = 1.594 \times 10^{-7}$. Hypha area: Kruskal-Wallis test, $p = 9.53 \times 10^{-7}$. Letters display group significant differences from Conover's multiple comparisons test.

Table 6: Overview of the biological activities exerted by the three flavonoids on *A. dauci* *in vitro*.
In brackets are the concentration range in which a significant difference with DMSO was observed.
*final concentration of Chry7R in the F_β fraction (containing 73% Chry7R and 8.7% Api7R).

	Api7R	Lut7R	F _β fraction
Germination	Stimulation (0.2 – 2 mM)	Stimulation (0.2 – 2 mM)	Unchanged (0.2 – 2 mM)*
Germ tube emission	Stimulation (0.2 – 2 mM)	Stimulation (0.2 – 2 mM)	Slight inhibition (1 – 2 mM)*
Average hyphal area	Decrease (0.2 – 2 mM)	Decrease (0.2 – 2 mM)	Increase (2 mM)*

3.3.4. Capacity of the emitted hyphae to infect carrot leaves

So far, in the study, there has been no visible evidence of cellular damage to the hyphae associated with the three flavonoids. As candidates for mediating resistance to ALB in carrots, the pathogenicity of *A. dauci* conidia treated with each of them was of particular interest, given the divergent biological activity exerted *in vitro* by Api7R and Lut7R on the one hand and by the F_β fraction on the other. Unfortunately, the lack of the F_β fraction did not allow us to go any further in deciphering the influence of Chry7R on the onset of the disease on carrot leaves. Hence, this second part of the study focused only Api7R and Lut7R.

The third fully developed leaves of the accession H1 (susceptible to ALB) were inoculated by depositing a total of 50 drops of inoculum on the leaf surface according to the protocol in (Boedo et al., 2010). The assessment encompassed two types of pathological phenotyping of the leaves. Firstly, the number of successful infections was counted at 13 days post-inoculation, assuming that one drop of inoculum contained one conidium. It appeared that leaf infection was initiated at a relatively low rate (nearly 10 spots out of 50) in the DMSO treatment group (**Figure 47**). As suggested by the statistics, a significant number of necrotic spots appeared on leaves where the conidia had been suspended in a given flavonoid solution. It was twice as high as in the reference group, when Api7R was at either 0.2 mM or 2 mM. A similar trend was observed with Lut7R at 0.2 mM, while even more necrosis was found with 2 mM of Lut7R (**Figure 47**).

Furthermore, the percentage of severely blighted leaf surface remained relatively low in the control condition one week later, but increased consistently in the Api7R 0.2 mM group, and to a lesser extent with Lut7R at 0.2 and 2 mM and finally with Api7R at 2 mM (**Figure 48**). Despite these visible trends, the statistical results confirmed a significant difference only between the control and the modalities containing Api7R 0.2 mM, without neglecting a relatively large data scatter in the other groups (**Figure 49**).

Taken together, these observations indicated in all that the presence of Api7R and Lut7R tended to promote the onset of the pathogenic interaction between the carrot leaf and *A. dauci*, suggesting that the emitted hyphae were functional. Yet, regardless of the statistical results, the disease did not seem to progress in the same way not only between the

two compounds but also between concentrations, showing that the influence of Api7R in this process was more pronounced at 0.2 mM and tended to decrease at 2 mM in the vicinity of the Lut7R groups.

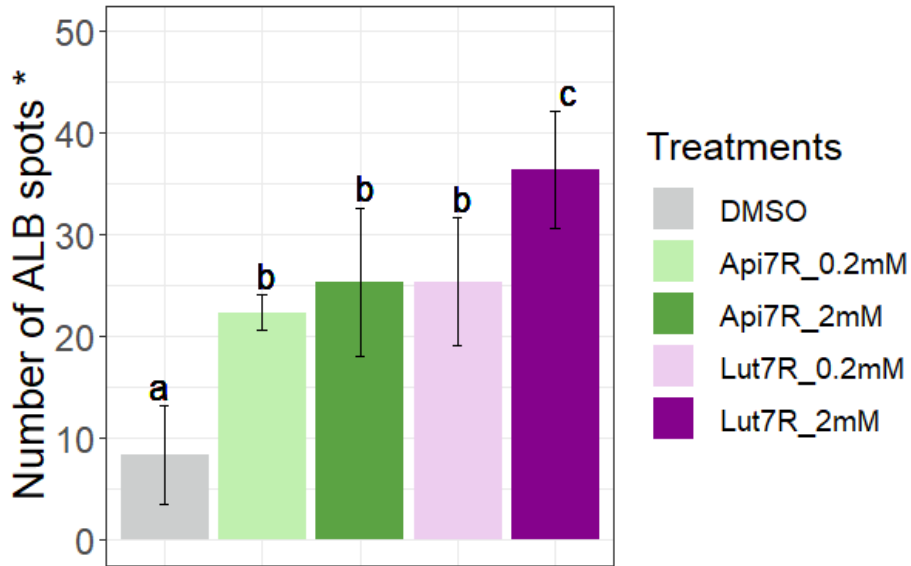


Figure 47: Number of successful infection sites at 13 days post-inoculation over fifty inoculum drops of different treatments applied on the leaf of H1 (Susceptible).

Five replications per modality. ANOVA, $p = 3.901 \times 10^{-6}$. Group differences are displayed by the letters from a Tukey’s multiple comparison test. Error bars correspond to standard deviation.

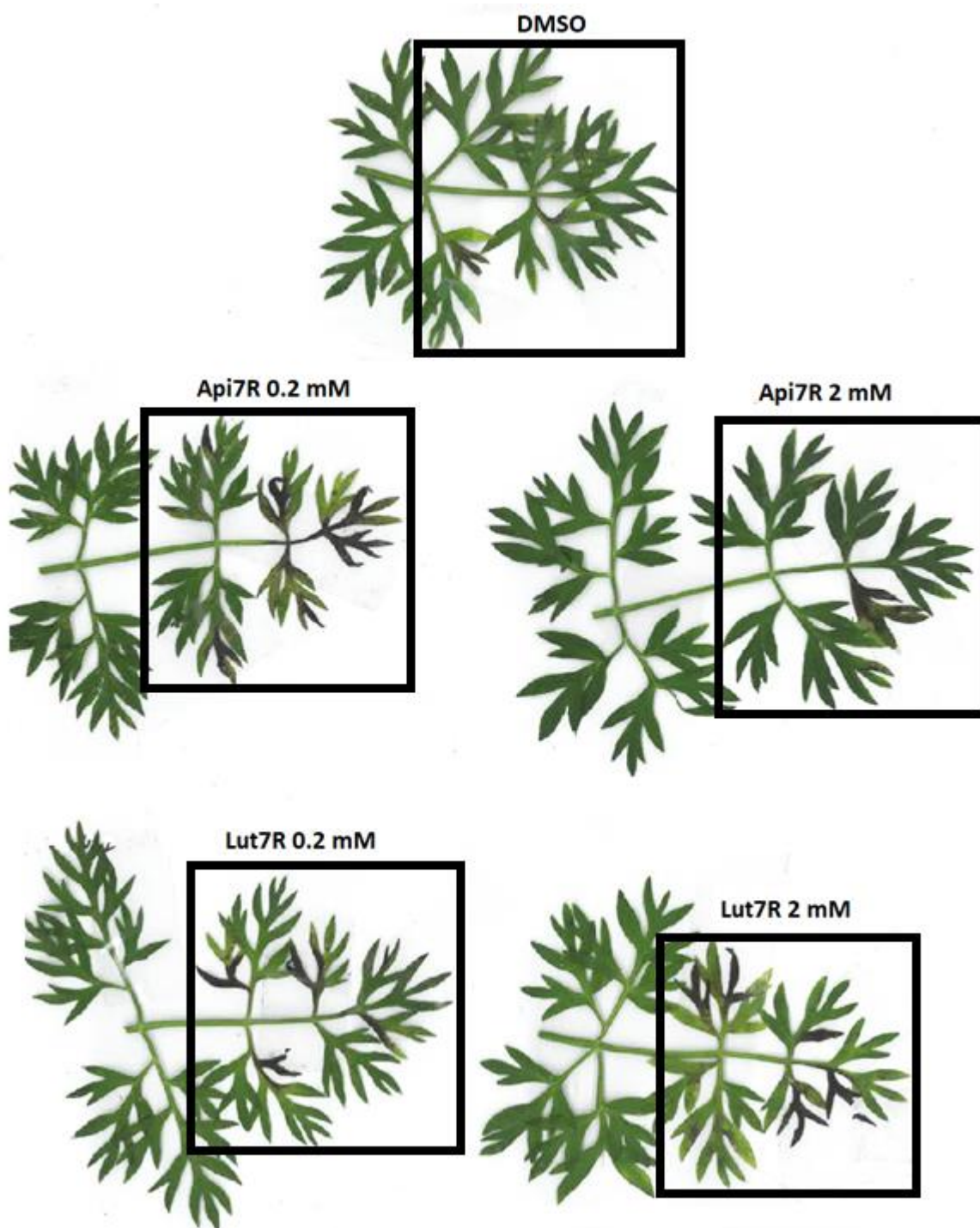


Figure 48: ALB symptom severity at 7 days after the occurrence of necrotic spots (13 days post-inoculation) on leaves of H1 (susceptible), inoculated with *A.dauci* conidia exposed to Api7R or Lut7R at two concentrations or to 1% DMSO. Frames delimit the parts of the leaf surface that were inoculated.

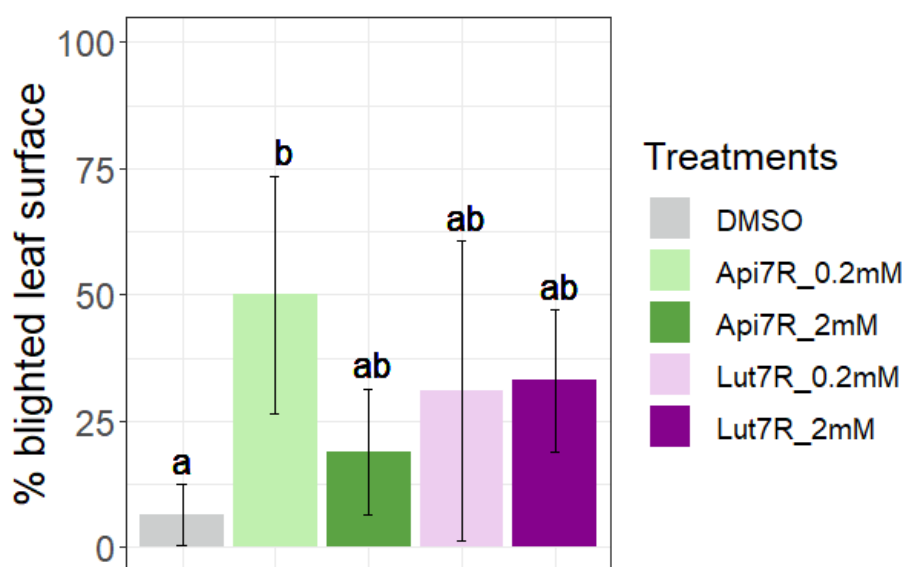


Figure 49: Percentage of blighted leaf surface at 7 days after the occurrence of necrotic spots on the leaves of H1 (susceptible), inoculated with *A. dauci* conidia exposed to Api7R or Lut7R at two concentrations or to DMSO 1%.

Five replications per modality. ANOVA, $p = 0.021$. Group differences are displayed by the letters from a Tukey's multiple comparison test. Error bars correspond to standard deviation.

DISCUSSION AND PERSPECTIVES

The candidate flavonoids were constitutively accumulated in the leaves of the partially resistant accession (I2), suggesting that they may be phytoanticipins. The mechanism of candidate flavonoid-mediated resistance to ALB was unravelled by first investigating a putative direct effect on the pathogen. To this end, an existing *in vitro* assay protocol within the QuaRVeg team (Koutouan et al., 2023) was intended to be applied to the present study. Such a method required a large amount of purified compounds, thus, efforts were made to obtain a relatively consistent amount of each of the candidates. In this process, priority was given to the purification of Lut7R from *Mentha x piperita* (peppermint) and Chry7R from *Daucus carota* leaves, as Api7R was commercially available and affordable, in order to manage time. The fractionation-purification strategy of leaf extracts was efficient for both methanolic *Mentha x piperita* and hydromethanolic *Daucus carota* extracts. This facilitated the next step of purification by reverse phase flash chromatography. The challenge in isolating Chry7R was mainly related to the unmet need for LC-UV-MS data at the beginning of the process during the extraction and fractionation optimisation. Although the collaboration with the team in Colmar was deeply helpful, the need for a different LC method unexpectedly led to a misleading result and to the purification of a co-eluting compound instead. In fact, Chry7R was referred to as the major peak of some fractions, which was not the case. This partially explained the low amount of Chry7R obtained from the process, in addition to the low content of this compound in the carrot leaf extract. Actually, the selected carrot accession was relatively the most enriched in this compound compared to others in our in-house collection, but essentially this compound was quite low in the leaves to allow efficient purification of a consistent amount. Unless a

more enriched candidate source is identified in the future, the extraction-fractionation-purification process will have to be repeated on the actual accession to access a new batch of Chry7R that could be further purified to achieve a higher level of purity.

Given the relatively limited amount of purified flavonoids, the context did not allow the process to continue with the previously established bioassay protocol as it was. Hence, the fine-tuning of a slide culture assay protocol was really instrumental in reducing the experimental scale and overcoming this issue. This preliminary phase took some time, as here was a need to identify the most suitable medium as well as the compound concentrations to be applied. The concentration range of the candidate flavonoids in the leaves of I2 (partially resistant) was estimated to be around 0.5 mM on the basis of previous metabolite quantification. It was also important to find the right volume of solvent preparation, which would allow good solubility of the flavonoids, in order to avoid any side effect on the conidia. In addition, the optimal incubation time was determined and several systems to stop fungal growth (adding acetic acid, storing the slides at 4 °C or -80 °C) prior to imaging were tested. There was also a need to define a method for measuring conidial attributes on thousands of images in a relatively reasonable time. Thus, two *in vitro* assays were actually carried out, but the methodology was not fully refined during the first series of tests (**Appendix - Figure 9**, **Appendix - Figure 10**). Nevertheless, the results are consistent with those described in this chapter. Firstly, it was noted that there were inter-day variabilities between control groups, assumed to come from the varying temperature in the laboratory during conidial preparations. For this reason, treatment groups were only referred to their respective control group and therefore comparisons between different compounds were compromised. The results showed that Api7R and Lut7R had a stimulatory effect on the germination of *A. dauci* conidia, reaching 3 times higher than in DMSO whereas no apparent effect was observed with the F_β fraction (73 % Chry7R and 8.7 % Api7R), confirmed by the second experiment (**Appendix - Figure 8**). In the control condition, not all cells of a relatively large conidium were germinating at the time of observation (4h post-incubation). More specifically, *A. dauci* conidia are multinucleate and each cell that forms the conidial body has the potential to germinate and develop an hypha. The stimulatory action exerted by Api7R and Lut7R resulted in hyphal outgrowth from several cells of the conidia, leading to a higher number of hyphae per conidium than in the control condition. However, this difference was less evident in relatively small conidia. In addition, there seemed to be an inversely proportional relationship between the number of hyphae per conidium and their size. This could be interpreted, in terms of the energetic cost of growing longer hyphae, suggesting that a large conidium would theoretically have to expend energy on several cells at once, as opposed to smaller conidia where the denominator would be lower. But more than that, this biological activity was strikingly at odds with the conventional wisdom about a compound that qualifies as a phytoanticipin (Oros and Kállai, 2019). Not only did the presence of either flavonoids stimulate hyphal formation, but the hyphae also appeared just as intact as in the control condition.

With five repetitions, despite the time and molecules shortages that prevented from further replications, *in planta* bioassays on the susceptible H1 carrot accession clearly demonstrated the ability of these hyphae to penetrate and infect the carrot leaf, thus promoting the onset of pathogenesis observed 13 days post-inoculation. Despite the

scarcity of necrotic spots in the control condition, the amplitude of the infection rate in the presence of these flavonoids generally reflected the stimulation of the pathogen observed *in vitro*, although it was higher for Lut7R 2 mM than for the others. Even so, in the DMSO modality, it could be that not all inoculum drops contained a conidium as expected, or that the germination rate was simply very low. Microscopic observation would have helped to ensure that the leaves were homogeneously inoculated under all conditions. In any case, it is likely that the biological activity of these two compounds does not involve alteration of hyphal functionality in *A. dauci*.

Disease progressed more in the presence of the flavonoids than with DMSO, one week after necrotic spots were observed, *i.e.* 20 days post-inoculation. Regarding the control condition, disease severity ratings in greenhouse pathological test usually require about 4 weeks after inoculation to observe a well-developed symptom in the H1 accession. Therefore, this result may not be of concern from this point of view. However, between Api7R and Lut7R, it appears that the disease generally progressed more slowly when the conidia had been exposed to Lut7R regardless of the concentration (0.2 and 2 mM) or to Api7R but only at a relatively high concentration (2 mM), despite a visible intra-group variation (**Appendix - Figure I2** for illustration). These results may highlight a putative fungistatic activity in terms of mycelial development. In this sense, Api7R would be a less efficient fungistatic compound compared to Lut7R. Certainly, this would have been confirmed by extending the *in vitro* test to this stage of fungal growth. Nonetheless, this hypothesis could be relevant and in line with the observations made by Boedo and colleagues years ago. In this respect, *A. dauci* conidia produced more germ tubes when inoculated on leaves of Boléro (partially resistant) than on Presto (susceptible), although the disease progressed more slowly on the partially resistant cultivar (Boedo et al., 2010). Moreover, as seen in the previous chapter and in (Koutouan et al., 2018), Boléro had a similar profile to I2 in terms of candidate flavonoid enrichment. Furthermore, it cannot be excluded that the exogenous application of the flavonoids, contained into the inoculum in the current experiment, had limited the ALB symptom by (also) exerting a protective effect on the leaf tissue if applied on the leaves before the conidial solution because of the antioxidant properties of the flavonoids. It has been reported that Lut7R has a relatively more efficient free radical scavenging activity than Api7R, which is related to the presence of the catechol group in the ring B of luteolin (Kim et al., 2000; Wang et al., 2003; Nagy et al., 2009). The physiological response of the leaf treated with the flavonoids only was not considered in the current experiment, but could be further investigated to corroborate this hypothesis. The inclusion of I2 in the evaluation would also allow a better understanding of the observations made.

Evaluation of the biological activity of the F_β fraction, in the counterpart, pointed out that Chry7R does not seem to have any effect on the conidial germination in term of percentage of germinated conidia. However, it was found that *A. dauci* conidia produced significantly fewer hyphae at 1 mM and 2 mM of Chry7R than in the control condition. It is important to remind that at these concentrations of Chry7R, Api7R reached 0.16 mM and 0.33 mM in the fraction, respectively. The stimulatory effect of Api7R is therefore expected to be visible as in the previous tests at least in the last modality. The scenario of an inhibitory effect would therefore prevail in the hypothesis of a possible buffering with the activity of Api7R. Pending the availability of reasonably pure Chry7R, it is also important to consider that an unidentified peak eluted at RT= 2.254 min was also present in this fraction at 11.5 % (**Appendix - Table 1**). According

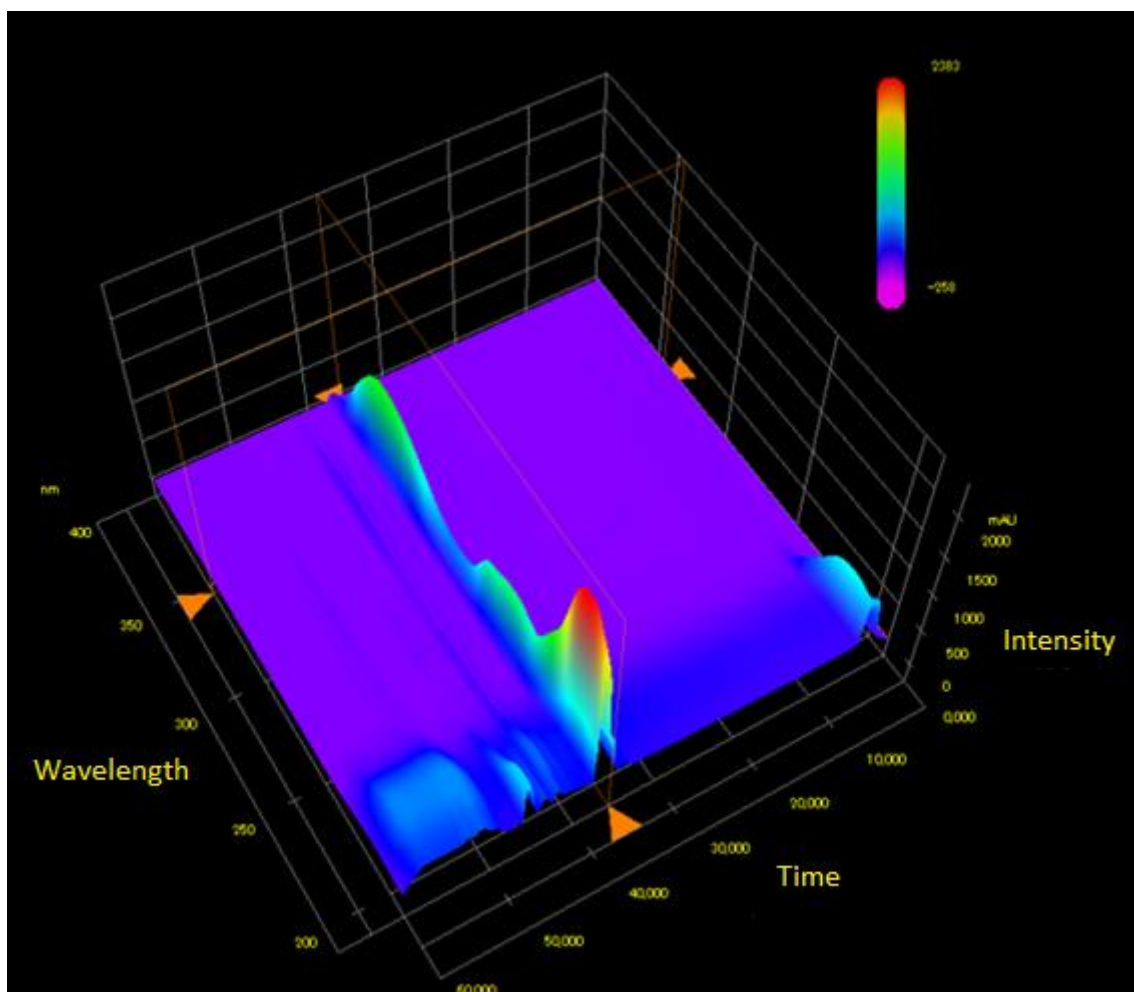
to the absorption spectra of the detected compounds from the HPLC-DAD analysis, this peak would be neither a flavonoid nor a phenolic compound (Plazonić et al., 2009; Argentieri et al., 2020; Kaeswurm et al., 2021). It is also possible that it corresponds to an injection artefact, meaning the F_β fraction would be of higher purity than presented in this manuscript. In view of this, it is crucial to obtain Chry7R with a very high degree of purity in order to provide substantial evidence, *in vitro* and on carrot leaves, as has already been done for Api7R and Lut7R.

In summary, several answers were obtained to the initial research questions. The candidate flavonoids had a direct effect on *A. dauci* conidia with an apparently opposite effect *in vitro*, between that of Chry7R and the others, although it has not yet been rigorously elucidated for the former. The stimulation of pathogenesis by Api7R and Lut7R on the carrot accession studied was followed by a slow progression of the disease, but more pronounced with Lut7R. This raises the question of whether the observed protective effect is still linked to a direct effect on *A. dauci* or whether it is a consequence of an induced defence response in the host. The defence reaction in the leaves can be evaluated using the high throughput gene expression tool qPFD®, which has already been used by the QuaRVeg team in previous evaluations of elicitors in carrot accessions. So far, these results do not allow us to conclude how important the candidate flavonoids are in the process of ALB resistance, among other bioactive compounds that could be found in the leaves of I2. Bio-guided fractionation of carrot leaf extracts would shed more light on this. Regarding the diversity of the pathogen, a conidial strain of intermediate aggressiveness was used in the current evaluation. It is known that several strains of *A. dauci* are differentially aggressive towards carrot genotypes, but with no significant genotype x cultivar interaction (Boedo et al., 2012; Le Clerc et al., 2014). The consistence of a flavonoid-mediated resistance could still be considered in the future as part of a biological activity assessment on a wider range of fungal strains.

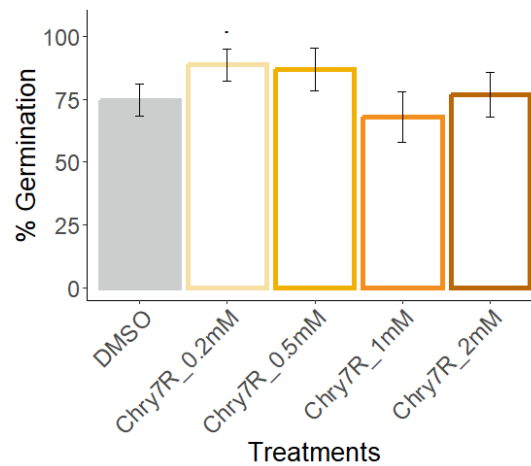
APPENDICES

Appendix - Table 1: HPLC-ELSD data of the F_{β} fraction.
Brown: unknown compound, blue: Api7R, green: Chry7R.

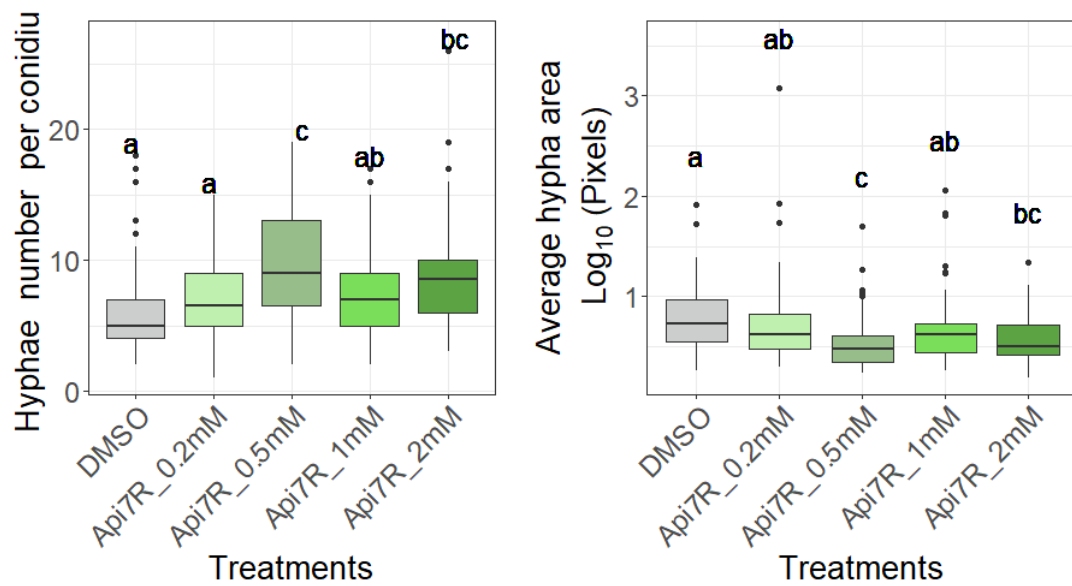
Ret. Time (min)	Area	Area%
1,970	298760	1,158
2,254	2958831	11,472
35,836	2250401	8,725
37,058	18893027	73,250
42,143	446097	1,730
43,663	162198	0,629
45,407	783136	3,036
	25792451	100,000



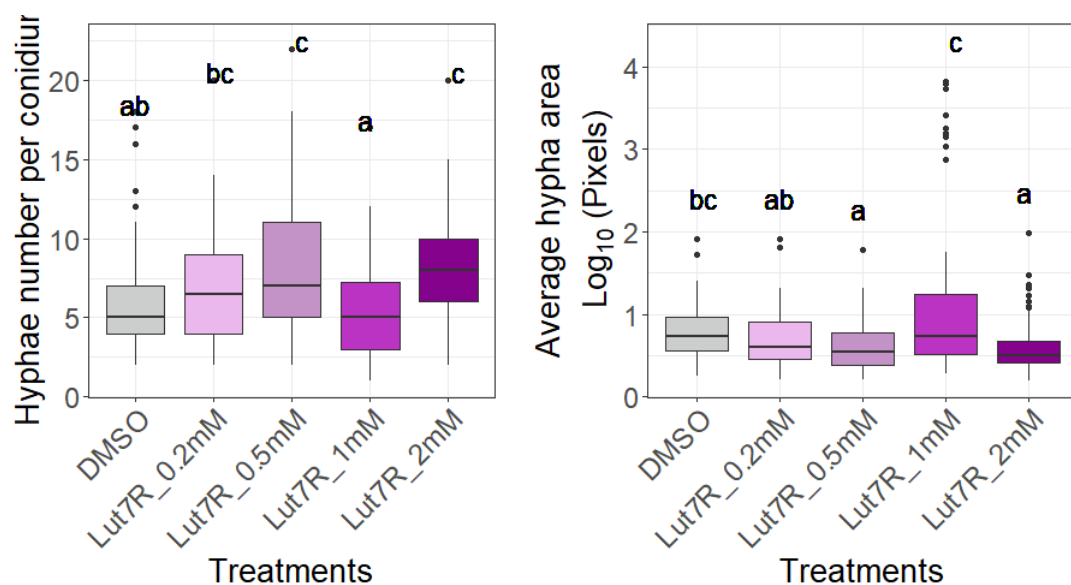
Appendix - Figure 7: 3D representation of the Fb fraction HPLC-DAD chromatogram.
Y axis: Wavelength (nm), X axis: Time (min), Z axis: Peak intensity.



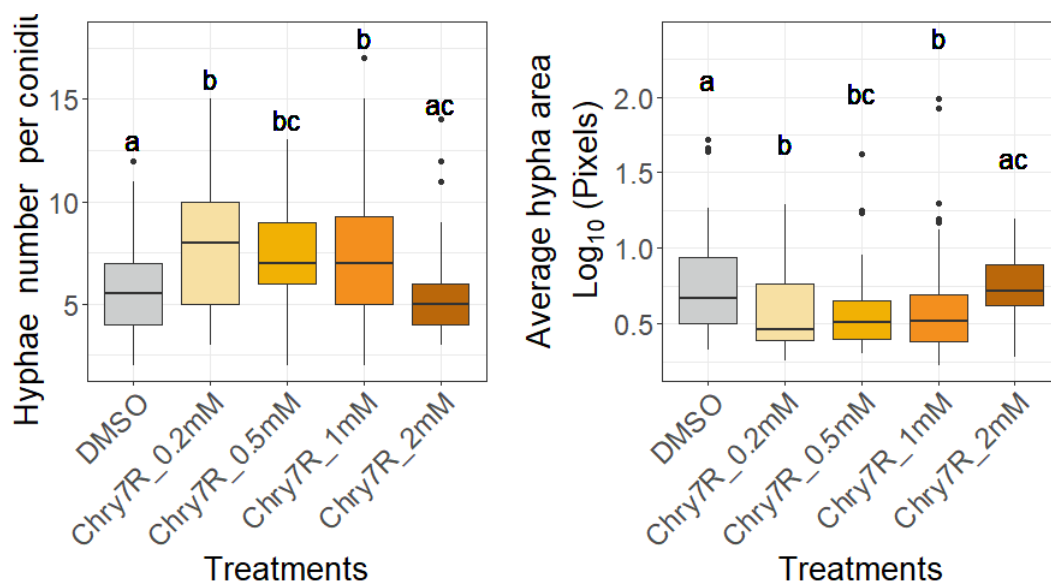
Appendix - Figure 8: Second in vitro assay assessing the effect of the F_{β} fraction on the germination of *A. dauci* conidia. ANOVA $p = 0.014$. Four replications of 100 conidia per modality, Symbols display Dunnett's test: **** $p < 0.0001$, *** $p < 0.001$, ** $p < 0.01$, * $p < 0.05$, . $p < 0.1$. Error bars indicate standard deviation.



Appendix - Figure 9: Preliminary vitro assay evaluating the effect of Api7R on the hyphal growth. 80 conidia per modality. Hyphae number (left): ANOVA on power transformed data, $p = 1.408 \times 10^{-7}$. Letters display Tukey's multiple comparison test. Hypha area (right): Kruskal-Wallis test, $p = 2.316 \times 10^{-6}$. Letters display group significant differences from Conover's multiple comparisons test.



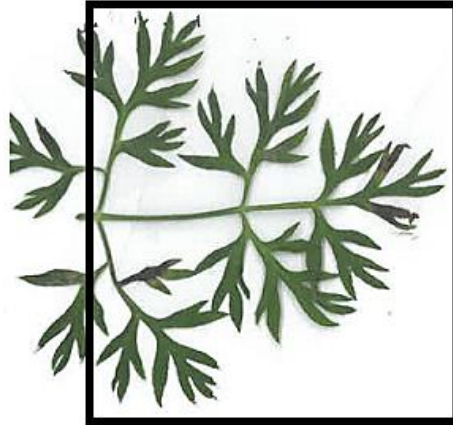
Appendix - Figure 10: Preliminary vitro assay evaluating the effect of *Lut7R* on the hyphal growth. 80 conidia per modality. Hyphae number (left): ANOVA on power transformed data, $p = 7.215 \times 10^{-7}$. Hypha area (right): ANOVA on power transformed data, $p = 8.499 \times 10^{-7}$. Letters display Tukey's multiple comparison test.



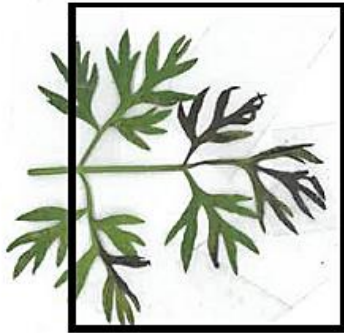
Appendix - Figure 11: Additional in vitro assay evaluating the effect of F_{β} fraction on the hyphal growth. 80 conidia per modality. Hyphae number (left): Kruskal-Wallis test, $p = 0.0001$. Hypha area (right): Kruskal-Wallis test, $p = 6.483 \times 10^{-5}$. Letters display group significant differences from Conover's multiple comparisons test.

Rep. 2

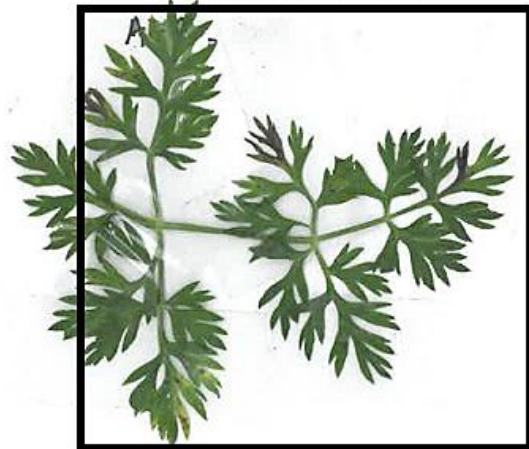
DMSO



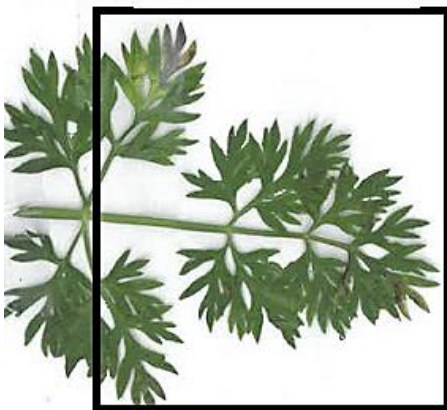
Api7R 0.2 mM



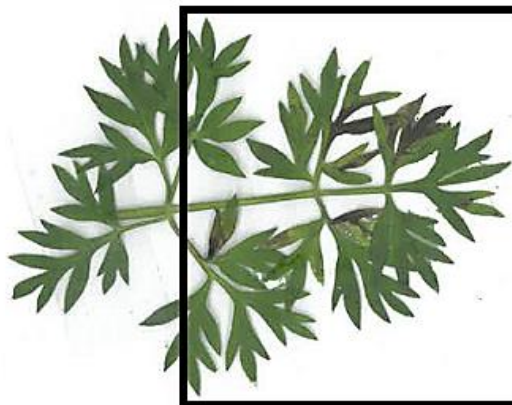
Api7R 2 mM



Lut7R 0.2 mM

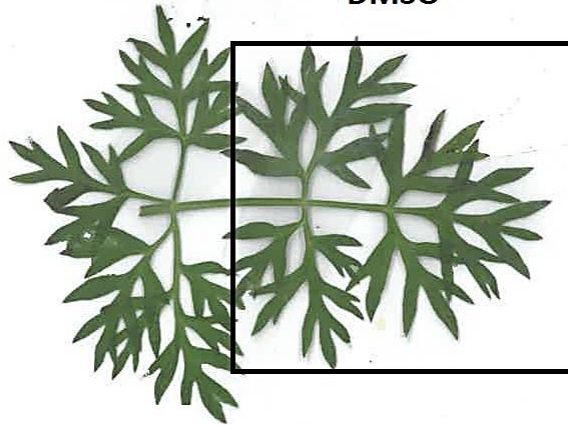


Lut7R 2 mM

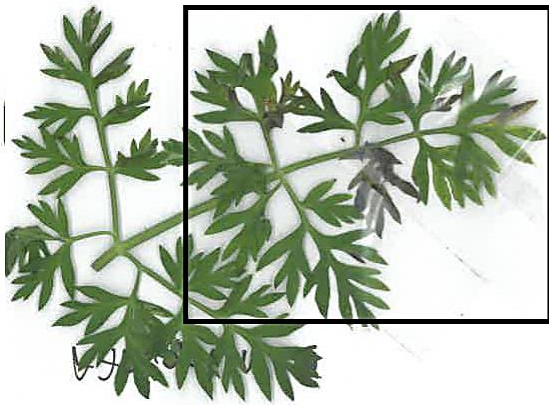


Rep.3

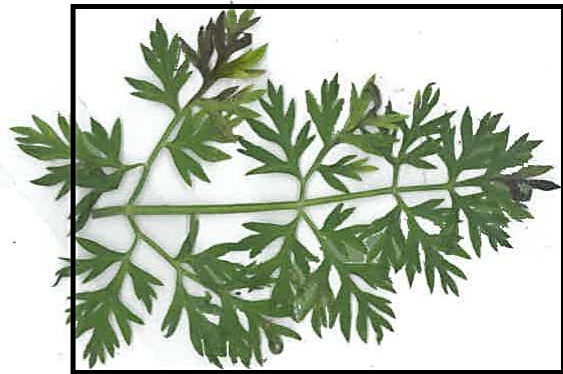
DMSO



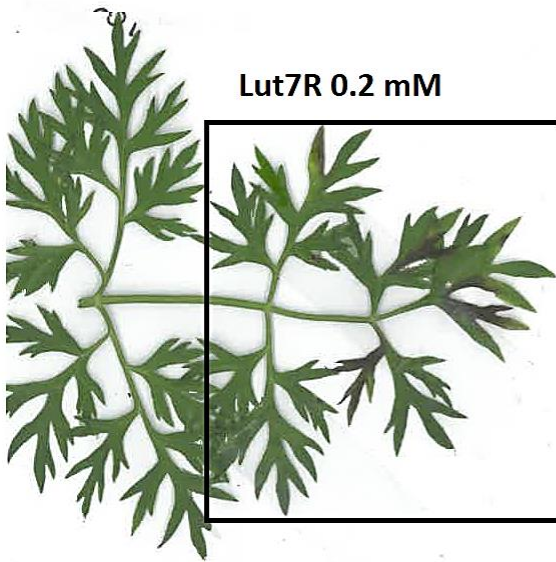
Api7R 0.2 mM



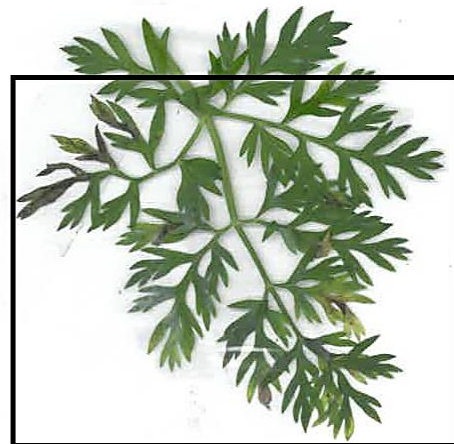
Api7R 2 mM



Lut7R 0.2 mM

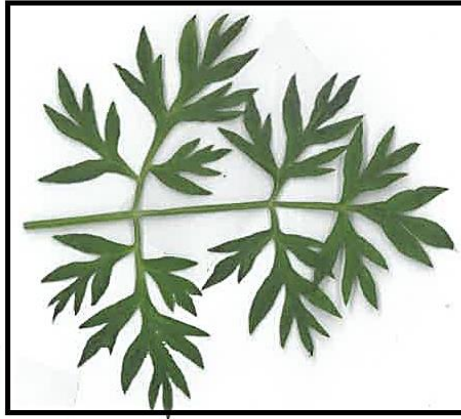


Lut7R 2 mM

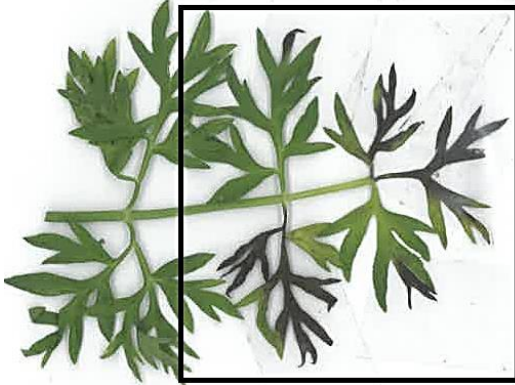


Rep.4

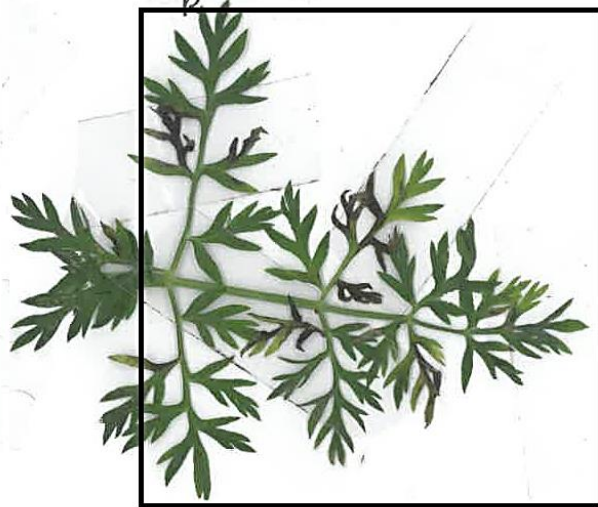
DMSO



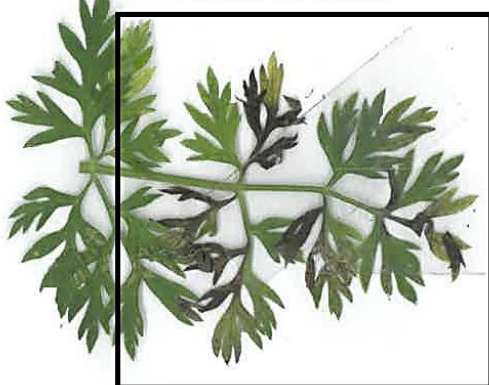
Api7R 0.2 mM



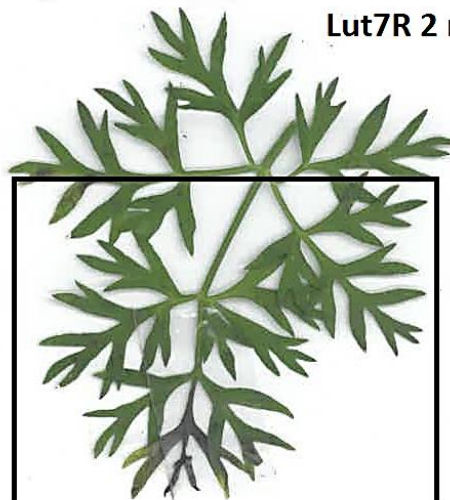
Api7R 2 mM

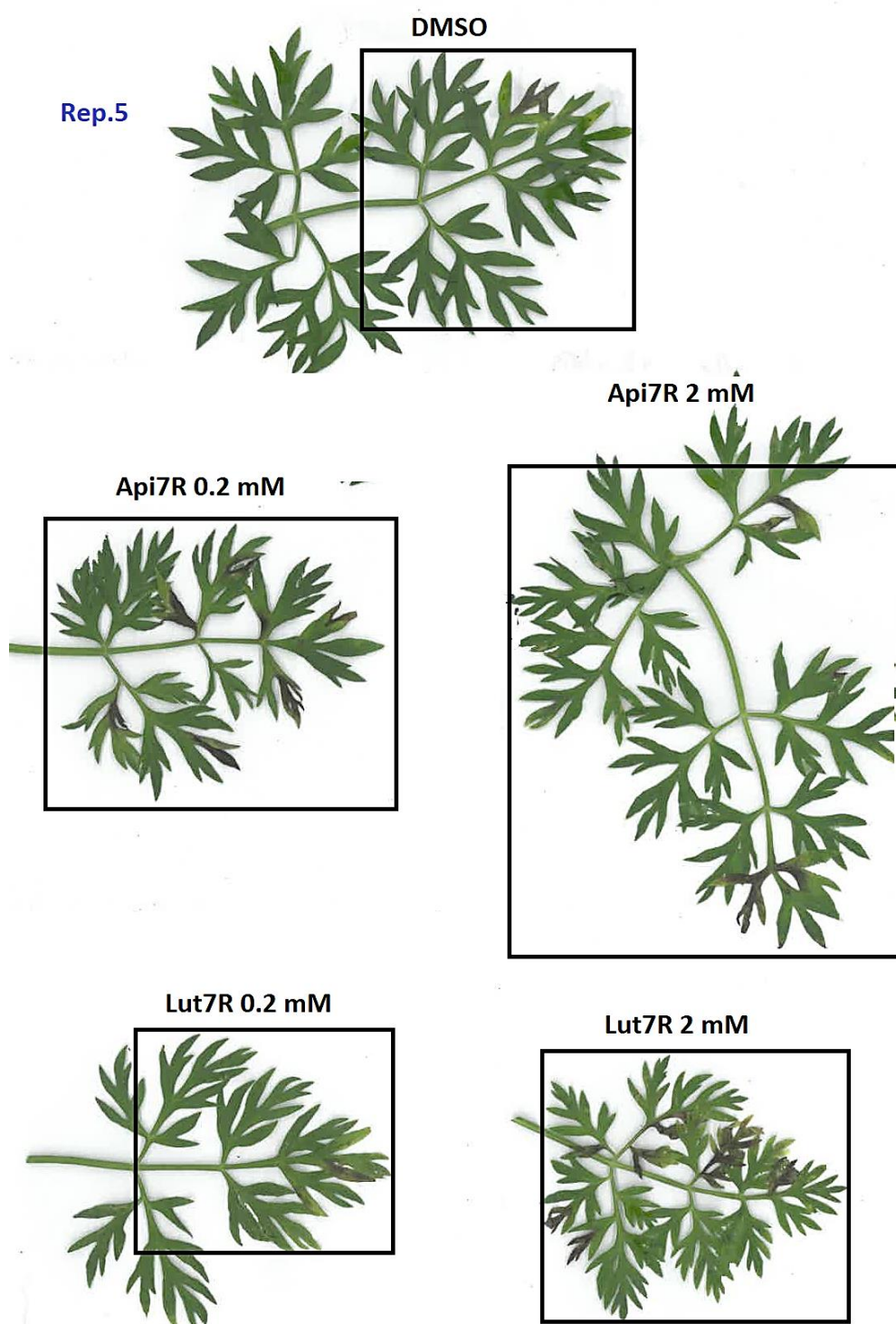


Lut7R 0.2 mM



Lut7R 2 mM





Appendix - Figure 12: Biological replications of inoculated leaves of H1 during the assessment of Lut7R and Api7R in greenhouse conditions.

ALB symptom severity rated at 7 days after the occurrence of necrotic spots (13 days post-inoculation). Frames delimit the parts of the leaf surface that were inoculated.

CHAPTER IV: FUNCTIONAL ANALYSIS OF CANDIDATE GENES PUTATIVELY DICTATING THE ACCUMULATION OF THE CANDIDATE FLAVONOIDS IN CARROT LEAVES

So far, the study of the role of flavonoid candidates in ALB resistance has provided partial answers by evaluating carrot accessions, and testing the biological activity of these compounds. Of the three candidates, Api7R and Lut7R tended to stimulate the pathogen *in vitro*, whereas Chry7R did not seem to have any apparent effect and a hypothetical inhibitory effect, which had to be confirmed. *In vivo*, the presence of Lut7R on the leaf surface seemed to limit disease progression after the onset of pathogenesis, more than Api7R. In the partially resistant accession I2, these three compounds together were correlated with ALB resistance. The involvement of other putative bioactive compounds in the leaves has not yet been investigated so far to clearly define whether these three candidates are major components of the carrot-*A. dauci* interaction, or whether there are other compounds equally involved. Therefore, considering the relatively low content of metabolites in the leaves of H1 compared to I2, enhancing their biosynthesis in the former was one of the strategies to associate a shift in metabolite content with a shift in resistance phenotype.

The discovery of the three candidate flavonoids was enabled by the joint analysis of metabolomic data and results from genetic analyses using forward genetic approaches. Their accumulation in carrot leaves was shown to be highly heritable ($H^2 = 0.926$, $H^2 = 0.889$ and $H^2 = 0.915$ for the broad sense heritability of the accumulation of Api7R, Lut7R, and Chry7R, respectively). Favourable alleles arose from the accession I2, and the additive effect of the alleles was between 0.3-0.5 (Ph.D. thesis Koutouan, 2019). Attempting to introduce this trait into less flavonoid-accumulating accessions such as H1 may therefore be worth considering in future breeding programmes, following validation of potential genes of interest. Metabolite QTLs co-localised with major resistance QTLs on chromosome 6 explained more than 50 % the accumulation of candidate metabolites in leaves of I2, according to the same study: $R^2 = 50$ % for Api7R, $R^2 = 68$ % for Lut7R and $R^2 = 71$ % for Chry7R. Contrasting the transcriptomes of I2 and H1 was helpful in zooming in on these important genomic regions and narrowing down the list to two candidate genes putatively governing the biosynthesis of the three flavone-rutinosides. The up-regulation of the loci 108226497 and 108227155 (<https://www.ncbi.nlm.nih.gov/gene/>) in I2 leaves) coincided with the accumulation of candidate flavonoids (unpublished data), encouraging the current investigation of their function. The LOC108226497 was predicted to encode a bHLH118-like protein of 207 amino acids. It has a highly conserved bHLH superfamily domain, spanning 82 residues from its N-terminal side (NCBI) (**Figure 50**). This region contains a DNA binding site of 6 residues, which should recognise E-box consensus sequences in various gene promoters. It also has a dimer interface of 16 residues where polypeptide binding is expected to occur. Heterodimerisation could be mentioned in particular, as the bHLH transcription factor (TF) family is known to regulate gene expression in interaction with other proteins (R2R3 MYB and WD40) (Xu et al., 2015) to regulate flavonoid biosynthesis at the transcriptional level. The involvement of this complex has been extensively documented with respect to flavonoid accumulation in various plant tissues such as

in leaves or in pigmented fruits and storage roots (Kodama et al., 2018; Zhao et al., 2018; Guo et al., 2020; Meng et al., 2020).

The second candidate (LOC108227155) was predicted to be an *anthocyanidin 3-O-glucosyltransferase 2-like* gene encoding a 482 amino acid enzyme from the UDP-flavonoid glycosyltransferase (UGT) family. As such, it has global features in common with other enzymes of the glycosyltransferase family. Its homodimer interface is formed by 5 amino acid residues scattered over the first 442 amino acid residues from the N-terminus (**Figure 51**). The 356-residue active site is formed by 14 amino acid residues, in which a sugar donor binding site of 6 amino acid residues could be found and an acceptor substrate binding site of 1 amino acid residue located at the 15th residue from the N-terminus (**Figure 51**). Similar enzymes have often been assigned a role in flower or storage organ pigmentation in different plant species (Gachon et al., 2005; Yin et al., 2015), which is not the concern in the present study. However, some flavonoid O-glycosyltransferases have a poor substrate specificity *in vitro* (Liu et al., 2018) and potentially *in vivo*; therefore the role of this enzyme in the biosynthesis of the candidate compounds could be conceivable, without mentioning the correlation between metabolite accumulation and gene expression levels in previous studies on carrot (PhD Koutouan, 2019).

As a first step in the functional characterisation of these candidate genes, it was crucial to understand where in the biosynthetic pathway they operate. This may be difficult to answer for a transcription factor that may be involved in multiple pathways, but it could pave the way for understanding the *in vivo* substrate specificity of the glycosyltransferase. To this end, each gene was overexpressed in the H1 carrot accession, which is relatively poor in the candidate flavones. The phenotypic shift was monitored on carrot calli with respect to the quantitative aspect of the candidate metabolites compared to the untransformed callus of H1, its empty vector transformants and to the untransformed callus of I2. In a further study, the putative biological activity of callus extracts on *A. dauci* conidia was investigated. Finally, a series of plantlets were monitored *in vitro* and under greenhouse conditions to determine the feasibility of phenotyping plant regenerants or seeds.

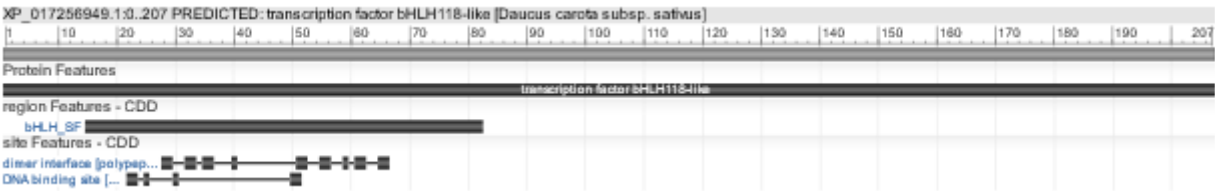


Figure 50: Conserved domains of DcbHLH118-like protein sequence (NCBI)..

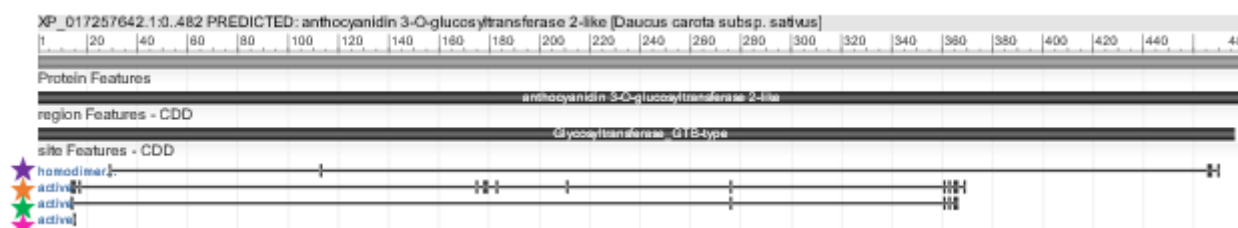


Figure 51: Conserved domains of the anthocyanidin 3-O-glucosyltransferase 2-like (NCBI).

Purple star: Homodimer interface, orange star: active site, green star: TDP-binding site and pink star: acceptor substrate-binding pocket.

4.1 Investigation of candidate gene function on calli

Selection of potentially transformed calli exposed to *A. tumefaciens* was based on their ability to develop on kanamycin-supplemented medium and the observation of a GFP fluorescence signal. A first visual evaluation of all modalities showed that H1 calli exposed to *A. tumefaciens* carrying plasmid with UFGT as insert did not develop optimally compared to empty plasmid or with bHLH gene (not shown). Therefore, only the effect of the bHLH candidate on metabolite levels could be further investigated. Transformants with empty plasmid will be further called EV for empty vector while transformants harbouring the LOC108226497 under the control of the CaMV 35S promoter, allowing a constitutive overexpression of the candidate gene, will be called bHLH over-expressors. Untransformed calli will be referred to as NT. The *DcbHLH118-like* gene will be simply called *bHLH*.

As a first step, samples from two or three independent transformation events were pooled to provide sufficient material for molecular and metabolite analyses. After what, as soon as a minimum of five independent events were sufficiently multiplied, they were phenotyped individually.

4.1.1. Gene expression level and metabolite enrichment of pooled transformation events

This evaluation allowed to assess whether a freshly sub-cultured callus is phenotypically different from a few weeks old callus in terms of cellular activity or not. Gene expression analysis showed that all *bHLH* over-expressors had at least a thousandfold higher gene expression than in empty vector (EV) modalities. This difference was very pronounced when the samples were cultured for several weeks (**Figure 52**). The metabolic parallel to this is that, overall, both groups had a comparable pattern, given their respective sampling dates: all had a very low level of Api7R, regardless of the construct and the sampling date. Although no statistical analysis can be performed on these pooled samples, we can note that the level of Chry7R was at an intermediate level, following the highest level observed for Lut7R (**Figure 53**). Irrespective of the construction, EV or *bHLH* over-expressors, a higher level of both Chry7R and Lut7R was observed in freshly sub-cultured calli compared to older calli. Furthermore, if differences between EV and *bHLH* over-expressors are still visible for Lut7R levels in the latter, this is no more the case for Chry7R levels (**Figure 53**).

From these observations, it was clear that placing the calli on a fresh medium for a week was sufficient to obtain the desired measurements.

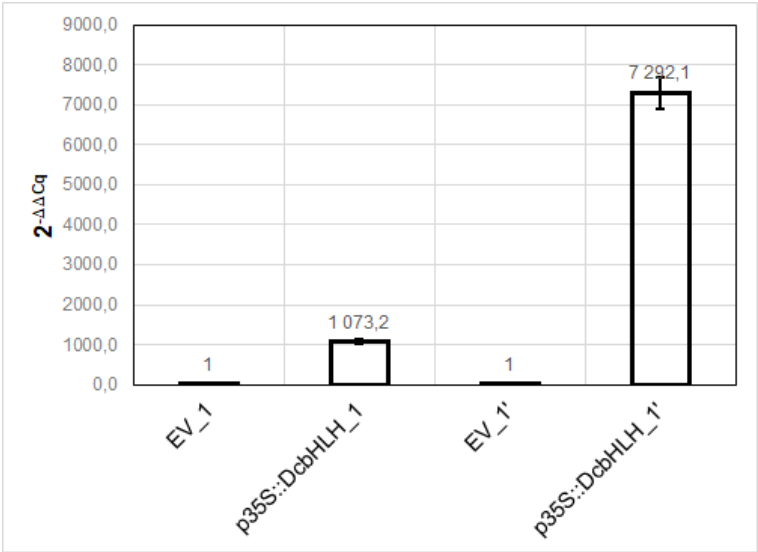


Figure 52: Expression level of DcbHLH118-like in pooled samples from H1 calli sub-cultured for one week (_1) or three weeks (_1').

EV: empty plasmid vectors. P35S::DcbHLH: tranformants carrying inserted LOC108226497 under the CaMV 35S promoter.

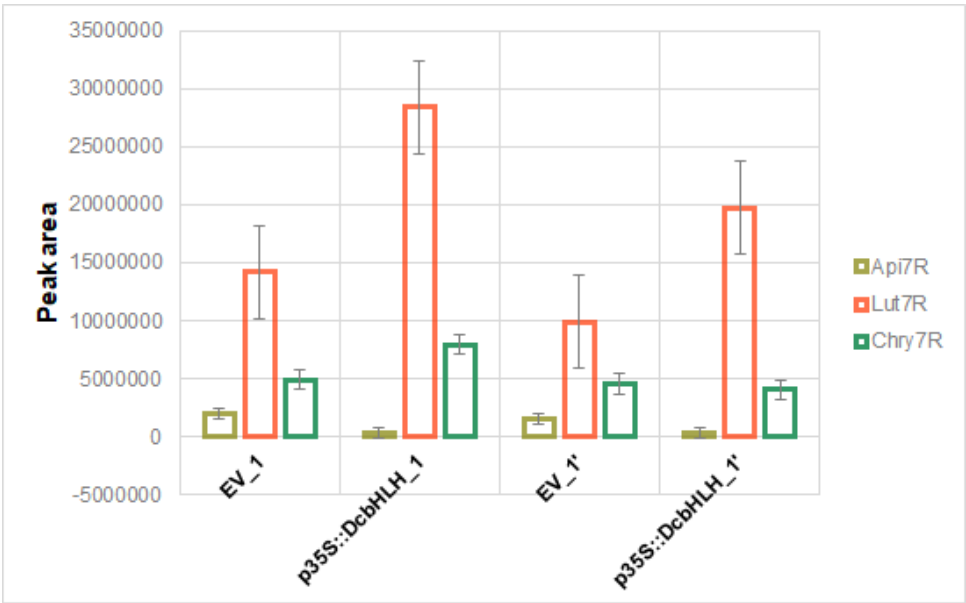


Figure 53: Candidate metabolite content in pooled samples from H1 calli sub-cultured for one week (_1) or three weeks (_1'). EV: empty plasmid vectors. P35S::DcbHLH: tranformants carrying inserted LOC108226497 under the CaMV 35S promoter. Y axis refers to peak area of eluted compound of interest monitored at 280nm by LC-DAD. Error bars correspond to the standard error of the mean.

4.1.2. Genetic and metabolic phenotyping of single transformation events

Using the H1_EV modality (average result of 7 EV events) as a control sample, each of the *bHLH118-like* putative over-expressors expressed the gene at more than 800-fold higher, confirming a successful transformation. Six samples out of eleven samples (events n°4, 5, 6, 7, 9, 10) showed a very similar level of expression, while two (events n°1, 8) showed an even higher level of expression and the remaining three (events n°11-13) a rather lower level of expression (**Figure 54**). Furthermore, the gene was clearly up-regulated 119-fold higher in NT I2 calli, which was also much higher, compared to NT H1 calli showing a 3-fold higher expression level than the EV sample.

Regarding the metabolic phenotype, the general trend mimicked the previous observations made on pooled samples, with Lut7R being the most abundant in both EV and bHLH over-expressors, followed by Chry7R. Api7R was not detected in any of them (**Figure 55**). In addition, it had much lower levels in both native H1 and I2 calli. Despite the differences highlighted for the levels of gene transcripts within the bHLH transformant events or between them and EV or NT calli, the accumulation of Lut7R did not follow a particularly similar pattern: in fact, it was noted that events with a relatively high fold change in gene expression, such as in events n° 1 and 8, could have a higher or a much lower metabolite content than the EV, respectively. Chry7R, on the other hand, did not seem to vary much between events and was clearly lower in bHLH over-expressors than in EV.

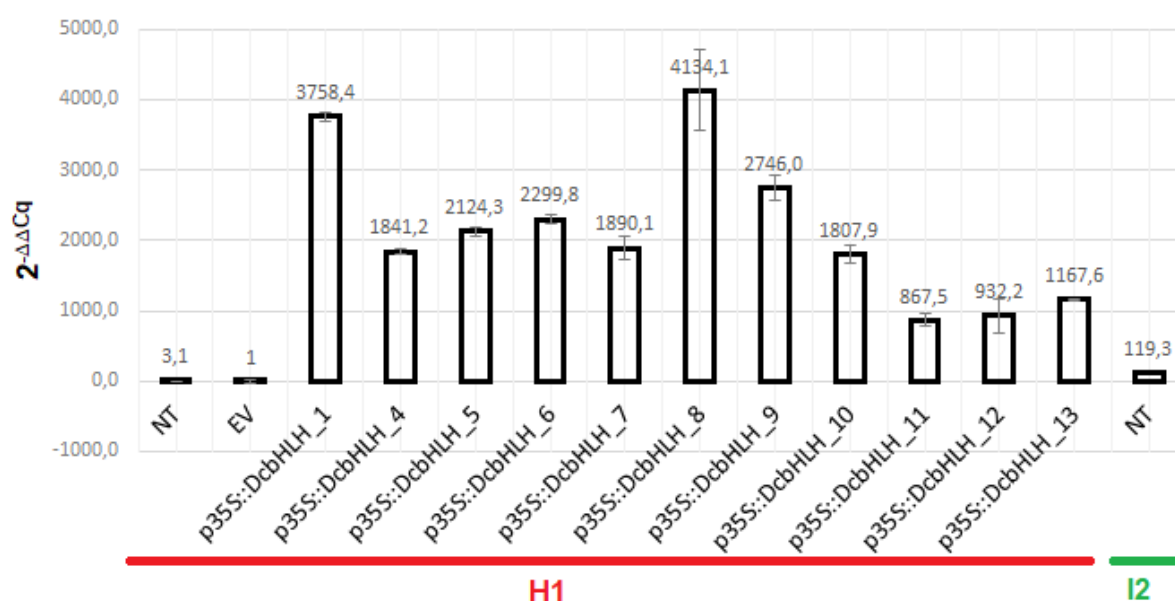


Figure 54: Expression level of *DcbHLH118-like* in NT H1 and bHLH over-expressors as well as in NT I2, referred to a pool of 7 H1 empty vector (EV) transformants.

NT: untransformed calli. Error bars display standard deviation of three technical replicates in a qPCR run.

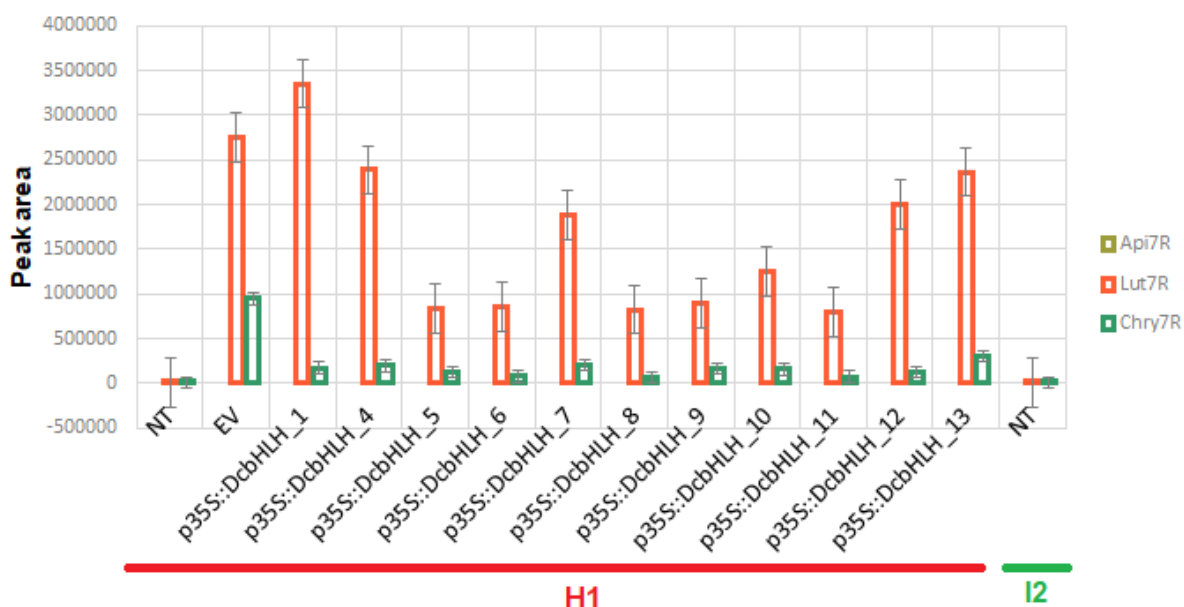


Figure 55: Phenotypic homogeneity between independent transformation events of H1 DcbHLH118-like over-expressors, compared to untransformed (NT) H1, NT I2 and a pool of 7 samples from empty-vector transformants (EV). Y axis correspond to LC-DAD peak area monitored at 280 nm.

4.1.3. Biological activity assessment of callus extracts on *A. dauci*

Events n° 11-13 were selected according to material availability and sampled together with non-transformed H1 and I2 to obtain calli extracts from a hydro-alcoholic solvent system (MeOH/H₂O 75/25). The dry crude extracts were prepared at 20 mg/mL and 100 mg/mL for biological assay and analytically characterised (HPLC-UV) with reference to standards at 1 mg/mL. The resulting chromatograms showed the predominance of relatively more polar compounds referred to the candidate compounds, thus overshadowing the compounds of interest detected at the level of the background noise (*Appendix - Figure 13*). The data obtained were therefore not interpretable to assign a precise qualitative or a quantitative profile to each extract for a comparative overview. Nevertheless, the observation of a putative biological activity on the development of *A. dauci* was thought to provide a bridge to a more integrative and large-scale analysis, using a more efficient approach in the future. In fact, prior to a non-targeted metabolomic study or a whole plant disease resistance phenotyping of the bHLH over-expressors, the response exhibited by *A. dauci* to these extracts was explored to analyse the impact of a metabolic shift on the fungus. A similar approach to that described in the previous chapter was used to assess the ability of *A. dauci* conidia to germinate and to examine the number and integrity of the hyphae produced *in vitro*. Unfortunately, the application developed in Chapter III to analyse hyphal dimension was not usable due to a high hyphal disintegration as explained below, which has led us to remove this criterion.

4.1.3.1 Germination rate of *A. dauci*

Exposure to callus extracts tended to increase the germination rate of *A. dauci* conidia, but the difference from the control condition (1% DMSO) was not significant when the extract came from NT H1 calli (**Figure 56**). The difference between NT H1 and NT I2 extracts was statistically confirmed, particularly at 100 mg/mL of I2 extract where the germination rate of *A. dauci* was the highest. H1 at 100 mg/mL could be considered comparable to NT I2 at 20 mg/mL regarding their effect. However, no significant difference was observed between the two concentrations of I2 extract. Furthermore, when H1 over expressed the *bHLH* candidate gene, the deriving callus extracts regardless of the concentration had a comparable effect as well to that of NT H1 at 100 mg/mL as to that of NT I2 callus extracts. In brief, *A. dauci* conidia germinated significantly in the presence of extracts from a *bHLH* overexpressing H1 or NT I2 and to a lesser extent with NT H1 extract at the highest concentration.

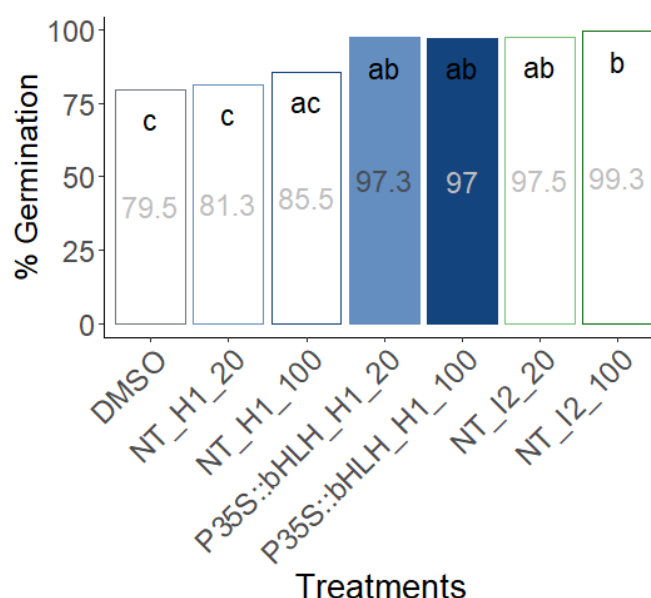


Figure 56: Conidial germination percentage.

ANOVA on transformed data (Arcsine square root transformation), $p = 1.184 \times 10^{-5}$. Blue coloured bars pointed out extracts of transformed events at 20 mg/mL (clear blue) or 100 mg/mL (dark blue). Letters display group significance from Tukey's multiple comparison test. Error threshold = 0.05.

4.1.3.2 Counting of formed hyphae

Hyphae formed from emitted germ tubes were counted on germinating conidia, whether their aspect disrupted or not. Conidia emitted significantly more hyphae when exposed to 100 mg/mL extract of H1 over-expressing the *bHLH*, similar to NT I2 at both concentrations tested (**Figure 57**). Conidia treated with NT H1 extract at 100 mg/mL had the

fewest hyphae, with statistically indistinguishable group in between, comprising conidia exposed to the control treatment DMSO, H1_bHLH over-expressor at 20 mg/mL and NT H1 at 20 mg/mL.

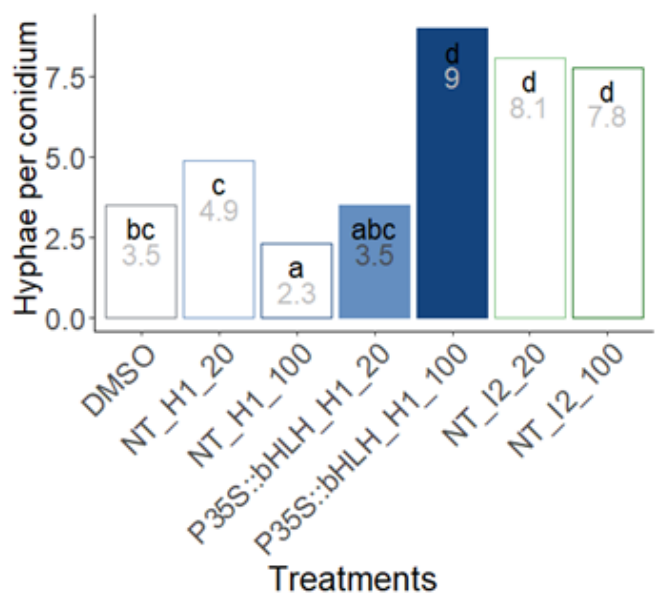


Figure 57: Average hypha number per conidium.

ANOVA, $p < 2.2e-16$. Blue coloured bars pointed out extracts of transformed events at 20 mg/mL (clear blue) or 100 mg/mL (dark blue). Letters display group significance from Tukey’s multiple comparison test. Error threshold =0.05.

4.1.3.3 Hyphal integrity evaluation

There are three different groups: a group with little hyphal destructuration comparable to the DMSO control with NT_H1_20 and bHLH_H1_20 , a group with very strong destructuration including high concentrations whatever the genotype or construction NT_H1_100, bHLH_H1_100 and NT_I2_100) and an intermediate group with quite strong destructuration but quite less than the first group (Figure 58, Table 7).

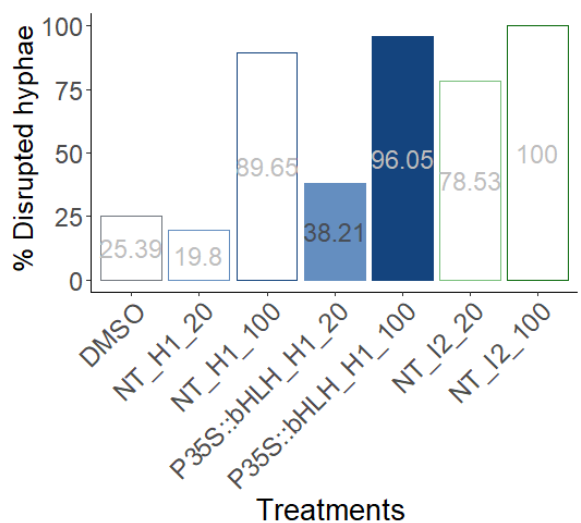


Figure 58 : Percentage of disrupted hyphae on germinating conidia.

Blue coloured bars pointed out extracts of transformed events at 20 mg/mL (clear blue) or 100 mg/mL (dark blue). Observations on 400 conidia per treatment.

In summary, four profiles can be drawn from the results. Firstly, in the control condition and NT_H1_20, which had a lower germination rate than the other groups, relatively fewer hyphae were formed but significantly less hyphal disruption was observed (**Figure 59, Table 7**); secondly, in NT_H1_100, conidial germination was stimulated, but with a significant reduction in the number of hyphae per conidium and an increase in hyphal disruption. The third profile (*p35S::bHLH_H1_20*) showed a marked increase in germination rate, no obvious effect on the hyphal number compared to the first group, except for an increased rate of hyphal disruption (**Figure 59, Table 7**). The last group (*p35S::bHLH_H1_100*, NT_I2_20, NT_I2_100), showed a relatively high germination rate, with a significantly higher hyphal number, but also the highest hyphal breakage rate (**Figure 59, Table 7**).

These observations led to the question of the behaviour of *A. dauci* conidia in interaction with regenerated transformed plants. However, the limited amount of biological material available at this stage and the lack of clear response elements regarding the role of the candidate genes made it risky to delve into this road. Therefore, in order to prepare this process, the possibility of regenerating whole plants *in vitro* and growing them for a certain period of time under greenhouse conditions was evaluated using empty-vector transformants of I2 and H1.

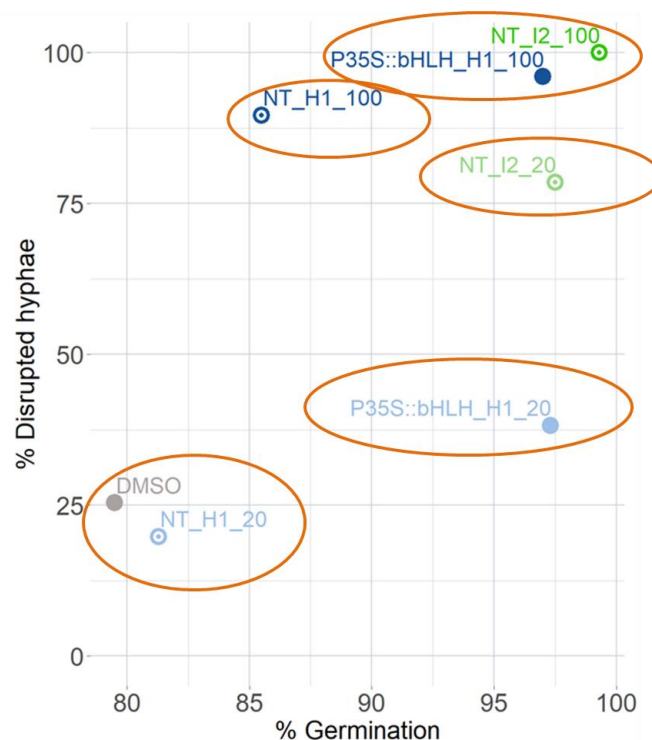
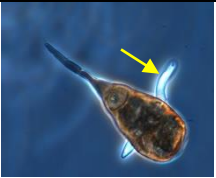








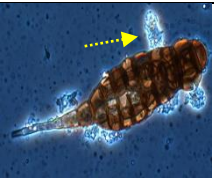

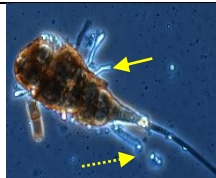
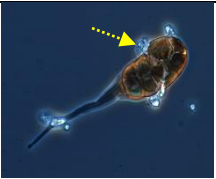

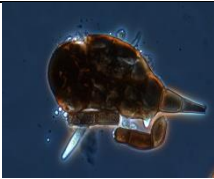
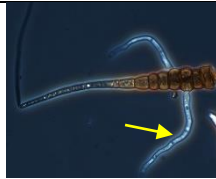






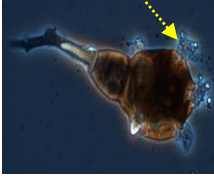

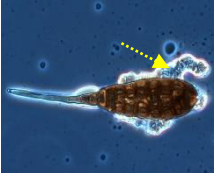
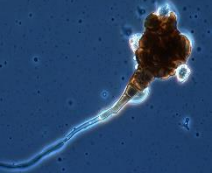
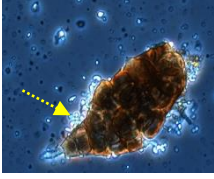



Figure 59: Hyphal disruption related to the germination rate of *A. dauci* conidia *in vitro*, after exposure to different callus extracts at two concentrations (20 and 100 mg/mL), and the control (1% DMSO).

NT: untransformed.

Table 7: Hyphal integrity of *A. dauci* conidia in vitro, after exposure to different callus extracts at two concentrations (20 and 100 mg/mL), and the control (1% DMSO).

NT: non-transformed calli; H1- p35S::DcbHLH calli transformed with LOC108226497 under the control of the CaMV P35S promoter. Images shown are arbitrarily representative samples of 400 observed conidia per modality. Solid arrow: examples of intact hyphae, dashed arrow: examples of disrupted hyphae.

DMSO				
NT H1- 20 mg/mL				
NT H1-100 mg/mL				
p35S::DcbHLH-H1 20 mg/mL				
p35S::DcbHLH-H1 100 mg/mL				
NT I2-20 mg/mL				
NT I2-100 mg/mL				

These observations led to the question of the behaviour of *A. dauci* conidia in interaction with regenerated transformed plants. However, the limited amount of biological material available at this stage and the lack of clear

response elements regarding the role of the candidate genes made it risky to delve into this road. Therefore, in order to prepare this process, the possibility of regenerating whole plants *in vitro* and growing them for a certain period of time under greenhouse conditions was evaluated using empty-vector transformants of I2 and H1

4.2 Follow up of H1 and I2 T₀ regenerants

In this context, I2 and H1 calli underwent *A. tumefaciens* - mediated transformation to acquire the empty vector containing the *NPTII* gene as a selectable marker, independent of the previous experiment. A total of 149 plants were regenerated *in vitro* on a selective medium, theoretically based on the ability the transgenic plants to tolerate a high dose of kanamycin (50 mg/L) (**Figure 60**). As no genetic characterisation had been carried out due to the limited amount of plant tissue available, it was assumed that plants that appeared to be vigorous at this stage had acquired the *NPTII* gene from the genetic transformation, conferring resistance to kanamycin, and were therefore highly likely to have been successfully transformed. Of these 149 plants, 65.9 % of I2 (83/126) and 43.5 % of H1 (10/23) were selected for acclimation in the S2 greenhouse. Nevertheless, I2 seemed to develop well *in vitro* compared to H1 (**Figure 61**), which led to a large number of vigorous plants and an overrepresentation of this accession in the greenhouse (**Figure 60**). Furthermore, it was also evident that I2 had already initiated root filling, whereas H1 had not. A difference in growth rate and/or physiological state between genotypes is commonly observed *in vitro*, although possible effect of the genetic engineering process could not be excluded.

Under greenhouse conditions, a 5-month follow-up was carried out to assess their fitness and to assess the possibility of maintaining the plants long enough to reach the reproductive phase. This aim of this approach was to produce seeds from self-pollinated plants for further phenotyping the progeny. The result showed that approximately 30% of the plants survived for either H1 or I2. However, given the number of I2 plants transferred *ex vitro*, the loss appeared to be more dramatic, with only 19 plants out of 83 continuing to grow in the greenhouse, compared with 3 out of 10 for H1 (**Figure 60**). Genotyping of some of these plants showed that all I2 plants genetically assessed had acquired the *NPTII* gene, whereas there were none for H1 (**Figure 62**). It is therefore tempting to assume that the genetic transformation in H1 was not very efficient in this experiment, although several plants were already lost and could not be genotyped in time. No further comment on the transformation success in I2 can be made, as not all of the growing plants were genotyped.

An overview of this process made it clear that the chances of obtaining seeds from regenerated transformants would be quite low. Furthermore, this observation reflected the challenge of obtaining homogeneous T₀ plants, thus potentially adding another level of complexity to the process of phenotyping different constructions that are expected to be at the same physiological and developmental stage. These results reinforced the fact that genotyping and

phenotyping of embryogenic calli after their exposure to *A. tumefaciens* seems to be more appropriate in order to avoid any possible loss due to the fragility of the accession or transformant *in vitro*.

	Regenerated <i>in vitro</i>	Acclimation month 1 ^a	Growing month 5 ^b	<i>NPTII</i> detection ^c
I2	126	83	19	10/10
H1	23	10	3	0/3

Figure 60: Plant tracking from *in vitro* to greenhouse.

a: Acclimation of selected vitroplants in the S2 greenhouse. b: Remaining plants that survived 5 months of greenhouse conditions. c: number of plants in which *NPTII* was successfully detected in the total number of plants genotyped.

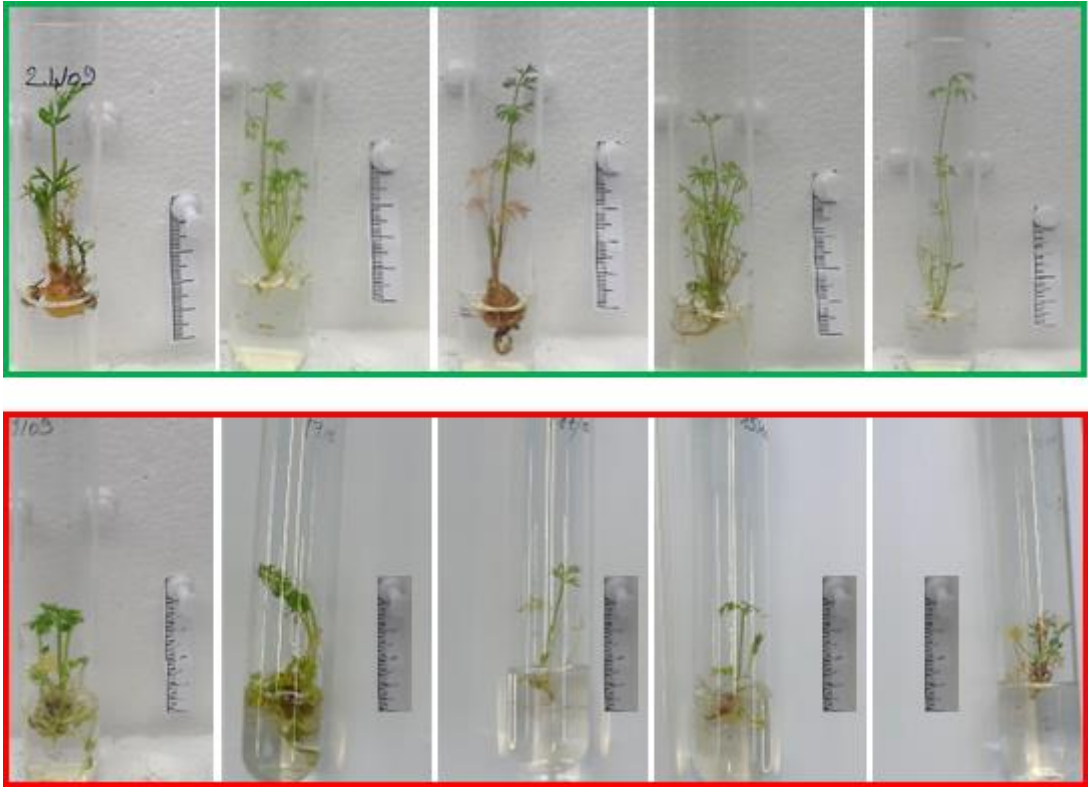


Figure 61: Phenotype of the plantlets *in vitro*.
Top framed in green: I2, bottom framed in red: H1.

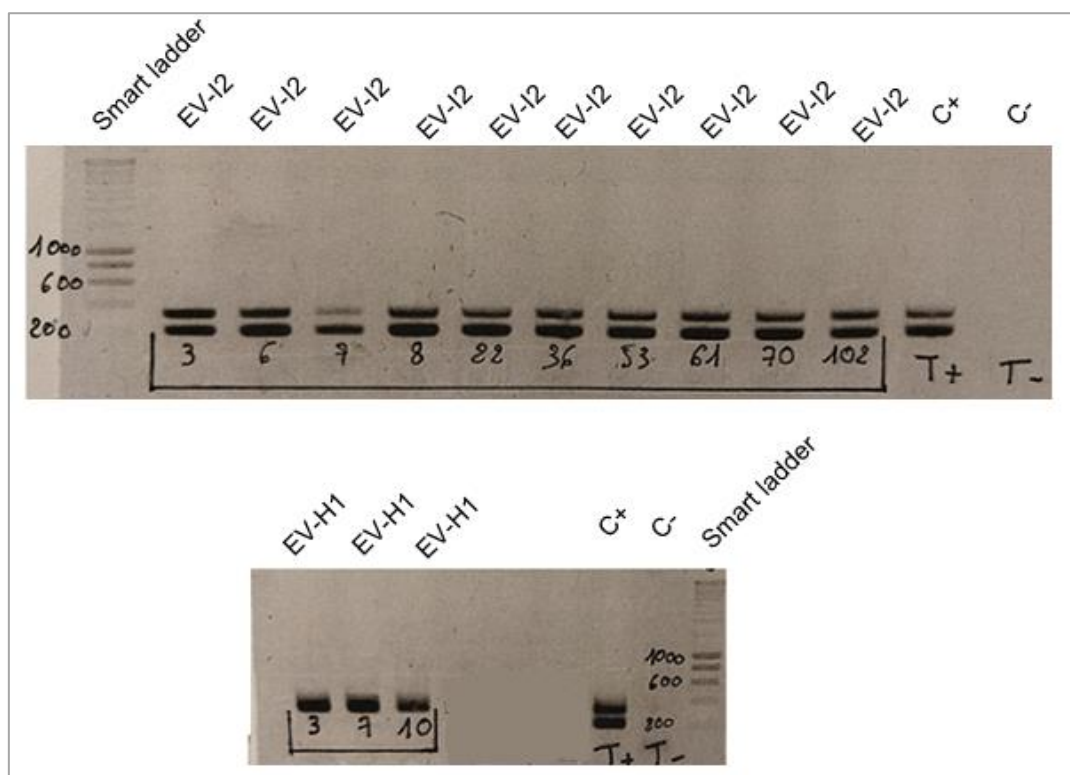


Figure 62: Amplification of *NPTII* (~200 bp) in empty vector events of *I2* (top) and *H1* (bottom). EV: empty vector, C: control.

DISCUSSION AND PERSPECTIVES

The regeneration of transformants from different carrot accessions has been successful. However, although carrot is a model in which somatic embryogenesis was first described (Reinert, 1958; Steward, 1958), mastering all the stages of this biological process on several accessions and fine-tuning the induction of transgenesis remain a challenge and an obstacle to validating gene function. From a technical point of view, it is also important to note that the analysis of DNA and RNA from callus required relatively lengthy method development, because the undifferentiated cells were vacuolated and the amounts of genetic material were small. Several extraction methods were tested on fresh and freeze-dried materials: by kit, or by applying a CTAB (Cetyltrimethylammonium bromide) protocol (Hamama et al., 2012). Different DNA concentrations were considered, before coming up with the methods described in this manuscript (Chapter V-5.3.7).

With regard to the function of the LOC108227155, which encodes a putative glycosyltransferase protein (anthocyanidin 3-O-glucosyltransferase 2-like), the calli did not grow optimally, indicating that the genetic transformation probably affected developmental processes. This observation is not surprising as glycosyltransferases can have a wide range of substrates including flavonoids and phytohormones such as auxin (Griesser et al., 2008; Hectors et al., 2012; Song et al., 2015; Kuhn et al., 2016; Kantharaj et al., 2022). In this sense, the permanent availability of a multi-substrate enzyme may induce a change in the metabolite ratio, thus promoting the glycosylation

of temporally and spatially inappropriate compounds. This may lead to the accumulation of flavonoids that directly interfere with hormonal balance and transport (Buer et al., 2013; Kuhn et al., 2016). Overexpression of flavonoid glycosyltransferases has been shown to induce changes in the growth and development of *Arabidopsis thaliana*, either positively or negatively, depending on the glycosyltransferase candidate gene (Yao et al., 2019). Auxin biosynthesis is generally mentioned as being regulated in interaction with flavonol biosynthesis (Kuhn et al., 2016). It (indole 3-acetic acid) is also a substrate of glycosyltransferases, and its glucosylation has been shown to positively regulate plant growth by upregulating important genes involved in cell division (Kantharaj et al., 2022). Therefore, overexpression of a flavonoid glycosyltransferase not directly linked to auxin biosynthesis, may simply have depleted the auxin glucosylation machinery with available activated sugars. Since that time of evaluation, more or less nine months ago, cell proliferation and differentiation have been enhanced in these calli. Studies similar to those described in this chapter could therefore be undertaken in the near future.

Regarding the overexpression of the LOC108226497 (*bHLH 118-like*) in pooled calli samples, the accumulation of Lut7R was clearly enhanced in *bHLH* over-expressors in comparison to the EV lines. Although a similar trend was observed for calli subcultured for one week or three weeks, the metabolite content decreased slightly in the latter. This may be due to cellular exhaustion or simply occurred when the medium was depleted in nutrient. In single transformation events, higher levels of Lut7R and, to a lesser extent, Chry7R were observed in EV and in *bHLH* over-expressors, but not well detected in untransformed calli of H1 and I2. Preliminary analyses have already shown that the level of candidate metabolites in untransformed calli tend to be below the detection limit in LC-MS analyses. In any case, the level of Api7R was very low to be detected. Although gene expression is clearly what is expected from successful transformations, metabolite levels do not appear to be directly related to the overexpression of the *bHLH* gene. In fact, it was unexpected to observe an induction of metabolite accumulation in the EV lines, which had a relatively higher levels of Lut7R and Chry7R and not Api7R, compared to the non-transformed and *bHLH* overexpressing lines. The accumulation of these metabolites does not appear to depend on this gene at first. This reminds the importance of going to the end of the functional validation procedures, to demonstrate the involvement of a candidate gene or candidate metabolites in any type of biological process highlighted by genetic studies. This phenomenon seems to indicate that exposure to *A. tumefaciens* may have induced a defensive response in the carrot cells, which led to a change in the metabolite levels in EV calli. This could be validated by inoculating carrot calli with wild type *A. tumefaciens* compared to those carrying the plasmid used in this study. Results obtained from transformation of *Cucurbitaceae* species by *Rhizobium rhizogenes* showed a similar phenomenon but rather caused reduction in cucurbitacin content (Almeida et al., 2023), contrarily to our observation. The authors also observed a shift in the plant transcriptome in EV lines compared to non-transformed lines, highlighting the identification of several differentially expressed transcription factors. In our study, gene expression analysis did not show any effect of the transformation process on the expression of the candidate *bHLH* gene in EV calli, but it could have indeed affected other transcription factors such as *MYB* and *WDR* which are other components in the regulation of flavonoid

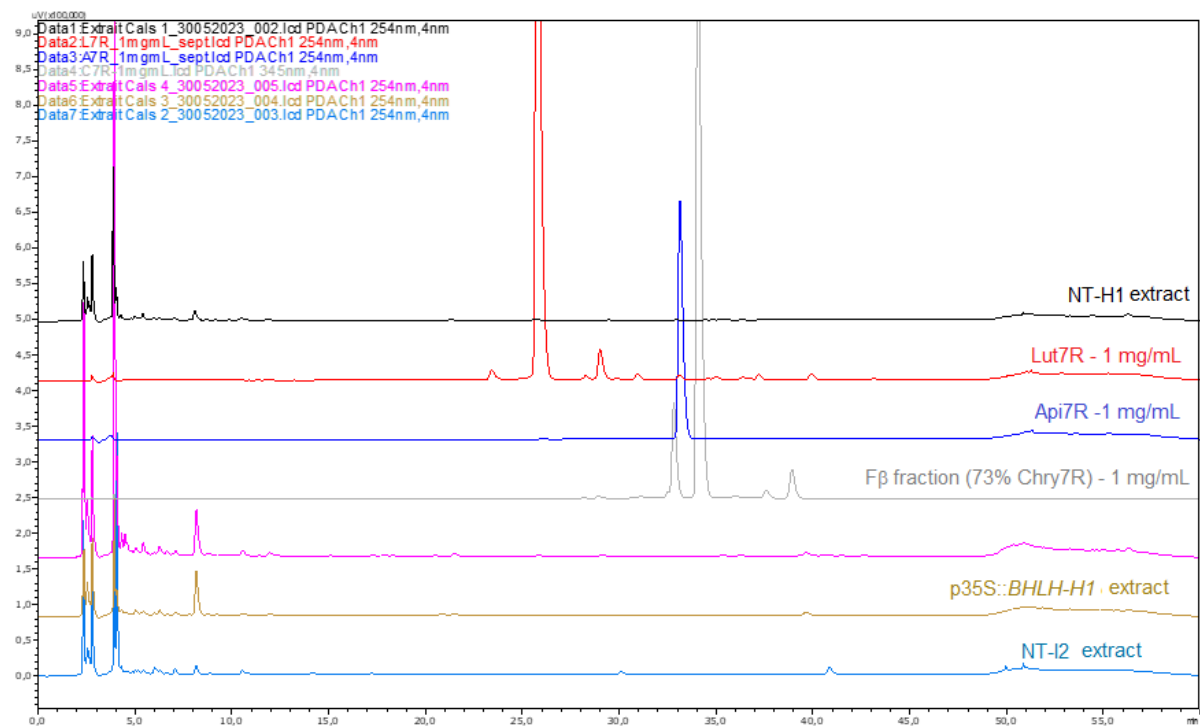
biosynthesis (Xu et al., 2015; Nemesio-Gorriz et al., 2017). Almeida and colleagues also observed that overexpression of a *bHLH* gene known to induce the accumulation of cucurbitacins resulted in a phenotype that counteracted the decrease in metabolite levels observed in EV lines (Almeida et al., 2023). From this point of view, the candidate gene in our study would be a negative regulator of Lut7R and Chry7R accumulation, despite a clear accumulation of these compounds at higher levels compared to untransformed calli. To test this hypothesis, gene silencing with RNAi or CRISPR/Cas system in the carrot accession I2 could be made.

Considering the putative role of this gene in ALB resistance, its upregulation in I2 was associated with metabolite accumulation (Ph.D Koutouan, 2019). It is possible that this correlation is spurious and that this gene is indirectly linked to the accumulation of candidate metabolites through regulation of other resistance mechanisms. Nevertheless, the acquisition of a flavonoid accumulating phenotype in H1 was encouraging to perform a biological assay of their extract, before the possibility of carrying out an integrative analysis of the metabolome and transcriptome, as well as the obtention of regenerated plants for a whole plant pathological assay. The inclusion of untransformed I2 calli in the biological assay was also hoped to provide complementary data on the possible presence of other bioactive compounds in the totum. The results showed a clear effect of high extract concentrations or transformation of the H1 calli on conidial development. There seems to be a link between the increase in Lut7R and Chry7R in the transformed calli and the increased toxicity of the extracts, although their HPLC-UV profiles did not allow proper quantitative and qualitative analysis (**Appendix - Figure 13**). The content of the compounds in the extracts may have been too diluted to allow an optimal signal detection. In parallel with the previous Chapter, Lut7R tested separately from others, stimulated conidial germination but has no deleterious effect on hyphal integrity. This difference may be due to the relatively high concentration of extract tested (20 mg/mL and 100 mg/mL) or/and to the presence of other compounds, which at such concentrations of the extract would also have a toxic effect. The first assumption at least appeared valid, as the damages were relatively reduced for the conidia treated with callus extracts at 20 mg/mL. However, the conidia were less impacted when exposed to extracts at 20 mg/mL from *bHLH* over-expressor and untransformed H1 calli, than with untransformed I2. This is in line with the second assumption, suggesting that the totum of untransformed I2 may be qualitatively and quantitatively different from that of *bHLH* overexpressing H1 calli. Assuming that there is no major effect of the *bHLH* overexpression on the composition of the totum, other than on Lut7R and on Chry7R, the stimulatory effect of Lut7R on conidial germination adds to the results observed in Chapter III. However, Chry7R could be responsible for the toxic effects, but this is difficult to assess in these conditions once again. An overview of the shift in the metabolome and the transcriptome would enable to establish a sound relationship between candidate gene expression and its effect on the flavonoid pathway. Moreover, as this candidate gene encodes a transcription factor, predicting its potential targets would allow to truly uncover the metabolic pathway(s) or mechanism that it regulates.

In order to prepare for the regeneration of transformants in future studies, the growth of EV lines produced independently from those metabolically profiled here was followed. Difference in growth rate observed *in vitro* may

be genotype dependent as H1 tended to be relatively less vigorous than I2 even when non transformed (similar at a whole plant scale, Chapter II). Genotyping at the acclimation stage in greenhouse may have been misleading as a large number of plants died before genotyping could be done and some of these might have been successfully transformed. Failure to detect selectable markers in H1 plants could indicate the development of escapes, which are commonly encountered in callus transformation (Klimek-Chodacka et al., 2018). Initially, the acclimation follow-up was intended to provide information on the fitness of the transformants under greenhouse conditions, but it would not be indicative of the performance of *bHLH* transformants anyway, as no over-expressor lines had been regenerated so far. Considering all the challenges mentioned, it seems opportune to phenotype at an early stage of plant development, as phenotypic differences in terms of resistance to *A. dauci* exudate have already been observed and validated at the cellular level between untransformed H1 and I2 (Lecomte et al., 2014; Courtial et al., 2018).

APPENDICES



Appendix - Figure 13: HPLC-UV profiles at 254nm of the callus extracts at 100 mg/mL, compared to standard solutions.

CHAPTER V: MATERIALS AND METHODOLOGIES

5.1 CHAPTER II

5.1.1. Plant materials, field trials and sampling

5.1.1.1 H1 and I2 field trial

Previously studied accessions I2 and H1 (**Table 8**) were grown from seeds in Angers (Latitude 47.4711; Longitude -0.5518, Maine-et-Loire France). Seeds were sown in four rows of 20 linear meters per accession, to obtain approximately 1600 plants per row and per accession (**Figure 63**). Each accession was sampled at seven developmental stages from 2 to 12-leaf stages (**Figure 64**). Four samples (one per row) were collected at each stage. A sample, representative of a row, was taken from eight different plants distributed at different points along the row. From 2 to 4-leaf stages, the entire leaf part was withdrawn, whereas for the older stages only the three intermediate leaves were taken. Samples were stored and transported from the field to the laboratory in liquid nitrogen.

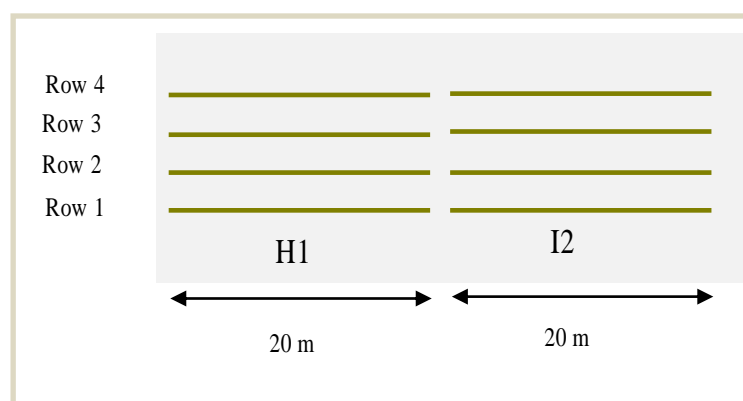


Figure 63: Design of the field trial for the metabolite content evaluation of H1 and I2.

Table 8: Origin of the carrot accessions and resistance level to ALB.

Accessions Boléro and Presto are commercial references frequently grown by farmers in French carrot production basins and used as references on ALB 'resistance / susceptibility' by the GEVES (Variety and Seed Study and Control Group).

Accessions	Description / Supplier	Type	Resistance level
Presto	Commercial F1 hybrid / Vilmorin	Nantaise	Susceptible
H1	S3 line / (Le Clerc et al., 2014)	Touchon Origin	Susceptible
Valor	Commercial F1 hybrid / HM-Clause	Nantaise	Intermediate
B18	Maternal line / QuaRVeg breeding program	Flakkee Origin	Intermediate
A92	Maternal line / QuaRVeg breeding program	Lobbericher Origin	Partially resistant
I2	S2 line / (Le Clerc et al., 2014)	Kuroda Origin	Partially resistant
Boléro	Commercial F1 hybrid / Vilmorin	Nantaise	Partially resistant
Brilliance	Commercial F1 hybrid / Nunhems	Nantaise	Partially resistant

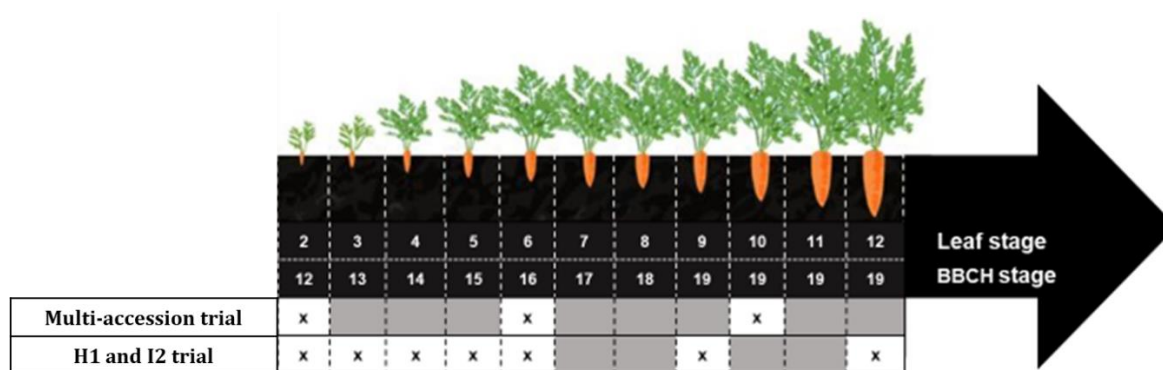


Figure 64: Sampling along the developmental stages of carrot, during the two trials.

Leaf stage corresponds to the number of true leaves well developed. BBCH is an international scale for plant development

5.1.1.2 Multi-accession field trial

Eight accessions (**Table 8**) were later planted from seeds on the same field plot, in a randomized block design (**Figure 65**). H1 and I2 evaluated with other accessions of different resistance levels to ALB at three stages of development (**Figure 64**). Seeds of each accession were sown in two rows of 1 linear meter per block, to obtain about eighty plants per row.

Sampling was carried out as already described in the previous trial.

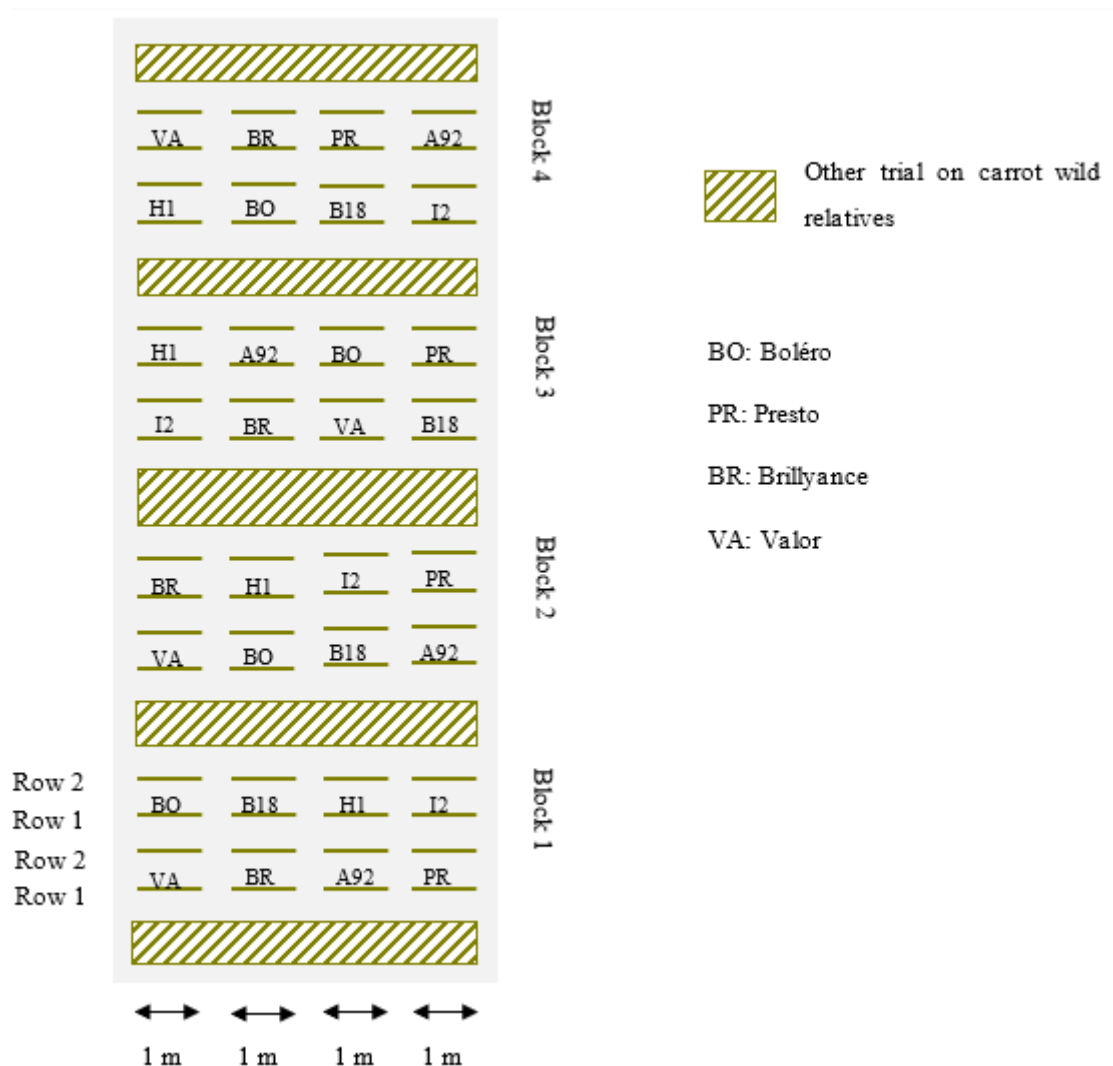


Figure 65: Design of the field experimentation relative to the 8 carrot accessions.

5.1.2. Production of leaf extracts and flavonoid quantification

Leaf samples devoid of petioles were ground into a fine powder in liquid nitrogen using a mortar and pestle, and then freeze-dried using -80°C freezer and a SRK GT2/8 lyophiliser (VWR).

Flavonoid quantification was carried out in collaboration with UMR SVQV of INRAE in Colmar, FRANCE. For this purpose, 10 mg of freeze-dried leaf powder per sample were delivered in 2 mL screw-capped tubes. An ultrasound-assisted extraction (15 min bath) was performed from the 10 mg dry leaf powder, with 150 µL per mg of leaf powder of methanol containing 5 µg/mL of chloramphenicol as an internal standard. The homogenates were then centrifuged at 12000 rpm for 10 min, to recover 100 µL of the supernatant for the subsequent analysis.

The supernatants were analysed by reversed phase ultrahigh performance liquid chromatography (Dionex Ultimate 3000; Thermo Fisher Scientific) associated to a detection system consisting of a diode array detector (DAD) and an Exactive Orbitrap mass spectrometer with an electrospray ionization (ESI) source operating in positive mode (mass detection accuracy < 1 part per million (ppm)).

The same analytical conditions as in (Koutouan et al., 2018) were applied. Briefly, 1 µL of methanolic leaf extract was injected into a Nucleodur HTec column (150 × 2 mm, 1.8 µm particle size from Macherey-Nagel) thermostated at 30 °C. Components of the leaf extract were eluted in gradient mode using acetonitrile/formic acid (0.1%, v/v) as eluent A and water/formic acid (0.1%, v/v) as eluent B, according to the programme (**Table 9**). Apigenin-7-*O*-glucoside was injected at 1 mg/mL to allow a relative estimation of the metabolite content per gram of dry material. Eluted peaks at 280 nm were integrated and retrieved for subsequent data analysis.

Table 9: Liquid chromatography elution gradient applied for the analyses of carrot leaf extracts and candidate flavonoid quantification.

Flow rate: 0.25mL/min	
Time	% B
0 – 4 min	80-70
4 – 5 min	70-50
5 – 6.5 min	50
6.5 – 8.5 min	50 - 0
8.5 – 10 min	0

5.1.3. Disease severity scoring

Symptom severity scores were assigned to the plants in the field once natural infection had occurred. At this time, the plants were at approximately (13-14)-leaf stage. Lesion severity was assessed visually on a statistical unit, *i.e.*, a group of ~ 50 plants per modality per block, considered as one biological replicate. The intensity of ALB symptoms on the upper and on the lower parts of the leaf was examined and compared to a disease scoring scale going from 0 to 9 (**Figure 66**, **Table 10**), as developed by (Pawelec et al., 2006).



Figure 66: Visual disease evaluation scale, from zero (symptomless) to 9 (highly blighted leaves). Credit: V. LE CLERC.

Table 10: Disease evaluation scores

Score	Lesion severity
0	No lesion
1	Very scarce necrotic spots
2	Highly reduced blight on lower leaves
3	Lower leaves lightly blighted
4	Medium attack on the lower leaves and low attack on the upper leaves
5	High attack on the lower leaves and weak attack on the upper leaves
6	High attack on the lower leaves and medium attack on the upper leaves
7	Lower leaves completely blighted and high attack on the upper leaves
8	Lower leaves completely blighted and very high attack on upper leaves
9	Upper and lower leaves completely blighted

5.1.4. Data processing and statistical analysis

Statistical analyses were performed on the corrected values, using the R software version 4.2.2 (2022-10-31) -- "Innocent and Trusting".

Data from LC-UV analyses were retrieved, particularly for the three candidate compounds. A correction factor was applied to the value of each flavonoid peak area, based on the amplitude of the response shift exhibited by the internal standard in each sample. Specifically, the corrected value of the metabolite peak area (M') was obtained by adding the correction factor to the initial value (M). The correction factor took into account the value of M multiplied by the ratio between the internal standard peak area in one sample (IS) and the mean of all internal standard peak areas in the analysis (Mean IS) subtracted from 1 (Eq. 1).

$$M' = M + M \times \left(1 - \frac{IS}{Mean\ IS}\right)$$

(Eq. 1)

In the H1-I2 trial, the influence of the two factors (accession and developmental stage) on the response variables (the content of the three flavonoids) was evaluated using a two-factor interaction model of analysis of variance (Eq. 2). The assumptions underlying the use of a parametric analysis of variances (ANOVA) were checked: 1) independence of the observations, 2) normality of the distribution of the residuals using the Shapiro Wilk test, 3) homogeneity of the residual variances using Bartlett's test. In the case of a non-normal distribution of the residuals, a Box-Cox transformation (Box and Cox, 1964) was applied, giving new values of the response variables through a power or a logarithmic transformation, according to the estimate of λ (Eq. 3). Thereafter, these assumptions were checked again

on the transformed data. A non-parametric test was used in the case of anormal distribution or an ANOVA with Welch's correction if only variance homoscedasticity was not validated.

$$Y_{ijr} = \mu + \alpha_i + \beta_j + (\alpha\beta)_{ij} + \epsilon_{ijr}$$

(Eq. 2)

Y_{ijr} : Observed value of Y associated to the i levels of the first factor, j levels of the second and the sample replication (r).

μ : Global theoretical mean of Y

α_i : main effect imputed to the i level of the first factor

β_j : main effect imputed to the j level of the second factor

$\alpha\beta_{ij}$: effect of the interaction between both factors

ϵ_{ijr} : residual error associated with i and j effect in r replications

$$B(x, \lambda) = \begin{cases} \frac{x^\lambda - 1}{\lambda}, & \lambda \neq 0 \\ \log(x), & \lambda = 0 \end{cases}$$

(Eq. 3)

$B(x, \lambda)$: value of the variable x , after transformation upon the estimate of λ

x : observed value of the response variable

λ : power transformation

Multiple pairwise comparisons between groups were performed, using a Tukey or Conover's *post hoc* test following a group significant difference in the parametric and non-parametric analysis of variances respectively. A Games-Howell's test was used instead if a Welch Anova had previously been used. In principle, when analysing the difference between accessions, the levels of the developmental stage factor were fixed; *i.e.*, the accessions were compared between them at each developmental stage. Conversely, the variation in metabolite content during development was analysed in one accession at a time. For a non-significant effect of the factor interaction, a simple two-factor model was used for the analysis of variance (Eq.4).

$$Y_{ijr} = \mu + \alpha_i + \beta_j + \epsilon_{ijr}$$

(Eq. 4)

Y_{ijr} : Observed value of Y associated to the i levels of the first factor, j levels of the second and the sample replication (r).

μ : Global theoretical mean of Y

α_i : main effect imputed to the i level of the first factor

β_j : main effect imputed to the j level of the second factor

ϵ_{ijr} : residual error associated with i and j effect in r replications

Data on the multi-accession trial underwent the same data preparation as in the H1-I2 experiment, prior statistical analyses (Eq. 1). The same principle was used to perform ANOVA on a two-factor interaction model was applied, as already detailed above (Eq. 2),(Eq. 3),(Eq. 4). In addition, the difference between accessions in disease symptom severity was assessed by ANOVA, subject to validation of all conditions. Furthermore, an additional analysis was performed, in which metabolite content and disease scores were considered as qualitative variables with several

levels. Metabolite content was divided into four classes (levels) of metabolite enrichment, according to quartile distribution. Each quartile was assigned a label indicating content < 25%, content [25-50%], content [50-75%] and content > 75%. Disease severity scores were divided into three classes (levels) of disease intensity: low score, intermediate score, and high score. Fisher's exact test was then used to evaluate the dependence of these data ($p < 0.05$), followed by factorial correspondence analysis on Fisher's test significance.

Correlation analysis between flavone rutinosides was performed on scaled data using Pearson's method in case of data normality ($p < 0.05$).

5.2 CHAPTER III

5.2.1. Plant materials

Green Globe artichoke seeds were first sown in greenhouse. They were afterwards transferred to the open field in Angers as soon as the frost season was over. Capitula were harvested and transported in crates to the laboratory, where they were immediately cut in quarters, conditioned and stored in a -80°C freezer until use.

Dried leaves of *Mentha x piperita* were provided by the Faculty of Pharmacy of the University of Angers (supplied by Cailleau Herboristerie <https://www.herbo-cailleau.com/>).

Carrot accessions A92 and C12 are maternal lines obtained from the QuaRVeg team breeding programme. They were grown from seed in the field in Angers, until reaching approximately the 12-leaf stage. The leaves were collected in plastic crates covered with moist cloths during transport to the laboratory. They were conditioned and frozen at -80°C before lyophilisation. Once lyophilized they were ground into a fine powder.

5.2.2. Isolation and purification of Luteolin-7-O-rutinoside (L7R)

5.2.2.1 Ultrasound-assisted extraction (UAE) from Peppermint leaves

Ultrasound-assisted extraction was performed with a PEX03 Sonifier (REUS, Contes, France) operating at a frequency of 25 kHz and with a maximum input power of 150 W. The double-layered mantle facilitated the temperature control of the suspension at 15°C thanks to a Julabo F250 compact recirculating system. Powdered dried *Mentha x piperita* leaves (142 g and 144 g) were sonicated twice for 30 min in 1.4 L of MeOH under mechanical stirring at 1300 rpm. After each run, the suspension was filtered through a Celite pad. The first filtrate was evaporated under reduced pressure. The solvent was recycled and used immediately for the second extraction. Both extracts for each batch of leaves were combined and thoroughly concentrated to dryness under reduced pressure to yield 40.6 g of crude extract (14.2% yield).

5.2.2.2 HPLC-UV leaf extract analysis

Leaf extracts were suspended in HPLC grade methanol at 5 mg/mL, homogenised in ultrasonic bath and centrifuged for 2 min at 8500 rpm. Analysis was carried out by injecting 10 µL of solution on an Uptisphere UP3ODB C18 column (150 mm x 4.6 mm, 5 µm, Interchim – France) using a Waters Alliance 2695 HPLC module (Waters, Massachusetts, USA) with H₂O as solvent A and HPLC grade MeOH as solvent B. Elution followed gradient in eluent B at 0.7 mL/min program : 35% for 3 min, 35-45% in 3 min, 45 % for 4 min, 45-55% in 5 min, 55% for 5 min, 55-100% in 2 min, 100% for 3 min, 100-35% in 1 min, 35% for 4 min. A Lut7R standard (Sigma Aldrich, Missouri, USA) was dissolved in HPLC grade MeOH and injected to determine the retention time. Signals were monitored at 254 nm and 320 nm, but peak integration was performed on signals observed at 254 nm to obtain data relative to peak intensity and area under the curve.

5.2.2.3 Leaf extract fractionation: stationary phase screening

Starting from a batch of 5 g of leaf extract at once, two different types of stationary phase were confronted for their efficiency to roughly separate the leaf component focusing on compound polarity in one hand and on their size in another.

Method A: a unique separation was carried out by flash chromatography using a 80 g Silica column (Interchim, France). 5 gram of extract was dissolved in methanol and 10 grams of silica was added to reach a 1:2 ratio in weight. The solvent was evaporated until a dry solid deposit was obtained. It was transferred to a pre-column.. Elution was performed on a Combiflash RF-200 automated system (Teledyne ISCO, Nebraska USA) following a gradient method with AcOEt/ formic acid (FA) 100/1 as solvent A while solvent B was a 50/50/1 mixture of ethyl acetate (AcOEt), MeOH and FA: 0% for 4 min, 0-10 % in 3 min, 10% for 3 min, 10-20% in 3 min, 20% for 7 min, 20-30 % for 3 min, 30-29.8% in 10 min, 29.8-33.5% in 1.1 min, 33.5-50% in 1.9 min, 50% for 5.7 min. The eluent flow rate was set at 40mL/min and the absorbance was measured at 254nm and 320nm. Fractions were further characterised by HPLC-UV using the methanol gradient described in 5.2.2.2. H₂O as solvent A and HPLC grade MeOH as solvent B. Elution followed gradient in eluent B at 0.7 mL/min program : 35% for 3 min, 35-45% in 3 min, 45 % for 4 min, 45-55% in 5 min, 55% for 5 min, 55-100% in 2 min, 100% for 3 min, 100-35% in 1 min, 35% for 4 min. . Signals were monitored at 254 nm and 320 nm.

Method B: a Sephadex LH-20 adsorbent (Sigma Aldrich, Missouri USA) was used after the report from (Inoue et al., 2002) with adaptations. Four independent and consecutive separations were made on the same stationary phase. Prior to the fractionation procedure, 50 g of Sephadex LH-20 were swollen overnight in methanol and then transferred into a glass column (2.5 cm). The obtained stationary phase was conditioned overnight in 60/40 MeOH/H₂O to form a ready-to-use column of about 40 cm long and 2.5 cm external diameter. The following day, 5 g of leaf crude extract

were progressively dissolved in a minimum volume of MeOH and homogenised in an ultrasonic bath. Isocratic elution was applied, using the same eluent as for the column conditioning step and assisted by compressed air. Fractions of 30 mL were collected and analysed by HPLC-UV to identify the ones containing Lut7R. Fractions of interest were from both methods were dried using a rotary evaporator at 40°C.

5.2.2.4 Purification by reverse phase flash chromatography

Sample was prepared and loaded through a solid deposit contained in a C18-bound silica powder pre-column. Purification was performed on a 12 g or 25 g C18 column (Interchim, France) depending on the amount of starting materials. For the latter, fractions from two different experiments were combined for a unique flash chromatography purification. Peaks were eluted at 20 mL/min on a 12g column and 30 ml/min on a 25 g counterpart (Solvent A: H₂O, solvent B : MeOH). Percentage of solvent B in initial conditions was gradually increased 20-40% across purifications to come up with a final method that was set to purify the combined fractions only : 0-5 min 40%, 8-16 min 50%, 19-25 min 60%, 27-32 min 100% and 35-39.9 min 50%.

Absorbance was monitored at 254 nm and 320 nm and fractions of interest were further analysed by HPLC-UV. Solvents were successively removed using a rotary evaporator and a freeze-drier.

5.2.3. Isolation and purification of Chrysoeriol-7-O-rutinoside

5.2.3.1 UAE from carrot leaves

Prior to large scale extraction, a set of three solvent systems were primarily assessed to select for the highest extraction potential: MeOH 100%, MeOH/H₂O 50/50 and MeOH/H₂O 75/25. At this scale, 1 g of dry leaves was suspended in 10 mL of each solvent system and let in an ultrasonic bath for 20 min. The same steps as for the UAE made on peppermint leaves was followed. This enabled to validate the system containing MeOH/H₂O 75/25 for carrying out the extraction from twice 100 g of dry leaves of A92 accession only following the protocol in 5.2.2.1.

5.2.3.2 Characterisation of carrot leaf extracts by HPLC-UV

Extracts from preliminary and large scale experiments were analysed on a Uptisphere UP30DB C18 column (150 x 4.6 mm, 5µm) from Interchim, France. MeOH gradient developed in 5.2.2.2 was applied prior to switching to a more convenient elution system. The LC method proposed by (Plazonić et al., 2009) was adapted to the used column by reducing the mobile phase flow rate from 1mL/min to 0.7 mL/min. The final method used solvent A: acetonitrile (ACN)/H₂O 5/95 + 0.1% FA and solvent B: ACN/ H₂O 50/50 + 0.1% FA as eluents at 0.7mL/min for 60 min. Gradient in solvent B was: 20% for 10 min, 20-40% in 30 min, 40% for 5 min, 40-100% in 3 min, 100% for 6 min, 100-0% in 3 min, 0% for 3 min. Peaks were monitored and integrated at 254 nm, 280 nm and 345 nm.

5.2.3.3 Carrot leaf extract fractionations

The same Sephadex LH-20 column used in 5.2.2.3 was washed and re-used. Fractionation followed the same instructions as detailed earlier in 5.2.2.3, except the conditioning and elution solvent was a 50/50 proportion of MeOH/H₂O. A first fractionation was carried out from combined crude extracts from all the preliminary extractions made (1.188 g). A second fractionation at a larger scale started from 5 g of dry crude extract of the A92 accession. In both cases, fractions were collected every 30 mL and qualitatively characterised by HPLC-UV using the optimised method in 5.2.3.2. At last, they were dried using a vacuum rotative evaporator and a freeze-drier.

5.2.3.4 Purification of target peak by reverse phase flash chromatography

As in 5.2.2.4, all preparation steps were similarly applied herein. The desired peak was purified from 105.6 mg of dried fractions of interest. Prior to solid deposit preparation, the fractions were suspended in MeOH, homogenised in ultrasonic bath and centrifuged at 10000 rpm for 2min. The supernatant was recovered, mixed with 210 mg of C18-bound silica and dried. The separation was carried out on a 4g C18 column from Interchim France, at 12 ml/min (Solvent A: ACN /H₂O 5/95 + FA 0,1% and solvent B: ACN /H₂O 50/50 + FA 0,1%). The gradient in solvent B percentage was: 10% for 5min, 10-20% in 5 min, 20% for 10 min, 20-30% in 6 min, 30% for 8 min, 30-100% in 6 min, 100% for 5 min, 100-70% in 3 min, 70% for 6 min. Absorbance was measured at 254 nm and 344 nm and fractions were characterised by HPLC-UV as in 5.2.3.2. Solvents were at last dried using a rotative evaporator, in a 40°C bath.

5.2.4. Lut7R and Chry7R purity rate validation: HPLC-DAD-ELSD

Fractions from HPLC-UV analysis were prepared at 1 mg/mL in HPLC-grade methanol and analysed according to the LC method developed for each purpose (5.2.2.2 and 5.2.3.2 respectively) using Uptisphere UP30DB C18 column (150 x 4.6 mm, 3µm), from Interchim France. The injected volume was 10 µL, refrigerated at 5 °C. A LC-2030C 3D HPLC module from Shimadzu (Kyoto, Japan) was connected to a Diode Array Detector (DAD) monitoring the absorbance from 190 to 400 nm and to an Evaporative Light Scattering Detector (ELSD SEDEX 90 LT, SEDERE). ELSD experiments were performed at 50 °C, and nitrogen was used as the nebulization gas (3.5 bar). Data were acquired and processed with LabSolutions Software (Shimadzu, Noisiel, France).

5.2.5. Validation of Lut7R and Chry7R identity by LC-HRMS and LC-DAD-MS

For LC-HRMS analyses, the purified derivatives were dissolved in LC-MS grade methanol at a 1 mg/mL concentration. Solutions homogenised in an ultrasonic bath and afterwards filtered through a nylon membrane (0.2µ,13mm) prior to the injection of 1 µL. Liquid chromatography methods were run on a UPLC Acquity Hclass Plus (Waters, Massachusetts USA) using an Acquity UPLC CSH C18 column (1.7 µm, 2.1x 100mm) from the same manufacturer. Two different solvent gradients using H₂O and ACN/H₂O/FA 5/95/0.1 as solvent A. For the identification of Lut7R, the gradient with MeOH as the solvent B was: 35% for 1 min, 35-45% in 1 min, 45 % for 1.5 min, 45-55% in 1.5 min, 55% for 1.5 min, 55-100% in 1 min, 100% for 1.5 min, 100-35% in 1.5 min, 35% for 4.5 min. For the identification of Chry7R, the gradient with ACN/H₂O/FA 50/50/0.1 as solvent B was: 20% in 4 min, 20-40% in 7 min, 40% for 2 min, 40-52% in 1 min, 52% for 1 min, 52-100% in 1 min, 100% for 2 min, 100-0% in 2 min, 0% for 4 min.

Ionisation and detection of eluted peaks were performed on a XeVo G2-XS Quadrupole-time of flight (QTOF) system from Waters. Spectral analyses were performed in both positive and negative mode, upon response of desired compounds. Peaks corresponding to the candidate flavones were searched by entering their respective exact masses (578.16355 g/mol for Api7R, 594.15847 g/mol for Lut7R and 608.17412 g/mol for Chry7R). Fragmentation pattern of the molecular ions were retrieved and compared to existing data in the literature.

Analyses were also run by LC-DAD-ESI-MS in Colmar following the procedure as detailed in (Koutouan et al., 2018). A Nucleodur HTec C18 column (150 × 2 mm, 1.8 µm) from Macherey-Nagel Germany was used with eluents A: ACN + 0.1% FA and B : H₂O + 0.1% FA. Mobile phase flow rate was at 0.25 mL/min. B gradient was : 80–70% in 4 min, 70–50% in 1 min, 50% for 1.5 min , 50–0% in 2 min and 0% for 1.5 min.

5.2.6. Slide culture assays

Four concentrations of Api7R (Extrasynthèse, France), the purified Lut7R and the F_β fraction (containing 73 % Chry7R and 8.7 % Api7R) were considered for the *in vitro* assays: 0.2 mM, 0.5 mM, 1 mM and 2 mM. The fraction was weighted according to the final concentration of Chry7R to be achieved. Stock solutions were prepared at 2 mM in filter sterilised dimethyl sulfoxide (DMSO) and then supplemented with potato dextrose broth medium (PDB) to give a percentage of 1 % DMSO in the final volume. The solutions were homogenised in an ultrasonic bath before preparing the dilutions in PDB.

The P2 strain of *A. dauci* was cultured on V8 medium as described in (Pawelec et al., 2006) for one week prior to the assays. Conidia were harvested by flooding sporulating mycelia with sterile distilled water and gently scrapping the surface of the medium. The suspension was filtered through sterile compress, to eliminate coarse mycelial fragments.

The concentration of the conidial suspension was adjusted to 4×10^4 conidia/mL and tween 20 was added to make up 0.05 % of the suspension. A volume of 500 μ L of the suspension was pipetted into small tubes and the conidia were sedimented using a benchtop centrifuge for 10s. The supernatant was thereafter discarded and the sediment was resuspended in 500 μ L of each of the corresponding compound solutions prepared above. DMSO 1 % was used as a reference group.

The solutions were gently homogenised on a vortex before a 100 μ L drop was placed between a microscope slide and its coverslip. A total of 4 slides were prepared per modality as biological replications. Slides were then incubated in the dark at 22 °C for 4 hours and growth was stopped by transfer to -80 °C.

Germination percentage was estimated on 100 conidia randomly found at the central area of a slide. This counting was repeated on the four slides. The number of hyphae per conidium was manually counted on 20 random germinating conidia per slide. The image of individual conidia was captured using a Leica DMR HC light microscope (ref: 1188054) coupled to a QImaging Retiga 2000R Color CCD camera. Conidia were magnified 250x for the evaluation of Api7R and Lut7R, whereas 200x for the F β fraction. Conidial size and hyphal length were estimated by measuring their area using an image analysis tool developed in collaboration with the ImHorPhen team of IRHS that will be soon available under request.

5.2.7. Pathogenicity tests in greenhouse conditions

Api7R and Lut7R were prepared in 1 % DMSO in sterile distilled water, to give each 0.2 mM and 2 mM of solutions. 1 % DMSO in water was used as reference treatment. Methods used in (Boedo et al., 2010) were used with slight adaptations. Seeds of the susceptible H1 were sown in 0.5 L pots, filled with traysubstrat from Klasmann-Deilmann®, to obtain five plants per modality (one per pot). Then they were grown in greenhouse conditions with a photoperiod of 16h day and 8h night, with temperature of 20°C +/-2 for day and 18°C +/-2 for night. After five weeks, the third fully developed leaf of the plant was isolated in a Petri dish without being detached from the plant (**Figure 67**) for inoculation at the third leaf stage. Inoculum suspensions were prepared in the same way as for the slide assay culture and transported to the greenhouse on ice. Leaf surface inoculation consisted of the application of 50 drops of 5 μ L (**Figure 67**), with one conidium expected per inoculum drop. ALB necrotic spots were counted at 13 days post-inoculation and symptom development was assessed 7 days later as the percentage of blighted leaf surface within the inoculated area.



Figure 67: Drop-inoculation of the third leaf stage of H1 with fifty drops of *A. dauci* conidial suspension in greenhouse.

5.2.8. Development of machine learning tools for a batch image analysis

The most predominant object of an image was detected and expected to be an *A. dauci* conidium. This object was then segmented according to four different object classes assigned as conidium, hyphae, blemish and background (**Figure 68**) using a random forest pixel classification model, from the Ilastik software. The developed plugin was hosted in Napari, where images were submitted in batch output data were accessible. The surface area of the conidium, the number of hyphae and their total surface area were measured.

The development of this tool was achieved in three main steps: 1) model training, 2) testing and 3) validation. A set of 32 images with different exposures and backgrounds were used to train the model for class identification. The performance of the model was evaluated on a total of 1959 images, and validated after the implementing minor adjustments. The accuracy of the class prediction was visually monitored.

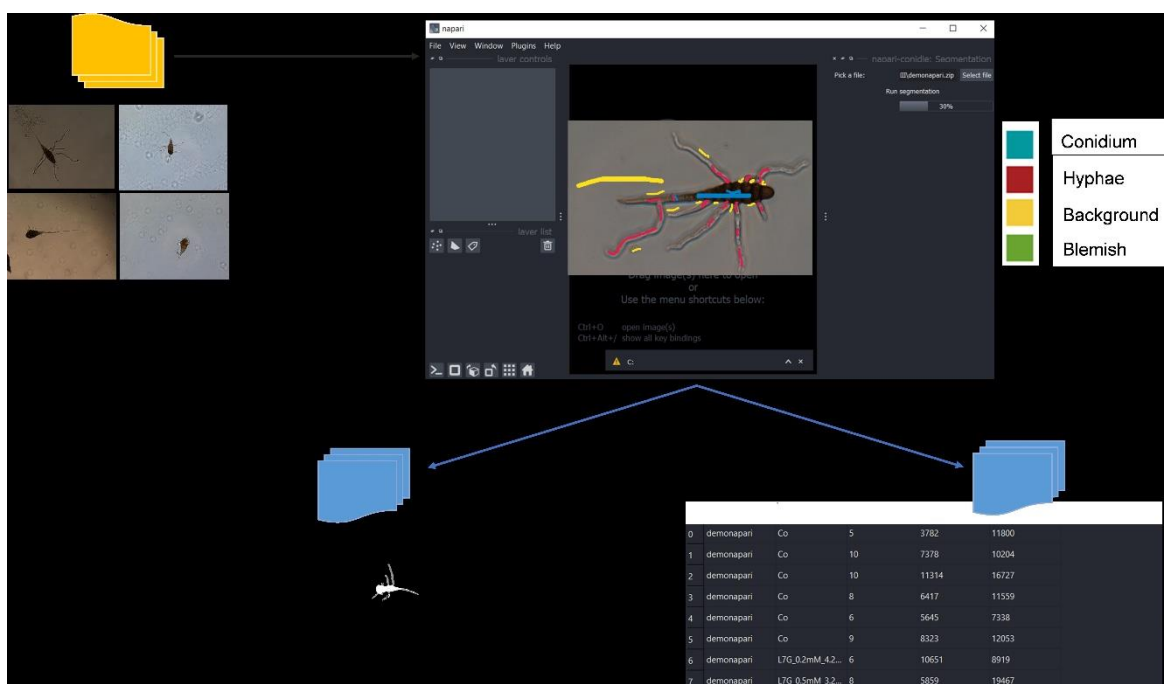


Figure 68: Napari interface showing a pixel classification on the image from an input dataset (yellow folders) and the type of data retrieved in output dataset (blue folders).

5.2.9. Data processing and statistical analysis

Data were analysed using the software R version 4.2.2 (2022-10-31) -- "Innocent and Trusting".

The experiment with Api7R and Lut7R was not carried out simultaneously as the F_{β} fraction. Therefore, a ratio of the germination percentage at different concentrations of the tested compound to the corresponding control was calculated. In addition, separate comparative analyses of each compound to the respective reference were performed.

Surface area data obtained from Napari were logarithmically transformed prior to further analysis. The mean surface area of a hypha was calculated as the ratio of the total hypha area to the number of hyphae per conidium.

Power-transformed data (Box-Cox transformation) were analysed instead of raw data when the transformation allowed to the assumptions for performing a one-way ANOVA to be met. Upon validation of residual normality and homogeneity of variance, ANOVA was used; and if significant ($p < 0.05$), was completed with Dunnett's test to compare the modalities to a reference group or Tukey's test for pairwise multiple comparisons. Where variance homogeneity only was not respected, ANOVA with Welch's correction was used, followed by Dunnett's test or Games-Howell multiple comparison test. If residual normality was not satisfied, a Kruskal-Wallis test followed by Conover's tests was applied, either for comparison with the control or for multiple comparisons.

5.3 CHAPTER IV

5.3.1. Carrot accessions

Two accessions of contrasted resistance level to *A. dauci* were considered in this investigation: H1 (susceptible) and I2 (partially resistant) (**Table 8**).

5.3.2. Induction of callogenesis and somatic embryogenesis from carrot petioles

Surface disinfected seeds of H1 and I2 were placed on a moistened Whatman® filter paper placed in a Petri dish, to germinate. Disinfection involved a first step of 1 minute bath in 70% ethanol. A second step involved a 15 min bath in 2.6 % sodium hypochlorite and three rinses with an autoclaved water. Seedlings were then transferred to a B5 Gamborg ½ medium until the formation of leaves.

Petioles were then withdrawn from the obtained seedlings and cut into 4-5 mm long pieces. Each petiole fragment was cut lengthwise and the wounded side was placed on the same medium supplemented with 1 mg/L 2,4-dichlorophenoxyacetic acid (2,4-D). Petri dishes were kept in the dark at 22°C and subcultured every three weeks until friable cell mass was obtained.

Embryogenic calli of each accession were obtained by transferring the callus masses on a B5 Gamborg ½ medium supplemented with 0.1 mg /L 2,4-D, and placing the dishes under low light intensity 20 µmol/m²/s for 6 weeks.

5.3.3. Gene cloning and transfection of *A. tumefaciens*

BHLH DNA sequences were synthesised and cloned into a pTwist entry vector by Twist Bioscience (San Francisco, California, USA). The entry vectors were then introduced into *Escherichia coli* strain TOP10 by thermal shock at 42 °C for 30 seconds. *E. Coli* clones were selected after a one day of cultivation on LB medium supplemented with kanamycin (50 µg/mL) at 37 °C. Plasmids were extracted using the Nucleospin plasmid extraction kit (Macherey-Nagel, Düren, Germany) and characterised by sequencing, using M13 universal primers (M13-F: 5'-GTAAAACGACGGCCAG-3' and M13-R: 5'-CAGGAAACAGCTATGAC-3'). Each gene of interest was then cloned into a pK7WG2D destination vector (

Figure 69) (Karimi et al., 2002) using an LR Clonase II kit (Invitrogen, Waltham, Massachusetts, USA). Ligation products were transferred into *E.coli* strain TOP10 following the same procedure as described above and positive clones were selected on LB medium supplemented with spectinomycin (100 µg/mL) at 37 °C. Plasmids were extracted from the selected clones using the Nucleospin Plasmid Extraction Kit (Macherey-Nagel) and their sequences were confirmed by using the *p35S* primer (*P35S_pK7WG2D_For* 5'-AAGAAGACGTTCCAACCACG-3'). The destination vectors were transferred into *Agrobacterium tumefaciens* strain EHA105 (pBBR1-MCS-5) by

electroporation and selected after a three days of cultivation on LB medium supplemented with rifampicin (50 µg/mL), gentamicin (10 µg/mL) and spectinomycin (100 µg/mL) at 28 °C.

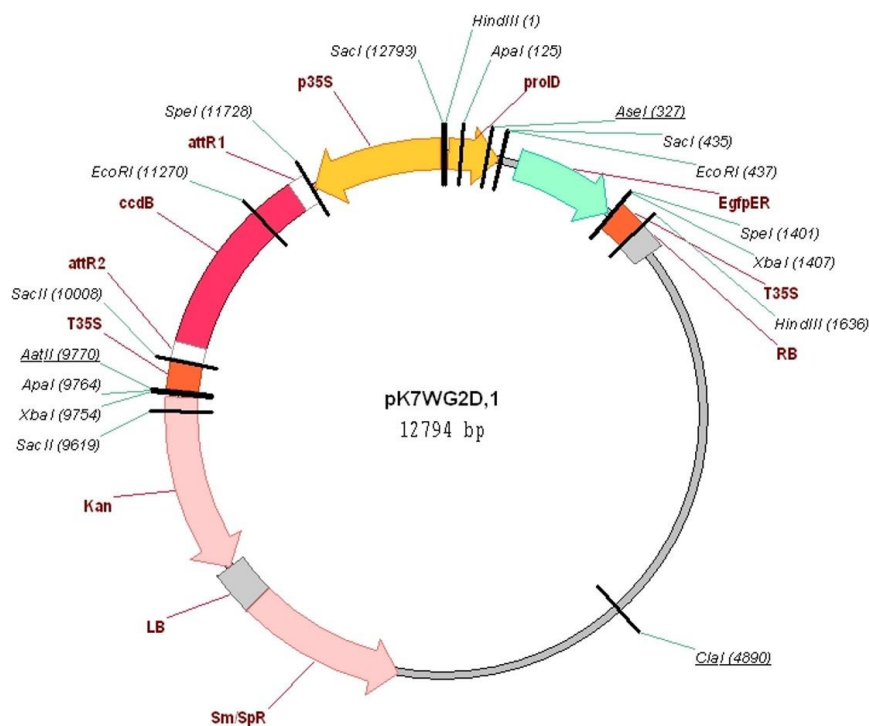


Figure 69: Configuration of the destination vector.

EgfpER (gene encoding for green fluorescent protein) for visual follow up of the transformation events, Kan (NPTII: neomycin phosphotransferase gene) for selection of carrot transformants upon resistance to kanamycin. Photo: Ghent University.

5.3.4. Preparation of the bacterial suspensions and carrot cell transformation

One *A. tumefaciens* colony of each desired plasmid construction (native, with *bHLH*) was plated on a LB medium supplemented with rifampicin (50 mg/L) and spectinomycin (100 mg/L) and gentamycin (10 mg/L) for two days. The resulting cultures were suspended in a MinA medium containing 100µM of acetosyringone and shaken at 150 rpm for 2h at 28°C.

Carrot embryogenic calli grown on B5 Gamborg ½ medium were exposed to *A. tumefaciens* suspension at $D_{0600} = 0.1$ for 10 min and then co-cultured on Whatman paper placed on top of the culture medium in the dark at 19- 23°C for 1 day. Transformant selection was subsequently initiated by transferring the calli on a fresh medium supplemented with 100 mg/L kanamycin and 500 mg /L cefotaxime, to discard NT calli and *A. tumefaciens* respectively. Calli were subcultured every three weeks on a B5 Gamborg ½ medium supplemented with 50 mg/L kanamycin until callus masses homogeneously expressing *GFP* were observed by fluorescence microscopy.

5.3.5. Whole plant regeneration

Calli were subcultured every three weeks on B5 Gamborg ½ medium supplemented with 50 mg/L kanamycin, without growth regulators. Petri dishes were placed in growth chambers under a light period of 16 hours at 70 $\mu\text{mol}/\text{m}^2/\text{s}$ at 23°C and a dark period of 8 hours at 19°C. Subculturing cycles lasted approximately 3 months before carrot plantlets were obtained.

For modalities which had difficulty to grow, the medium was supplemented with 1 mg/mL of 6-Benzylaminopurine (BAP).

5.3.6. Selection of transformation events for phenotyping

Two separate experiments were carried out. The first was preliminary and aimed at following up the development of the putative transformants *in vitro* and in the acclimation greenhouse plantlets were planted into 80-cell seed trays filled with traysubstrat from Klasmann-Deilmann®, (one plantlet per hole). Then they were grown under a photoperiod of 16h day and 8h night, with temperature of 20°C +/-2 for day and 18°C +/-2 for night. The attention was focused on modalities containing the plasmid without an insert. Whole plant regeneration from calli was undertaken and plantlets that appeared vigorous after several cycles of selective subculturing were considered for acclimation in greenhouse (**Figure 70**). In order to assess the feasibility of leading the plants to seed setting, a regular follow-up was carried out and the number dead plants was recorded during a 5-month interval. A selection of plants remaining in the greenhouse at the end of the 5 months was genetically characterised.



Figure 70: Acclimation of plantlets in seed trays under greenhouse conditions.

In the second experiment, genotyping and phenotyping were performed at the callus stage only. The fluorescence of the GFP in the calli was visualised using an SZX16 stereomicroscope (Olympus, Tokyo, Japan): $\lambda_{\text{excitation}} = [460-480\text{nm}]$, $\lambda_{\text{emission}} = [495-540\text{nm}]$ (**Figure 71**). The 15 most homogeneously fluorescing callus masses were considered as 15 separate transformation events for one construction and spotted for multiplication. Calli not exposed to *A. tumefaciens* were used as a negative control (untransformed NT). Multiplication consisted of sub culturing of one callus mass in one Petri dish of Gamborg ½ medium with 0.1mg/L 2,4-D and 50 mg/L kanamycin, placed in the dark. Multiplied events and NT calli were sub cultured on a fresh medium 3 weeks before sampling. Untransformed calli were cultured on a kanamycin-free medium to prevent their loss.

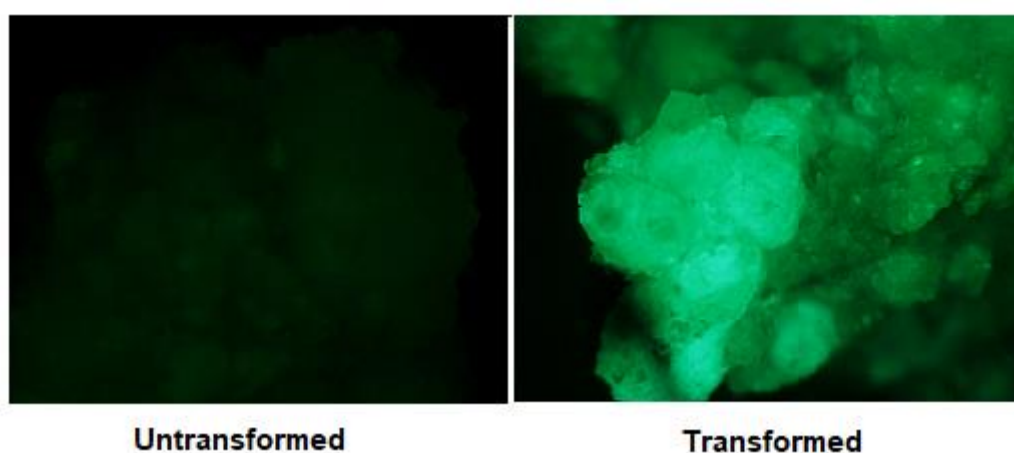


Figure 71: Fluorescence of the GFP in transformed calli (right), compared to the ones that were not exposed to *A. tumefaciens* (left).

5.3.7. Verification of the genetic transformation in regenerated plants

Leaves were withdrawn from greenhouse grown plants and ground to a fine powder in liquid nitrogen, using a mortar and pestle. DNA was extracted from 10 mg of fresh leaf powder using the Nucleospin® Plant II kit (Macherey-Nagel), according to the manufacturer's protocol. Integration of the selectable marker gene (*NPTII*, *NPTII*-F: 5'-GAGGCTATTCGGCTATGACTG-3' and *NPTII*-R: 5'-ATCGGGAGCGGCGATACCGTA-3') into the carrot genome was verified by endpoint PCR: 10 µL reactional volume contained 1X Taq buffer, 0.15 mM of each deoxyribonucleotide triphosphate (dNTP) (Promega, Madison, Wisconsin, USA), 2 mM MgCl₂, 0.15 µM of each of the primer pair, 0.5 units of Taq DNA polymerase (Promega, Madison, Wisconsin, USA). The PCR program was as follows: 94 °C 2 min, 35 cycles (94 °C 30 s, annealing temperature 15 s, 72 °C 30 s) and 72 °C 7 min. PCR products were dyed with Midori Green (Nippon Genetics Co., Ltd., Tokyo, Japan) fluorescent dye and electrophoretically migrated on 1% agarose gel for 25 min, before visualisation under UV light.

5.3.8. Gene expression analysis in carrot calli

RNA extraction was carried out from 50 mg of fresh calli, using the NucleoSpin RNA Plus kit (Macherey-Nagel), according to the manufacturer's protocol (Macherey-Nagel, 2016). Total extracted RNA was quantified using a NanoDrop ND-1000 spectrophotometer (NanoDrop Technologies, Wilmington, Delaware, USA). The absence of genomic DNA was verified by endpoint PCR (94 °C for 5min, 35 cycles of (94 °C for 30s, 56 °C for 90s, 68 °C for 60s) , 68 °C for 10 min, 4 °C for 5min) using primer pairs targeting an intronic sequence of the *EF1- α* gene (*EF1- α -int-F* 5'- GCTTTACTTGCATTTACCCTTGGT-3' and *EF1- α -int-R* 5'-ACCCAACCTTCTTCAAGTAAGATGA-3'. Insertion of the *NPTII* gene was also verified by endpoint PCR as in 5.3.7.

Reverse transcription (RT) of RNA was performed on 2 µg total RNA in a 25 µL reaction volume using the M-MLV Reverse Transcriptase Kit (Promega, Madison, Wisconsin, USA). The reaction program was: 42 °C for 60 min, 70 °C for 10min and 4 °C for 10 min.

Quantitative real-time PCR (qRT-PCR) was performed on the obtained cDNA using the GoTaq®qPCR Master Mix kit (Promega) according to the manufacturer's protocol and using a Chromo4 Real-time PCR detector (Bio-Rad, Inc., Hercules, CA, USA): 95 °C for 5min, 40 times (95 °C for 3s, 60 °C for 1min), 60 °C to 95 °C for 5s and plate reading.

Three housekeeping genes *GAPDH*, *α tubulin* and *actin* (primer sequences in Patent No. DI-RV-19-0075, an extension of the Patent No. WO/2011/161388) were used as reference genes to evaluate the expression level of the candidate gene (*BHLH-F* 5'- ATATTCGCGTCTCCTTTTATGC-3' and *BHLH-R* 5'- GCCGATCCCTCCTGCAAT-3'). Three technical replicates per sample were included in the analysis.

5.3.9. Metabolite quantification: LC-ESI-MS

Approximately 1 g of callus was withdrawn and placed in a 2 mL screw-capped tube. The calli were freeze-dried. Fifty milligrams of the dry material was weighted for hydromethanolic extraction and the other 50 mg for subsequent metabolic analysis. The analytical method was similar to that described in paragraph 5.1.2.

5.3.10. Callus hydromethanolic extracts for biological activity assay

The calli were ground in an ice-cold mortar. The powder obtained was suspended in 7.5 mL of hydromethanolic solvent (MeOH/H₂O 75/25 v/v), including the suspension volume of the powder and two rinses of the mortar. The solution obtained was placed in an ultrasonic bath for 20 min. The liquid extract was recovered and another 2 x 2.5 mL of residual extract from the rinsing of the material and the container was added. 10 µL of DMSO was then added to the suspension before the container was returned to the ultrasonic bath for another 20 min. The liquid extract was filtered through a 25 µM metal filter and completed with 3 x 2.5 mL of the wash. The extracts obtained were centrifuged twice at 8500 rpm for 5 min. The supernatant was collected and the solvent was dried using a rotary

evaporator in a 40 °C bath. Dried callus extracts were resuspended in MeOH/H₂O 53/1 v/v and filtered on cellulose (0.45 µM).

5.3.11. *In vitro* biological activity test of callus extracts

Stock solutions of callus extract were prepared at 100 mg/mL in PDB with 1% DMSO, at 1/10 m/v ratio (mg / µL). A 5-fold dilution was prepared in PDB to give the solutions at 20 mg/mL. PDB with 1 % DMSO was used as a reference treatment. The conidial strain used and the preparation of the conidial suspension were as described in paragraph 5.2.6. Germination rate was estimated on 4 times 100 conidia per microscope slide. Formed hyphae in 80 germinating conidia were counted manually. The hyphae were visually inspected to note a possible hyphal destructure. In this assessment, a conidium is considered germinated as long as it has a visible hypha regardless of its integrity

5.3.12. Data processing and statistics

Quantitative PCR data were retrieved from the Bio-Rad CFX Maestro1.1 software. Gene expression level was normalised upon the expression of the housekeeping genes. The $2^{-\Delta\Delta C_q}$ method (Livak and Schmittgen, 2001) was used to obtain the expression level of the target gene referring to its expression level in the empty vector modality of H1 and of the same accession. For this purpose, the average expression level of 7 empty vector control in H1 transformation events were calculated and used as a reference thereafter.

Data from biological assays were analysed using an ANOVA with R version 4.2.2 (2022-10-31) -- "Innocent and Trusting", following the procedures described in 5.2.9. conidial germination rate values were divided by 100 and subjected to an arcsine transformation before meeting the conditions for ANOVA. The number of hyphae per conidium was analysed by ANOVA without primary data transformation. Significant differences (0.05 threshold) were followed by Tukey's multiple comparison test (0.05 threshold).

GENERAL DISCUSSION

In retrospect, each piece of results highlighted in Chapters II, III and IV points towards the same direction: two of the three candidates are potentially the most involved in ALB resistance, and probably the most relevant for future use in breeding programmes. However, there are still grey areas in each step of the investigation that are worth discussing with a general overview of the role of such a family of compounds in plant-fungus pathogenic interactions.

Kinetics of flavonoid accumulation in carrot accessions along the vegetative growth phase and location

The differential accumulation of the three flavonoids between the accessions H1 and I2 was previously observed at approximately the 6-leaf to 8-leaf stage (Koutouan et al., 2018). The follow-up of their accumulation in the leaves at different stages of the vegetative growth showed that this difference is already marked as soon as the 2-leaf stage and stabilises until the 12-leaf stage. This accumulation pattern was not comparable to that in other species, which followed the seasonal variation and progression of the growth stage (Ryu et al., 2017) or varied according to the source-sink relationship in the plant, as for the anthocyanin content in the leaves of purple yam (*Dioscorea alata*), which shifted in coordination with their content in the roots along the growth stage (Yin et al., 2015). In carrot, the root content of the three candidates was not studied, but even if variations occurred in the roots, they do not seem to affect the leaves, as here it was shown that the candidates flavonoids not only to constitutively accumulate in the leaves of I2, but also that their content is rather stable along the plant development. Their possible link with root metabolism could still be investigated. What is also new compared to previous findings is that, when the differences are smaller than those between H1 and I2, *i.e.*, between H1 and intermediate accessions, only Lut7R and Chry7R correctly discriminated susceptible accessions from partially resistant ones from the 2-leaf stage onwards. Api7R is in fact not discriminatory enough to highlight minor differences. Since *A. dauci* can also infect inflorescences (Strandberg, 1983) and is transmissible through seeds (Netzer and Kenneth, 1969; Maude et al., 1992), the flavonoid content of seeds should be regarded in parallel with their ability to develop seedlings after ALB infection. Quantification of rice seed flavones in dry and germinating embryos suggested that the overall levels of flavones and glycosylated flavones did not change significantly after reactivation of the seed metabolism (Galland et al., 2014). Their study also highlighted that the levels of chrysoeriol and of luteolin-4'-O-glucoside decreased, in contrast to the levels of Chy7R, which increased slightly during germination. These results suggest that the accumulation of the glycosylated forms starts early after imbibition. The early accumulation of Chry7R after seed imbibition would make sense in carrot seeds, to protect the seedlings from stressful stimuli such as the occurrence of ALB. It would be therefore particularly relevant to study this early phase of plant development, as this could provide a new lever for crop protection at the planting stage.

Furthermore, the present study breaks the limit of correlative analyses of metabolomic and genetic data observed on only one genetic background, and imposes the need to extend the study to an even a greater range of population

diversity. The lack of resolution in the previous study (Ph.D. Koutouan 2019) could, on the one hand, be related to an accumulation of the rutinosylated forms in leaves in the order Api7R > Lut7R > Chry7R, presumably simply due to the up-regulation of multi-substrate glycosyltransferase genes in I2. This enzyme would, theoretically, have a better affinity with the structure of apigenin than those of luteolin or chrysoeriol. This aspect should be further explored with the candidate glucosyltransferase discussed in Chapter IV. On the other hand, it could also be imagined that these enzymes have the same affinity for both genins and that its activity depends on the availability of precursors. In this sense, genes encoding flavone 3'-hydroxylase and 3'-O-methyltransferase would be upregulated in accessions differentially accumulating Lut7R and Chry7R, as to allow the 3'-O-hydroxylation of apigenin to produce luteolin and, the methylation of the 3'-OH group of luteolin to give chrysoeriol, respectively. One way to answer this question is by comparative gene expression analysis between accessions, but this requires prior identification of the correct candidate genes.

Accessions accumulating higher levels of Lut7R and Chry7R compared to H1 had a resistance level comparable to that of I2. For now, it would be interesting to identify the threshold in metabolite content that confers a minimum phenotypic improvement. Working with a diversity set implies taking into account all other major resistance factors within an accession. The resistance of I2 and other accessions may depend substantially on their levels of the candidate flavonoids, although, it is not irrelevant to consider leaf vigour as part of a mechanical defence strategy. Features of the aerial tissue, to mention only foliage height and density, are non-negligible components that can modulate the establishment of *A. dauci* (Santos et al., 2000). Moreover, leaf hardness, in combination with leaf surface hydrophobicity, is a determinant factor inducing conidial germination in the tomato-*Botrytis cinerea* pathosystem (Doehleemann et al., 2006). To investigate these other factors, more precise phenotyping will have to be developed. Variation in the chemical composition of the leaf cuticular wax may also comfort or hinder the pathogen in the infection process (Gniwotta et al., 2005). The frequency of trichomes on the leaf has been shown to play a role as well, due to the presence of protective compounds in the secretory products that help to damaging oxidative burst (Tattini et al., 2000; Tattini et al., 2005). This raises the more general question of the localisation of candidates in the plant. Previous histo-cytological observations of leaf surfaces by the QuaRVeg team have already shown differences in the number of trichomes between susceptible and partially resistant genotypes and observations of vesicles in basal cells (unpublished data). Therefore, one hypothesis here could be a localisation of candidate metabolites in the basal cells of trichomes as a ready-to-use weapon against *A. dauci*. To investigate this further in the future, laser capture microdissection coupled with metabolite dosages as well as laser scanning confocal microscopy could be considered.

Biological activity and mechanisms of action of the candidate flavonoids

Unexpectedly, Api7R and Lut7R exhibited stimulation of the conidial germination and hyphal emergence in *A. dauci*. As candidates for resistance, it is surprising to uncover this mode of action. Stimulation of fungal growth by

flavonoid glycosides has been observed before, but in the context of a beneficial plant-fungus interaction (Lagrange et al., 2001). Probably one of the rarest cases of pathogenic interactions, (Ruan et al., 1995) have found that apigenin-7-*O*-glucoside and pisatin from pea (*Pisum sativum*) root exudates stimulated the germination of *Fusarium solani* f. sp. *Pisi* spores. A complementary pharmacological experiment elucidated the signalling pathway activated in the fungus and demonstrated that this phenomenon could be due to tolerance to phytoalexin (regarding pisatin). As this compound also induced *nod* gene expression during interaction with rhizobacteria, it was, therefore, considered to be a host recognition compound in *F. solani*. Based on these observations, the stimulation of pathogen development by defence-related flavonoids was interpreted as an adaptation of the pathogen to its host, revealing a more specialised interaction between the host and the pathogen, as summarised by (Straney et al., 2002). Observations made on the tomato (*Solanum lycopersicum*)–*Fusarium oxysporum* f. sp. *Lycopersici* pathosystem confirmed the involvement of phenolic compounds in the onset of the plant-pathogen interaction, although their results contradicted the concept of host selectivity being mediated by these compounds (Steinkellner et al., 2005). It is therefore possible that *A. dauci* has already overcome the protection that Api7R may have conferred the carrot plant in the past, at least for the fungal strain used in this study. Fungal pathogens can evade host defence mechanisms by detoxifying active compounds from the host plant and by secreting catabolic enzymes (Westrick et al., 2021). In the case of *Sclerotinia sclerotiorum*, its virulence against *Arabidopsis thaliana* was associated with its ability to metabolise rutin, by releasing the rutinose moiety, prior to degradation of the aglycone by a quercetin 2,3-dioxygenase (Chen et al., 2019). In the tomato (*Solanum lycopersicum*)–*Cladosporium fulvum* interaction, the increased virulence of the pathogen was conferred by a tomatinase enzyme, capable of degrading α -tomatin, a saponin reported to have antimicrobial activities in plants (Kmen et al., 2013). Similar mechanisms may exist in *A. dauci*. However, till date, its aggressiveness has been mostly linked to the production of phytotoxins (Courtial et al., 2018). The resistance to *A. dauci* exhibited by flavonoid accumulating carrot accessions (I2 and Boléro) has been shown to include resistance to phytotoxins (Lecomte et al., 2014; Courtial et al., 2018). In the current study, the late protective effect of Lut7R observed *in planta* could be due to two possible mechanisms: the first, by protecting the plant from the damaging effects of the toxin, which could be through a more efficient antioxidant activity than Api7R or by inducing defence response in the host. Such a mechanism might be more efficient if the metabolites were applied before the inoculum rather than in the inoculum, to prime the plant. To test this, Lut7R and Api7R would be applied on the leaves at different times before the conidial solution. The second mechanism could be a reduced toxin production in *A. dauci*. This compound may have impacted toxin biosynthesis in this fungus, while limiting the effect of oxidative bursts in carrot leaves as well (Shivashankar and Sumathi, 2022). With regard to *Fusaria* species, it was reported that through the high antioxidant potential of luteolin, it caused 49-99 % decrease in trichothecene production by the fungi, and exposure to this compound among other flavonoids inhibited trichothecene biosynthesis genes (Bilska et al., 2018). The authors emphasised that the relatively weak inhibitory activity exerted by apigenin may have come from its much lower antioxidant activity compared to luteolin. In resistant maize lines, increasing flavonoid content was correlated with limited accumulation of *Aspergillus flavus* toxins in the kernels (Castano-Duque et al., 2021). For the carrot-

A. dauci pathosystem, this mechanism could be explored in depth, by first exposing different strains of *A. dauci* to the candidate flavonoids before quantifying their content of the aldaulactone toxin (Courtial et al., 2018) or measuring the expression levels of candidate polyketide synthase genes, recently identified as directly related to aldaulactone biosynthesis in *A. dauci* (Courtial et al., 2022). We did not see an early deleterious effect of Lut7R on the fungus during our *in planta* biological assays, which could have prevented any onset of symptoms, but we can hypothesize that the stimulation of conidial germination occurred as soon as Lut7R and conidia were in contact, whereas a possible change in aldaulactone levels would take more time. To evaluate this, metabolite-conidia confrontations of different durations could be performed.

Nevertheless, from an evolutionary point of view, the addition of another step in the flavone pathway by increasing the structural complexity of the apigenin through luteolin and chrysoeriol, could indicate an adaptation to a changing environment. More clearly, the biosynthesis of the chrysoeriol from luteolin may reflect a need to regain full control over the pathogen, which probably already uses Lut7R as a host recognition molecule as well. This makes sense from this point of view, as the fraction containing Chry7R in our study did not stimulate germination, suggesting that it could have inhibited hyphal development if it was present in much higher purity in the fraction. This compound is more likely to have a direct effect on the pathogen by inhibiting its development, and perhaps its ability to produce toxins, yet to be demonstrated. This would be a nice example of co-evolutionary story between a plant and a pathogenic fungus: i) Carrot first resisted until the fungus adapted itself to Api7R and used this molecule to recognize the host ii) Carrot developed a more complex molecule from Api7R that is Lut7R efficient until a new fungal adaptation iii) Carrot evolved a more complex molecule from Lut7R that is Chry7R. Investigation of fungal *A. dauci* strains isolated from highly susceptible wild carrot resources would perhaps help to evaluate this.

So far in the discussion, the three candidate flavonoids differ only in the substitution at the 3' position of their respective B-ring. In carrot leaves, luteolin glucoside was reported to be the most abundant (Teubert et al., 1977; Brooks and Feeny, 2004). In accession I2, 7-O-glucosylated forms of these flavones were also present (Koutouan et al., 2018), but did not correlate with mQTL upregulation (not published). We therefore planned to test the biological activity of the 7-O-glucosides, in order to evaluate the importance of the addition of a rhamnosyl group in ALB resistance. Unfortunately, these compounds precipitated in the medium and did not allow optimal visualisation of the *A. dauci* conidia. Nevertheless, glycosylation is known to be associated with improved hydrophilicity of compounds, facilitating their transport to less lipophilic target sites such as the cell wall, or their transport to the vacuole (Le Roy et al., 2016). Aglycones are often considered toxic to the plant itself, therefore their release at the target site requires both glycosylation to inactivate them in the cellular matrix, and hydrolysis by a cell wall-associated glucosidase, allowing the aglycones to complete their function as antioxidants in the extracellular space (Chong et al., 1999). This would be a future area of investigation for studying the interaction between carrot and *A. dauci*.

Overexpression of *DcbHLH118-like* in H1 and *Dc3-O-Glucosyltransferase2-like*

The overexpression of the candidate *bHLH* in H1, seemed to indicate an indirect role in the biosynthesis of the candidate flavonoids. However, the reduction of the metabolite levels in these over-expressors compared to the EV calli could indicate a negative regulation of the flavonoid biosynthesis by this gene, although this interpretation could be biased, as *A. tumefaciens* may have caused a transcriptional shift in the calli. In addition, this gene was naturally up-regulated in the accession I2 and positively correlated with metabolite accumulation compared to H1, according to previous results (Ph.D. Koutouan 2019). Available data in the literature indicate that among the *bHLH* family, some are up-regulators of the flavonoid biosynthesis, while others act as repressors (Hichri et al., 2010; Song et al., 2013; Kodama et al., 2018). *BHLH* repressors can also bind directly to gene promoters to counteract the effect of activators (Song et al., 2013). Likewise, R2R3-MYB transcription factors can act as repressors of the flavonoid biosynthesis (F., Xu et al., 2014), and it could be imagined that this type of MYB was activated after the incorporation of the plasmid into calli; thus, counteracting the putative up-regulation of the flavonoid biosynthesis by the candidate *bHLH*. At this stage, it is difficult to speculate on the direction of action our candidate *bHLH* goes, as we do not have a clear view into the transcriptional reprogramming that may have been induced in carrot calli by *A. tumefaciens*. Our results should be complemented with data from RNA sequencing and metabolomic analyses of the transformants, to identify the potential target genes.

For the glucosyltransferase candidate, metabolomic analyses should be performed to provide a global view of its potential substrates *in planta*.

Conclusion and perspectives:

This Ph.D. programme made it possible to obtain more precision on the correlative evidence between the content of metabolites in carrot leaves and the level of resistance to *A. dauci*. It enabled to reveal the importance of each compound, which according to our results, is not at the same level. Mechanistic hypotheses were put forward. For example, the evaluation of their biological activity *in vitro* and *in planta* underpinned that the pathogen may have completely bypassed the resistance mechanism through the accumulation of Api7R in carrot leaves, and now uses this compound as a host recognition signal. The Fungisem team at the IRHS, which is investigating the pathogenesis of *A. dauci*, could look at a possible effect of this compound on the *A. dauci* transcriptome. The resistance provided by Lut7R would be partially sustained by a probable double action: a direct effect that the pathogen has already circumvented, and an indirect effect on the plant that still confers protection. The QuaRVeg team could go further in describing the effect of exogenous application of Lut7R on defence reactions in carrot leaves inoculated or not by *A. dauci* as well as quantifying fungal biomass in treated infected leaves by real-time PCR. Chry7R may play a crucial role in the carrot resistance to *A. dauci*. More purified Chry7R should be obtained as a priority to validate the assumption of its inhibitory effect on the conidial development and possibly on limiting disease development on carrot leaves. At this stage, the available information suggests that Lut7R and Chry7R would be of interest as

resistance markers. When this mechanism can be implemented in new cultivars by metabolite-assisted selection, identification of the genetic determinants will be necessary to enable the use of new breeding techniques in other contexts. Even though the role of the candidate genes in metabolite accumulation is not clear, their role in mediating ALB resistance is still relevant, in the light of past genetic analyses. This should be supported by the phenotyping of regenerated transformants for resistance to *A. dauci*. As transformants are now available, functional analysis on the second candidate gene, encoding UDP-flavonoid-glycosyltransferase needs to be completed.

Concerning the follow up of a diversity set of carrot, experiment on a much larger population should be carried out in the same way and the features of the aboveground parts should be characterised in parallel with the genetic diversity analysis. SNP (Single Nucleotide Polymorphism) and DcS-ILP (*Daucus carota* Stowaway-like MITE (Miniature Inverted-repeat Transposable Element) based Intron Length Polymorphism) have been recommended as cost- and time-effective tools (Stelmach et al., 2017; Stelmach et al., 2021), they could be used to genetically characterise genotypes to ensure that the set is largely diverse. Furthermore, it is clear that the three compounds coexist in the leaves and therefore the accumulation of Api7R is a weak point of the system. Estimating the minimal metabolite ratio in Api7R / Lut7R / Chry7R with their relative content would be more relevant for breeders, to identify the minimal threshold that confers an improvement in ALB resistance.

The compatibility between several resistance mechanisms in a cultivar should also be evaluated, for example, in combination with the accumulation of terpenes. Indeed, it is known that the resistance of accession K3 is due to its terpene content (Koutouan et al., 2018), therefore, enhancing the accumulation of flavonoids in this accession would allow to explore a putative complementarity between the two mechanisms that could result in a higher level of resistance.

With regard to root quality, it has been shown that root carotenoid content can be affected by infection with *A. dauci*, suggesting that there is a possible trade-off between foliar defence and root carotenoid metabolism (Perrin et al., 2017). The same study also highlighted that the impact of *A. dauci* could be even more important in combination with drought stress. The relevance of flavonoid-mediated resistance should therefore be considered in the development of new cultivars for diverse climatic contexts in which carrot is produced.

Lastly, this work reminds us that the host and the pathogen are constantly evolving and adapting to each other over time (**Figure 72**). We lack time scale for how long it takes for *A. dauci* to become less affected by the metabolic evolution of the carrot and vice versa. Faced with the unknown, we are urged to dig deeper into priority elements identified in the present study, to help carrot growers and the French authorities anticipate the withdrawal of harmful phytopharmaceuticals still in use.

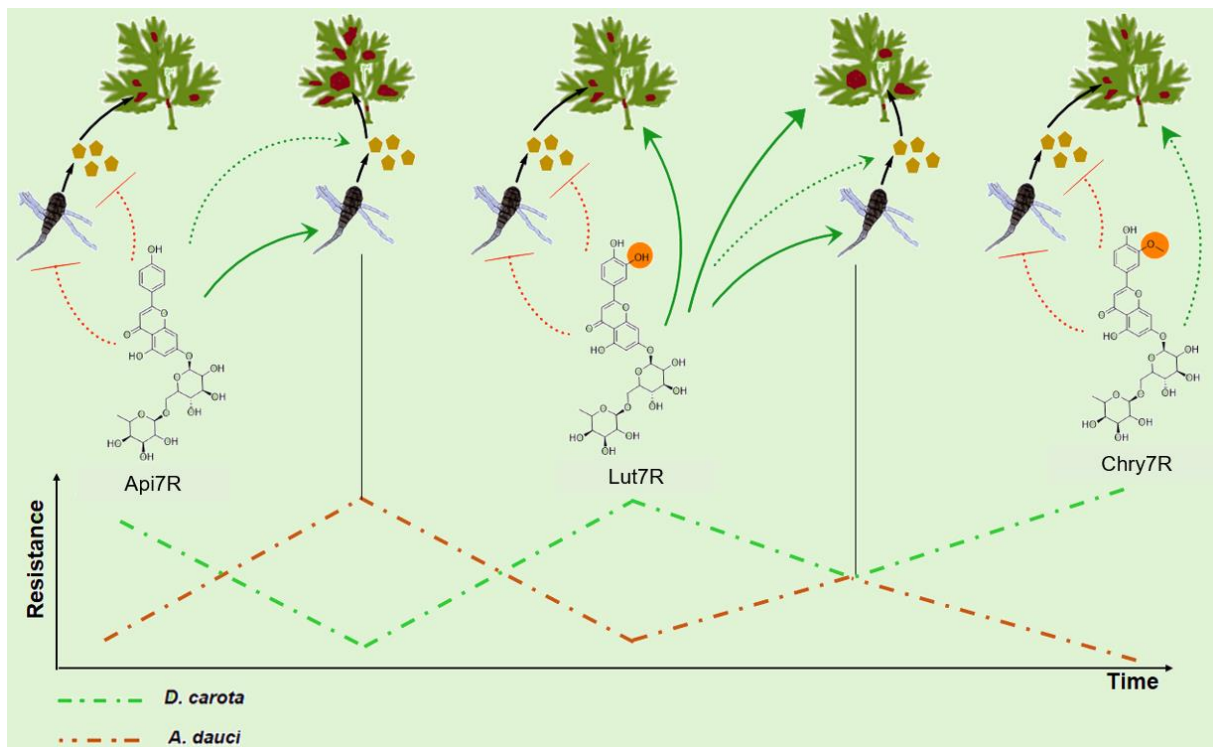


Figure 72: Co-evolution of carrot and *A. dauci* regarding flavonoid-mediated ALB resistance. Dashed arrows: hypothetical; Solid arrows: observed. Api7R: apigenin-7-O-rutinoside, Lut7R: luteolin-7-O-rutinoside, Chry7R: chrysoeriol-7-O-rutinoside.

BIBLIOGRAPHY

- Abu-Reidah, I.M., Arraez-Roman, D., Segura-Carretero, A. & Fernandez-Gutierrez, A. (2013) Extensive characterisation of bioactive phenolic constituents from globe artichoke (*Cynara scolymus* L.) by HPLC-DAD-ESI-QTOF-MS. *Food Chemistry*, 141, 2269–2277. <https://doi.org/10.1016/j.foodchem.2013.04.066>.
- Acosta-Motos, J.R., Díaz-Vivancos, P., Becerra-Gutiérrez, V., Cortés, J.A.H. & Barba-Espín, G. (2021) Comparative characterization of eastern carrot accessions for some main agricultural traits. *Agronomy*, 11. <https://doi.org/10.3390/agronomy11122460>.
- Agati, G., Biricolti, S., Guidi, L., Ferrini, F., Fini, A. & Tattini, M. (2011) The biosynthesis of flavonoids is enhanced similarly by UV radiation and root zone salinity in *L. vulgare* leaves. *Journal of Plant Physiology*, 168, 204–212. <https://doi.org/10.1016/j.jplph.2010.07.016>.
- Agati, G., Matteini, P., Goti, A. & Tattini, M. (2007) Chloroplast-located flavonoids can scavenge singlet oxygen. *New Phytologist*, 174, 77–89. <https://doi.org/10.1111/j.1469-8137.2007.01986.x>.
- Agati, G., Stefano, G., Biricolti, S. & Tattini, M. (2009) Mesophyll distribution of ‘antioxidant’ flavonoid glycosides in *Ligustrum vulgare* leaves under contrasting sunlight irradiance. *Annals of Botany*, 104, 853–861. <https://doi.org/10.1093/aob/mcp177>.
- Ahmad, L. & Siddiqui, Z.A. (2017) Effects of *Meloidogyne incognita*, *Alternaria dauci* and *Fusarium solani* on carrot in different types of soil. *Acta Phytopathologica et Entomologica Hungarica*, 52, 39–47. <https://doi.org/10.1556/038.52.2017.012>.
- Ahmad, T., Cawood, M., Iqbal, Q., Ariño, A., Batool, A., Sabir Tariq, R.M., et al. (2019) Phytochemicals in *daucus carota* and their health benefits—review article. *Foods*, 8, 424.
- Almeida, A., Favero, B.T., Dong, L., Cárdenas, P.D., Saenz-Mata, J., Lütken, H., et al. (2023) Lessons learned from metabolic engineering in hairy roots: Transcriptome and metabolic profile changes caused by *Rhizobium*-mediated plant transformation in *Cucurbitaceae* species. *Plant Physiology and Biochemistry*, 201. <https://doi.org/10.1016/j.plaphy.2023.107797>.
- Amirov, B.M., Amirova, Z.S., Manabaeva, U.A. & Zhasybaeva, K.R. (2014) Carrot breeding for *Alternaria* leaf blight resistance. *Acta Horticulturae*, 1053, 223–226. <https://doi.org/10.17660/ActaHortic.2014.1053.24>.
- Ancuceanu, R., Hovaneț, M.V., Anghel, A.I., Dinu, M., Dune, A., Ciolea, M., et al. (2017) Variation of polyphenols and iron concentration in *Mentha X piperita* L. By development stage and soil type. *Farmacia*, 65, 748–754.
- Anhalt, S. & Weissenböck, G. (1992) Subcellular localization of luteolin glucuronides and related enzymes in rye mesophyll. *Planta*, 187, 83–88. <https://doi.org/10.1007/BF00201627>.
- Ardila, H.D., Martínez, S.T. & Higuera, B.L. (2013) Levels of constitutive flavonoid biosynthetic enzymes in carnation (*Dianthus caryophyllus* L.) cultivars with differential response to *Fusarium oxysporum* f. sp. *dianthi*. *Acta Physiologiae Plantarum*, 35, 1233–1245. <https://doi.org/10.1007/s11738-012-1162-0>.
- Argentieri, M.P., Madeo, M., Avato, P., Iriti, M. & Vitalini, S. (2020) Polyphenol content and bioactivity of *Achillea moschata* from the Italian and Swiss Alps. 75, 57–64.
- Arscott, S.A. & Tanumihardjo, S.A. (2010) Carrots of many colors provide basic nutrition and bioavailable phytochemicals acting as a functional food. *Comprehensive Reviews in Food Science and Food Safety*, 9, 223–239. <https://doi.org/10.1111/j.1541-4337.2009.00103.x>.
- Banga, O. (1957) The development of the original European carrot material. *Euphytica*, 6, 64–76. <https://doi.org/10.1007/BF00179519>.
- Baranski, R., Klocke, E. & Nothnagel, T. (2007) Enhancing resistance of transgenic carrot to fungal pathogens by the expression

of *Pseudomonas fluorescens* microbial factor 3 (MF3) gene. *Physiological and Molecular Plant Pathology*, 71, 88–95. <https://doi.org/10.1016/j.pmpp.2007.12.002>.

- Barba, F.J., Zhu, Z., Koubaa, M., Sant'Ana, A.S. & Orlie, V. (2016) Green alternative methods for the extraction of antioxidant bioactive compounds from winery wastes and by-products: A review. *Trends in Food Science and Technology*, 49, 96–109.
- Ben-Noon, E., Shtienberg, D., Shlevin, E. & Dinoor, A. (2003) Joint Action of Disease Control Measures: A Case Study of Alternaria Leaf Blight of Carrot. *Phytopathology*, 93, 1320–1328. <https://doi.org/10.1094/PHTO.2003.93.10.1320>.
- Ben-Noon, E., Shtienberg, D., Shlevin, E. & Vintal, H. (2001) Optimization of chemical suppression of Alternaria dauci, the causal agent of Alternaria leaf blight in carrots. *Plant Disease*, 85, 1149–1156. <https://doi.org/10.1094/PDIS.2001.85.11.1149>.
- Bernonville, T.D. de, Gaucher, M., Guyot, S., Durel, C.E., Dat, J.F. & Briset, M.N. (2011) The constitutive phenolic composition of two Malus domestica genotypes is not responsible for their contrasted susceptibilities to fire blight. *Environmental and Experimental Botany*, 74, 65–73. <https://doi.org/10.1016/j.envexpbot.2011.04.019>.
- Bhandari, S.R., Rhee, J., Choi, C.S., Jo, J.S., Shin, Y.K., Song, J.W., et al. (2022) Morphological and Biochemical Variation in Carrot Genetic Resources Grown under Open Field Conditions: The Selection of Functional Genotypes for a Breeding Program. *Agronomy*, 12. <https://doi.org/10.3390/agronomy12030553>.
- Bilska, K., Stuper-Szablewska, K., Kulik, T., Buśko, M., Załuski, D., Jurczak, S., et al. (2018) Changes in phenylpropanoid and trichothecene production by Fusarium culmorum and F. Graminearum sensu stricto via exposure to flavonoids. *Toxins*, 10. <https://doi.org/10.3390/toxins10030110>.
- Boedo, C., Benichou, S., Berruyer, R., Bersihand, S., Dongo, A., Simoneau, P., et al. (2012) Evaluating aggressiveness and host range of Alternaria dauci in a controlled environment. *Plant Pathology*, 61, 63–75. <https://doi.org/10.1111/j.1365-3059.2011.02494.x>.
- Boedo, C., Berruyer, R., Lecomte, M., Bersihand, S., Briard, M., Le Clerc, V., et al. (2010) Evaluation of different methods for the characterization of carrot resistance to the alternaria leaf blight pathogen (Alternaria dauci) revealed two qualitatively different resistances. *Plant Pathology*, 59, 368–375. <https://doi.org/10.1111/j.1365-3059.2009.02218.x>.
- Boedo, C., Le Clerc, V., Briard, M., Simoneau, P., Chevalier, M., Georgeault, S., et al. (2008) Impact of carrot resistance on development of the Alternaria leaf blight pathogen (Alternaria dauci). *European Journal of Plant Pathology*, 121, 55–66. <https://doi.org/10.1007/s10658-007-9241-6>.
- Boiteux, L.S., Vecchia, P.T. Della & Reifschneider, F.J.B. (1993) Heritability Estimate for Resistance to Alternaria dauci in Carrot. *Plant Breeding*, 110, 165–167. <https://doi.org/10.1111/J.1439-0523.1993.TB01230.X>.
- Bollina, V., Kumaraswamy, G.K., Kushalappa, A.C., Choo, T.M., Dion, Y., Rioux, S., et al. (2010) Mass spectrometry-based metabolomics application to identify quantitative resistance-related metabolites in barley against Fusarium head blight. *Molecular Plant Pathology*, 11, 769–782. <https://doi.org/10.1111/j.1364-3703.2010.00643.x>.
- Bounds, R.S., Hausbeck, M.K. & Podolsky, R.H. (2007) Comparing Disease Forecasters for Timing Fungicide Sprays to Control Foliar Blight on Carrot. <https://doi.org/10.1094/PD-90-0264>, 90, 264–268. <https://doi.org/10.1094/PD-90-0264>.
- Box, G.E.P. & Cox, D.R. (1964) An Analysis of Transformations. *Journal of the Royal Statistical Society: Series B (Methodological)*, 26, 211–243.
- Brooks, J.S. & Feeny, P. (2004) Seasonal variation in Daucus carota leaf-surface and leaf-tissue chemical profiles. *Biochemical Systematics and Ecology*, 32, 769–782. <https://doi.org/10.1016/j.bse.2004.01.004>.
- Buer, C.S., Kordbacheh, F., Truong, T.T., Hocart, C.H. & Djordjevic, M.A. (2013) Alteration of flavonoid accumulation patterns in transparent testa mutants disturbs auxin transport, gravity responses, and imparts long-term effects on root and shoot architecture. *Planta*, 238, 171–189. <https://doi.org/10.1007/s00425-013-1883-3>.

- CAB International (2021) Carrots and related Apiaceae crops. Geoffriau, E. and Simon, P.W. (Eds.). CABI International.
- Carvalho, A.D.F., Silva, G.O., Pereira, R.B. & Pinheiro, J.B. (2015) Produtividade e tolerância à queima-das-folhas de diferentes genótipos de cenoura de verão. *Horticultura Brasileira*, 33, 299–304. <https://doi.org/10.1590/S0102-053620150000300004>.
- Castano-Duque, L., Gilbert, M.K., Mack, B.M., Lebar, M.D., Carter-Wientjes, C.H., Sickler, C.M., et al. (2021) Flavonoids Modulate the Accumulation of Toxins From *Aspergillus flavus* in Maize Kernels. *Frontiers in Plant Science*, 12, 2534. <https://doi.org/10.3389/FPLS.2021.761446/BIBTEX>.
- Chen, J., Ullah, C., Reichelt, M., Gershenzon, J. & Hammerbacher, A. (2019) Sclerotinia sclerotiorum circumvents flavonoid defenses by catabolizing flavonol glycosides and aglycones. *Plant Physiology*, 180, 1975–1987. <https://doi.org/10.1104/pp.19.00461>.
- Chong, J., Baltz, R., Fritig, B. & Saindrenan, P. (1999) An early salicylic acid-, pathogen- and elicitor-inducible tobacco glucosyltransferase: Role in compartmentalization of phenolics and H₂O₂ metabolism. *FEBS Letters*, 458, 204–208. [https://doi.org/10.1016/S0014-5793\(99\)01154-0](https://doi.org/10.1016/S0014-5793(99)01154-0).
- Chung, M.J., Pandey, R.P., Choi, J.W., Sohng, J.K., Choi, D.J. & Park, Y. Il (2015) Inhibitory effects of kaempferol-3-O-rhamnoside on ovalbumin-induced lung inflammation in a mouse model of allergic asthma. *International Immunopharmacology*, 25, 302–310. <https://doi.org/10.1016/j.intimp.2015.01.031>.
- Le Clerc, V. & Briard, M. (2020) Carrot disease management. In: Geoffriau, E. and Simon, P.W. (Eds.) Carrots and related Apiaceae crops. CABI, pp. 115-129.
- Le Clerc, V., Briard, M., Cottet, V., Dandin, S. & Geoffriau, E. (2021) Carrot, a major vegetable crop in France. *Chronica Horticulturae*. pp. 27–33.
- Le Clerc, V., Marques, S., Suel, A., Huet, S., Hamama, L., Voisine, L., et al. (2015) QTL mapping of carrot resistance to leaf blight with connected populations: stability across years and consequences for breeding. *Theoretical and Applied Genetics*, 128, 2177–2187. <https://doi.org/10.1007/s00122-015-2576-z>.
- Le Clerc, V., Pawelec, A., Birolleau-Touchard, C., Suel, A. & Briard, M. (2009) Genetic architecture of factors underlying partial resistance to *Alternaria* leaf blight in carrot. *Theoretical and Applied Genetics*, 118, 1251–1259. <https://doi.org/10.1007/s00122-009-0978-5>.
- Le Clerc, V., Suel, A., Pawelec, A., Marques, S., Huet, S., Lecomte, M., et al. (2014) Is there variety × isolate interaction in the polygenic quantitative resistance of carrot to *Alternaria dauci*? *Euphytica*, 202, 235–243. <https://doi.org/10.1007/s10681-014-1279-x>.
- Courtial, J., Hamama, L., Helesbeux, J.-J., Lecomte, M., Renaux, Y., Guichard, E., et al. (2018) Aldaulactone – An Original Phytotoxic Secondary Metabolite Involved in the Aggressiveness of *Alternaria dauci* on Carrot. *Frontiers in Plant Science*, 9. <https://doi.org/10.3389/fpls.2018.00502>.
- Courtial, J., Helesbeux, J.-J., Oudart, H., Aligon, S., Bahut, M., Hamon, B., et al. (2022) Characterization of NRPS and PKS genes involved in the biosynthesis of SMs in *Alternaria dauci* including the phytotoxic polyketide aldaulactone. *Scientific Reports* 2022 12:1, 12, 1–20. <https://doi.org/10.1038/s41598-022-11896-0>.
- Davis, R.M. (2004) Carrot Diseases and their Management. Diseases of Fruits and Vegetables. Kluwer Academic Publishers, pp. 397–439.
- Doehlemann, G., Berndt, P. & Hahn, M. (2006) Different signalling pathways involving a Gα protein, cAMP and a MAP kinase control germination of *Botrytis cinerea* conidia. *undefined*, 59, 821–835. <https://doi.org/10.1111/J.1365-2958.2005.04991.X>.
- Dugdale, L.J., Mortimer, A.M., Isaac, S. & Collin, H.A. (2000) Disease response of carrot and carrot somaclones to *Alternaria dauci*. *Plant Pathology*, 49, 57–67. <https://doi.org/10.1046/j.1365-3059.2000.00389.x>.

- Dugdale, Mortimer, Isaac & Collin (2000) Disease response of carrot and carrot somaclones to *Alternaria dauci*. *Plant Pathology*, 49, 57–67. <https://doi.org/10.1046/j.1365-3059.2000.00389.x>.
- El-Nagar, A., Elzaawely, A.A., Taha, N.A. & Nehela, Y. (2020) The antifungal activity of gallic acid and its derivatives against *alternaria solani*, the causal agent of tomato early blight. *Agronomy*, 10, 1–23. <https://doi.org/10.3390/agronomy10091402>.
- El-Negoumy, S.I., Abdalla, M.F. & Saleh, N.A.M. (1986) Flavonoids of *Phlomis aurea* and *P. floccosa*. *Phytochemistry*, 25, 772–774.
- Ellison, S.L. (2017) Carrot Domestication. The carrot Genome, Compendium of plant Genomes. pp. 77–91.
- FAO (2020) *Fruit and vegetables – your dietary essentials*. Rome.
- Farrar, J.J., Pryor, B.M. & Davis, R.M. (2004) *Alternaria* Diseases of Carrot. *Plant Disease*, 88, 776–784. <https://doi.org/10.1094/PDIS.2004.88.8.776>.
- Fecka, I., Kowalczyk, A. & Cisowski, W. (2004) Optimization of the separation of flavonoid glycosides and rosmarinic acid from *Mentha piperita* on HPTLC plates. *Journal of Planar Chromatography - Modern TLC*, 17, 22–25. <https://doi.org/10.1556/JPC.17.2004.1.5>.
- Fialova, S., Veizerova, L., Nosalova, V., Drabikova, K., Tekelova, D., Grancai, D., et al. (2015) Water Extract of *Mentha x villosa*: Phenolic Fingerprint and Effect on Ischemia-Reperfusion Injury. *Natural product communications*, 10, 937–940. <https://doi.org/10.1177/1934578x1501000636>.
- Foury, C. (2003) Carottes et panais. Histoire de légumes. pp. 126–137.
- FranceAgrimer (2022) Analyse compétitivité filière carotte en Europe en 2020.
- Gachon, C.M.M., Langlois-Meurinne, M. & Saindrenan, P. (2005) Plant secondary metabolism glycosyltransferases: The emerging functional analysis. *Trends in Plant Science*, 10, 542–549.
- Galeotti, F., Barile, E., Lanzotti, V., Dolci, M. & Curir, P. (2008) Quantification of Major Flavonoids in Carnation Tissues (*Dianthus caryophyllus*) as a Tool for Cultivar Discrimination. *Z Naturforsch*, 63, 161–168.
- Galland, M., Boutet-Mercey, S., Lounifi, I., Godin, B., Balzergue, S., Grandjean, O., et al. (2014) Compartmentation and dynamics of flavone metabolism in dry and germinated rice seeds. *Plant and Cell Physiology*, 55, 1646–1659. <https://doi.org/10.1093/pcp/pcu095>.
- Garcia-Mas, J. & Rodriguez-Concepcion, M. (2016) The carrot genome sequence brings colors out of the dark. *Nature Genetics*, 48, 589–590. <https://doi.org/10.1038/ng.3574>.
- Gniwotta, F., Vogg, G., Gartmann, V., Carver, T.L.W., Riederer, M. & Jetter, R. (2005) What Do Microbes Encounter at the Plant Surface? Chemical Composition of Pea Leaf Cuticular Waxes. *Plant Physiology*, 139, 519. <https://doi.org/10.1104/PP.104.053579>.
- Grace, B.S. & Müller-Schärer, H. (2003) Biological control of *Senecio vulgaris* in carrots (*Daucus carota*) with the rust fungus *Puccinia lagenophorae*. *Basic and Applied Ecology*, 4, 375–384. <https://doi.org/10.1078/1439-1791-00171>.
- Griesser, M., Vitzthum, F., Fink, B., Bellido, M.L., Raasch, C., Munoz-Blanco, J., et al. (2008) Multi-substrate flavonol O-glucosyltransferases from strawberry (*Fragaria xananassa*) achene and receptacle. *Journal of Experimental Botany*, 59, 2611–2625. <https://doi.org/10.1093/jxb/ern117>.
- Gu, N., Qiu, C., Zhao, L., Zhang, L. & Pei, J. (2020) Enhancing UDP-rhamnose supply for rhamnosylation of flavonoids in *Escherichia coli* by regulating the modular pathway and improving NADPH availability. *Journal of Agricultural and Food Chemistry*, 68, 9513–9523. <https://doi.org/10.1021/acs.jafc.0c03689>.
- Guédon, D.J. & Pasquier, B.P. (1994) Analysis and Distribution of Flavonoid Glycosides and Rosmarinic Acid in 40 *Mentha X*

piperita Clones. *Journal of Agricultural and Food Chemistry*, 42, 679–684. <https://doi.org/10.1021/jf00039a015>.

- Gugino, B.K., Carroll, J.E., Widmer, T.L., Chen, P. & Abawi, G.S. (2007) Field evaluation of carrot cultivars for susceptibility to fungal leaf blight diseases in New York. *Crop Protection*, 26, 709–714. <https://doi.org/10.1016/J.CROPRO.2006.06.009>.
- Guo, J., Wu, Y., Wang, G., Wang, T. & Cao, F. (2020) Integrated analysis of the transcriptome and metabolome in young and mature leaves of Ginkgo biloba L. *Industrial Crops and Products*, 143, 111906. <https://doi.org/10.1016/j.indcrop.2019.111906>.
- Hamama, L., Naouar, A., Gala, R., Voisine, L., Pierre, S., Jeauffre, J., et al. (2012) Overexpression of RoDELLA impacts the height, branching, and flowering behaviour of Pelargonium × domesticum transgenic plants. *Plant Cell Reports*, 31.
- Hannoufa, A., Varin, L. & Ibrahim, R.K. (1991) Spatial distribution of flavonoid conjugates in relation to glucosyltransferase and sulfotransferase activities in flaveria bidentis. *Plant Physiology*, 97, 259–263. <https://doi.org/10.1104/pp.97.1.259>.
- Haraguchi, H., Yoshida, N., Ishikawa, H., Tamura, Y., Mizutani, K. & Kinoshita, T. (2010) Protection of Mitochondrial Functions against Oxidative Stresses by Isoflavans from Glycyrrhiza glabra . *Journal of Pharmacy and Pharmacology*, 52, 219–223. <https://doi.org/10.1211/0022357001773724>.
- Hassabou, N.F. & Farag, A.F. (2020) Anticancer effects induced by artichoke extract in oral squamous carcinoma cell lines. *Journal of the Egyptian National Cancer Institute*, 32. <https://doi.org/10.1186/s43046-020-00026-4>.
- Hatzipapas, P., Kalosak, K., Dara, A. & Christias, C. (2002) Spore germination and appressorium formation in the entomopathogenic Alternaria alternata. *Mycological Research*, 106, 1349–1359.
- Hauser, T.P. & Shim, S.I. (2007) Survival and flowering of hybrids between cultivated and wild carrots (Daucus carota) in Danish grasslands. *Environmental biosafety research*, 6, 237–247. <https://doi.org/10.1051/eb:2007044>.
- Hectors, K., Oevelen, S. Van, Guisez, Y., Prinsen, E. & Jansen, M.A.K. (2012) The phytohormone auxin is a component of the regulatory system that controls UV-mediated accumulation of flavonoids and UV-induced morphogenesis. *Physiologia Plantarum*, 145, 594–603. <https://doi.org/10.1111/j.1399-3054.2012.01590.x>.
- Hichri, I., Heppel, S.C., Pillet, J., Léon, C., Czempl, S., Delrot, S., et al. (2010) The basic helix-loop-helix transcription factor MYC1 is involved in the regulation of the flavonoid biosynthesis pathway in grapevine. *Molecular Plant*, 3, 509–523. <https://doi.org/10.1093/mp/ssp118>.
- Hodaei, M., Rahimalek, M., Arzani, A. & Talebi, M. (2018) The effect of water stress on phytochemical accumulation, bioactive compounds and expression of key genes involved in flavonoid biosynthesis in Chrysanthemum morifolium L. *Industrial Crops and Products*, 120, 295–304. <https://doi.org/10.1016/j.indcrop.2018.04.073>.
- Inoue, T., Sugimoto, Y., Masuda, H. & Kamei, C. (2002) Antiallergic effect of flavonoid glycosides obtained from Mentha piperita L. *Biological and Pharmaceutical Bulletin*, 25, 256–259. <https://doi.org/10.1248/bpb.25.256>.
- Iorizzo, M., Ellison, S., Senalik, D., Zeng, P., Satapoomin, P., Huang, J., et al. (2016) A high-quality carrot genome assembly provides new insights into carotenoid accumulation and asterid genome evolution. *Nature Genetics*, 48, 657–666. <https://doi.org/10.1038/ng.3565>.
- Iorizzo, M., Senalik, D.A., Ellison, S.L., Grzebelus, D., Cavagnaro, P.F., Allender, C., et al. (2013) Genetic structure and domestication of carrot (Daucus carota subsp. sativus) (Apiaceae) 1. *American Journal of Botany*, 100, 930–938. <https://doi.org/10.3732/ajb.1300055>.
- Jang, S.W., Cho, C.H., Jung, Y.S., Rha, C., Nam, T.G., Kim, D.O., et al. (2018) Enzymatic synthesis of α-flavone glucoside via regioselective transglucosylation by amylosucrase from Deinococcus geothermalis. *PLoS ONE*, 13, 1–11. <https://doi.org/10.1371/journal.pone.0207466>.
- Jean Bruneton (1999) Pharmacognosie : phytochimie et plantes médicinales. Paris, France: Tech & Doc (Editions).

- Jeandet, P., Hébrard, C., Deville, M.A., Cordelier, S., Dorey, S., Aziz, A., et al. (2014) Deciphering the role of phytoalexins in plant-microorganism interactions and human health. *Molecules*, 19, 18033–18056. <https://doi.org/10.3390/molecules191118033>.
- Kaeswurm, J.A.H., Scharinger, A., Teipel, J. & Buchweitz, M. (2021) Absorption coefficients of phenolic structures in different solvents routinely used for experiments. *Molecules*, 26, 1–15. <https://doi.org/10.3390/molecules26154656>.
- Kantharaj, V., Ramasamy, N.K., Yoon, Y.-E., Cheong, M.S., Kim, Y.-N., Lee, K.-A., et al. (2022) Auxin-Glucose Conjugation Protects the Rice (*Oryza sativa* L.) Seedlings Against Hydroxyurea-Induced Phytotoxicity by Activating UDP-Glucosyltransferase Enzyme. *Frontiers in Plant Science*, 12, 3388. <https://doi.org/10.3389/fpls.2021.767044>.
- Karimi, M., Inzé, D. & Depicker, A. (2002) GATEWAY vectors for Agrobacterium-mediated plant.pdf. *TRENDS in Plant Science*, 7, 193–195.
- Kim, N.M., Kim, J., Chung, H.Y. & Choi, J.S. (2000) Isolation of Luteolin 7-O-rutinoside and Esculetin with Potential Antioxidant Activity from the Aerial Parts of *Artemisia montana*. *Archives of Pharmacal Research*, 23, 237–239. <https://doi.org/10.1007/BF02976451>.
- Klimek-Chodacka, M., Oleszkiewicz, T., Lowder, L.G., Qi, Y. & Baranski, R. (2018) Efficient CRISPR/Cas9-based genome editing in carrot cells. *Plant Cell Reports*, 37, 575–586. <https://doi.org/10.1007/s00299-018-2252-2>.
- kmen, B., Etalo, D.W., Joosten, M.H.A.J., Bouwmeester, H.J., Vos, R.C.H. de, Collemare, J., et al. (2013) Detoxification of α -tomatine by *Cladosporium fulvum* is required for full virulence on tomato. *New Phytologist*, 198, 1203–1214. <https://doi.org/10.1111/nph.12208>.
- Ko, J.H., Kim, B.G., Kim, J.H., Kim, H., Lim, C.E., Lim, J., et al. (2008) Four glucosyltransferases from rice: cDNA cloning, expression, and characterization. *Journal of Plant Physiology*, 165, 435–444. <https://doi.org/10.1016/j.jplph.2007.01.006>.
- Kodama, M., Brinch-Pedersen, H., Sharma, S., Holme, I.B., Joernsgaard, B., Dzhanfezova, T., et al. (2018) Identification of transcription factor genes involved in anthocyanin biosynthesis in carrot (*Daucus carota* L.) using RNA-Seq. *BMC Genomics*, 19, 1–13. <https://doi.org/10.1186/s12864-018-5135-6>.
- Koutouan, C., Le Clerc, V., Baltenweck, R., Claudel, P., Halter, D., Huguene, P., et al. (2018) Link between carrot leaf secondary metabolites and resistance to *Alternaria dauci*. *Scientific Reports*, 8, 1–14. <https://doi.org/10.1038/s41598-018-31700-2>.
- Koutouan, C.E., Le Clerc, V., Suel, A., Hamama, L., Claudel, P., Halter, D., et al. (2023) Co-Localization of Resistance and Metabolic Quantitative Trait Loci on Carrot Genome Reveals Fungitoxic Terpenes and Related Candidate Genes Associated with the Resistance to *Alternaria dauci*. *Metabolites*, 13, 71. <https://doi.org/10.3390/metabo13010071>.
- Kröner, A., Marnet, N., Andrivon, D. & Val, F. (2012) Nicotiflorin, rutin and chlorogenic acid: Phenylpropanoids involved differently in quantitative resistance of potato tubers to biotrophic and necrotrophic pathogens. *Plant Physiology and Biochemistry*, 57, 23–31. <https://doi.org/10.1016/j.plaphy.2012.05.006>.
- Kuhn, B.M., Errafi, S., Bucher, R., Dobrev, P., Geisler, M., Bigler, L., et al. (2016) 7-Rhamnosylated Flavonols Modulate Homeostasis of the Plant Hormone Auxin and Affect Plant Development. *Journal of Biological Chemistry*, 291, 5385–5395. <https://doi.org/10.1074/jbc.M115.701565>.
- Lagrange, H., Jay-Allgmand, C. & Lapeyrie, F. (2001) Rutin, the phenolglycoside from eucalyptus root exudates, stimulates *Pisolithus* hyphal growth at picomolar concentrations. *New Phytologist*, 149, 349–355. <https://doi.org/10.1046/j.1469-8137.2001.00027.x>.
- Lattanzio, V., Kroon, P.A., Linsalata, V. & Cardinali, A. (2009) Globe artichoke: A functional food and source of nutraceutical ingredients. *Journal of Functional Foods*, 1, 131–144. <https://doi.org/10.1016/j.jff.2009.01.002>.
- Lecomte, M., Berruyer, R., Hamama, L., Boedo, C., Hudhomme, P., Bersihand, S., et al. (2012) Inhibitory effects of the carrot metabolites 6-methoxymellein and faltarindiol on development of the fungal leaf blight pathogen *Alternaria dauci*. *Physiological and Molecular Plant Pathology*, 80, 58–67. <https://doi.org/10.1016/j.pmp.2012.10.002>.

- Lecomte, M., Hamama, L., Voisine, L., Gatto, J., Hélesbeux, J.-J., Séraphin, D., et al. (2014) Partial Resistance of Carrot to *Alternaria dauci* Correlates with In Vitro Cultured Carrot Cell Resistance to Fungal Exudates Wilson, R.A. (Ed.). *PLoS ONE*, 9, e101008. <https://doi.org/10.1371/journal.pone.0101008>.
- Lee, H., Woo, E.R. & Lee, D.G. (2018) Apigenin induces cell shrinkage in *Candida albicans* by membrane perturbation. *FEMS Yeast Research*, 18. <https://doi.org/10.1093/femsyr/foy003>.
- Leja, M., Kamińska, I., Kramer, M., Maksylewicz-Kaul, A., Kammerer, D., Carle, R., et al. (2013) The Content of Phenolic Compounds and Radical Scavenging Activity Varies with Carrot Origin and Root Color. *Plant Foods for Human Nutrition*, 68, 163–170. <https://doi.org/10.1007/s11130-013-0351-3>.
- Leyte-Lugo, M., Richomme, P., Poupard, P. & Peña-Rodriguez, L.M. (2020) Identification and Quantification of a Phytotoxic Metabolite from *Alternaria dauci*. *Molecules* 2020, Vol. 25, Page 4003, 25, 4003. <https://doi.org/10.3390/MOLECULES25174003>.
- Li, C., Qiu, J., Ding, L., Huang, M., Huang, S., Yang, G., et al. (2017) Anthocyanin biosynthesis regulation of DhMYB2 and DhbHLH1 in *Dendrobium* hybrids petals. *Plant Physiology and Biochemistry*, 112, 335–345. <https://doi.org/10.1016/j.plaphy.2017.01.019>.
- Lin, L.C., Pai, Y.F. & Tsai, T.H. (2015) Isolation of Luteolin and Luteolin-7-O-glucoside from *Dendranthema morifolium* Ramat Tzvel and Their Pharmacokinetics in Rats. *Journal of Agricultural and Food Chemistry*, 63, 7700–7706. <https://doi.org/10.1021/jf505848z>.
- Linke, B., Alessandro, M.S., Galmarini, C.R. & Nothnagel, T. (2017) Carrot Floral Development and Reproductive Biology. In: Kole, C. (Ed.) *The carrot Genome, Compendium of plant Genomes*. © Springer Nature Switzerland AG 2019, pp. 27–57.
- Liu, S., Lyu, Y., Yu, S., Cheng, J. & Zhou, J. (2021) Efficient Production of Orientin and Vitexin from Luteolin and Apigenin Using Coupled Catalysis of Glycosyltransferase and Sucrose Synthase. *Journal of Agricultural and Food Chemistry*, 69, 6578–6587. <https://doi.org/10.1021/acs.jafc.1c00602>.
- Liu, X., Lin, C., Ma, X., Tan, Y., Wang, J. & Zeng, M. (2018) Functional characterization of a flavonoid glycosyltransferase in sweet orange (*Citrus sinensis*). *Frontiers in Plant Science*, 9, 1–14. <https://doi.org/10.3389/fpls.2018.00166>.
- Livak, K.J. & Schmittgen, T.D. (2001) Analysis of relative gene expression data using real-time quantitative PCR and the 2- $\Delta\Delta CT$ method. *Methods*, 25, 402–408. <https://doi.org/10.1006/meth.2001.1262>.
- Mace, M.E., Bell, A.A. & Stipanovic, R.D. (1978) Histochemistry and identification of flavanols in *Verticillium* wilt-resistant and -susceptible cottons. *Physiological Plant Pathology*, 13, 143–149. [https://doi.org/10.1016/0048-4059\(78\)90027-9](https://doi.org/10.1016/0048-4059(78)90027-9).
- Macherey-Nagel (2016) RNA isolation User manual NucleoSpin® RNA Plus. 1–25.
- Mandel, J.R., Ramsey, A.J., Iorizzo, M. & Simon, P.W. (2016) Patterns of gene flow between crop and wild carrot, *Daucus carota* (Apiaceae) in the United States. *PLoS ONE*, 11. <https://doi.org/10.1371/journal.pone.0161971>.
- Marcuzzo, L.L. & Tomasoni, C.M. (2020) Development of a weather-based forecasting model for *Alternaria* leaf blight of carrot / Desenvolvimento de um modelo de previsão climático para a queima das pontas da cenoura NOTAS CIENTÍFICAS Development of a weather-based forecasting model for *Alternari*. 18–20. <https://doi.org/10.1590/0100-5405/216538>.
- Markham, K.R., Ryan, K.G., Bloor, S.J. & Mitchell, K.A. (1998) An increase in the luteolin: Apigenin ratio in *Marchantia polymorpha* on UV-B enhancement. *Phytochemistry*, 48, 791–794. [https://doi.org/10.1016/S0031-9422\(97\)00875-3](https://doi.org/10.1016/S0031-9422(97)00875-3).
- Maude, R.B. (1966) Studies on the etiology of black rot, *Stemphylium radicum* (Meier, Drechsl. & Eddy) Neerg., and leaf blight, *Alternaria dauci* (Kühn) Groves & Skolko, on carrot crops; and on fungicide control of their seed-borne infection phases. *Annals of Applied Biology*, 57, 83–93. <https://doi.org/10.1111/j.1744-7348.1966.tb06869.x>.
- Maude, R.B., Drew, R.L.K., Gray, D., Petch, G.M., Bujalski, W. & Nienow, A.W. (1992) Strategies for control of seed-borne *Alternaria dauci* (leaf blight) of carrots in priming and process engineering systems. *Plant Pathology*, 41, 204–214. <https://doi.org/10.1111/J.1365-3059.1992.TB02339.X>.

- McIsaac, G.E., Sanderson, K.R., Peters, R.D., Garbary, D.J. & Fillmore, S.A.E. (2013) Impact of commercial foliage trimming on disease suppression and yield of processing carrots in Nova Scotia, Canada. *Canadian Journal of Plant Science*, 93, 1155–1163. <https://doi.org/10.4141/CJPS2013-249/ASSET/IMAGES/CJPS2013-249TAB4.GIF>.
- Melake-Berhan, A., Butler, L.G., Ejeta, G. & Menkir, A. (1996) Grain Mold Resistance and Polyphenol Accumulation in Sorghum. *Journal of Agricultural and Food Chemistry*, 44, 2428–2434. <https://doi.org/10.1021/jf950580x>.
- Meng, G., Clausen, S.K. & Rasmussen, S.K. (2020) Transcriptome Analysis Reveals Candidate Genes Related to Anthocyanin Biosynthesis in Different Carrot Genotypes and Tissues. *Plants*, 9, 344. <https://doi.org/10.3390/plants9030344>.
- Mierziak, J., Kostyn, K. & Kulma, A. (2014) Flavonoids as important molecules of plant interactions with the environment. *Molecules*, 19, 16240–16265. <https://doi.org/10.3390/molecules191016240>.
- Moazeni, M., Hedayati, M.T., Nabili, M., Mousavi, S.J., Abdollahi Gohar, A. & Gholami, S. (2017) Glabridin triggers over-expression of MCA1 and NUC1 genes in *Candida glabrata*: Is it an apoptosis inducer? *Journal de Mycologie Medicale*, 27, 369–375. <https://doi.org/10.1016/j.mycmed.2017.05.002>.
- Muhlemann, J.K., Younts, T.L.B. & Muday, G.K. (2018) Flavonols control pollen tube growth and integrity by regulating ROS homeostasis during high-temperature stress. *Proceedings of the National Academy of Sciences of the United States of America*, 115, E11188–E11197. <https://doi.org/10.1073/pnas.1811492115>.
- Nagy, M., Križková, L., Mučaji, P., Kontšeková, Z., Šeršeň, F. & Krajčovič, J. (2009) Antimutagenic activity and radical scavenging activity of water infusions and phenolics from *Ligustrum* plants leaves. *Molecules*, 14, 509–518. <https://doi.org/10.3390/molecules14010509>.
- Naoumkina, M.A., Zhao, Q., Gallego-Giraldo, L., Dai, X., Zhao, P.X. & Dixon, R.A. (2010) Genome-wide analysis of phenylpropanoid defence pathways. *Molecular Plant Pathology*, 11, 829–846. <https://doi.org/10.1111/j.1364-3703.2010.00648.x>.
- Negro, D., Montesano, V., Grieco, S., Crupi, P., Sarli, G., Lisi, A. De, et al. (2012) Polyphenol Compounds in Artichoke Plant Tissues and Varieties. *Journal of Food Science*, 77. <https://doi.org/10.1111/j.1750-3841.2011.02531.x>.
- Nemesio-Gorritz, M., Blair, P.B., Dalman, K., Hammerbacher, A., Arnerup, J., Stenlid, J., et al. (2017) Identification of Norway Spruce MYB-bHLH-WDR Transcription Factor Complex Members Linked to Regulation of the Flavonoid Pathway. *Frontiers in plant science*, 8, 305. <https://doi.org/10.3389/fpls.2017.00305>.
- Netzer, D. & Kenneth, R.. (1970) Apparent heterokaryosis in *Alternaria daucil* Identification and Frequency of Auxotrophic Isolates in Nature. *Canadian Journal of Botany*, 48, 831–835.
- Netzer, D. & Kenneth, R.G. (1969) Persistence and transmission of *Alternaria dauci* (Kühn) Groves & Skolko in the semi-arid conditions of Israel*. *Annals of Applied Biology*, 63, 289–294. <https://doi.org/10.1111/J.1744-7348.1969.TB05490.X>.
- Nothnagel, T., Budahn, H. & Krämer, R. (2017) Characterization of resistance to *Alternaria* spp. in wild relatives of carrot (*Daucus carota* L. ssp. *carota*). *Acta Horticulturae*, 1153, 251–258. <https://doi.org/10.17660/ActaHortic.2017.1153.37>.
- Omezzine, F., Daami-Remadi, M., Ladhari, A. & Haouala, R. (2014) Variation in phytochemical content and antifungal activity of *Trigonella foenum-graecum* L. with plant developmental stage and ploidy level. *South African Journal of Botany*, 92, 120–125. <https://doi.org/10.1016/j.sajb.2014.02.014>.
- Oros, G. & Kállai, Z. (2019) Phytoanticipins: The Constitutive Defense Compounds as Potential Botanical Fungicides. In: Sudisha Jogaiah and Abdelrahman, M. (Eds.) *Bioactive Molecules in Plant Defense*. Springer Nature Switzerland AG 2019, pp. 179–229.
- Pandino, G., Lombardo, S., Mauromicale, G. & Williamson, G. (2011) Profile of polyphenols and phenolic acids in bracts and receptacles of globe artichoke (*Cynara cardunculus* var. *scolymus*) germplasm. *Journal of Food Composition and Analysis*, 24, 148–153. <https://doi.org/10.1016/j.jfca.2010.04.010>.
- Pardede, A., Adfa, M., Juliari Kusnanda, A., Ninomiya, M. & Koketsu, M. (2017) Flavonoid rutinosides from *Cinnamomum*

parthenoxylon leaves and their hepatoprotective and antioxidant activity. *Medicinal Chemistry Research*, 26, 2074–2079. <https://doi.org/10.1007/s00044-017-1916-8>.

- Pawelec, A., Dubourg, C. & Briard, M. (2006) Evaluation of carrot resistance to alternaria leaf blight in controlled environments. *Plant Pathology*, 55, 68–72. <https://doi.org/10.1111/j.1365-3059.2006.01290.x>.
- Pélissier, R., Buendia, L., Brousse, A., Temple, C., Ballini, E., Fort, F., et al. (2021) Plant neighbour-modulated susceptibility to pathogens in intraspecific mixtures. *Journal of Experimental Botany*, 72, 6570–6580. <https://doi.org/10.1093/jxb/erab277>.
- Pereira, R.B., Carvalho, A.D.F. de, Pinheiro, J.B., Silva, G.O. da & Vieira, J. V. (2012) Resistência de populações de cenoura à queima-das-folhas com diferentes níveis de germoplasma tropical. *Horticultura Brasileira*, 30, 489–493. <https://doi.org/10.1590/S0102-05362012000300022>.
- Perrin, F., Dubois-Laurent, C., Gibon, Y., Citerne, S., Huet, S., Suel, A., et al. (2017) Combined *Alternaria dauci* infection and water stresses impact carotenoid content of carrot leaves and roots. *Environmental and Experimental Botany*, 143, 125–134. <https://doi.org/10.1016/j.envexpbot.2017.09.004>.
- Petropoulos, S.A., Fernandes, Â., Antoniadis, V., Ntatsi, G., Barros, L. & Ferreira, I.C.F.R. (2018) Chemical composition and antioxidant activity of *Cichorium spinosum* L. leaves in relation to developmental stage. *Food Chemistry*, 239, 946–952. <https://doi.org/10.1016/j.foodchem.2017.07.043>.
- Plazonić, A., Bucar, F., Maleš, Željani, Mornar, A., Nigović, B. & Kujundžić, N. (2009) Identification and quantification of flavonoids and phenolic acids in burr parsley (*caucalis platycarpus* L.), using high-performance liquid chromatography with diode array detection and electrospray ionization mass spectrometry. *Molecules*, 14, 2466–2490. <https://doi.org/10.3390/molecules14072466>.
- Pryor, B.M., Strandberg, J.O., Davis, R.M., Nunez, J.J. & Gilbertson, R.L. (2002) Survival and persistence of *Alternaria dauci* in carrot cropping systems. *Plant Disease*, 86, 1115–1122. <https://doi.org/10.1094/PDIS.2002.86.10.1115>.
- Punja, Z.K. (2005) Transgenic carrots expressing a thaumatin-like protein display enhanced resistance to several fungal pathogens. *Canadian Journal of Plant Pathology*, 27, 291–296. <https://doi.org/10.1080/07060660509507227>.
- Rackova, L., Firakova, S., Kostalova, D., Stefek, M., Sturdik, E. & Majekova, M. (2005) Oxidation of liposomal membrane suppressed by flavonoids: Quantitative structure-activity relationship. *Bioorganic and Medicinal Chemistry*, 13, 6477–6484. <https://doi.org/10.1016/j.bmc.2005.07.047>.
- Ramaroson, M., Koutouan, C., Helesbeux, J., Hamama, L., Geoffriau, E. & Briard, M. (2022) Role of Phenylpropanoids and Flavonoids in Plant Resistance to Pests and Diseases.
- Reinert, J. (1958) Untersuchungen über die Morphogenese an Gewebekulturen. *Ber. Dtsch. Bot. Ges.* https://doi.org/https://doi.org/10.1007/978-3-642-81784-7_8.
- Rio, J.A. Del, Gonzalez, A., Fuster, M.D., Botia, J.M., Gomez, P., Frias, V., et al. (2001) Tylose formation and changes in phenolic compounds of grape. *Phytopathologia Mediterranea*, 40, 394–399.
- Rodríguez De Luna, S.L., Ramírez-Garza, R.E. & Serna Saldívar, S.O. (2020) Environmentally Friendly Methods for Flavonoid Extraction from Plant Material: Impact of Their Operating Conditions on Yield and Antioxidant Properties. *Scientific World Journal*, 2020.
- Rogers, P.M. & Stevenson, W.R. (2010a) Integration of host resistance, disease monitoring, and reduced fungicide practices for the management of two foliar diseases of carrot. <https://doi.org/10.1080/07060660609507313>, 28, 401–410. <https://doi.org/10.1080/07060660609507313>.
- Rogers, P.M. & Stevenson, W.R. (2010b) Aggressiveness and Fungicide Sensitivity of *Alternaria dauci* from Cultivated Carrot. <https://doi.org/10.1094/PDIS-94-4-0405>, 94, 405–412. <https://doi.org/10.1094/PDIS-94-4-0405>.
- Rong, J., Janson, S., Umehara, M., Ono, M. & Vrieling, K. (2010) Historical and contemporary gene dispersal in wild carrot (*Daucus carota* ssp. *carota*) populations. *Annals of Botany*, 106, 285–296. <https://doi.org/10.1093/aob/mcq108>.

- Rong, J., Lammers, Y., Strasburg, J.L., Schidlo, N.S., Ariyurek, Y., Jong, T.J. De, et al. (2014) New insights into domestication of carrot from root transcriptome analyses. *BMC Genomics*, 15, 1–15. <https://doi.org/10.1186/1471-2164-15-895>.
- Rottem, J. (1994) The Genus *Alternaria*. Biology, Epidemiology and Pathogenicity. American P. Saint Paul [USA].
- Roy, J. Le, Huss, B., Creach, A., Hawkins, S. & Neutelings, G. (2016) Glycosylation is a major regulator of phenylpropanoid availability and biological activity in plants. *Frontiers in Plant Science*, 7. <https://doi.org/10.3389/fpls.2016.00735>.
- Ruan, Y., Kotraiah, V. & Straney, D.C. (1995) Flavonoids stimulate spore germination in *Fusarium solani* pathogenic on legumes in a manner sensitive to inhibitors of cAMP-dependent protein kinase. *Molecular Plant-Microbe Interactions*, 8, 929–938.
- Ryan, K.G., Swinny, E.E., Markham, K.R. & Winefield, C. (2002) Flavonoid gene expression and UV photoprotection in transgenic and mutant *Petunia* leaves. *Phytochemistry*, 59, 23–32. [https://doi.org/10.1016/S0031-9422\(01\)00404-6](https://doi.org/10.1016/S0031-9422(01)00404-6).
- Ryu, H.W., Yuk, H.J., An, J.H., Kim, D.Y., Song, H.H. & Oh, S.R. (2017) Comparison of secondary metabolite changes in *Camellia sinensis* leaves depending on the growth stage. *Food Control*, 73, 916–921. <https://doi.org/10.1016/j.foodcont.2016.10.017>.
- Santos, P., Student, G., Pathology, P. & Nunez, J.J. (2000) Influence of Gibberellic Acid on Carrot Growth and Severity of *Alternaria* Leaf Blight.
- Saude, C., McDonald, M.R. & Westerveld, S. (2014) Nitrogen and Fungicide Applications for the Management of Fungal Blights of Carrot. *HortScience*, 49, 608–614. <https://doi.org/10.21273/HORTSCI.49.5.608>.
- Schouten, H.J., Tongeren, C.A.M. van & Bulk, R.W. van den (2002) Fitness effects of *Alternaria dauci* on wild carrot in The Netherlands. *Environmental biosafety research*, 1, 39–47. <https://doi.org/10.1051/eb:2002004>.
- Schulz, E., Tohge, T., Zuther, E., Fernie, A.R. & Hinch, D.K. (2016) Flavonoids are determinants of freezing tolerance and cold acclimation in *Arabidopsis thaliana*. *Scientific Reports*, 6. <https://doi.org/10.1038/srep34027>.
- Schütz, K., Kammerer, D., Carle, R. & Schieber, A. (2004) Identification and quantification of caffeoylquinic acids and flavonoids from artichoke (*Cynara scolymus* L.) heads, juice, and pomace by HPLC-DAD-ESI/MSn. *Journal of Agricultural and Food Chemistry*, 52, 4090–4096. <https://doi.org/10.1021/jf049625x>.
- Schütz, K., Muks, E., Carle, R. & Schieber, A. (2006) Quantitative determination of phenolic compounds in artichoke-based dietary supplements and pharmaceuticals by high-performance liquid chromatography. *Journal of Agricultural and Food Chemistry*, 54, 8812–8817. <https://doi.org/10.1021/jf062009b>.
- Shallan, M.A., Ali, M.A., Meshrf, W.A. & Marrez, D.A. (2020) In vitro antimicrobial, antioxidant and anticancer activities of globe artichoke (*Cynara cardunculus* var. *scolymus* L.) bracts and receptacles ethanolic extract. *Biocatalysis and Agricultural Biotechnology*, 29. <https://doi.org/10.1016/j.bcab.2020.101774>.
- Shivashankar, S. & Sumathi, M. (2022) Gallic acid induces constitutive resistance against *Bactrocera dorsalis* infestation in mango fruit by its dual action. *Pesticide Biochemistry and Physiology*, 188, 105268. <https://doi.org/10.1016/J.PESTBP.2022.105268>.
- Silva, G.O., Vieira, J. V., Vilel, M.S., Reis, A. & Boiteux, L.S. (2009) Parâmetros genéticos da resistência ao complexo da queima-das-folhas em populações de cenoura. *Horticultura Brasileira*, 27, 354–356. <https://doi.org/10.1590/S0102-05362009000300017>.
- Simon, P.W., Iorizzo, M., Grzebelus, D. & Baranski, R. (2017) The Carrot Genome. Chittaranjan Kole (Ed.). © Springer Nature Switzerland AG 2019.
- Simon, P.W. & Strandberg, J.O. (1998) Diallel Analysis of Resistance in Carrot to *Alternaria* Leaf Blight. *Journal of the American Society for Horticultural Science*, 123, 412–415. <https://doi.org/10.21273/JASHS.123.3.412>.
- Song, C., Gu, L., Liu, J., Zhao, S., Hong, X., Schulenburg, K., et al. (2015) Functional Characterization and Substrate

- Promiscuity of UGT71 Glycosyltransferases from Strawberry (*Fragaria × ananassa*). *Plant and Cell Physiology*, 56, 2478–2493. <https://doi.org/10.1093/PCP/PCV151>.
- Song, S., Qi, T., Fan, M., Zhang, X., Gao, H., Huang, H., et al. (2013) The bHLH Subgroup III d Factors Negatively Regulate Jasmonate-Mediated Plant Defense and Development. *PLoS Genetics*, 9, 1–19. <https://doi.org/10.1371/journal.pgen.1003653>.
- Song, Z., Chen, W., Du, X., Zhang, H., Lin, L. & Xu, H. (2011) Chemical constituents of *Picea neoveitchii*. *Phytochemistry*, 72, 490–494. <https://doi.org/10.1016/j.phytochem.2011.01.018>.
- Stein, M. & Nothnagel, T. (1995) Some remarks on carrot breeding (*Daucus carota sativus* Hoffm.). *Plant Breeding*, 114, 1–11. <https://doi.org/10.1111/j.1439-0523.1995.tb00750.x>.
- Steinkellner, S., Mammerler, R. & Vierheilig, H. (2005) Microconidia germination of the tomato pathogen *Fusarium oxysporum* in the presence of root exudates. *undefined*, 1, 23–30. <https://doi.org/10.1080/17429140500134334>.
- Stelmach, K., Macko-Podgórn, A., Allender, C. & Grzebelus, D. (2021) Genetic diversity structure of western-type carrots. *BMC plant biology*, 21, 200. <https://doi.org/10.1186/s12870-021-02980-0>.
- Stelmach, K., Macko-Podgórn, A., Machaj, G. & Grzebelus, D. (2017) Miniature inverted repeat transposable element insertions provide a source of intron length polymorphism markers in the carrot (*Daucus carota* L.). *Frontiers in Plant Science*, 8, 1–9. <https://doi.org/10.3389/fpls.2017.00725>.
- Steward, F.C. (1958) Growth and Organized Development of Cultured Cells. *American Journal of Botany*, 45, 709–713.
- Stolarczyk, J. & Janick, J. (2011) Carrot: History and Iconography. *Chronica Horticulturae*, 51, 13–18.
- Strandberg, J. (1983) Infection and Colonization of Inflorescences and Mericarps of Carrot by *A. dauci*. 1351–1353.
- Strandberg, J.O., Bassett, M.J., Peterson, C.E. & Berger, R.D. (1972) Source of resistance to *Alternaria dauci*. *Horticultural Science*, 7.
- Straney, D., Khan, R., Tan, R. & Bagga, S. (2002) Host recognition by pathogenic fungi through plant flavonoids. *undefined*, 505, 9–22. https://doi.org/10.1007/978-1-4757-5235-9_2.
- Sung, W.S. & Lee, D.G. (2010) Antifungal action of chlorogenic acid against pathogenic fungi, mediated by membrane disruption. *Pure and Applied Chemistry*, 82, 219–226. <https://doi.org/10.1351/PAC-CON-09-01-08>.
- Surles, R.L., Weng, N., Simon, P.W. & Tanumihardjo, S.A. (2004) Carotenoid profiles and consumer sensory evaluation of specialty carrots (*Daucus carota*, L.) of various colors. *Journal of Agricultural and Food Chemistry*, 52, 3417–3421. <https://doi.org/10.1021/jf035472m>.
- Swanton, C.J., O’Sullivan, J. & Robinson, D.E. (2010) The Critical Weed-Free Period in Carrot. *Weed Science*, 58, 229–233. <https://doi.org/10.1614/ws-09-098.1>.
- Tagousop, C.N., Tamokou, J.D.D., Ekom, S.E., Ngnokam, D. & Voutquenne-Nazabadioko, L. (2018) Antimicrobial activities of flavonoid glycosides from *Graptophyllum grandulosum* and their mechanism of antibacterial action. *BMC Complementary and Alternative Medicine*, 18, 252. <https://doi.org/10.1186/s12906-018-2321-7>.
- Takaichi, M. & Oeda, K. (2000) Transgenic carrots with enhanced resistance against two major pathogens, *Erysiphe heraclei* and *Alternaria dauci*. *Plant Science*, 153, 135–144. [https://doi.org/10.1016/S0168-9452\(99\)00254-X](https://doi.org/10.1016/S0168-9452(99)00254-X).
- Tan, B.A., Daim, L.D.J., Ithnin, N., Ooi, T.E.K., Md-Noh, N., Mohamed, M., et al. (2016) Expression of phenylpropanoid and flavonoid pathway genes in oil palm roots during infection by *Ganoderma boninense*. *Plant Gene*, 7, 11–20. <https://doi.org/10.1016/j.plgene.2016.07.003>.
- Tattini, M., Gravano, E., Pinelli, P., Mulinacci, N. & Romani, A. (2000) Flavonoids accumulate in leaves and glandular trichomes of *Phillyrea latifolia* exposed to excess solar radiation. *New Phytologist*, 148, 69–77.

<https://doi.org/10.1046/j.1469-8137.2000.00743.x>.

- Tattini, M., Guidi, L., Morassi-Bonzi, L., Pinelli, P., Remorini, D., Degl'Innocenti, E., et al. (2005) On the role of flavonoids in the integrated mechanisms of response of *Ligustrum vulgare* and *Phillyrea latifolia* to high solar radiation. *New Phytologist*, 167, 457–470. <https://doi.org/10.1111/j.1469-8137.2005.01442.x>.
- Taylor, L.P. & Grotewold, E. (2005) Flavonoids as developmental regulators. *Current Opinion in Plant Biology*, 8, 317–323.
- Teubert, H., Wunscher, G. & Herrmann, K. (1977) Flavonole und Flavone der Gemüsearten. *Zeitschrift für Lebensmittel-Untersuchung und -Forschung*, 152, 134–137. <https://doi.org/10.1007/BF01830525>.
- Tian, F., Woo, S.Y., Lee, S.Y., Park, S.B., Im, J.H. & Chun, H.S. (2023) Plant-based natural flavonoids show strong inhibition of aflatoxin production and related gene expressions correlated with chemical structure. *Food Microbiology*, 109, 104141. <https://doi.org/10.1016/j.fm.2022.104141>.
- Du Toit, L.J., Le Clerc, V. & Briard, M. (2019) Genetics and Genomics of Carrot Biotic Stress. The carrot Genome, Compendium of plant Genomes. Springer Nature Switzerland AG 2019, pp. 317–362.
- Du Toit, L.J., Pathologist, V.S., State, W., Vernon, M., Crowe, F.J., Pathologist, P., et al. (2005) Bacterial Blight in Carrot Seed Crops in the Pacific Northwest. *Plant disease*, 89.
- Tokuji, Y. & Hiroo, F. (1999) A Rapid Method for Transformation of Carrot (*Daucus carota* L.) by Using Direct Somatic Embryogenesis. *Bioscience, Biotechnology, and Biochemistry*, 63, 519–523.
- Valle, J.C. Del, Buide, M.L., Whittall, J.B. & Narbona, E. (2018) Phenotypic plasticity in light-induced flavonoids varies among tissues in *Silene littorea* (Caryophyllaceae). *Environmental and Experimental Botany*, 153, 100–107. <https://doi.org/10.1016/j.envexpbot.2018.05.014>.
- Vieira, V., Dias Casali, V., Milagres, J., Cardoso, A. & Regazzi, A. (1991) Heritability and genetic gain for resistance to leaf blight in carrot (*Daucus carota* L.) populations evaluated at different times after sowing. *Revista Brazilian de Genetica*, 14, 501–508.
- Vinatoru, M., Mason, T.J. & Calinescu, I. (2017) Ultrasonically assisted extraction (UAE) and microwave assisted extraction (MAE) of functional compounds from plant materials. *TrAC - Trends in Analytical Chemistry*, 97, 159–178.
- Vintal, H., Ben-Noon, E., Shlevin, E., Yermiyahu, U., Shtienberg, D. & Dinoor, A. (1999) Influence of rate of soil fertilization on *Alternaria* leaf blight (*Alternaria dauci*) in carrots. *Phytoparasitica*, 27, 193–200. <https://doi.org/10.1007/BF02981458>.
- Vogt, T. & Taylor, L.P. (1995) Flavonol 3- O-G I y cosy I t ransferases Associated w i t h Petu n ia Pollen Produce Gametophyte-Specific Flavonol Diglycosides '. 903–911.
- Wang, L., Ran, L., Hou, Y., Tian, Q., Li, C., Liu, R., et al. (2017) The transcription factor MYB115 contributes to the regulation of proanthocyanidin biosynthesis and enhances fungal resistance in poplar. *New Phytologist*, 215, 351–367. <https://doi.org/10.1111/nph.14569>.
- Wang, M., Simon, J.E., Aviles, I.F., He, K., Zheng, Q.Y. & Tadmor, Y. (2003) Analysis of antioxidative phenolic compounds in artichoke (*Cynara scolymus* L.). *Journal of Agricultural and Food Chemistry*, 51, 601–608. <https://doi.org/10.1021/jf020792b>.
- Wang, Q., Cui, W., Liu, M., Zhang, J., Liao, R.Q., Liao, X.L., et al. (2015) An improved synthesis of apigenin. *Journal of Chemical Research*, 39, 67–69. <https://doi.org/10.3184/174751915X14204548288464>.
- Wang, X. gui, Wei, X. yi, Tian, Y. qing, Shen, L. tao & Xu, H. hong (2010) Antifungal Flavonoids from *Ficus sarmentosa* var. *henryi* (King) Corner. *Agricultural Sciences in China*, 9, 690–694. [https://doi.org/10.1016/S1671-2927\(09\)60144-9](https://doi.org/10.1016/S1671-2927(09)60144-9).
- Wang, Y.C., Qian, W.J., Li, N.N., Hao, X.Y., Wang, L., Xiao, B., et al. (2016) Metabolic Changes of Caffeine in Tea Plant (*Camellia sinensis* (L.) O. Kuntze) as Defense Response to *Colletotrichum fructicola*. *Journal of Agricultural and Food Chemistry*, 64, 6685–6693. <https://doi.org/10.1021/acs.jafc.6b02044>.

- Westrick, N.M., Smith, D.L. & Kabbage, M. (2021) Disarming the Host: Detoxification of Plant Defense Compounds During Fungal Necrotrophy. *Frontiers in Plant Science*, 12, 1–18. <https://doi.org/10.3389/fpls.2021.651716>.
- Wu, Q.W., Wei, M., Feng, L.F., Ding, L., Wei, W.K., Yang, J.F., et al. (2022) Rhamnosyltransferases involved in the biosynthesis of flavone rutinosides in *Chrysanthemum* species. *Plant Physiology*, 190, 2122–2136. <https://doi.org/10.1093/plphys/kiac371>.
- Xu, F., Ning, Y., Zhang, W., Liao, Y., Li, L., Cheng, H., et al. (2014) An R2R3-MYB transcription factor as a negative regulator of the flavonoid biosynthesis pathway in *Ginkgo biloba*. *Functional and Integrative Genomics*, 14, 177–189. <https://doi.org/10.1007/s10142-013-0352-1>.
- Xu, S., Yan, F., Ni, Z., Chen, Q., Zhang, H. & Zheng, X. (2014) In vitro and in vivo control of *Alternaria alternata* in cherry tomato by essential oil from *Laurus nobilis* of Chinese origin. *Journal of the Science of Food and Agriculture*, 94, 1403–1408. <https://doi.org/10.1002/jsfa.6428>.
- Xu, W., Dubos, C. & Lepiniec, L. (2015) Transcriptional control of flavonoid biosynthesis by MYB-bHLH-WDR complexes. *Trends in Plant Science*, 20, 176–185. <https://doi.org/10.1016/j.tplants.2014.12.001>.
- Yao, P., Deng, R., Huang, Y., Stael, S., Shi, J., Shi, G., et al. (2019) Diverse biological effects of glycosyltransferase genes from Tartary buckwheat. *BMC Plant Biology*, 19, 1–15. <https://doi.org/10.1186/s12870-019-1955-z>.
- Yin, J.M., Yan, R.X., Zhang, P.T., Han, X.Y. & Wang, L. (2015) Anthocyanin accumulation rate and the biosynthesis related gene expression in *Dioscorea alata*. *Biologia Plantarum*, 59, 325–330. <https://doi.org/10.1007/s10535-015-0502-5>.
- Zagrean-Tuza, C., Mot, A.C., Chmiel, T., Bende, A. & Turcu, I. (2020) Sugar matters: Sugar moieties as reactivity-tuning factors in quercetin: O-glycosides. *Food and Function*, 11, 5293–5307. <https://doi.org/10.1039/d0fo00319k>.
- Zhang, J., Liu, M., Cui, W., Yang, J. & Liao, X.L. (2013) Efficient synthesis of apigenin. *Journal of Chemical Research*, 37, 694–696. <https://doi.org/10.3184/174751913X13815091347640>.
- Zhang, Q.W., Lin, L.G. & Ye, W.C. (2018) Techniques for extraction and isolation of natural products: A comprehensive review. *Chinese Medicine*, 13, 20.
- Zhang, X., Huang, X., Li, Y., Tao, F., Zhao, Q. & Li, W. (2021) Polar auxin transport May Be responsive to specific features of flavonoid structure. *Phytochemistry*, 185, 112702. <https://doi.org/10.1016/j.phytochem.2021.112702>.
- Zhao, F., Li, G., Hu, P., Zhao, X., Li, L., Wei, W., et al. (2018) Identification of basic/helix-loop-helix transcription factors reveals candidate genes involved in anthocyanin biosynthesis from the strawberry white-flesh mutant. *Scientific Reports*, 8, 1–15. <https://doi.org/10.1038/s41598-018-21136-z>.
- Zhu, J., Xu, Q., Zhao, S., Xia, X., Yan, X., An, Y., et al. (2020) Comprehensive co-expression analysis provides novel insights into temporal variation of flavonoids in fresh leaves of the tea plant (*Camellia sinensis*). *Plant Science*, 290, 110306. <https://doi.org/10.1016/j.plantsci.2019.110306>.
- Zhu, X., Zhang, H. & Lo, R. (2004) Phenolic Compounds from the Leaf Extract of Artichoke (*Cynara scolymus* L.) and Their Antimicrobial Activities. <https://doi.org/10.1021/jf0490192>.

RÉSUMÉ

Les flavones apigénine-7-O-rutinoside (Api7R), lutéoline-7-O-rutinoside (Lut7R) et chrysoériol-7-O-rutinoside (Chry7R) étaient différentiellement accumulés entre les accessions de carotte partiellement résistante (I2) et sensible (H1) à la brûlure foliaire (ALB) due à *A. dauci* (Ad), dès le stade 2 feuilles et ont persisté au cours de la croissance végétative. La co-occurrence de leur accumulation avec la résistance à ALB a été vérifiée dans plusieurs accessions d'origines diverses. Cependant, seuls les niveaux de Lut7R et Chry7R discriminent les niveaux de résistance intermédiaire. L'étude de l'activité biologique d'Api7R pure, de Lut7R purifiée à 95-97% et de Chry7R à 73% a montré que Api7R et Lut7R ont stimulé la germination des conidies du champignon *in vitro*, tandis que Chry7R a eu un léger effet inhibiteur sur la croissance des hyphes. Api7R et Lut7R ont également stimulé l'infection de H1 *in planta*. Néanmoins, une expansion plus limitée des symptômes avec Lut7R, suggère un potentiel effet protecteur différé. L'obtention de transformants surexprimant un gène codant un facteur de transcription BHLH118-like (bHLH) ou un gène codant une UDP-flavonoid-glycosyltransférase n'a pas permis de mettre en évidence leur rôle potentiel dans la biosynthèse des 3 candidats, mais des extraits de cals de H1 surexprimant bHLH et accumulant fortement Lut7R et Chry7R ont stimulé, de façon prononcée, la germination des conidies d'Ad *in vitro*, tel des extraits de cals I2 non transformés (I2-NT), toutefois sans modifier l'intégrité des hyphes contrairement à I2-NT. D'autres composés bioactifs sont donc à rechercher. Les résultats confortent l'idée d'utiliser Lut7R et Chry7R en tant que marqueurs de résistance dans les programmes de sélection.

mots-clés : Résistance quantitative, Métabolites spécialisés, Génétique fonctionnelle, Purification, LC-MS

ABSTRACT

Differential accumulation of the flavones apigenin-7-O-rutinoside (Api7R), luteolin-7-O-rutinoside (Lut7R) and chrysoeryol-7-O-rutinoside (Chry7R) was observed between carrot accessions partially resistant (I2) and susceptible (H1) to *A. dauci* (Ad) leaf blight (ALB) from the 2-leaf stage and persisted during vegetative growth. The co-occurrence of their accumulation with ALB resistance has been demonstrated in several accessions of diverse origins. However, only Lut7R and Chry7R levels discriminate between intermediate levels of resistance. A study of the biological activity of pure Api7R, 95-97% purified Lut7R and 73% purified Chry7R showed that Api7R and Lut7R stimulated the germination of fungal conidia *in vitro*, whereas Chry7R had a slight inhibitory effect on hyphal growth. Api7R and Lut7R also stimulated H1 infection *in planta*. However, a more limited spread of symptoms with Lut7R suggests a possible delayed protective effect. Transformants overexpressing a gene encoding a BHLH118-like transcription factor (bHLH) or another encoding a UDP-flavonoid-glycosyltransferase were obtained. Although their potential role in the biosynthesis of the 3 candidates was not confirmed, extracts of H1 callus overexpressing bHLH and highly accumulating Lut7R and Chry7R strongly stimulated conidial germination of Ad *in vitro*, as did extracts of untransformed I2 callus (I2-NT), but without affecting the integrity of the hyphae, unlike I2-NT. Other bioactive compounds therefore need to be sought. The results support the idea of using Lut7R and Chry7R as resistance markers in breeding programmes.

keywords: Quantitative resistance, Specialised metabolites, Functional genetics, Purification, LC-MS.

ENGAGEMENT DE NON PLAGIAT

Je, soussigné(e) **RAMAROSON Marie Louisa**.....
déclare être pleinement conscient(e) que le plagiat de documents ou d'une
partie d'un document publiée sur toutes formes de support, y compris l'internet,
constitue une violation des droits d'auteur ainsi qu'une fraude caractérisée.
En conséquence, je m'engage à citer toutes les sources que j'ai utilisées
pour écrire ce rapport ou mémoire.

signé par l'étudiant(e) le **22 / 08 / 2023**

**Cet engagement de non plagiat doit être signé et joint
à tous les rapports, dossiers, mémoires.**

Présidence de l'université
40 rue de rennes – BP 73532
49035 Angers cedex



Titre : Rôle des flavonoïdes dans la résistance de la carotte à *Alternaria dauci*.

Mots clés : Résistance quantitative, Métabolites spécialisés, Génétique fonctionnelle, Purification, LC-MS

Les flavones apigénine-7-O-rutinoside (Api7R), lutéoline-7-O-rutinoside (Lut7R) et chrysoéryol-7-O-rutinoside (Chry7R) étaient différenciellement accumulés entre les accessions de carotte partiellement résistante (I2) et sensible (H1) à la brûlure foliaire (ALB) due à *A. dauci* (Ad), dès le stade 2 feuilles et ont persisté au cours de la croissance végétative. La co-occurrence de leur accumulation avec la résistance à ALB a été vérifiée dans plusieurs accessions d'origines diverses. Cependant, seuls les niveaux de Lut7R et Chry7R discriminent les niveaux de résistance intermédiaire. L'étude de l'activité biologique d'Api7R pure, de Lut7R purifiée à 95-97% et de Chry7R à 73% a montré que Api7R et Lut7R ont stimulé la germination des conidies du champignon *in vitro*, tandis que Chry7R a eu un léger effet inhibiteur sur la croissance des hyphes. Api7R et Lut7R ont également stimulé l'infection de H1 *in planta*.

Néanmoins, une expansion plus limitée des symptômes avec Lut7R, suggère un potentiel effet protecteur différé. L'obtention de transformants surexprimant un gène codant un facteur de transcription BHLH118-like (bHLH) ou un gène codant une UDP-flavonoid-glycosyltransférase n'a pas permis de mettre en évidence leur rôle potentiel dans la biosynthèse des 3 candidats, mais des extraits de cals de H1 surexprimant bHLH et accumulant fortement Lut7R et Chry7R ont stimulé, de façon prononcée, la germination des conidies d'Ad *in vitro*, tel des extraits de cals I2 non transformés (I2-NT), toutefois sans modifier l'intégrité des hyphes contrairement à I2-NT. D'autres composés bioactifs sont donc à rechercher. Les résultats confortent l'idée d'utiliser Lut7R et Chry7R en tant que marqueurs de résistance dans les programmes de sélection.

Title: Flavonoids and resistance of carrot to *Alternaria dauci*.

Keywords: Quantitative resistance, Specialised metabolites, functional genetics, purification, LC-MS

Abstract: Differential accumulation of the flavones apigenin-7-O-rutinoside (Api7R), luteolin-7-O-rutinoside (Lut7R) and chrysoeryol-7-O-rutinoside (Chry7R) was observed between carrot accessions partially resistant (I2) and susceptible (H1) to *A. dauci* (Ad) leaf blight (ALB) from the 2-leaf stage and persisted during vegetative growth. The co-occurrence of their accumulation with ALB resistance has been demonstrated in several accessions of diverse origins. However, only Lut7R and Chry7R levels discriminate between intermediate levels of resistance. A study of the biological activity of pure Api7R, 95-97% purified Lut7R and 73% purified Chry7R showed that Api7R and Lut7R stimulated the germination of fungal conidia *in vitro*, whereas Chry7R had a slight inhibitory effect on hyphal growth. Api7R and Lut7R also stimulated H1 infection *in planta*.

However, a more limited spread of symptoms with Lut7R suggests a possible delayed protective effect. Transformants overexpressing a gene encoding a BHLH118-like transcription factor (bHLH) or another encoding a UDP-flavonoid-glycosyltransferase were obtained. Although their potential role in the biosynthesis of the 3 candidates was not confirmed, extracts of H1 callus overexpressing bHLH and highly accumulating Lut7R and Chry7R strongly stimulated conidial germination of Ad *in vitro*, as did extracts of untransformed I2 callus (I2-NT), but without affecting the integrity of the hyphae, unlike I2-NT. Other bioactive compounds therefore need to be sought. The results support the idea of using Lut7R and Chry7R as resistance markers in breeding programmes.